A Methodology (CUPRITE) for Urban Network Travel Time Estimation by Integrating Multisource Data

THÈSE N^{O} 4416 (2009)

PRÉSENTÉE LE 3 JUINI 2009

À LA FACULTÉ ENVIRONNEMENT NATUREL, ARCHITECTURAL ET CONSTRUIT
LABORATOIRE DES VOIES DE CIRCULATION
PROGRAMME DOCTORAL EN ENVIRONNEMENT

ÉCOLE POLYTECHNIQUE FÉDÉRALE DE LAUSANNE

POUR L'OBTENTION DU GRADE DE DOCTEUR ÈS SCIENCES

PAR

Ashish BHASKAR

acceptée sur proposition du jury:

Dr D. Robinson, président du jury
Prof. A.-G. Dumont, Dr E. Chung, directeurs de thèse
Prof. M. Bierlaire, rapporteur
Dr N.-E. El Faouzi, rapporteur
Prof. M. Kuwahara, rapporteur

ÉCOLE POLYTECHNIQUE
FÉDÉRALE DE LAUSANNE

Suisse
2009

Abstract

Travel time is an important network performance measure and it quantifies congestion in a manner easily understood by all transport users. In urban networks, travel time estimation is challenging due to number of reasons such as, fluctuations in traffic flow due to traffic signals, significant flow to/from mid-link sinks/sources, etc. In this research a methodology, named CUmulative plots and PRobe Integration for travel timE estimation (CUPRITE), has been developed, tested and validated for average travel time estimation on signalized urban network. It provides exit movement specific link travel time and can be applied for route travel time estimation.

The basis of CUPRITE lies in the classical analytical procedure of utilizing cumulative plots at upstream and downstream locations for estimating travel time between the two locations. The classical procedure is vulnerable to detector counting error and non conservation of flow between the two locations that induces *relative deviation amongst the cumulative plots* (RD).

The originality of CUPRITE resides in integration of multi-source data: detector data and signal timings from different locations on the network, and probe vehicle data. First, cumulative plots are accurately estimated by integrating detector and signal timings. Thereafter, cumulative plots are integrated with probe vehicle data and RD issue is addressed.

CUPRITE is tested rigorously using traffic simulation for different scenarios with different possible combinations of sink, source and detector error. The performance of the proposed methodology has been found insensitive to percentage of sink or source or detector error. For a link between two consecutive signalized intersections and during undersaturated traffic condition, the concept of virtual probe is introduced and travel time can be accurately estimated without any real probe. For oversaturated traffic condition, CUPRITE requires only few probes per estimation interval for accurate travel time estimation.

CUPRITE is also validated with real data collected from number plate survey at Lucerne, Switzerland. Two tailed t-test (at 0.05 level of significance) results confirm that travel time estimates from CUPRITE are statistically equivalent to real estimates from number plate survey.

The testing and validation of CUPRITE have demonstrated that it can be applied for accurate and reliable travel time estimation. The current market penetration of probe vehicle is quite low. In urban networks, availability of a large number of probes per estimation interval is rare. With limited number of probe vehicles in urban networks, CUPRITE can significantly enhance the accuracy of travel time estimation.

Keywords: Travel time, urban network, signalized network, cumulative plots, probe vehicle, detector error, mid-link sink, mid-link source.

Résumé

Sur un réseau routier, le temps de parcours est un indicateur de performance très important qui quantifie la congestion d'une façon compréhensible par tous les usagers. En environnement urbain, l'estimation des temps de parcours peut s'avérer complexe en raison d'un certain nombre d'éléments: fluctuations du débit due aux feux de signalisation, débit non négligeable provenant de sources/puits de mi-parcours etc. Dans ce travail, une méthodologie, nommé CUPRITE (CUmulative plots and PRobe Integration for Travel timE estimation), a été développée, testée et validée pour l'estimation d'un temps de parcours moyen sur un réseau urbain signalisé. Elle fournit un temps de parcours en fonction du mouvement spécifique de sortie sur un lien et peut être appliquée pour l'estimation du temps de parcours du trajet.

La procédure de base de CUPRITE consiste à utiliser la classique procédure analytique d'utilisation des courbes cumulatives en amont et en aval d'un point donné dans le but d'estimer le temps de parcours entre deux points. Toutefois, cette procédure est vulnérable face aux erreurs de mesure des capteurs et à la non-conservation du débit entre deux points, ce qui entraine des erreurs relatives entre les courbes cumulatives (ER).

L'originalité de CUPRITE réside dans l'intégration de données multi-source: données boucle et phases de feux pour différents endroits du réseau et données de véhicules traceurs. Dans un premier temps, les courbes cumulatives sont estimées précisément à l'aide des données boucles et phases de feux puis ces courbes cumulatives sont intégrées avec les données des véhicules traceurs pour résoudre le problème des erreurs relatives (ER).

CUPRITE a été testée rigoureusement avec des simulations de plusieurs scénarii pour différentes combinaisons possibles de puits (perte de véhicules à mi-parcours), de sources ou d'erreurs de capteurs. Les performances restent stables quels que soient les pourcentages de ces différentes perturbations. Pour un lien entre deux intersections signalisées en régime non saturé, le concept de véhicule traceur *virtuel* est introduit, qui permet d'estimer précisément les temps de parcours sans véhicule traceur réel. Pour des conditions saturées, CUPRITE requiert seulement quelques données de véhicules traceurs par intervalle pour une estimation précise du temps de parcours.

CUPRITE a également été validée avec des données réelles collectées par reconnaissance de plaques d'immatriculation à Lucerne (Suisse). Les résultats des tests de Student bilatéraux (à un degré de significativité de 0.05) confirment que les estimations de temps de parcours de CUPRITE sont statistiquement équivalentes aux estimations réelles à partir des plaques d'immatriculation.

Les tests et la validation de CUPRITE ont montré que la méthode peut être appliquée pour des estimations précises et fiables de temps de parcours. Actuellement, le taux de pénétration des véhicules traceurs dans le marché actuel est assez faible et il y a peu de données en milieu urbain. Cependant, même avec peu de données "traceurs", CUPRITE peut améliorer de façon significative la précision des estimations de temps de parcours.

Mots clés: Temps de parcours, réseau urbain, réseau signalisé, courbes cumulatives, véhicules traceurs, erreurs de capteurs.

Acknowledgements

I take this opportunity to thank those who made this dissertation possible.

Foremost, I would like to express my sincere appreciation to my supervisors Professor André-Gilles Dumont and Professor Edward Chung. I am grateful to Professor Dumont for accepting me as a PhD candidate and for giving me an opportunity to work in the European atmosphere. He has provided full support for conducting the research and has shown confidence in me. I am thankful for his comments and suggestions. Professor Edward has gone deep into the topic. He has not only been an invaluable source of guidance, advice and suggestions but has also provided understanding throughout my research. I appreciate all his contributions of time, ideas, discussions and patience to make my PhD experience productive. His analytical skills and logical ways of thinking have been of great value for me.

I would like to express my thanks to jury members for their constructive comments. Their comments and suggestions are helpful to improve the quality of the report.

I wish to express my gratitude to Professor Masao Kuwahara the discussion with whom during his two months of sabbatical at EPFL were valuable during the early phase of this research.

Furthermore, I would like to recognize the contribution from Dr. Thomas Riedel (VS-PLUS, Switzerland) for his timely support to obtain the real data from Lucerne. I am grateful to Mr Inerio Betto (Lucerne Transport Authority, Lucerne, Switzerland) for giving me access to the detector and signal data. I am also thankful to my colleagues Mr Jean-Jacques Hefti, Mr Charles Gilliard, Minh-Hai, Patrick and Etienne, and hired students who had helped to collect the number plate survey data.

I warmly thank Dr. Olivier de Mouzon, Dr. Shamas Bajwa and Professor Takashi Oguchi for their insight.

The financial support from Swiss Federal Road Office (FEDRO), Switzerland is deeply appreciated. I am thankful to the members of the *commission suivi* for providing encouragement.

Thanks also to the members and ex-members of LAVOC for their support. To mention a few, Mehdi, Minh-Hai, Emmanuel, Patrick, Nicolas, Margarita, Chiara, Daniel,… Thanks to

Ms Dominique Corday for her friendly attitude and taking care of the administrative tasks. Dr Alexandre Torday deserves special thanks for helping me to find the doctoral position at EPFL and also to settle down in a new culture and atmosphere.

It is difficult to name all, but I am thankful to all those, especially Shashank, Romain, and Saurabh … who have helped in a way or other.

I owe special gratitude to my family: my wife Pooja, my daughter Aashi, my parents and my sisters for their continuous and unconditional support, affection, wishes and encouragement. They have always stood by me throughout. Pooja has always been very supportive and understanding, especially during the challenging periods of the research.

Finally, I thank to God for providing me the confidence and strength.

(Ashish, BHASKAR)

Table of contents

List of figures

List of tables

List of abbreviations and symbols

Following are the common used abbreviations and symbols throughout the thesis. Abbreviations specific to a chapter are provided as a separate list in the chapter, if required.

Abbreviation	**Meaning**
A_M	Accuracy obtained from Mean Absolute Percentage Error. Equation (4.15).
A_5	Accuracy obtained from 95th percentile of error. Equation (4.17).
ANPR	Automatic Number Plate Recognition.
AVI	Automatic Vehicle Identification.
C	Signal cycle time.
CP	Cumulative plot.
CUPRITE	CUmulative plots and PRobe Integration for Travel timE estimation.
d/s	Downstream exit of the study link. Here, entrance of the downstream intersection.
D(t)	Cumulative plot at *d/s* location. Also the counts corresponding to time *t*.
FIFO	First-In-First-Out.
g	Signal effective green time.
ITS	Intelligent Transportation Systems.
MAPE	Mean Absolute Percentage Error.
R_C	Component based path travel time.
RD	Relative deviation amongst the cumulative plots.
R_E	Extreme based path travel time.
s	Saturation flow rate. (Also used for seconds, unit of measure).
S_n	Fixed number of probes per estimation interval.
S_p	Fixed percentage of probes per estimation interval.
T_{EI}	Travel time estimation interval.
t_d	Time when probe vehicle is at *d/s* location.
t_D	Time when a vehicle is represented in D(t).

Abbreviation	Meaning
$[t_d]$	List of t_d values from different probe vehicles.
t_{ff}	Free-flow travel time from *u/s* to *d/s*.
t_{GE}	Time corresponding to end of effective signal green phase.
t_{RS}	Time corresponding to start of effective signal red phase.
t_u	Time when probe vehicle is at *u/s* location.
t_U	Time when a vehicle is represented in U(t).
$[t_u]$	List of t_u values from different probe vehicles.
$t_{\alpha/2,n}$	t-statistics with α level of significance and *n* degrees of freedom.
u/s	Upstream entrance of the study link. Here, entrance of the upstream intersection.
U(t)	Cumulative plot at *u/s* location. Also the counts corresponding to time *t*.
X	Degree of saturation at downstream intersection.

Abbreviation	Unit of measure
cm	centimeter
ft	feet
h	hour
kHz	kilohertz
Km	Kilometer
m	meter
mi	mile
mi/h	miles per hour
min	minute
pcu	passenger car unit
pcu/h	passenger car unit per hour
s	seconds (Also used for saturation flow rate)
s/km	seconds per kilometer
veh	vehicle
veh/s	vehicle per second

Abbreviation	**Meaning**
veh/km	vehicle per kilometer
Symbol	**Meaning**
μ_C	Mean of the population estimates from CUPRITE application.
μ_s	Mean of the population estimates from survey data.

1 Introduction

This chapter introduces the problem addressed in this research followed by research objectives and significance. Finally, the outline of the dissertation is provided.

1.1 Background

Travelling is an inevitable part of life either due to spatially separated activities or for other social, economic and behavioral reasons. With economic and population growth there is an increase in demand for travel and vehicle ownership. The supply (capacity of transportation infrastructure and modes) of infrastructure and transportation system is limited and the increase in supply does not match with increase in demand. This is one of the reasons for traffic congestion. Traffic congestion is an inevitable condition in almost all major cities. The increase in congestion on the road network results in:

i. Economic loss: In Europe, the external social economic cost of congestion is estimated to be around 2% of GDP (Kinnock, 1995), which amounts to annual social loss of more than 120 billion Euros.

ii. Environmental impact: Congestion results in stop-and-go running conditions, which not only increases energy consumption but also causes more air and noise pollution.

iii. Adverse physiological, psychological and social effects.

It is almost impossible to eliminate peak period congestion. However, the problem can be reduced by efficient and intelligent traffic management. For instance, Intelligent Transportation Systems (ITS) where network performance information is automatically gathered, managed, and relayed through a network of transportation facilities such as roadways and terminals.

Travel time is defined as the time needed to travel from one point to another on the network. Travel time information quantifies the performance of the network and is generally considered as the most important performance measure in transportation studies. Excess travel

time (delay) leads to indirect costs to the drivers in terms of lost time, discomfort and frustration and a direct cost in terms of fuel consumption during idling. Excessive delay reflects inefficiency in the system performance. Travel time information is easy to perceive by the road users and has the potential to reduce congestion on both temporal and spatial scale. Reducing congestion maximizes the efficiency and capacity of the network, providing smooth traffic flow which in turn reduces vehicle emissions and energy consumption.

Different techniques are applied to estimate travel time on the traffic networks. These techniques depend on the type of the traffic data retrieval system, that vary from traditional inductive loop detectors to advance vehicle tracking equipments such as GPS and mobile phone carried by driver. The state-of-the-art for travel time estimation techniques is provided in Chapter 2.

Traffic data obtained from detectors provide information for the point where detectors are installed (point measure). Whereas, probe vehicle data, provides information for the behavior of the probe vehicle on the network. The traffic information obtained from a point measure should be carefully utilized to estimate the spatial behavior of traffic. Similarly, the information obtained from a probe vehicle should be carefully utilized to estimate the behavior of all the vehicles traversing.

In this dissertation, vehicle equipped with vehicle tracking equipments is termed as probe vehicle. Probe data in addition to detector and traffic signal data at different locations on the network are multisource data utilized for travel time estimation.

1.2 Research motivation

The primary use of the detectors at most of the signalized arterials is for signal control. More and more vehicles are equipped with position tracking equipments and such vehicles can be used as probe vehicles. For instance, GPS equipped taxis where the data is used for fleet management. If the data from these multisources (detector and signal controller at different locations on the network and probe vehicle) is also used for accurate travel time estimation and feed back to the traffic management system then it would be a significant contribution to better urban traffic control and management.

In Switzerland, generally most of the intersections have stop-line inductive loop detectors, i.e., detectors just before or after the stop-line at the intersection (Detectors after the stop-line

are generally installed to check the red light violation.). These detectors are 1.5 ~ 2 m in length and are capable of providing vehicle counts. The methodology in this research is developed based on stop-line detectors and is able to incorporate data from detectors at different locations. A short description of detector layout in urban networks is provided in Appendix A.

Figure 1-1 illustrates the data required for the methodology development i.e., detector data, signal control data and probe vehicle data. The potential applications for the integration of these multisource data are also illustrated. The detail of these applications is discussed in Section 1.8.

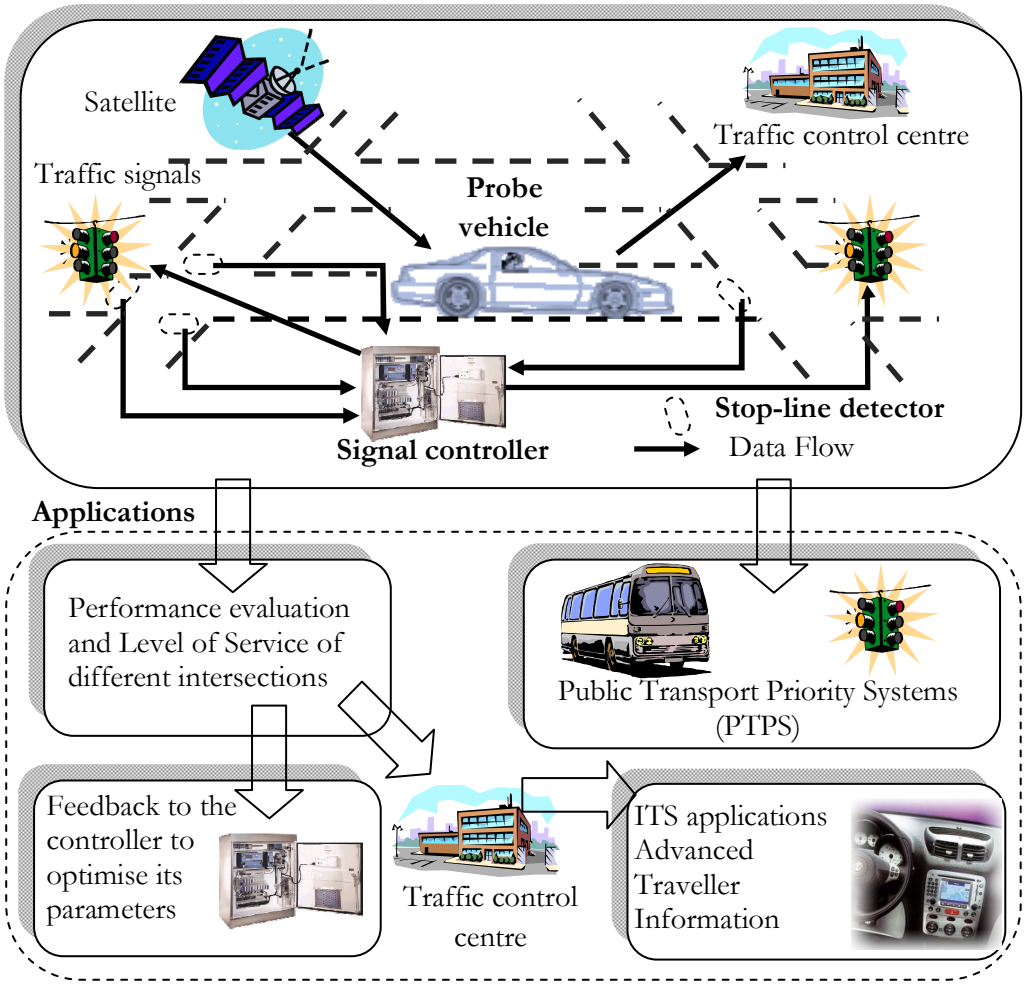

Figure 1-1: Representation of the data requirement for the methodology and its applications.

1.3 Problem statement

Most of the researches on travel time estimation are limited to freeways and researchers have applied different methodologies ranging from simple statistical modeling to sophisticated artificial intelligence. Traffic flows on freeways are treated as *uninterrupted traffic flow* where flow conditions are primarily the result of internal friction i.e., interactions among the vehicles and interactions between the vehicle and infrastructure. There are no external causes of interruption (such as, traffic signals) to the continuous movement of vehicles. On freeways, the spot-speed at the detector location can be easily correlated to the travel time of the section from (few hundred meters) upstream to downstream of the detector location. There is no significant variation of the travel time between two consecutive vehicles. Hence, few probe vehicles can be a good representation of all the vehicles traversing the link. However, travel time estimation is more challenging on urban facilities as explained in the following subsection (1.3.1).

1.3.1 Complexities with urban network

Interruptions in flow due to conflicting areas: On urban networks external control such as, traffic signals, yield signs and stop signs are needed to ensure safety at conflicting areas (intersections). The flow thus not only depends on internal friction but also on the external factors resulting in *interrupted traffic flow*. Vehicles are at stop-and-go running conditions and the delays experienced at the intersections are significant part of the travel time on the urban link. Hence, the spot-speed from a detector cannot be correlated to travel time on a link between intersections. In addition to the delays at the intersections, vehicles are also prone to *mid-link delays* due to a number of reasons such as, pedestrians, vehicles entering from side-streets, on-street bus stops etc.

There can be significant variation in travel time between two consecutive vehicles depending on the time when the vehicle arrives at an intersection. For instance, if the leading vehicle arrives during signal green phase and the following vehicle arrives during signal red phase then the following vehicle has to stop at intersection resulting in significantly higher travel time. Therefore, average travel time estimation solely based on probe data requires significantly large number of probes per estimation interval.

Significant proportion of flow to/from mid-link sinks/sources: The proportion of such flows is dynamic and varies with time of the day and day of the week. Generally, detectors are

not installed on mid-link sinks/sources. Practically, the loss/gain of flow to/from a mid-link sink/source is unknown. Models solely based on detector data only capture the flow at the detector location and its performance can significantly deteriorate in the presence of significant flow to/from mid-link sinks/sources. Also, the performance is affected by the errors in detector counting.

Average link travel time may not be representative of travel time for different exit movements: An urban link is associated with different exit turning movements for instance, travel time for through, left and right movements. Average travel time on the link may not be a true representative of the travel time for different movements. For ITS applications (such as route guidance) one is more interested in movement specific travel time than average link travel time. For movement specific travel time we need to know the demand for each movement and it is more complicated to estimate than average travel time on the whole link.

1.4 Research goal and objectives

The main goal of this research is to develop a methodology that should address the problem discussed in the previous section.

The first objective of this research is to **develop a methodology** for movement specific travel time estimation on urban signalized networks utilizing the multisource data.

The second objective is to **test the methodology** under controlled environment. The performance of the methodology is to be evaluated through simulation of different scenarios.

The third objective is to **validate the methodology** with real data from a typical urban network with mid-link sources and sinks etc. Validation with field data is necessary to justify the potential of the methodology for implementation on real transport network.

1.5 Research scope

The methodology developed in this research is to estimate average travel time during certain travel time estimation interval. For instance, average travel time for five signal control cycles. It should not be confused with “Individual vehicle travel time” or “Short-term travel time prediction”. Individual vehicle travel time on signalized urban networks is random and is subjected to the time when the vehicle arrives at the intersection. Short-term travel time prediction is the prediction of future travel time. In literature, time series modeling tools such

as AutoRegressive Integrated Moving Average (ARIMA), are utilized for travel time prediction. Such models require an input of time series of experienced travel time. The performance of such models highly depends on the quality of the input. The estimates of travel time from this research should be a valuable input for such models.

1.6 Classical analytical procedure for travel time estimation

The methodology developed in this research is based on classical analytical procedure of estimating travel time using cumulative plots. This section introduces the procedure and discusses the issues related to application of cumulative plots for travel time estimation on urban networks.

1.6.1 Cumulative plot

Cumulative plot (Figure 1-2) is graph of a function that defines the cumulative number of values (counts of vehicles passing an observer) at time *t*, starting from an arbitrary initial count, e.g., at *t=0*. Cumulative plots are used as a tool in number of engineering applications such as "mass curve analysis" in hydraulic engineering. In traffic engineering, Newell (1982) is pioneer to use cumulative plots for dynamic analysis of deterministic congested systems.

Suppose at a specific location on the road there is an observer or a detector which detects the time when the vehicle is at the location, then accumulating vehicles vertically in the order of their detection time provides the discrete points of cumulative vehicle counts versus time (*see* Figure 1-2). Discrete points are obtained because vehicles are discrete. These discrete points can be joined smoothly by considering fluid approximation to the vehicle flow and the defined curve is the cumulative plot.

Cumulative plot is monotonically increasing and can be assumed to be differential with respect to time. The slope of the plot at time *t* is the instantaneous traffic flow at time *t*. The value of the cumulative counts at time *t* is CP(t). For time *t* and *t*+Δt, the difference in the corresponding cumulative counts (CP(t + Δt) - CP(t)) gives traffic counts during time interval Δt. The average flow during the time interval is the ratio of counts and time interval i.e., (CP(t + Δt) - CP(t))/ Δt .

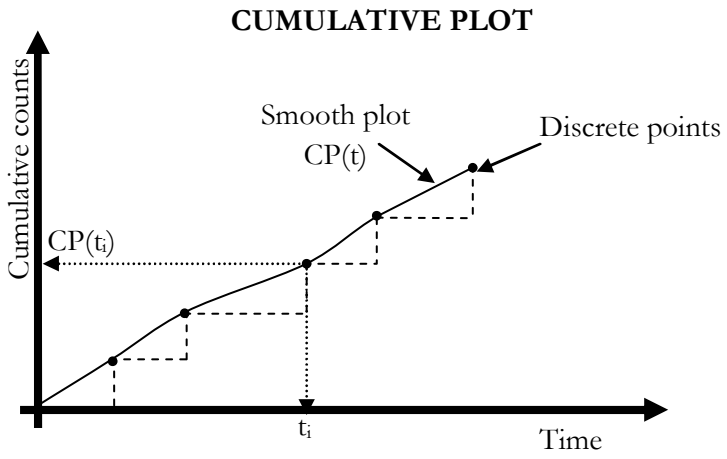

Figure 1-2: Cumulative plot obtained by smoothly joining the discrete points of cumulative counts versus time.

1.6.2 Travel time estimation using cumulative plots

Refer to Figure 1-3, two cumulative plots U(t) and D(t) are obtained at locations upstream (*u/s*) and downstream (*d/s*) of a road, respectively. Assuming: a) First-In-First-Out (FIFO) discipline is respected for all vehicles traversing from *u/s* to *d/s* (i.e., there is no vehicle overtaking); and b) the vehicles are conserved (i.e., there is no loss or gain of vehicles between *u/s* and *d/s*). The vertical distance (along Y-axis) between the two plots at time *t* defines the instantaneous number of vehicles (*n*) between the two locations. The horizontal distance (along X-axis) for count *i* define the travel time (tt_i) for the i^{th} vehicle. The classical analytical principle for average travel time estimation defines total travel time for all the *N* vehicles departing during travel time estimation interval (T_{EI}) (from the location *d/s*) as the area (*A*) between the two cumulative plots. Average travel time per vehicle is the ratio: *A/N*. Interested readers can refer to Page 1-24 of Newell (1982) and Chapter 2 of Daganzo (1997) for complementary reading.

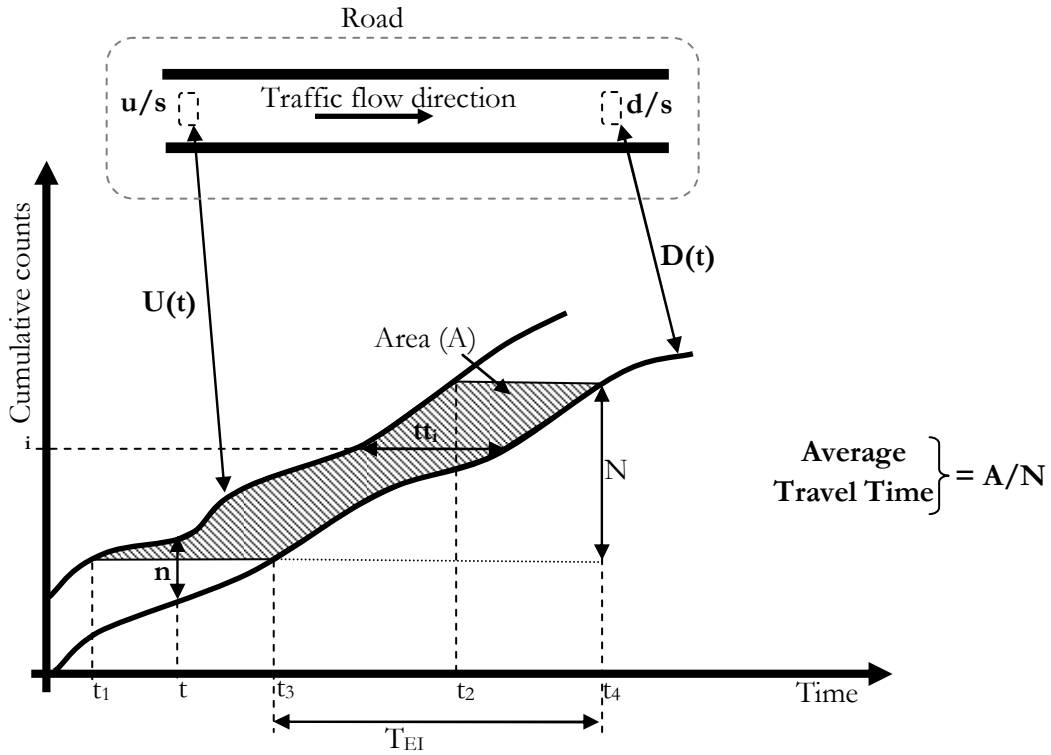

Figure 1-3: Classical analytical procedure for average travel time estimation.

Note: even if FIFO discipline is not respected, the area (*A*) between the two plots represents the total travel time as long as all the vehicles which arrive at upstream during time t_1 and t_2 actually depart at downstream during time t_3 and t_4, and vice versa. Here t_1 and t_2 are time corresponding to the start and end of U(t) represented in the area, respectively; and similarly t_3 and t_4 are time corresponding to the start and end of D(t) represented in the area, respectively.

1.6.3 Issue for application of classical analytical procedure on urban network

For the application of the above mentioned classical procedure, not only cumulative plots should be accurately estimated but also there should not be *relative deviation amongst the plots*. The ideal situation is when detectors are perfect (i.e., they provide accurate vehicle by vehicle information) and vehicles are conserved between the upstream and downstream locations. However, these conditions are difficult to obtain in practice, especially in urban networks due to reasons mentioned below:

i. *Detector Error*: Loop detectors even under normal running conditions have counting error of around 5%. However, for cumulative plot these errors are also cumulative and can result in exponential *relative deviation amongst the plots*.

ii. *Mid-link sources and sinks* such as, parking, mid-link street, residential and commercial areas etc., violate the requirement for conservation of vehicles between the two locations where cumulative plots are defined.

iii. *Unknown cumulative plots for different link movements:* An urban link can have complex combinations of flow to and from a link. For instance, shared use lane at upstream link with unknown real turning proportions can complex the process of estimating cumulative plot at upstream location. Moreover, for exit movement specific travel time, the unknown cumulative plot for each exit movement is also to be estimated.

For detailed discussion of the above issues with an example refer to Section 4.1 and Section 5.1.2.

Based on the above mentioned classical analytical procedure, in this research analytical modeling is performed for accurate estimation of cumulative plots and accuracy is enhanced by integrating cumulative plots with probe vehicle data (Figure 1-1). The methodology developed in this dissertation is named as CUmulative plots and PRobe Integration for Travel timE estimation (CUPRITE[1]).

1.7 Scientific relevance

The key contributions of this research to the scientific community can be summarized as follows:

i. *Methodology for real-time average travel time estimation on signalized urban networks:* The methodology is thoroughly tested for different traffic conditions and validated with the real data.

ii. *Consideration of mid-link sinks and sources, and detector counting error:* Most of the in-practice models overlook the flow to/from mid-link sinks/sources and

[1] Pronunciation: kyü-prīt.

In literature, *cuprite* is a red mineral consisting of copper oxide (Cu_2O) and is a minor ore of copper. It is also one of the rarest and most sought of collector's gems. http://en.wikipedia.org/wiki/Cuprite

also the effect of detector counting error. This research develops a methodology which is robust with respect to mid-link sinks and sources, and detector counting error.

iii. *Exit movement specific travel time estimation:* This research provides travel time for different exit movements on the link, and also for a route. Existing models are applicable for average link travel time which on urban networks can be significantly different from travel time on different exit movements associated with the link.

iv. *Integration of probe information for better accuracy and reliability*: Most of the existing models either consider probe data or detector counts. This research integrates both the data and the issues (such as, detector counting error and low number of probe samples) related with individual data are resolved.

1.8 Practical relevance

The practical applications of this research can be summarized as follows:

i. *Performance evaluation of the system and Level Of Service (LOS) of the intersection*: Excess travel time is an important network performance measure. It is the criteria for the estimation of LOS of the intersection. Network-wide performance evaluation provides information to the traffic operators to identify critical junctions in the network for which traffic management and strategic measures can be applied to increase the efficiency of the network. This research can be applied to estimate the network wide performance of the system and LOS of different intersections.

ii. *ITS applications:* The travel time estimates from this research can be used for Intelligent Transportation Systems (ITS*)* applications such as, Advanced Traveler Information System (ATIS). The real-time travel time information can be provided to the users through internet and other mediums. The information has the potential for spatial and temporal dispersion of congestion.

iii. *Feedback to signal controller to optimize its parameters*: Most of the adaptive traffic signal control algorithms optimize its parameters based on objective functions defined in terms of “key parameters” such as, delay and number of stops at intersections for SCOOTS (Hunt et al., 1981) and Degree of Saturation

(DS) value for SCATS (Lowrie, 1990). Travel time estimates from this research can act as a feedback to the controller to optimize its parameters and hence increase the effectiveness of the control algorithm. Moreover, CAREEN[2] (Asano, 2004), an adaptive control algorithm developed by University of Tokyo, Japan, generates signal control parameters (green split, cycle time, offset) by minimizing total delay at the intersection obtained from cumulative plots. Similarly, CUPRITE's cumulative plots could be used to adjust the signal timings to minimize delay.

iv. *Short-term travel time prediction*: Historical time series of travel time is a necessary input for any prediction algorithm (such as ARIMA). Integrating CUPRITE with such prediction algorithms should provide better predictions for short-term travel time.

v. *Public Transport Priority Systems (PTPS)*: Public transport priority systems give priority to the public transport (*PT*) (such as public buses) at signalized intersections. PTPS require priority strategies for *PT* vehicles so that they pass the signalized intersection without stopping at the intersections, i.e., provide green time to the *PT* vehicle when it reaches the intersection. For this, its arrival time at intersection is predicted well in advance when it is still at up-stream of the intersection. Therefore, the efficiency of such system is sensitive to the accuracy of the prediction of travel time. Errors in travel time prediction can lead the *PT* vehicle to miss the priority provided to them. CUPRITE has the potential to accurately estimate travel time and can be easily integrated with PTPS for better efficiency and reliability.

1.9 Outline of the dissertation

Figure 1-4 illustrates an overview of the core of this dissertation. Chapter 2 provides the state-of-the-art travel time estimation methodologies for both freeway and urban facilities. Chapter 3 provides fundamental understanding of the travel time estimation using cumulative

[2] Field demonstration of CAREEN, during ITS World Congress 2004, Nagoya, Japan, was performed and CAREEN was compared with in-practice fixed time control signal. According to the comparison, on average there were 20% reduction in travel time of main stream and 5-10% of most of other streams ASANO, M. (2004) Adaptive Traffic Signal Control Using Real-Time Delay Measurement. *Department of Civil Engineering, Faculty of Engineers.* Tokyo, Japan, University of Tokyo.

plots. It explores different models to estimate cumulative plots and finally, sensitivity analysis of the different parameters of the models is performed. Chapter 4 extends the classical cumulative plot estimation technique by integrating it with probe vehicle information and the methodology, CUPRITE, is developed. The chapter concludes by presenting the results of its thorough testing under controlled environment. Discussions on the application of CUPRITE for exit movement specific link travel time and route travel time are provided in Chapter 5. And the results of its validation with field data are provided in Chapter 6. Finally, the main contributions of this research and recommendations for future research are summarized in Chapter 7.

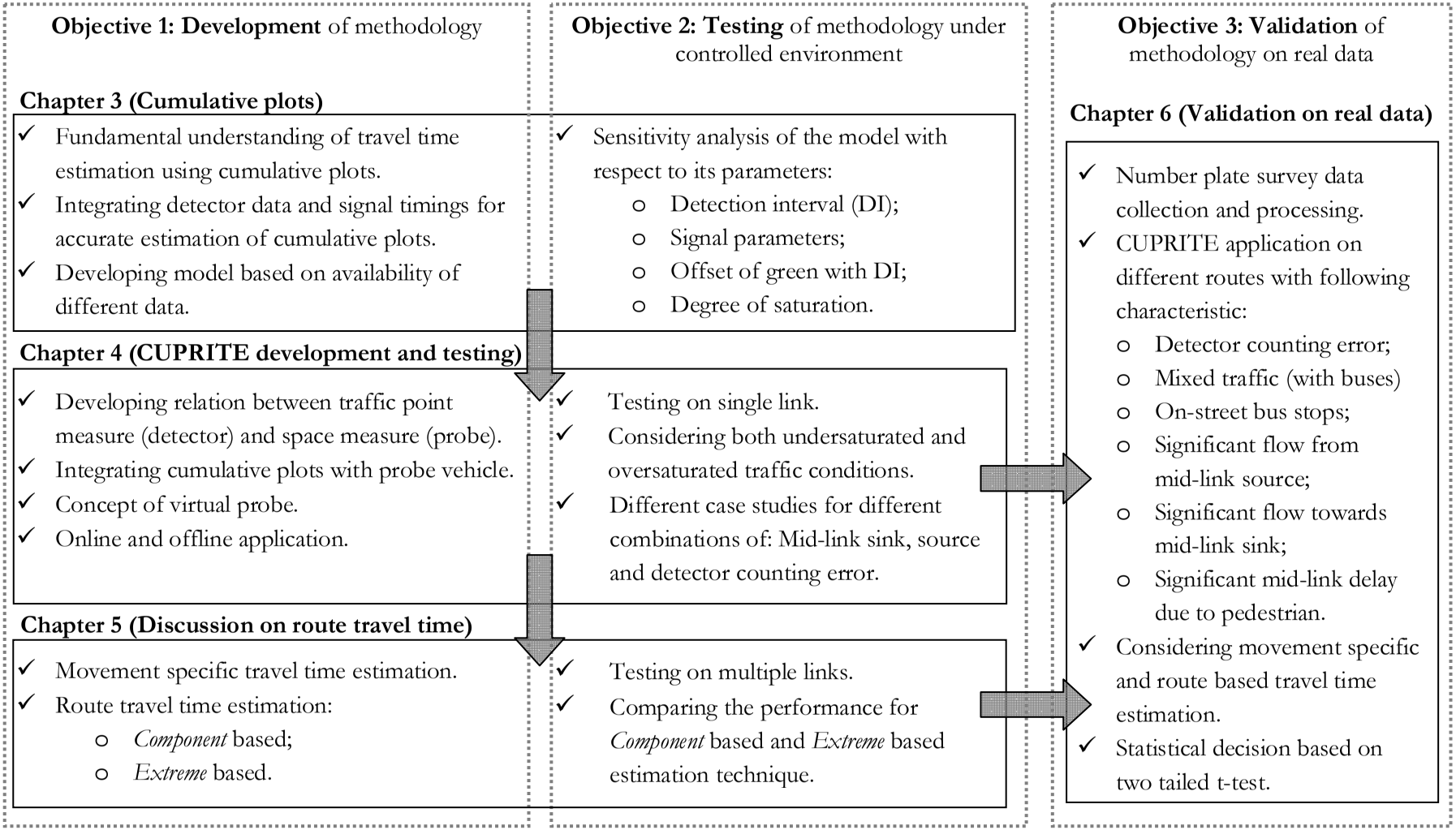

Figure 1-4: Systematic overview of the core of this dissertation.

2 Travel time estimation: A literature review

Travel time estimation has been an active area of research since 1950's. The activities related to ITS have increased the attention of researchers for better and accurate real time estimation of travel time. The goal of this chapter is to review and compare the latest developments in the travel time estimation methodologies for both urban and freeway facilities. The review is organized in chronological order, except for few instances where the order is altered for continuity of discussion.

2.1 Travel time estimation techniques

Advancement of technology has resulted in different traffic data retrieval systems from traditional road sensors embedded in the pavements to advanced electronic systems onboard a vehicle, such as Vehicle Information and Communication Systems (VICS, 2008). These data retrieval systems can be broadly categorized into two categories: fixed sensors; and mobile sensors.

Fixed sensors, such as inductive loop detectors provide traffic information at the specific location on the network whereas, mobile sensors such as probe vehicle provide data for the entire journey of the vehicle. Based on the type of data available different techniques are applied to estimate average travel time for all the vehicles traversing the road. Moreover, the availability of data from different systems provide avenue for application of data fusion techniques for more reliable and robust travel time estimation. Therefore, this chapter classifies different travel time estimation models as follows:

i. Fixed sensor based;

ii. Mobile sensor based; and

iii. Data fusion based.

2.2 Fixed sensor based

Fixed sensors, such as inductive loop detectors, ultrasonic detectors, microwave detectors etc. are installed at a fixed location and hence can provide continuous temporal traffic characteristics only at a fixed point and not the spatial behavior of traffic. Loop detectors are the oldest and widely used data sources mainly because they can provide vehicle flow (counts) which is one of the basic parameter for planning, design and operation of roadway facilities. In addition to flow they can also provide occupancy[3]. Literature is abundant with models ranging from naïve regression to advanced neural networks to relate detector data to travel time estimates.

Here, the models based on fixed sensor data are categorized into:

i. Regression based (Section 2.2.1);
ii. Queueing theory based (Section 2.2.2);
iii. Traffic flow theory based (Section 2.2.3);
iv. Pattern recognition based (Section 2.2.4);
v. Time series analysis (Section 2.2.5);
vi. Neural Networks based (Section 2.2.6);
vii. Probabilistic models (Section 2.2.7); and
viii. Automatic Vehicle Identification (AVI) technology (Section 2.2.8).

2.2.1 Regression based

Wardrop (1968) had defined regression equation (2.1) for average journey speed (v, unit: mi/h) in central urban areas as a function of: average traffic flow (q, unit: pcu/h); width of carriageway (w, unit: ft); number of controlled intersections per miles (f); and average proportion of effective green time (λ). He found that journey speed is inversely proportions to number of signalized intersections per unit distance. And for a given number of intersections, the speed is largely defined by the traffic intensity[4].

[3] In addition to flow and occupancy different sensors can provide speed, though not measured directly. Speed can be estimated from a dual loop detectors placed at known distance apart or with a single loop using algorithm based on average vehicle length.

[4] Traffic intensity is defined as ratio of flow to carriageway width (unit: pcu/h/ft)

$$\frac{1}{v} = \frac{1}{31 - \frac{140}{w} - 0.0244\frac{q}{w}} + \frac{f}{1000 - 6.8\frac{q}{\lambda w}} \quad (2.1)$$

Gault (1981) has defined following two models based on simulated data to estimate travel time from detectors at signalized arterial. The optimum detector location for both the models is reported to be 40 m upstream of the stop-line.

i. *Arrival Time* model: is extension of Gipps (1997) work that predicts a vehicle travel time (*T*) as a function of the time when the vehicle arrives at the detector and the detector occupancy just prior to the departure of the vehicle (2.2). This model often underestimates travel time and could not be applied for situation where average occupancy was higher than 50%.

$$T = (1-\delta)a(rt - (C - G + lag) + \delta g^{1.6} + K \quad (2.2)$$

Where:

a, *g* and *K* are regression coefficients defined in terms of linear combination of: free flow travel time of the link (Termed as undelayed link travel time by Gault.); degree of saturation for the approach to the traffic stream; and offset between the upstream and downstream signals;

rt is the register time (in seconds) that is defined so that, on average, undelayed vehicle which pass over the detector at register time zero just reach the stop-line as the signal turn red;

G and *C* are signal green time and cycle time, respectively;

$\delta = 0$ if $rt \leq R$ else $\delta = 1$; *R* is signal red time; and

Lag is the average time for an undelayed vehicle to travel from the detector to the stop-line.

ii. *Occupancy* model or *British* model: defines a linear regression relationship (2.3) between average detector occupancy (*O*) and link average travel time (t_{avg}). The linear relationship is applicable only for occupancy less than 70%.

$$t_{avg} = aO + b \quad (2.3)$$

Where: *a* and *b* are regression coefficients defined in terms of linear combination of: free flow travel time of the link; degree of saturation for the approach to the traffic stream; and ratio of signal green split at upstream and downstream intersections.

Gault has evaluated the performance of the above models using simulated data and 20 min detector aggregation period. It was found that *Occupancy* model performs slightly better than the *Arrival Time* model. Gault has also emphasized on the importance of using the correct value of desired speed (Free flow travel time depends on the desired speed.) for the models application.

Young (1988) also observed a linear relationship between average delay per vehicle and average occupancy per vehicle per detector for a signalized junction. The relationship is valid only if the detectors are far upstream of the stop-line and queue clears the detector during the green phase. He did not provide any calibrated model but emphasized on the role of detector layout for the applicability of the above linear relationship.

Sisiopiku and Rouphail (1994a) have provided a review of models for travel time estimation based on detector data. The paper can be a good complementary reading for review of the detector output based models introduced before year 1993.

Sisiopiku et al., (1994) have analyzed the relationship between through-movement link travel time and detector flow and occupancy (average for 15 min). They found that:

i. Travel time is independent of both flow and occupancy under low traffic demand;

ii. Percentage occupancy is a better predictor of link travel time than traffic flow; and

iii. Travel time is linearly related to occupancy in the range of 17% to 60%, approximately. For occupancy below 17% travel time is independent of occupancy values and for occupancies above 60% conclusion cannot be drawn as real data was not available.

They conclude that for a mid-link detector, with queue that does not persist over a detector location, a regression relationship can be fitted for certain ranges of occupancies to obtain link travel time.

Sisiopiku and Rouphail (1994b) have also defined a simple travel time (t) estimation model, *Illinois model* (2.4), as a linear combination of free-flow travel time (t_f) and delay. The delay (2.4) is expressed in terms of: ratio of the distance between the detector setback from the stop-line to link length (dl); detector occupancy (O); and green split (g).

$$t = t_f + delay \tag{2.4}$$

$$delay = \beta_0 + \beta_1 dl + \beta_2 O + \beta_3 g \tag{2.5}$$

Where: β_o, β_1 and β_2 are regression coefficient.

Zhang (1999) has proposed a journey-speed ($\overline{u_c}$) model (2.6), named *Iowa* model, as a linear combination of two speed estimated: a) average speed ($\overline{u_{V/C}}$) (2.7) from non linear regression of critical volume to capacity (V/C) ratio; and b) average speed ($\overline{u_{q/O}}$) (2.8) from loop detector flow (q) and occupancy (O) measurements.

$$\overline{u_c} = \gamma \overline{u_{V/C}} + (1-\gamma)\overline{u_{q/O}} \tag{2.6}$$

Where $0 \leq \gamma \leq 1$; $\gamma = 0$ for congested traffic and $\gamma = 1$ for light traffic.

$$\overline{u_{V/C}} = u_f - \alpha e^{\beta V/C} \tag{2.7}$$

$$\overline{u_{q/O}} = 0.379 \frac{\sum_i q}{\sum_i O} \tag{2.8}$$

Where: 0.379 is a constant converting occupancy to density;

α and β are calibration parameter; and

u_f is free flow speed.

Zhang has calibrated *Iowa* model with real data and has compared it with *British* model (2.3) and *Illinois* model (2.4). All the three models perform well at low speed. At high speed *Iowa* model performs better than the other two, though *British* model performs better than *Illinois* model. It was also found that none of the three models performs well during transition traffic state.

Xie et al., (2001) have provided a model, named *Singapore* model, to estimate average speed for a link defined from upstream intersection down to 40 m to 50 m from the downstream intersection. The model simply considers travel time (2.9) as a linear combination of cruise

time and delay. Cruise time (2.10) is the ratio of the link length (L_1) and maximum of the speed (u_{det}) obtained from the detectors at the upstream and downstream of the link. Note that the link is not between two intersections; it starts from the upstream intersection and ends 40 m ~ 50 m (=L_2) upstream of the downstream intersection.

$$Travel\,time = Cruise\,time + Signal\,Delay \tag{2.9}$$

$$Cruise\,time = \frac{L_1}{u_{\det}} \tag{2.10}$$

Delay is defined as a function of Webster deterministic delay equation (For Webster delay model refer to equation (2.14).). Webster delay equation is the total delay near the stop-line of intersection. The delay defined in equation (2.11) is the proportion of total delay in the link of interest.

$$\begin{aligned} Signal\,Delay &= 0.9\varphi\left[\frac{C(1-\lambda)^2}{2(1-\lambda x)} + \frac{x^2}{2q(1-x)}\right] \\ \varphi &= \begin{cases} \dfrac{(C-G)q - L_2}{(C-G)q}, if\ (C-G)q \geq L_2 \\ 0, if\ (C-G)q < L_2 \end{cases} \end{aligned} \tag{2.11}$$

Where: C and G are downstream intersection signal cycle length and green time, respectively;

x is degree of saturation at downstream intersection; and

q is flow measured at upstream intersection.

Xie et al., have compared *Singapore* model with *British* (2.3), *Iowa* (2.6) and *Illinois* (2.4) models. Their results indicates that the performance of all the four models is more or less the same (RMSE < ±5 km/h) under moderate to congested traffic conditions. They argue that *Singapore* model has slightly better accuracy than that of the *British* and *Iowa* models and is slightly lower than the *Illinois* model. However, being calibration-free, their model is simple for practical implementation.

Rice and Van Zwet (2004) have observed a linear relationship between future travel time and current status travel time using the real data from Los Angeles freeway. The slope and Y-intercept of this relationship may change subject to time of the day and time until departure, but linearity persists. Based on this observation they have defined a linear regression model with time varying coefficients (TVC) for travel time estimation on freeways.

Zhang and Rice (2003) have observed that the quality of the training data set used to estimate TVC have significant impacts on the prediction accuracy.

Comments: Regression relationship developed for mid-link detector should not be applied for stop-line detectors. Similarly, the regression relationship obtained for through exit movement is not necessary valid for other exit movements. For an effective regression model, effect of parameters such as detector location, effective green time, progression quality, link length, opposing flow for permissive phasing, traffic composition etc. should not be overlooked. The model calibrated for a specific condition should not be generalized without further testing and calibration. Generally regression models are site specific and their transferability is limited. Moreover, if regression models parameters are calibrated with simulated data, then it is necessary that simulation model[5] should be properly calibrated with field observations.

2.2.2 Queueing theory based

Queueing theory is a tool to analyze congested systems. Most of the mathematical queueing theory models are developed for steady-state but stochastic (random) systems. However, real queues are dynamic for instance, congestion during peak period and researchers have developed analytical models capable of considering dynamic variations in arrival and service rates. Here, the queueing theory models are differentiated into:

i. *Static* models that average steady-state stochastic traffic situation; and

ii. *Dynamic* models that consider change in traffic situations over time. These models are analytical deterministic models and are more appropriate for real time applications.

2.2.2.1 Static models

2.2.2.1.1 Volume-delay functions

Initial motivation for travel time estimation models were their application in considering congestion effects in conventional traffic assignment step used in four-step transportation planning methods. Travel time functions (also known as speed/flow curves; congestion

[5] Simulation model is a controlled environment and has the potential to provide rich quantity of data for different traffic conditions and patterns but the simulation results are sensitive to the simulation model calibration parameters. Field observations are from an uncontrolled environment and it is real world conditions.

functions or volume-delay functions) such as: Bureau of Public Roads (2.12) (BPR, 1964); Davidson's function (2.13); modified Davidson's function (Akçelik, 1978, Tisato, 1991); conical-volume delay functions (Spiess, 1990); and Akcelik function (Akçelik, 1991) etc. are based on developing relationship between travel time (or cost) on a road link and traffic intensity (flow/capacity ratio).

$$\overline{TT} = t_{ff}(1+\alpha(\frac{q}{c})^{\beta}) \tag{2.12}$$

Where: $\overline{TT}$, t_{ff}, q and c are average travel time, free-flow travel time, flow and capacity for the link, respectively;

α and β are calibration parameters.

$$t = t_0(1+J_D(\frac{X}{1-X})) \tag{2.13}$$

Where: t = average travel time per unit distance (s/km);

t_o = free-flow travel time per unit distance (s/km);

J_D = a delay parameter (or 1 – J_D = a quality of service parameter);

$x = q / c$ = degree of saturation;

q = demand (arrival) flow rate (in veh/h); and

c = capacity (in veh/h).

Webster delay model (2.14) (Webster and Cobbe, 1966) is the earliest and most famous model for estimating average deterministic delay at undersaturated signalized intersection. It estimates average intersection delay per vehicle as a function of signal parameters (cycle length, green split), demand (arrival flow rate) and supply (capacity).

$$\begin{aligned} D &= \sum_{ij} D_{ij}^{W} = \sum_{ij} \frac{(1-u_i)^2 c}{2(1-u_i\rho_{ij})} + \frac{\rho_{ij}^2}{2q_{ij}(1-\rho_{ij})} - 0.65(\frac{c}{q_{ij}^2})^{1/3}\rho_{ij}^{2+5(g_i/c)} \\ \rho_{ij} &= \frac{q_{ij}}{s_j u_i};\ u_i = \frac{g_i}{c} \end{aligned} \tag{2.14}$$

Where: D is average delay per vehicle;

D_{ij} and q_{ij} is the average delay and arrival flow rate, respectively for signal phase i and traffic stream j;

g_i and u_i is the green time and green split for signal phase i;

c is the signal cycle length; and

s_j is the saturation flow rate for traffic stream j.

Webster delay model was developed using traffic simulation on a single lane approach to a signalized intersection. The model has three terms: a) the first one corresponds to the average delay per vehicle under uniform arrival (deterministic delay); b) the second term attributes to the probability that sudden fluctuations in vehicle arrival may temporary cause oversaturation at the intersection; and c) the last part is the adjustment factor to account for the correction for the curve fitting to the simulated average delay per vehicle due to the traffic signals.

Webster delay model is the basis of all the subsequent delay models as many researchers such as, Akçelik (Akçelik, 1988, Akcelik and Rouphail, 1993, Akcelik and Rouphail, 1994) and Highway Capacity Manual (TRB, 2000, TRB, 1998) follow Webster's work and proposed delay models to suit different field conditions. For instance, vehicle arrival in platoon is considered by Akçelik and Rouphail (1994) by extension of deterministic delay models to consider the effect of platoon.

Comments: The simplicity of these function make them favorable candidate for transport planning and policy analysis where the analysis is done using average demand within a period (e.g., an hour). The variability of traffic demands within a given control period is not fully considered. These models are not suited for ITS applications where more accurate and reliable analysis for shorter period, of order of signal cycle time, in real time is required.

2.2.2.1.2 Japanese Sand-glass model & Delay-time model

Takaba et al., (1991) have developed following two models: sand-glass model; and delay-time model.

Sand-glass model

Sand-glass model is based on the analogy of vehicle on the link with sand in the glass. Vehicle in the queue is considered similar to sand level in the glass and discharge rate at critical intersection is considered similar to down flow rate at the bottom of the glass. Travel time is defined by equation (2.15).

$$TT = \frac{N_q}{Q} + \frac{(L - L_q)}{v_{ff}} \tag{2.15}$$

Where: TT is the travel time;

N_q and L_q are number of vehicles in the queue and queue length, respectively;

L and v_{ff} are the length and free-flow speed of the link, respectively; and

Q is the link capacity (discharge flow volume).

Takaba et al. (1991) have defined a procedure for estimating number of vehicles in the queue. For this density (k) is defined as inverse of average spacing (2.16):

$$k = \frac{N_q}{L_q} \tag{2.16}$$

Density is approximated as linear function of flow (Q) as:

$$k = k_j - aQ \tag{2.17}$$

Where k_j is the jam density and a is regression coefficient.

Equation (2.15) is rewritten by substituting equations (2.16) and (2.17) as follows:

$$TT = \frac{k_j L_q}{Q} - aL_q + \frac{(L - L_q)}{v_{ff}} \tag{2.18}$$

The model (2.15) requires estimation of queue length (L_q) and number of vehicles in the queue (N_q) which is practically difficult to obtain. The procedure (equations (2.16) and (2.17)) suggested by Takaba et al. for estimating number of vehicles in the queue requires regressive regression on link capacity and density parameters.

Delay-time model

Delay-time model defines travel time (TT) in the congested section as the sum of delay time (D) and running time (F). Delay time is defined by equation (2.19) and running time by equation (2.20).

$$
\begin{aligned}
&D = d * m \\
&Where: \\
&\quad d = C - G \\
&\quad\;\; = G - C * Q / s \\
&\quad m = \frac{k_j * L_q}{Q * C}
\end{aligned}
\tag{2.19}
$$

$$F = \frac{L_q}{v} + (\frac{L - L_q}{v_f}) \tag{2.20}$$

$$
\begin{aligned}
TT &= D + \frac{L_q}{v} + (\frac{L - L_q}{v_f}) \\
&= \frac{k_j L_q}{Q} - L_q(k_j * s - 1/v) + (\frac{L - L_q}{v_f})
\end{aligned}
\tag{2.21}
$$

Where: d is the delay time per signal cycle;

m is the number of cycles while vehicles runs through the congested section;

C, G and s are signal cycle time, effective green time, and saturation flow rate, respectively;

Q is the link capacity (discharge flow volume).

L_q is queue length;

L is link length;

v is running speed; and

TT is travel time on the link

The first two terms in the equation (2.21) is the average travel time in congested section and last term is average travel time in uncongested section.

Comments: The sand-glass (2.18) and delay-time model (2.21) are the same when the regression coefficient a for sand-glass model is equal to (k_j*s – $1/v$).

Though the above two models are simple to understand, but the required parameters are difficult to obtain and requires extensive calibration for reasonable accuracy. Once calibrated, the models can be applied for transportation planning application. However, the stochastic variations in the parameters make them unfavorable for real time application.

2.2.2.1.3 Other stochastic queueing theory models

The above discussed delay models provide average delay and few researchers have focused on stochastic delay models to provide the respective statistical distribution instead of the average value. Brilon and Wu (1990) have developed a stochastic delay model based on Markov chains. The model provides average delay per vehicle at fixed signal control under Poisson or non-Poisson flow conditions. Heidemann (1994) derived the statistical distributions of queue length and delay at fixed signal control under Poisson arrival process. He developed the probability generating function of the queue length distribution, from which the Laplace-transformation of the delay distribution is obtained.

Comments: In stochastic queuing application, there is one basic underlying assumption that traffic facility in question operates under steady-state condition over the entire time period of interest. Steady-state assumption implies that the probability distribution function for the number of vehicles in the system at time *t*, does not vary with time (or in other words, the probability distribution function is independent of initial conditions at the start of the operation.). Strictly speaking, such assumptions are often unrealistic (For instance, the duration of peak periods encountered in practice is usually not long enough for the queues to settle down in the equilibrium.). If the time period of interest initiates with or includes a relaxation period then clearly the system is not continuously operating at steady-state. However, if the relaxation time is relatively small compared to total analysis period then the steady-state assumption violation might be considered insignificant. The validity of the steady-state assumption with respect to traffic flow facilities can be questionable under different periods of interest and relaxation time. However, in literature there is very little discussion on the relevance of the steady-state assumption or relative relaxation time. Son et al. (1995) had highlighted the issues of concern with regard to steady-state assumption by evaluating the appropriateness of the assumption based on simulation for highway queuing system. They found that the steady-state assumption may not always be reasonable and suggested that prior to exploiting stochastic queuing techniques, investigation concerning the steady-state tendencies of the facilities may be warranted.

Moreover, the basic limitation of the above mentioned models is the inability to predict delay for traffic conditions that are different from those assumed in the models. For example, unusual flow patterns which do not follow the traditional statistical distributions cannot be modeled.

2.2.2.2 Dynamic models

2.2.2.2.1 TRANSYT and SCOOT models

TRAffic Network StudY Tool (TRANSYT) and Split, Cycle and Offset Optimisation Technique (SCOOT) are developed by Transport Research Laboratory, UK for signal control optimisation. TRANSYT is for offline optimisation of fixed time coordinated traffic signal timings. SCOOT, evolved from TRANSYT, is for online optimisation and is able to adapt signal parameters considering the real time traffic flow parameters.

The basic optimisation model is same in both the tools. The objective function is to minimize network *performance index* expressed in terms of weighted links average queues (delay) and number of vehicles stops.

Robertson and Bretherton (1991) have explained the TRANSYT and SCOOT models. The models consider *cycle flow profiles* (CPF) at the upstream entrance of the SCOOT/TRANSYT link. CPF defines the demand for the link and is the average vehicle flow during each part of the cycle time of the upstream signal (1 s to 5 s for TRANSYT and 4 s for SCOOT.). This average flow in each part of the cycle is average of many cycles (e.g., peak hour in TRANSYT and is fixed to 4 s in SCOOT.). The growth and clearance of the queue (delay) is analytically estimated by considering CPF, link cruise speed, platoon dispersion, saturation flow rate and signal timings at downstream intersection (*see* Figure 2-1).

Comments: The models can be considered as identical to the classical analytical procedure of using cumulative plots described in Section 1.6.2. CPF is obtained by the detectors installed at the upstream entrance of the link (Figure 2-1). The performance of the model for travel time estimation with respect to the detector counting error and mid-link sources and sinks is not documented in the literature.

The objective of TRANSYT and SCOOT is to optimize signal parameters by considering total network delay and not to estimate accurate travel time (delay) for each link. Carden et al., (1989) have analyzed the SCOOT model accuracy through a case study on 17 links at Southampton, UK. They found that on average SCOOT delay estimates were within 5% of measured delay, though a large variability (50% coefficient of variation) in the measured delay between cycles were observed. The error in the SCOOT delay estimate was also variable with an average standard deviation of 80% of the measured delay. Further studies confirm that SCOOT overestimates delay in congested periods.

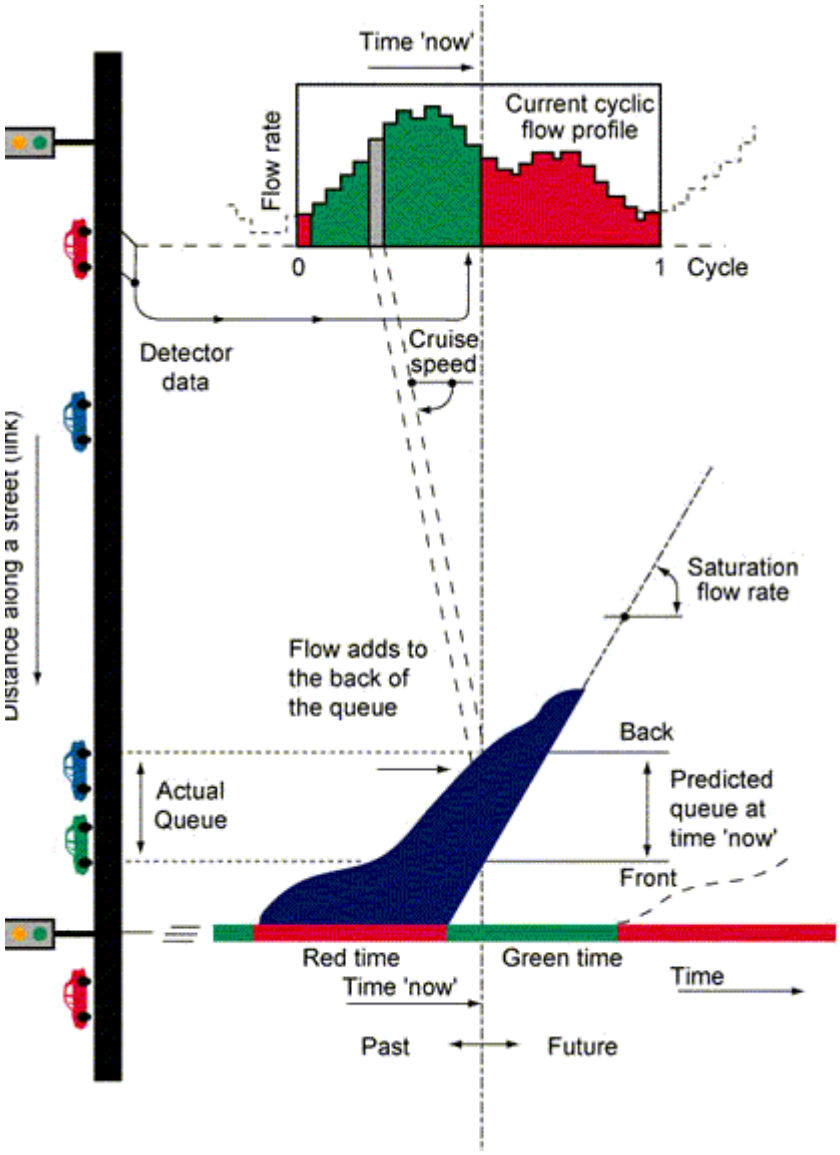

Figure 2-1: Representation of SCOOT model (source: www.scoot-utc.com).

2.2.2.2.2 Highway Capacity Manual 2000 delay model

Highway Capacity Manual 2000 (HCM 2000) provides average control delay (2.22) experienced by all vehicles that arrive in the analysis period, including delays incurred beyond the analysis period when the lane group is oversaturated.

$$d = d_1(PF) + d_2 + d_3 \tag{2.22}$$

$$d_1 = \frac{0.5C(1-\frac{g}{C})^2}{1-\left[\min(1,X)\frac{g}{C}\right]} \tag{2.23}$$

$$d_2 = 900T\left[(X-1)+\sqrt{(X-1)^2+\frac{8kIX}{cT}}\right] \tag{2.24}$$

$$d_3 = \frac{1800Q_b(1+u)t}{cT} \tag{2.25}$$

Where:

d = average control delay per vehicle (s/veh) that arrive during the analysis period. This includes movements at slower speeds and stops on intersection approaches as vehicles move up in queue position or slow down upstream of an intersection;

d_1 = uniform control delay assuming uniform arrival (s/veh) (2.23);

PF = uniform delay progression adjustment factor. This accounts for effects of signal progression. (Refer to equation (2.26), where P is proportion of vehicles arriving during green phase, f_{PA} is supplemental adjustment factor for platoon arriving during green phase;

$$PF = \frac{(1-P)f_{PA}}{1-\frac{g}{C}} \tag{2.26}$$

d_2 = incremental delay to account for effect of stochastic arrivals and oversaturation queues. This is adjusted for duration of analysis period and type of signal control. This delay component assumes that there is no initial queue for lane group at start of analysis period (s/veh) (2.24);

d_3 = initial queue delay, which accounts for delay to all vehicles in analysis period due to initial queue at start of analysis period (s/veh) (2.25);

C = signal cycle time;

g = signal green time for the lane group;

c = lane capacity (veh/h);

T = duration of analysis period (hour);

X = lane group flow by capacity ratio (v/c) or degree of saturation;

k, I = incremental delay calibration factors that are dependent on controller settings. k is a coefficient that accounts for randomness is arrivals ($0 < k < 0.5$). If variance of the arrival rate equals the mean arrival rate then k equals 0.5;

I is a coefficient that accounts for the metering effect of the upstream signals. If there is no metering effect then I equal unity. I is given by equation (2.27)

$$\begin{aligned} I &= 1 - 0.91X_u^{2.68} \quad if\ X_u \le 1 \\ &= 0.09 \qquad\qquad\ \ if\ X_u > 1 \end{aligned} \tag{2.27}$$

Where X_u is the degree of saturation at upstream intersection and is approximated as v/c ratio of upstream through movement.

Q_b = initial queue at start of period T (vehicle);

t = duration of unmet demand in T (hour);

u = delay parameter.

Comments: The HCM delay formula is well used delay formula is literature and can be applied for real time application, given that one can obtain the parameters defined above. Practically it is difficult to obtain the parameters such as Q_b and t in real time.

2.2.3 Traffic flow theory based

Lighthill, Whitham and Richards (LWR) (Lighthill and Whitham, 1955, Richards, 1956) have developed macroscopic hydrodynamic traffic flow theory using the analogy between traffic flow and fluid flow. They derived kinematic waves that satisfy first order partial differential equation which is also termed as *principle of conservation of vehicles* (2.28).

$$\frac{\partial q(x,t)}{\partial x} + \frac{\partial k(x,t)}{\partial t} = 0\,(or\ traffic\ generation\ rate) \tag{2.28}$$

Where: $q(x,t)$ and $k(x,t)$ is traffic flow (veh/h) and density (veh/km), respectively at location x at time t.

In practice, the model (2.28) is discretised in time and space, by considering time steps of Δt and dividing the freeway in sections of length Δx. For numerical stability of solutions equation (2.29) should be satisfied for all sections in network.

$$\Delta x > v\Delta t \tag{2.29}$$

Where: v is the speed in the section.

2.2.3.1.1 Nam and Drew model

Nam and Drew (1999) have developed analytical model for travel time estimation on freeways link. The link is defined between two detector locations and without any mid-link on-ramp or off-ramp. The model considers cumulative plots (from detector at upstream and downstream of the link) and principle of conservation of vehicles (between the two detector locations). Cumulative plots, at the location of the detector take into account the stochastic variations in the flow for real time application. The principle of conservation of vehicles (2.28) derives the flow-density-speed relationship as the rate of change of flow over distance is equal to the rate of change of density over time (2.30).

If the vehicles are conserved then, difference between the cumulative counts at two locations at time *t* defines number of the vehicles traversing the link at time *t*. The density (*k*) is the ratio of number of vehicles in the link and link length. Total travel time from upstream to downstream is the area between the cumulative plots at upstream and downstream. Nam and Drew have considered average flow at upstream and downstream. Hence, they have assumed trapezoidal area between the plots. This area is represented as a function of flow and density and is used to derive the equation (2.31) for average speed.

$$\frac{q(x_u,t)-q(x_d,t)}{\Delta x}=\frac{k(t+\Delta t)-k(t)}{\Delta t} \tag{2.30}$$

$$\begin{aligned} u(t_n) &= \frac{2*q(x_u,t_n)*q(x_d,t_n)}{q(x_u,t_n)*k(t_{n-1})+q(x_d,t_n)*k(t_n)} \quad if \quad Q(x_d,t_x) > Q(x_u,t_{n-1}) \\ &= \frac{2*q(x_d,t_n)}{k(t_{n-1})+k(t_n)} \quad if \quad Q(x_d,t_n) \le Q(x_u,t_{n-1}) \end{aligned} \tag{2.31}$$

Where: *q(x,t)* is the flow at location *x* at time *t*;

k(t) is the density at time *t*;

Δt are time interval when the first vehicle have entered the upstream and last vehicle have departed from downstream (The flow (*q*) is defined as the counts during Δt time interval);

Δx is the distance between the two locations;

x_u and x_d are the upstream and downstream detector station, respectively;

$u(t_n)$ is the speed at time interval t_n; and

Q(x,t) are cumulative counts at location *x* at time *t.*

Comments: Nam and Drew (1999) have validated the model on real data (From Queen Elizabeth Way in Toronto, Canada.) where performance of the model is evaluated by comparing it with true travel speed. They have documented RMSE to be close to 10%. They have assumed the true travel speed as the average of the speed obtained from upstream and downstream detectors. The way they have estimated the true travel speed is only valid when there is no congestion, or when traffic queue is half way between upstream and downstream of the link. The performance evaluation of the model does not differentiate between congested and non congested traffic condition. The performance evaluation of the model with better knowledge of true speed such as use of AVI data etc. should provide concrete model validation.

The basis of the equation (2.31) is the difference of cumulative counts at upstream and downstream of the links which in turn are sensitive to *relative deviation amongst cumulative plots*. Even in the absence of on-ramp and off-ramp there are chances of relative deviation due to detector counting error and for real application of the model detector counting error issue is to be resolved. Nam and Drew (1999) have found that the upstream counts were 3% higher than downstream counts. To account for this difference they have applied volume adjustment factor for each half hour and flow measurements at downstream location were multiplied by the volume adjustment factor. The explanation of how the volume adjustment factors are determined was not documented.

The model is limited to confined link of freeway (absence of on-ramp and off-ramp) under FIFO queueing discipline and cannot be applied as it is on urban networks due the following reasons:

i. Principle of conservation of vehicle is generally not valid on urban network due to mid-link sources and sinks etc.

ii. Due to traffic signals the flow is interrupted and equation (2.31) is not applicable. Equation (2.31) is derived considering trapezoidal shape between the two cumulative plots (For data aggregation interval (Δt) to be more than the free flow travel time of the link.). On urban network the shape of the cumulative plot highly depends on the location of the detector from the stop-line and stop-and-go running conditions at the trapezoidal shape is no longer valid.

2.2.3.1.2 Oh et al. model

Oh et al., (2003) have applied LWR hydrodynamic traffic flow theory to define travel time on a freeway section (2.32) as a function of section density (*k*, (2.33)) and flow at upstream and downstream of the section. The density and flow are estimated based on the counts from the detectors at each entrance and exit of the section.

$$tt_s = \frac{\Delta x}{v} = \frac{\Delta x k}{q} = \frac{\Delta x[k(t_{n+1}) + k(t_n)]}{[q(x_u, t_n) + q(x_d, t_n)]} \tag{2.32}$$

$$k(t_{n+1}) = k(t_n) + \frac{\Delta t}{l\Delta x}[lq_u(t) + l_{on}q_{on}(t) - \alpha(lq_d(t) + l_{off}q_{off}(t))] \tag{2.33}$$

Where: Δx is the length of the freeway section;

tt_s is section density based travel time;

q_u, q_d are flow at upstream and downstream of the section, respectively;

l is the number of lanes on the freeway section;

q_{on}, q_{off}, l_{on}, l_{off}, are flow and number of lanes for on ramp and off ramp, respectively;

α is the calibration parameter to take into account the systematic errors in detector counting.

Total vehicles inflow and outflow to the section should be identical for a larger period (Say six hours, from a free flow (at 2 p.m.) to next free flow traffic condition (8 p.m.).). α is obtained as the ratio of total cumulative inflow and cumulative outflow for a longer period as:

$$\alpha = \frac{\sum_t [lq_u(t) + l_{on}q_{on}(t)]}{\sum_t [lq_d(t) + l_{off}q_{off}(t)]} \tag{2.34}$$

The initial section-density is defined for homogeneous (Indicated by approximately equal values of occupancy at upstream and downstream detectors.) and uncongested traffic condition (Indicated by approximately free flow speed at upstream and downstream detectors.). Density is the function of average vehicle length and occupancy of the detector.

Comments: The model is applicable only for freeway sections between two detectors and it requires detectors on every on ramp and off ramp. The correction for the detector counting error (α, (2.34)) assumes that the error is consistent (systematic) for a large period. However, practically the counting error is not consistent for instance, detectors have tendency to

undercounts when vehicles are closely spaced. Hence, the estimation of section density during small estimation intervals (say each 5 min) is not correct resulting in error in section travel time estimate.

2.2.4 Pattern recognition based

Traffic flow parameters such as speed, occupancy and flow on spatial and temporal scale can define traffic pattern. Different techniques such as k-Nearest neighbor (k-NN) and cross-correlation are applied to match traffic patterns for travel time estimation.

2.2.4.1 k-Nearest Neighbor (k-NN)

The k-nearest neighbor, a non-parametric regression, technique is amongst the simplest of all machine-learning algorithms. In pattern recognition, the method identifies objects based on closest training example in the feature space. The basic idea behind the technique is if, historical observations of input and output variables are available then, matching the current set of input variables with historical database can provide a set of *k* historical observations that are similar to the current input. The current output can be then defined as a function of the values from the obtained set of *k* historical observations.

For travel time estimation, the technique is applied based on the assumption that traffic scenarios similar to the present traffic condition may have occurred before. Therefore, the present traffic pattern is compared with the historical database and *k* closet matching patterns (k-NN) are identified.

You and Kim (2000) have applied k-NN technique for travel time forecasting. Their model is based on segregating the original non-linear time series of travel time data into local linear trends. Thereafter, k-NN technique is applied to identify similar past cases compared with the slope of the present case.

Bajwa et al., (2003) have applied the technique on ultrasonic detector traffic data from Tokyo Metropolitan Expressway (MEX). They have identified traffic pattern as a function of distance weighted inverse speed obtained from the detectors. Nearest neighbor are obtained by minimizing the squared difference between the prediction time traffic pattern and historical traffic patterns in the database. The predicted travel time is defined as the average travel time of the *k*-nearest neighbor obtained. They have also applied genetic algorithm to optimize the parameters, such as the value of *k* and weights for traffic pattern (Bajwa et al., 2004) .

Comments: For pattern matching, the current pattern is compared with historical patterns having same day-type and time-type. Thus, any rare incident such as off-peak breakdown may not be captured. It is also assumed that the speed obtained from the detector is conserved along the whole section length. The assumption is valid only if the length of the section is small, and quantity of this assumption decreased during congestion dissipation and buildup. The model is tested on MEX where detectors are at 300 m spacing and performance of the model for longer detector spacing is not evaluated.

The above model is applicable on freeways. Robinson and Polak (2005) has applied k-NN technique on 15 min aggregated flow and occupancy from inductive loop detector data from central London SCOOT system. The database is developed based on the Automatic Number Plate Recognition (ANPR) cameras in the site. They have identified the pattern as a function of weighted flow and occupancy obtained from the detectors. Nearest neighbor is obtained by minimizing the square of the prediction time traffic pattern with historical pattern. Finally, the predicted travel time is defined as median of the *k*-nearest neighbor obtained. The MAPE from the testing of the model at Russell square in central London is reported at around 20%. They have also report that *"the model performed well at low and very high levels of actual travel time"*.

Comments: The basic requirement for the application of k-NN technique is to build historical database of the travel time and the parameters for the traffic pattern over the link. The performance of k-NN highly depends on the selection of its parameters in addition to the quantity and quality of the historical database. The attributes of the traffic patterns (input variables) can be easily stored from the sensors, though it may not be accurate. However, a methodology should be defined to obtain the travel time (output variable) to be stored in the historical database. The errors in the stored travel time values are reflected in the prediction. Robinson and Polak (2005) have tested the k-NN technique on the link where accurate travel time are obtained from ANPR, and traffic patterns are defined by the loop detectors. For potential application of the model, they have identified the use of GPS probe vehicle to define the historical database i.e., the travel time obtained from GPS vehicles to be stored with corresponding flow and occupancy reading from the detector. Probably the proposed potential application is satisfactory for freeways, but for urban environment, significantly larger number of probe vehicles per estimation interval is required as the travel time for each probe highly depends on its delay at intersection and it may not be a representative of the flow of vehicles during the estimation interval. Moreover, Robinson and Polak have defined flow as

an attribute for traffic pattern whereas, Bajwa et al., (2003) has identified that for travel time prediction, flow may not be a good variable for pattern recognition. This is because for a given flow there are two values of speed, one corresponding to free flow and another to congested traffic region.

2.2.4.2 Cross-correlation technique

Cross-correlation is the technique to measure the similarity between two waveforms as a function of time lag applied to one of them. For travel time estimation, the technique has been applied to data from traffic detector at upstream and downstream of the link.

Dailey (1993) has applied the cross-correlation technique to estimate average vehicle travel time between widely separated inductive (single) loops detectors on freeways. The flow at downstream is defined as a linear combination of: a) flow at upstream multiplied by a dispersion factor; b) change in flow due to on-ramp and off-ramp; and c) noise in the data. The cross-correlation is applied to the time series of traffic flow fluctuations about the average flow. Dailey observed that the technique provides reliable results only if there is sufficient correlation between the flows at upstream and downstream stations, i.e., correlation coefficient greater than or equal to 0.4. The criterion is not met for occupancy greater than 15%.

Comments: The model is only for freeways and cannot be applied for urban networks. As mentioned by the Dailey (1993) *"the cross-correlation technique modeled the traffic as fluctuations about a mean that propagated rigidly over the distance between the loops. This assumption of rigid propagation will be violated in high-occupancy or stop-and-go traffic."*

Petty et al., (1998) proposed a model based on platoon matching. They assume that for a given time interval, travel time of different vehicles on a freeway link is from same probability distribution. They estimate the probability distribution, and in particular its mode, from least-square regression on cumulative upstream and downstream arrival processes. For this they had define the flow at downstream detector at time t_d as the flow at upstream detector at time t_u times the probability that the travel time is $t_d - t_u$. They have shown that their model gives comparable results as that of Dailey (1993).

Comments: The model is applicable only for freeway section where platoon can exist i.e., absence of on-ramp and off-ramp. This platoon machining technique is unlikely to work in urban environment where the signals can induce significant fluctuations in the flow.

2.2.4.3 Vehicle reidentification

Vehicle reidentification technique matches a *vehicle signature* at upstream station and downstream station of a link and thereafter travel time is directly deduced from the difference of arrival time at two stations.

The data from conventional Inductive loop detectors (ILD) is a pulse data (i.e., data value is either "1" or "0" depending on the vehicle presence.). The length of a vehicle can be deduced from the pulse data, specifically from dual loop ILDs. ILD works on the principle of change in inductance due to presence of a vehicle. Advance ILD can provide the time series of changes in inductance, termed as inductance waveform. In literature, the following two indicators for *vehicle signature* are considered:

i. Vehicle length obtained from conventional ILD; and

ii. Inductance waveform from advance ILD.

2.2.4.3.1 Vehicle length as an indicator

Researchers (Coifman, 2001, Coifman and Cassidy, 2001, Coifman and Cassidy, 2002, Coifman and Ergueta, 2003, Coifman and Krishnamurthy, 2007) have applied vehicle reidentification technique considering vehicle length as an indicator for *vehicle signature* for travel time estimation on freeways. For short length vehicle such as passenger cars, the difference in vehicle lengths is small and hence many false positive matches are possible. The confidence in the match is higher if vehicles with long length such as heavy vehicles are considered. Coifman and Krishnamurthy (2007) have proposed a method to estimate the length of the vehicle by both dual loop and signal loop detector given that detector provides accurate pulse type data and for dual loop pulse data is available from both the loops.

Coifman (2001) matches individual heavy vehicle length within a search window define in terms of lower and upper bound for expected free flow travel time. The algorithm reidentifies vehicles only during free flow traffic condition, the reidentification ceases once traffic condition is congested and hence it acts as an indicator for free flow and congested traffic condition. For congested traffic condition Coifman and Cassidy (2002) considers platoon of 5-10 vehicles to match sequence of vehicle lengths for vehicle reidentification. For this, platoon should pass both upstream and downstream detectors in the same lane. The platoon is likely to be lost for longer link lengths with lane changing, merging and diverging traffic

behavior. Coifman and Krishnamurthy (2007) have extended the above models to allow vehicle reidentification even when vehicle changes lanes.

Comments: They have not reported the performance of their model in terms of standard statistical indicator such as MAPE. The model depends on the accuracy of the range for vehicle length estimated, which in turn depends on the detector accuracy. The model is developed and is tested for freeway. The application of the model for urban network is complicated due to following:

For a given vehicle length at downstream, there are different potential candidates at upstream. Model identifies travel time by assigning more weights to preceding vehicles with similar travel time (for details refer to (Coifman and Krishnamurthy, 2007)). On freeways, travel time from one vehicle to another during a given time frame does not varies significantly whereas, on urban network the travel time can significantly vary depending its delay at intersection. Moreover, the reidentification is considered for heavy vehicles which are relatively low on urban network.

2.2.4.3.2 Inductance waveform as an indicator

The shape of the inductance waveform depends on various factors (such as the length of the vehicle, speed of the vehicle, the amount of metal in the vehicle, distribution of the metal in the vehicle, height of the vehicle body from the road surface etc.). The inductance waveform has the potential to provide considerable amount of information about the vehicle. hence it has attracted the attention of researchers for number of applications such as estimating vehicle speed from single loop detector (Sun and Ritchie, 1999); vehicle classification (Sun, 2000); and vehicle reidentification (Kwon, 2006).

Sun and Ritchie (1999) have utilized the inductance waveform of a single loop detector data to estimate a vehicle speed from a single loop. They assume that the speed of the vehicle is correlated to rate of change in inductance of the waveform (slew rate). A linear regression model is defined to obtain a vehicle speed from its slew rate.

Sun (2000) has proposed two methods (Self-Organizing Feature Map; and heuristic discriminant algorithm) to classify vehicles into seven predefined vehicle classes. Ritchie et al., (2002, 2005) have demonstrated the potential application of above classification to estimate travel time on urban arterial by comparing the inductance waveform at downstream

detector with different upstream detectors. For this they have applied Probabilistic Neural Network (PNN) and heuristic method to identify the upstream origin of the vehicle.

The above approaches are based on raw inductance output from the detector. The raw inductance output from the detector is the moving average of inductance changes with the window size determined by the loop detection area. The reduction in the moving average effect from the raw inductance outputs should improve the reidentification rate as it exposes more uniqueness of each signature. Kwon (2006) has modeled inductance of loop detector as a convolution of original vehicle signature and loop system function (impulse response of loop detector). As both original vehicle signature and loop system functions are unknown therefore, they have formulated the problem as blind convolution problem.

Comments: The above approaches of advance signal processing are still in initial research states, and further study is needed to increase the accuracy, reliability and reidentification rate. Moreover, for implementation of inductance waveform based algorithm, existing infrastructure should be upgraded with advance detectors with inductance waveform capability and a high bandwidth in the data communication channel.

2.2.4.4 Regression tree

A regression tree is a tool for decision analysis in which data is classified based on its characteristics. A model for making a decision is constructed by recursively partitioning the data into homogeneous regions within which constant or linear estimates are generally fitted. The data is partitioned based on explanatory variables and certain criteria. Logendran and Wang (2008) have applied regression trees algorithm for speed estimation from detector output (volume and occupancy) on freeways. Their methodology included thirteen explanatory variables, categorized in four variable types: traffic flow; incident related; weather data; and time of day. They have used speed as a proxy for travel time on freeway segment between two detector locations, assuming speed does not change along the segment.
Comments: The approach is simple, but the development of regression tree requires wide range of accurate historical database.

2.2.5 Time series analysis

Models based on time series analysis such as, auto-regressive integrated moving average (ARIMA) (Hamed et al., 1995, Davis et al., 1990) and state-space model[6] (Kalman Filtering) (Yang, 2007, Stathopoulos and Karlaftis, 2003) have been applied for prediction of basic traffic parameters (volume, speed and occupancy). Vlahogianni et al. (2004) provides a good review of short-term traffic prediction models.

Comments: One of the limitations of these models includes averaging (smoothing) of input data over long time intervals. Hence they have the tendency to concentrate on the trend of the data and miss the extremes. Thus when traffic is in transition state of then such models cannot capture the behavior from congested to free-flow situation and vice versa. Specifically, in urban signalized networks, the short-term fluctuations (induced due to external control) are difficult to capture from these models. Such models are also dependent on historical database and for travel time prediction accurate historical database of travel time is not easily available.

2.2.6 Neural Networks based

Artificial intelligence (AI) is generally defined as study and design of a system (intelligent agents) that perceives its environment and takes actions that maximize its chances of success. Neural-networks are one of the tools for AI research and are originally applied for machine learning problems. Neural-networks algorithms are data driven tools with the potential to learn the complex non-linear relationship between variables by identifying the patterns in the data. Researchers have used the technique for short-term traffic and travel time forecasting on freeways. To improve estimation accuracy and efficiency researchers have proposed different approaches such as, modular neural networks (MNN) (Park and Rilett, 1998), spectral basis neural networks (SNN) (Park et al., 1999), state-space neural networks (SSNN) (van Lint et al., 2005) and neural networks with various hybrid approaches (Chen et al., 2001, Dia, 2001, Liu et al., 2006).

Comments: The application of these algorithms can be like a black box; and care should be taken to verify the reliability of the output and that the model is applied well within the limits for which it is trained. Data driven models, have the limitations of transferability, as the model is trained with data that is location specific, i.e., results obtained from one location are

[6] The term "State-space model" and "Kalman Filter model" refer to the same basic underlying theory. The term state space refers to the model and the term Kalman filter refers to the estimation of the state.

not transferable to another. Nevertheless, these models are applied in different engineering discipline and many promising results have been reported in literature. Dougherty (1995) provides a review of neural networks applied to transportation engineering.

2.2.7 Probabilistic models

Lin et al. (Lin et al., 2006, Tsekeris, 2006, Lin et al., 2004) utilize conditional probabilistic approach to predict the probability of the vehicle to be delayed at an intersection, given the delay condition at the upstream intersection, and hence the delay of the vehicle at an intersection. Dias (2007) has applied Bayesian network to predict travel time on an arterial route using probe data.

Comments: The probability transition matrix for delay estimation at an intersection is to be calibrated based on the flow level, the flow composition and the degree of signal coordination along the path of the route. Lin et al. (2004) identify the inherent limitations in the model *"…the nominal delay used in the formulation is based on the existing delay formula for intersection. It is well known that many existing delay formulas perform poorly under oversaturated situation. The performance of the model may be improved when more sophisticated delay formula become available"* (Lin et al., 2004).

The model by Dias (2007) is developed for undersaturated traffic conditions with fixed signal timings. Dias argues that under the assumption of undersaturated and fixed signal control the travel time prediction is obsolete. Nevertheless, it provides understanding the patterns in travel time distribution along signalized arterials.

2.2.8 Automatic Vehicle Identification (AVI) technology

Automatic Vehicle Identification (AVI) technology identifies the vehicle when it is observed at fixed AVI locations. AVI sensors include: video image processor; inductive loop; radio frequency optical/infrared (barcode); surface acoustical wave (SAW) etc. Video image processor (Automatic Number Plate Recognition (ANPR)) captures the license plate of the vehicle. Inductive loop technology uses an antenna embedded in the pavement at the station and transponder mounted at the underside of the vehicle communicates with the antenna. The barcode technology identifies the vehicle using barcode sticker located on the vehicle. The details of the sensor technology can be found in Klein (2001).

AVI sensors provide vehicle identity and time stamp when it is identified. Travel time of a vehicle identified between two AVI locations is the time difference between the time when it was identified at the respective locations.

ANPR utilizes image processing technology and the percentage of vehicles captured by these can range from 50% to 90%. For travel time estimation the vehicle ID should be recognized at both the AVI locations. In urban environment, the gap between the vehicles is likely to be lower and hence the ANPR of smaller vehicles (cars) can be hindered by larger vehicles (buses). The vehicle recognized at one site may not necessarily be recognized at other location. Therefore, the matching rate of a vehicle between two AVI locations can be lower in urban environment. Nevertheless, AVI technology captures a very good percentage of vehicles and can provide statistically accurate average travel time.

2.3 Mobile sensor based

Position detection equipments such as Global Positioning Systems (*GPS*), mobile phone or Personal Handy phone Systems (*PHS*) are capable of providing time-space trajectory of the vehicle equipped with such equipments. Here vehicle with such equipments is referred as probe vehicle[7], and data provided by these vehicles as probe vehicle data. The probe data obtained is its position coordinates (longitudes and latitudes) at different time intervals (defined by data transmission frequency). Thus it can provide direct travel time from point-to-point on the path traversed by the probe vehicle. For this, the coordinates are to be map-matched with the digital road network to know its position on the road. The accuracy of map-matching depends on the accuracy and frequency of the probe data in addition to the accuracy of the digital road network.

The estimate for the average link travel time, for all the vehicles (population) traversing the link, during certain interval is obtained by applying *statistical sampling theory* on the travel time obtained from the sample of different probe vehicles traversing the respective link at the respective time interval. The quality and reliability of the travel time estimates is sensitive to the number of probe observations on spatial-temporal scale which interests practitioners and

[7] In literature, probe vehicle is differentiated from floating car. Floating car (active vehicle) is a test vehicle where the driver is the member of the data collection team. The driving behaviour is controlled to match the desired driving style, such as average car. Whereas, probe vehicle (passive vehicle) is already in traffic steam and driver of the probe vehicle is not instructed to follow any specific driving style.

researches to know the minimum number of probes required to estimate statistically accurate average travel time.

2.3.1 Minimum number of probes (How many vehicles need to serve as probes?)

The above question can be mathematically formulated (2.35) as the minimum number of probes (n_p) required, on a given link in some time interval, to ensure that the estimated travel time value is within a predetermined statistical accuracy.

$$n_p : \text{Prob}\left[\left|\frac{\bar{x}-\mu}{\mu}\right| < \varepsilon_{\max}\right] \geq \alpha \tag{2.35}$$

Where: n_p is number of probes;

α is the level of significance and (1- α)*100 is the confidence level.

$\bar{x}$ is the mean estimate from the sample (probe vehicles);

μ is mean estimate from the population (all the vehicles)[8]; and

ε_{max} is the threshold relative error.

Equation (2.35), defines the number of probes required such that the probability (of relative absolute deviation $\left|\frac{\bar{x}-\mu}{\mu}\right|$ from estimate is less than ε_{max}) is more than α.

The solution for equation (2.35) is obtained from central limit theorem, assuming:

i. population is normally distributed;

ii. if population is not normally distributed than sample size should be large (>30).

If the estimation interval is short (for instance less and 15 min) and link is not heavily travelled then the assumptions are generally violated. In such situation, the sample size can be determined if probability density function of the mean travel time of all probes in the link during measurement time period is known. The estimation of probability density function is rather complicated therefore in literature a trade-off between the central limit theorem

[8] Here relative absolute deviation is considered instead of absolute deviation. Absolute deviation has different meaning for different travel time values i.e., it is more significant for smaller travel time than for larger travel time.

approximation and computation complexity is made. Applying the central limit theorem the required minimum number of probes is obtained as:

$$n_p = \frac{Z_{\alpha/2}{}^2 CV^2}{\varepsilon_{\max}{}^2};\ CV = \frac{\sigma}{\mu} \tag{2.36}$$

Where σ is the population standard deviation;

$Z_{\alpha/2}$ is the standard normal variates for α level of significance ($Z_{0.05/2}$ = 1.96 and $Z_{0.1//2}$ = 1.645); and

CV is the coefficient of variation of the population.

It is clear from equation (2.36) that for a given reliability criteria (level of significance and threshold relative error) sample size directly depends on the coefficient of variation (CV) of the population. Higher the coefficient of variation higher is the sample size (*see* Figure 2-2). The CV for urban links is expected to be larger than on freeways due to stop-and-go running conditions on urban networks[9].

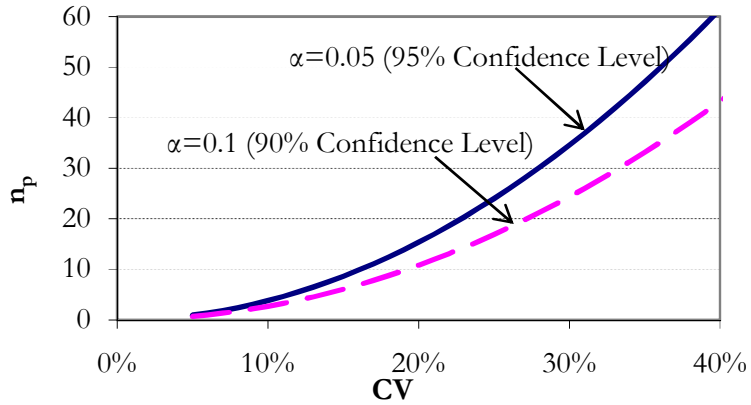

Figure 2-2: Relation between number of probes and coefficient of variation for 95% and 90% confidence level and 10 % error.

Using the empirical data from AVI installed on freeways in Houston, Turner and Holdener (1995) have reported the minimum required probe sample size for:

i. time periods (for travel time estimation) of 5 min and 15 min;

[9] The observed CV values for time periods of 5 min interval on an urban link A→D_{Lft} (see section 6.3.1) in Lucerne, Switzerland ranges from 26% to 55%.

Turner and Holdener (TURNER, S. M. & HOLDENER, D. J. (1995) Probe vehicle sample sizes for real-time information: the Houston experience. IN DAILEY DANIEL, J. & HASELKORN MARK, P. (Eds.) *Vehicle Navigation and Information Systems Conference (VNIS).* Seattle, WA, USA, IEEE.) have reported CV from a freeway in Houston for 5 min interval in range from 5% to 15%.

ii. (1- α): Confidence levels of 95% and 90%; and

iii. ε_{max}: relative error of 10% .

The estimate is based on 85% percentile CV values that range from 5% to 15% for 5 min interval and 5% to 19% for 15 min interval. The results are that for 5 min periods with 95% confidence level, the sample sizes range from 1 probe vehicle every 5 min for lanes having flow at free-flow conditions to 6 probe vehicles every 5 min for severely congested lanes. Sample sizes are slightly lower for a 90% confidence level. They have also provided a regression equation to estimate 85th percentile of coefficient of variation (CV) based on average speed and the required numbers of probe vehicles are estimated by equation (2.36). The validation of the regression equation is not reported.

The above study by Turner and Holdener does not take into account the adequate coverage of the network by the probe. Srinivasan and Jovanis (1996) have gone one step further and have defined a heuristic algorithm for estimating number of probe vehicles required in network (N) for reliable travel time estimation The algorithm accounts for the link reliability criterion defined in terms of level of significance (α) and relative error (ε) (Refer equation (2.36).) and for the network adequacy in terms of proportion of links to be covered (p_o).

The steps of the algorithm by Srinivasan and Jovanis are as follows:

Step 1 Determine the minimum number of probes required for each link during each measurement period (n_{plt});

Step 2 Sample N probe vehicles from the population of all vehicles trips assigned (dynamic or stochastic assignment) on the network;

Step 3 Assign the N probe vehicles trips using the dynamic or stochastic assignment model;

Step 4 Determine the proportion of links covered (p_t) reliably by probes (i.e., links in which number of probes in measurement period is greater than its corresponding minimum number determined in Step 1.);

Step 5 Average the proportion of link for the peak period to obtain the average link coverage p.

The above steps are repeated with increasing N until pre-specified proportion (p_o) of links is covered reliably ($p \geq p_0$). They have tested the algorithm using simulation and the results indicated that:

i. Total number of probes in the system (N) increases almost linearly with increasing value of minimum number of probes (n_p) required on each link during each estimation interval (tu). The increase is steeper if estimation interval is reduced from 20 min to 5 min;

ii. If the estimation interval (tu) decreases, then the number of probes (N) increases non-linearly. They found that there is a "knee" in the curve at a tu of about 10 min, particularly for higher value of n_p The measurement interval less than 10 min has steeper increase in N with decrease of tu;

iii. The proportion of link traversed increases at a decreasing rate with increasing N;

iv. It is also noted that freeways have significantly higher link traversals than the arterials. This result is attributed to the user-optimal route choice model which results in drivers choosing faster route (freeways) over the slower routes (arterials).

The above results are based on the simulation on a fixed network (Sacramento network) and depend on the OD and route choice parameters used. Nevertheless, it provide a good insight into the relation of different variables (N, n_p, tu and p) that affect the travel time estimation using probes.

2.3.2 Bias in probe on signalized links

Probe vehicle may not be true representative of the population of vehicle traversing. This issue is more severe in urban environment where there is significant fluctuation in the flow of vehicles and travel time for different exit movements on a link may be significantly different. Hellinga and Fu (1999) has demonstrated that bias in the proportion of probes associated with each link exit movements and/or arrival time distribution of probes can lead to sample mean that does not asymptotically approach the population mean, regardless of the sample size. To reduce the effect of the above bias they have proposed a methodology based on *stratified sampling technique*. The methodology requires the arrival time distribution of all the vehicles to weight each probe travel time report. The arrival time distribution is generally not known and they propose it to be estimated from detector or some other traffic surveillance method.

2.3.3 GPS based mobile sensors

GPS is the most accurate mobile sensor. Differential GPS can provide accuracy of 2 m to 10 m whereas kinematic GPS can provide accuracy of 5 cm to 15 cm. However, commercially available GPS equipments have relatively low accuracy with high data transmission frequency (Around 30 s or a minute.) (Kuwahara et al., 2004).

In urban environment, the network is generally dense with short link lengths; therefore data with low accuracy can result in significant error in map-matching and with high frequency can result in missing information for the travel on certain links. The effect of: a) accuracy of probe data; b) rate of data transmission; and c) density of urban network, on transport applications (such as travel time and OD estimation) should not overlooked (Chung and Kuwahara, 2007).

2.3.4 Emerging mobile sensors: Cellular phones

Every switched on mobile phone (CDMA, GSM, UMTS and GPRS) on a vehicle has the potential to become traffic probe. There is an increasing interest of researches to develop algorithms to use of mobile phone as traffic probes. PHS and mobile phone use network based position technology and have accuracy of around 50 ~ 100 m and 150 ~ 500 m, respectively. As the accuracy of localization of mobile phone is less accurate, therefore significant large number of mobile devices has to be tracked for travel time estimation. Mobile phone can act as a probe only if it is carried in the vehicle traversing the road. The data obtained from mobile phone is from all the users, hence the users in vehicle and outside vehicle are to be differentiated, which is complicated. For instance, if there is a metro track parallel to the road, then mobile phone data from a user traversing in the metro can be misinterpreted as traversing on the road, leading to wrong estimate of travel time. Similar misinterpretation can be for a pedestrian using a mobile phone and traversing slowly on the footpath along the road.

In addition, to above misinterpretations of cellular phone other issues such as potential public concerns about privacy; and growing awareness of the road safety implications is to be resolved. Moreover, for successful deployment of the cellular phone as mobile sensors, public-private partnerships between transport agencies and cellular carriers are also required (Rose, 2006, Yim, 2003, Holm et al., 2004).

2.3.5 Transit vehicles as mobile sensors

Transit vehicles, such as public buses, are increasingly equipped with automatic vehicle location (AVL) tracking equipments (e.g. GPS) with the objective of locating them for transit management and providing arrival time information to the passengers. They are inherently different from ordinary probe vehicles due to the following characteristics:

i. Buses stop at the bus stop to collect and discharge the passengers for certain dwelling time. If there is a bus bay, then they have to diverge from and merge to the traffic stream. In absence of bus bay they generally block the lane at the stop until the dwelling time.

ii. They generally travel to the right-most (right hand drive) or left-most (left hand drive) lane of the corridor. If the average speed differs among the lane then there is a bias in the travel time estimated from the bus.

iii. If there is a separate bus lane then travel time estimated from the bus is highly biased.

iv. They are both mechanically and operationally different from those of other cars running on the street.

Buses typically run on heavily travelled urban corridors- links where travel time information is mostly required. They run at high frequency during the peak-period, which provides better sample size of buses for time when information is most needed. Nevertheless, they have a potential to be a supplement source of travel time information.

Elango and Dailey (2000) and Cathey and Dailey (2001) have applied Kalman Filter technique to the noisy space-time measurements of AVL equipped transit vehicles for smooth estimates of transit vehicle speeds. They concluded that AVL data from a fleet of transit vehicles travelling along prescribed routes can be used to define *virtual speed sensors* along the route. The speed obtained from the virtual sensors defines the speed of the transit vehicles. To correlate the virtual sensor speed to the average speed of the link the relationship between the two should be explored.

Chakroborty and Kikuchi (2004) have examined the relationship between travel time of a transit vehicle (bus) and of other vehicle in the same traffic stream for stability and data adjustment needs. They used the data from major corridors in Delaware, USA, and found that the difference in travel time was relatively stable. Based on their findings they have suggested

functional form to predict average travel time of vehicle from observed travel time of bus in the same traffic stream. However, the functional form should be tested on different sites for a concrete conclusion. The applicability of the functional form with respect to road section, time of the day and other local factors should also be investigated.

2.3.6 General issues with mobile sensors

In addition to the issues mentioned above, following are the general issues with use of probe vehicle.

Note: the objective of this research is not to address different issues related to mobile sensors.

2.3.6.1 Gaps in data

The availability of transmission signals is a crucial factor to obtain real-time data from mobile probes. GPS system requires line-of-sight with at least four satellites to estimate its position. Due to unavailability of signals (communication error) there are instances when data is not recorded by GPS equipment. Communication error can occur when GPS equipment is in the vicinity of elevated structures such as buildings or is under an infrastructure such as tunnel. In urban environment due to dense elevated structures the error is more common and the effect is terms as *urban canyon*.

The traffic state between two successive data is not known, and assumptions such as uniform flow between two successive data are employed. Such assumptions may not be appropriate in urban environment and it may result in inaccurate determination of time when the probe vehicle is at a point of interest.

2.3.6.2 Sparse spatial-temporal coverage of probe vehicle

Probe vehicle only provides information for the areas covered by the probe and time interval in which probe is available. For instance, if taxi is used as a probe vehicle then higher confidence in travel time estimation is obtained only from areas heavily served by taxis. For continuous travel time estimation generally travel time is extrapolated for time intervals with no probe. Therefore, for spatial-temporal travel time estimation, probe vehicles must be supplemented by other sources.

2.3.6.3 Lag in travel time estimation

Travel time from the probe is only available when the probe has actually traversed the link i.e., it is the experienced travel time. It is not the predicted travel time. Say at time t_c, the measured travel time on a link from a probe is t_p. It means that at time, $t_c - t_p$, the link travel time was t_p. Depending on the link length and traffic condition, the actual link travel time at time t_c can be significantly different from t_p. If link length is long or traffic is during congestion build-up or dissipation process then there can be significant variation in link travel time at $t_c - t_p$ and t_c.

2.3.6.4 Probe market penetration

Level of market penetration of the probe vehicles is an important and essential factor in estimating travel time and its reliability using probe vehicle data. It is defined as the ratio of number of probe vehicles to total vehicles in the network. It is to be noted that the level of market penetration generally have spatial and temporal variation. Therefore, the definition of level of market penetration should be supported by its level of aggregation i.e., time interval and OD pair for which number of probes and total number of vehicles is determined.

Van Aerde et al. (1993) have studied the relationship between the reliability of the travel time estimates from probe and market penetration. They concluded that:

i. On signalized arterials: Interrupted nature of traffic in addition to low capacity results in high variability in the percentage of probes in the traffic stream. So, it is difficult to reliably estimate the travel time on arterials for low levels of market penetration;

ii. On freeways: Non-interrupted nature of traffic flow makes travel time estimation relatively more reliable than arterials. Moreover, due to high capacity there is increased likelihood of observing relatively more number of probes and therefore reliable travel time even from low levels of market penetration.

iii. An assessment based on availability of continuous and accurate probe information can be seriously flawed for low and medium levels of market penetration.

2.4 Data fusion based

Traffic data from different sources can have different accuracies which results in inconsistency and sometimes even contradictory estimates. Data fusion is the processing tool that takes into account the quality of the data provided by each source with the aim to increase the accuracy, reliability and robustness of the prediction. Interested readers can also refer to Hall and Llinas (1997) for introduction to data fusion and its applications. Different data fusion techniques for different engineering applications have been proposed in literature and can be classified into (El Faouzi, 2004):

i. Statistic based: weighted average, multivariate statistical analysis;

ii. Probabilistic based: Bayesian approach, evidence theory; and

iii. Neuromimetic networks based: including artificial intelligence, genetic algorithm and neural networks.

In weighted average based technique, an estimator of travel time from each source is derived and thereafter, estimates are combined according to the weighted mean. The weights are generally derived from variance-covariance estimation errors. Berka et al. (1995) fuses travel time (2.37) obtained from detectors (t_d) and mean probe travel time (t_{pm}) by method of weighted averages. For the computation of weights several variables are used, including: the sum of weights of reasonable probe reports (N_p); standard deviation of probe travel time (σ_p) and detector travel time (σ_d), respectively; weights assigned to detector travel time in data screening (W_d); and fusion adjustment factors (f_d, f_p) to control the contribution of each data source to the finally fused travel time (t_f).

The determination of these parameters is a rather complicated procedure and moreover, some of the model parameters have to be estimated from historical data.

$$t_f = \frac{f_p \frac{N_p}{\sigma^2_p} t_{pm} + f_d \frac{W_d}{\sigma^2_d} t_d}{f_p \frac{N_p}{\sigma^2_p} + f_d \frac{W_d}{\sigma^2_d}} \tag{2.37}$$

Westerman et al. (1996) have developed a model named COMETT in which they explore the fusion of probe vehicles and loop detector data for freeway travel time and incident detection in California Partners for Advance Transit and Highways (PATH) project. Travel time from loop detector data is based on defining cumulative plots. The divergence in the cumulative

plots due to detector counting error is corrected by resetting the counts to zero (re-calibration) when the following condition is met.

They assume that meso-fluctuations in traffic flow, defined as characteristic fluctuations over periods from half a minute to various minutes, are preserved over several kilometers. The meso-fluctuation in the pair of cumulative plots are correlated by minimizing, through least square, the surface area between the meso-fluctuation portions of the cumulative plots. Surface areas are defined through iteratively shifting the plot horizontally. If the surface area is below certain empirical threshold then they are considered to be correlated. Mean link travel time is the function of the horizontal shift of plots. If the difference of this mean link travel time with the travel time obtained from the mean speed measured from the upstream and downstream detector is below certain empirical threshold then the re-calibration is performed.

The above assumption of preservation of the meso-fluctuations in traffic flow is easily violated during congested conditions and interactions with flow from on-ramp and off-ramp, which therefore limits the application of the above model.

Westerman et al. have also developed a model to estimate link mean speed (travel time) based on data from probe vehicles and historical database. For this they assume that the probability density function of road link mean speed and traffic volume for a link is known or can be reliably obtained from the historical database. The required link mean speed is estimated using Bayes estimator and assuming: a) normal distribution of speeds from probe vehicle under free flow regime; and b) gamma distribution of individual probe vehicles speeds. For details refer to Chapter 3 of (Westerman et al., 1996). Once the average speed (travel time) from probe vehicles is estimated the above defined re-calibration process can be repeated by considering the average link travel time from the probe vehicles as the reference travel time.

As quoted in the report *"For using the probe vehicle data to perform additional re-calibration, it is important to ascertain that the road link mean speed obtained from the probe vehicle samples is correct."*. For small sample size of probes the model requires historical database of probability density functions which is not easily obtainable. Moreover, the validation of the above model is not quantitative and can only be applied for freeways. Nevertheless, the model addresses to the vulnerability of the cumulative plot for travel time estimation under detector error and mid-link sources and sinks.

Choi and Chung (2002) have applied the data fusion technique for 5 min average travel time estimates using detector and probe vehicle data. The algorithm first estimates space-mean speed from detector counts and occupancy using Dailey (1999) equation, which provides travel time estimated for each minutes. Each minutes travel time estimated are aggregated using *Voting Technique* for 5 min average travel time (TT_d). Average 5 min travel time (TT_g) from GPS probes are obtained using *Fuzzy regression.* Finally fused link travel time is obtained by applying *Bayesian Pooling Method* on TT_d and TT_g. The methodology is tested using real data collected on four consecutive urban links, in Suwon, Korea. It is not documented whether the links were signalized or not. As they have used both mid-link and stop-line detectors for space mean speed estimated, therefore it can be concluded that the links were not signalized. The MAPE for four links is reported in the ranges from 15% to 26.5%. The algorithm is tested for undersaturated traffic condition and should be tested for oversaturated traffic condition too. They quote that *"a different level of service might produce totally different weights of each data collection mechanism. In such cases, a different data fusion method and/or a revision of the proposed algorithm may be needed"*.

Xie et al., (2004) have applied two independent neural networks methodologies: Multi-Layer Perception (MLP) and Multi-Layer regression (MLR) models to combine output from loop detector and probe vehicles. For input to the data fusion: a) Singapore model (Xie et al., 2001) is applied to estimate the speed from the detector data; and b) Average travel time from probe samples are considered only if the sample size during estimation interval is more than 10 vehicles or is more than the minimum required sample size determined by central limit theorem. The model is tested using simulation and it is reported that RMSE for MLR and MLP model is 3.44 km/h and 2.52 km/h, respectively. The sensitivity analysis of estimation accuracy over probe vehicle penetration rate indicates that at least 3% of the probes are required for travel time estimates from probe and hence for data fusion. Moreover, there is marginal improvement in accuracy from data fusion if more than 18% of probes exist, as accuracy from probe only with such as high penetration rate is very good.

Data fusion of data from different sources has the potential to improve the accuracy and reliability of the estimates. However, the fusion of the data does not makes much sense if one of the sources has sufficient high accuracy as the improvement in accuracy is marginal or even negative. For instance, if probe sample size is very large (say penetration rate is more than 20%) then the travel time estimates from probes is relatively quite accurate. Fusion of the

information with travel time estimates from detectors with low accuracy may have little improvement.

In literature generally, different methodologies such as neural networks (Ivan, 1997, Ivan et al., 1995), Bayesian score rule (Thomas, 1998), and Dempster-Shafer theory (El Faouzi, 2006) are utilized to fuse detector and probe vehicle data for travel time estimation and incident detection. Klein et al. (2002) introduced Dempster-Shafer theory for data fusion for advance traffic management whilst El Faouzi (2004) provides an overview of data fusion in road traffic engineering and Dailey et al., (1996) summaries ITS data fusion projects.

Table 2-1: Critical overview of the literature

Model Type		Reference	A[10]	MS[11]	Mid[12]	DE[13]	Comments
Regression based		Wardrop (1968)	U	No	No	No	Generally regression models are site specific and their transferability is limited. Moreover, if regression models parameters are calibrated with simulated data, then it is necessary that simulation model should be properly calibrated with field observations. The model calibrated for a specific condition should not be generalized without further testing and calibration.
		Gipps (1997)		No	No	No	
		Gault (1981)		No	No	No	
		Young (1988)		No	No	No	
		Sisiopiku et al (1994)		No	No	No	
		Xie et al., (2001)		No	No	No	
		Rice and Van Zwet (2004)	F	No	No	No	
Queueing theory	Static	Bureau of Public Roads (1964), Davidson's function (Akçelik, 1978, Tisato, 1991), Conical-volume delay functions (1990), Akcelik function (1991) etc	U	No	No	No	Inability to estimate delay for traffic conditions that are different from those assumed in the models. For example, unusual flow patterns which do not follow the traditional statistical distributions cannot be modeled. The models are simple and favorable for transport planning and policy applications but not for ITS applications where more accurate and reliable travel time in real time is required.

[10] A: Application (F: Freeway facilities, U: Urban facilities)

[11] MS: Exit movement specific travel time estimation (ND: Not documented)

[12] Mid: Consideration of mid-link sources and sinks (ND: Not documented)

[13] DE: Consideration of detector error (ND: Not documented)

Model Type		Reference	A[10]	MS[11]	Mid[12]	DE[13]	Comments	
		Japanese Sand-Glass (Takaba et al., 1991)	F	No	No	No		
		Delay Time Model (Takaba et al., 1991)	U	No	No	No	Requires extensive calibration for reasonable accuracy.	
	Dynamic	TRANSYT/SCOOT (Carden et al., 1989)	U	ND	ND	ND	The objective of the model is to optimize signal parameters and not to estimate travel time. The performance of the model for travel time estimation with respect to the detector counting error and mid-link source/sinks is not documented in the literature.	
		Highway Capacity Manual 2000 (TRB, 2000)	U	No	No	No	The model is simple and favorable for transport planning and policy applications, where travel time for larger period is required. For real time application, the parameters such as left over queue is not easy to obtain.	
Traffic flow theory		Nam and Drew (1999)	F	No	No	Yes	The model is limited to confined link of freeway (no on/off ramp) under FIFO queueing discipline.	The detector error considered is approximation for a longer time period and fluctuations in the error especially during congested conditions is not considered.
		Oh et al., (2003)	F	No	Yes	Yes	Requires detectors at each mid-link sinks (off-ramp) and sources (on-ramp).	
Pattern recognition	k-NN	You and Kim (2000) Bajwa et al. (2003)	F	No	No	Yes	Not able to predict travel time for traffic patterns not present in historical database. The technique highly depends on the quality and quantity of the historical database. Error in the historical travel time estimation is reflected in the prediction. An accurate travel time estimation methodology is required to build the historical database.	
		Robinson and Polak (2005)	U	No	No	Yes		

Model Type		Reference	A[10]	MS[11]	Mid[12]	DE[13]	Comments
	Cross-correlation	Dailey (1993)	F	No	No	No	Only if sufficient correlation between the flow at two detectors. Model only for freeways with low occupancy (less than 15%).
		Petty et al., (1998)	F	No	No	No	The model is applicable only for freeway section where platoon can exist i.e., absence of on-ramp and off-ramp.
	Vehicle reidenti-fication	Coifman (2001, 2001, 2002, 2003, 2007).	F	No	No	No	Reidentification based on on vehicle length estimation. The reidentification rate depends on percentage of heavy vehicles and conservation of platoon in traffic flow from upstream to downstream.
		Ritchie et al. (2002, 2005) Kwon (2006)	F/U	No	No	No	Reidentification based on inductive waveform from advance inductive loop detectors.
	Regression trees	Logendran and Wang (2008)	F	No	No	No	Requires accurate historical database.
Time-series analysis	ARIMA	Hamed et al., (1995) Davis et al.(1990)	F	No	No	No	Applicable for forecasting. These models have the tendency to concentrate on the trend in the data and miss the extremes. Thus when traffic is in transition state then such models cannot capture the behavior from stop-and-go to free flow situation and vice versa.
	Kalman filtering	Yang (2007) Stathopoulos and Karlaftis(2003)					
Neural networks		Park and Rilett (1998) Park et al., (1999) van Lint et al., (2005) Chen et al.,(2001) Dia (2001)	F	No	No	No	The applications of these algorithms can be like a black box; and care should be taken to verify the reliability of the output and that the model is applied well within the limits for which it is trained. Models are location-specific.

Model Type	Reference	A[10]	MS[11]	Mid[12]	DE[13]	Comments	
	Liu et al.(2006)	U	No	No	No		
Probabilistic models	Lin et al., (2004, 2006) Tsekeris, (2006)	U	No	No	No	Probability transition matrix for delay estimation at an intersection is to be calibrated based on the flow level, the flow composition and the degree of signal coordination along the path of the route.	
	Dias (2007)	U	Yes	No	No	Only for undersaturated with fixed signal control. Requires building of historical database.	
Transit vehicles as mobile sensors	Elango and Dailey (2000) Cathey and Dailey (2001)	F/U	No	No	ND	The methodology provides speed of the transit vehicle. The correlation of the speed of transit vehicle with other vehicles should be explored.	Travel time information using transit vehicles can be integrated with other data sources using data fusion techniques for better accuracy and reliability.
	Chakroborty and Kikuchi (2004)	U	No	No	ND	The functional form to predict average travel time of vehicle from observed travel time of bus in the same traffic stream should be tested on different sites for a concrete conclusion.	

Model Type	Reference	A[10]	MS[11]	Mid[12]	DE[13]	Comments	
Data fusion	Westerman et al., (1996)	F	No	Yes	Yes	The assumption of preservation of "meso-fluctuations" in traffic flow is easily violated during congested conditions and interactions with flow from on/off ramp. Mean link speed from probe samples should be accurately estimated. The validation of the model is not quantitative. Nevertheless, the model addresses to the vulnerability of the cumulative plot for travel time estimation under detector error and mid-link sources and sinks.	Data fusion of data from different sources has the potential to improve the accuracy and reliability of the estimates. However, the fusion of the data does not make much sense if one of the sources has sufficient high accuracy or relatively low accuracy.
	Berka et al., (1995) El Faouzi (2004a, 2004b)		No	No	No	Weighted average of travel time from detectors and mean travel time from probes. The determination of weights is rather complicated.	
	Choi and Chung (2002)	U	No	No	No	Performance should be tested for different traffic conditions. Model requires calibration	
	Xie et al., (2004)	U	No	No	No	Validity of the model should be checked with read data	

2.5 Critical overview

Statistical comparison of different models using the same data set should be valuable. However, practically it is difficult due to different assumptions made, applicability in traffic conditions and variables involved. Only few examples in literature such as Xie et al., (2001) have compared their models with other similar models in literature.

A critical overview of the literature reviewed in this chapter is provided in the Table 2-1. Researchers have proposed number of models with various degree of complexities ranging from simple naïve regression, traffic flow theory based, pattern recognition to advance neural networks, and data fusion techniques.

Model specified for specific conditions should not be generalized without further testing and calibration. A majority of literature on travel time estimation is on freeways and cannot be applied as it is on urban networks due to the different behavior of traffic on the two facilities (Refer to Section 1.3.). The complexities related to the urban network includes: a) interrupted traffic due to conflicting areas such as intersections (signalized or non signalized) and significant delay from the interruption; b) significant traffic flow from a mid-link source and/or to a mid-link sink; c) significant difference in travel time for different turning movements associated with a link; and d) mid-link delay due to mid-link interruptions such as pedestrian crossing, or a leading vehicle turning towards a side street etc.

Majority of models for travel time estimation on urban networks considers the delay at intersection though the effect of flow to/from mid-link sinks/sources is not considered. The models generally provide average travel time for the whole link, which may not be a true representative of travel time for different link exit turning movements.

Moreover, the performance of the models with respect to detector counting error is not evaluated. Though, one can observe detector counting error of ±5% even under normal running conditions.

Models based on probe data assume that there is sufficient number of probe vehicles per estimation interval. The current market penetration of probe is low and the required number of probes per estimation interval is not easily available.

Researchers have also applied data fusion technique to fuse data from detector and probe vehicles. Integrating data from multisource have the potential to improve the accuracy and reliability of the estimates.

Literature is abundant with travel time estimation models though each model has its own limitations. New models are still being sought by many researchers as there are avenues for improvement especially in terms of transferability, applicability, robustness and sensitivity to sensor errors.

3 Cumulative plots estimation

This chapter provides fundamental understanding of the estimation of travel time using cumulative plots. It develops different models to generate cumulative plots for signalized urban networks. Finally, sensitivity analysis of the model with respect to its parameters is performed.

3.1 Introduction

Inductive loop detector can provide vehicle-by-vehicle counts, but the data obtained from the detector depends on the data acquisition software. Traditionally, detectors in urban networks are used for signal control and not for providing vehicle-by-vehicle counts. Therefore, at most of the urban networks, for instance in Geneva and Lausanne, Switzerland the counts from the detectors are acquired for certain aggregation interval, termed as detector detection interval.

Traffic flow on urban network is subjected to stop-and-go running conditions due to signals and other factors. At signalized intersection, vehicles stop during the signal red phase and queue builds up. During signal green phase the vehicles from the queue are discharged at saturation flow rate and remaining follow certain vehicle arrival pattern. Figure 3-1 represents a cumulative plot at the location of stop-line detector and corresponding traffic signals phases for the movement. It can be seen that there is no flow during signal red phase, i.e., slope of the plot is zero; and during signal green phase, a proportion of flow is at saturation flow rate. If aggregated counts for detector detection interval are available then the above mentioned fluctuation during the detection interval is unknown (In Figure 3-1, detection interval is equivalent to two signal cycles.).

For travel time estimation one is interested in pair of cumulative plots at upstream and downstream of the link. In Switzerland, stop-line detectors are available. Here a link is defined between consecutive signalized intersections. The upstream cumulative plot is obtained by integrating the data from stop-line detectors at upstream intersection. The downstream cumulative plot is obtained by the stop-line detector at downstream intersection.

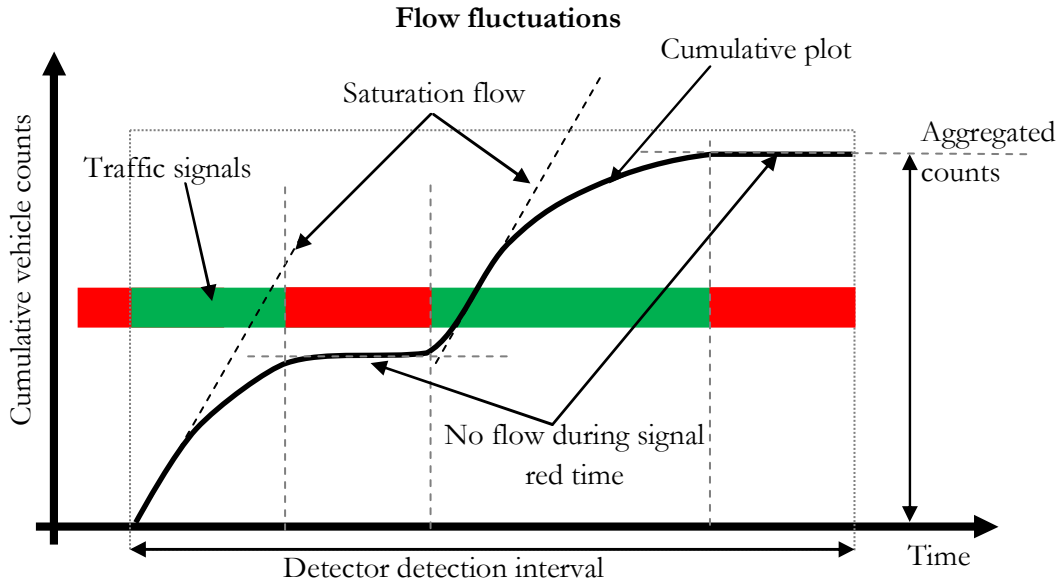

Figure 3-1: Cumulative plot at the location of stop-line detector. Shape of the cumulative plot is defined by the fluctuation in traffic flow due to signal.

3.2 Model development

If aggregated counts from the stop-line detectors are known and fluctuations in the flow due to signals are unknown then we make a hypothesis that if: a) stop-line detectors are present on all the lanes that contribute to cumulative plots; b) detectors are perfect and mid-block source and sinks are absent; and c) real turning proportions are known, then the integration of detector data with signal controller data should provide accurate cumulative plots. The aggregated counts defined here, are the respective counts for the study lane as obtained by appropriate scaling of the actual detector counts with known turning proportions.

Note: In this chapter the model is developed based on the above hypothesis. In next chapter (Chapter 4), we relax the above hypothesis and the model is extended to consider mid-block source and sink and detector counting error.

To generalize the model, cumulative plots at the location of the detector are estimated for the three cases depending on the availability of the data:

i. Case-D: Only detector data is available;

ii. Case-DS: Detector data and signal controller data is available; and

iii. Case-DSS: Detector data, signal controller data and saturation flow rate is available.

The slope of the plot defines the flow pattern at the respective entrance of the intersection. We define N_d and q as the counts and flow, respectively during the detection interval of DI seconds. A list of abbreviation used in this chapter is provided in Table 3-1.

Table 3-1: List of abbreviations in Chapter 3

Abbreviations	Meaning
q	Flow rate.
N_d	Counts during detection interval.
DI	Detector detection interval.
$g_{d,i}$	Signal green time corresponding to the i^{th} green period within the detection interval.
N_i	Counts during the i^{th} green period within the detection interval.
n_s	Counts in saturation flow rate.
N_g	Counts during a green phase.
N_{max}	Maximum counts during a green phase.
s	Saturation flow rate.
X	Degree of saturation.
g	Signal green time.
c	Signal cycle time.
g/c	Green split.
CP_{demand}	Demand cumulative plot at downstream.

3.2.1 Case-D

The flow pattern (*see* Figure 3-2) is assumed to be uniform throughout the detection interval (3.1). The assumption is reasonable for shorter detection intervals and in the absence of any further information can be applied for larger detection intervals.

$$q = \frac{N_d}{DI} \tag{3.1}$$

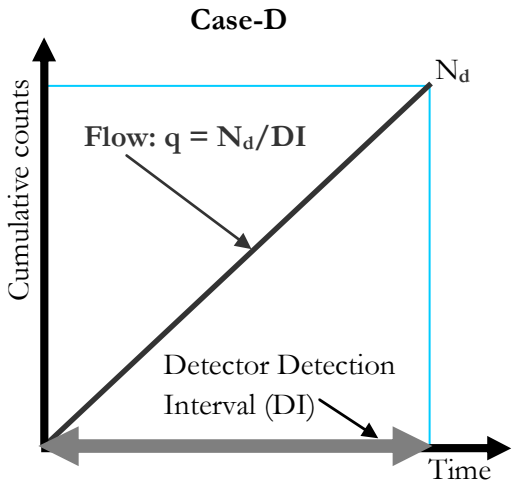

Figure 3-2: Flow profile for Case-D.

3.2.2 Case-DS

A stepwise flow pattern is defined (3.2) such that: a) flow is uniform only during the signal green period within the detection interval; and b) during signal red period there is no flow (*see* Figure 3-3). This captures the fluctuations in the flow pattern even for larger detection intervals. Flow patterns during each green period of the detection interval are parallel to each other.

$$q = \begin{cases} \dfrac{N_d}{\sum g_{d,i}} & \text{during green periods in the detection interval} \\ = 0 & \text{during red periods in the detection interval} \end{cases} \tag{3.2}$$

We define $g_{d,i}$ as the i^{th} green period within the detection interval.

In Figure 3-3, two green periods ($g_{d,1}$, $g_{d,2}$) are present during the detection interval and the counts are distributed to each green phase in proportion to the corresponding green time. The count, N_i, during each i^{th} green period ($g_{d,i}$) in the detection interval is assumed to be in proportion to $g_{d,i}$ (3.3).

$$N_i = \frac{N_d * g_{d,i}}{\sum_i g_{d,i}} \tag{3.3}$$

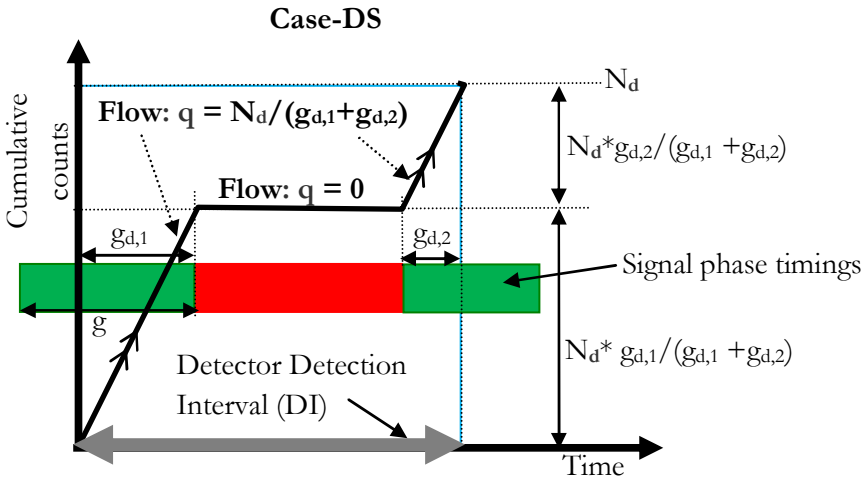

Figure 3-3: Flow profile for Case-DS.

3.2.3 Case-DSS

For realistic representation of the cumulative plots, saturation flow rate is considered and the counts during the green phase are segregated into counts from the saturation flow pattern and counts from the demand pattern.

We define the demand, which is the cumulative plot (CP_{demand}) at the location of the stop-line detector assuming point (vertical) queue at intersection. It can also be defined as the expected cumulative plot at the location of stop-line detector if there is no restriction, at the intersection, on the flow of the vehicles.

At a signalized intersection (during the green phase) the vehicles from the queue are effectively discharged at saturation flow. Thereafter, the flow pattern follows the demand pattern. If demand and saturation flow are known, then accurate and realistic flow pattern considering saturation flow and non-saturation flow can be estimated.

For simplicity, we focus on a green (g) for a complete signal cycle instead of $g_{d,i}$ (i^{th} green period during the detection interval). A g can extend in more than one detection interval. For instance, in Figure 3-3, the first green g has the component $g_{d,1}$ during the indicated detection interval. The count, N_g, during a g is obtained by respectively adding the counts from all its components, if split in more than one detection interval. Out of N_g vehicles, n_s vehicles enter the intersection at saturation flow pattern and the remaining (N_g - n_s) follow the demand pattern. The maximum number of vehicles which can depart during g is N_{max} (=s*g), where s is saturation flow rate (veh/s).

For a link between two consecutive intersections, the demand pattern, for the detector at the downstream end of the link, can be deduced from upstream cumulative plot U(t). However, for a network there can be certain links where U(t) is unknown such as at the entrance of the network, here demand can be assumed (*see* Figure 3-4). Therefore, the following two cases of assumed and deduced demand patterns are considered to estimate cumulative plots for Case-DSS.

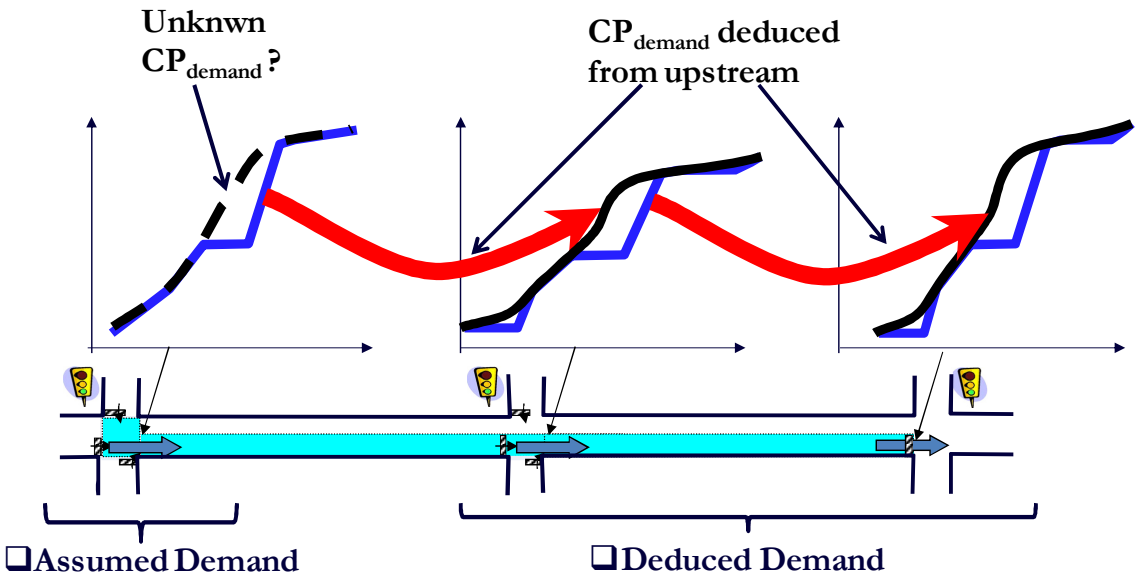

Figure 3-4: Example to illustrate *Assumed* and *Deduced* demand.

3.2.3.1 Assumed demand pattern

The detector counts represent demand for undersaturated situation. However, for oversaturated situation, the counts are upper bounded by capacity and that is less than true demand. Therefore, demand estimated in this case is termed as "assumed demand".

The demand flow pattern can be assumed to follow a uniform pattern (deterministic) or can be assumed to be distributed according to some probability distribution (stochastic). To simplify the analysis it is assumed that demand is uniform during the signal cycle. As shown in Figure 3-5, N_g numbers of vehicles are counted during the green phase that represents the uniform demand for the signal cycle. By superimposing saturation flow pattern (during the green phase) on the uniform demand pattern the following relationship can be geometrically obtained (Refer to Appendix B for the derivation of the equation):

$$\frac{n_s}{N_g} = \frac{(1 - g/c)}{(1 - X * \frac{g}{c})} \qquad for\ X < 1$$
$$= 1 \qquad for\ X \geq 1 \qquad (3.4)$$
$$where:$$
$$X = \frac{N_g}{N_{max}} \qquad when\ N_g < N_{max}$$

The saturation flow starts at the beginning of the green period and lasts for n_s/s time units. Therefore, the flow pattern is defined as:

$$\begin{aligned} &During\ Red\ Period \\ &\quad q = 0 \\ &During\ Green\ Period \\ &\quad q = \begin{cases} s & 0 < t < n_s / s \\ \dfrac{N_g}{c} & n_s / s \leq t \leq g \end{cases} \end{aligned} \qquad (3.5)$$

Where: t is the time since the start of the green within the green period.

Equation (3.4) provides the ratio of the counts in saturation flow rate (n_s) to the total counts during a green phase (N_g). For undersaturated situation, the ratio N_g/N_{max} represents degree of saturation (X) and n_s/N_g is the proportion of demand in saturation flow rate. For a given degree of saturation, the higher the green split (g/c) the lower the n_s/N_g ratio; and for near to saturation situations the ratio is close to one. This is as expected, because as the demand approaches capacity almost all the vehicles are at saturation flow rate.

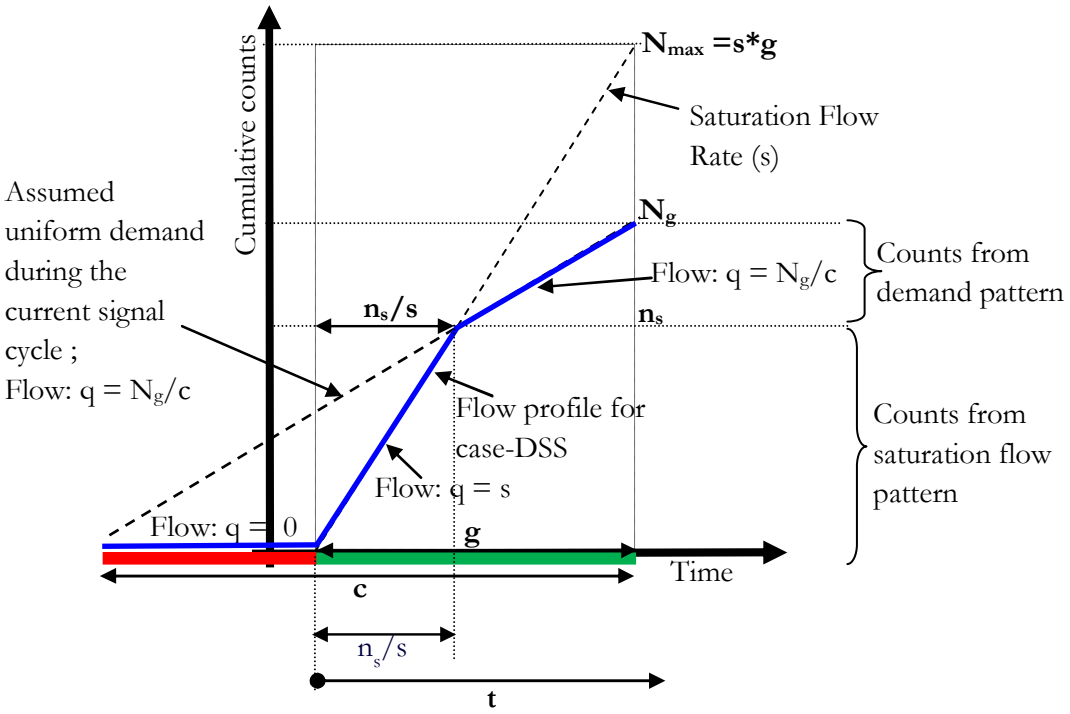

Figure 3-5: Geometrical relationship between n_s and N_g assuming uniform demand pattern (*Assumed demand*) during the current signal cycle.

3.2.3.2 Deduced demand pattern

In this case, we are interested in estimating downstream cumulative plot (D(t)), given the upstream cumulative plot (U(t)). The demand can be deduced from the upstream cumulative plot. We name this demand the *deduced demand* and it is the horizontal shift of the U(t) by free-flow travel time (t_{ff}) of the link i.e., U(t-t_{ff}), assuming no platoon dispersion. The assumption for no platoon dispersion is made for simplicity. It is found (presented in next section) that the model performs reasonably well with this assumption. For more accurate estimation a platoon dispersion model can be integrated to estimate the demand.

The flow is defined as zero for red phase. For green phase, if CP_{demand} is greater than the cumulative counts (D(t)) then the flow is at saturation flow rate otherwise the flow pattern is same as demand pattern (3.6).

$$
\begin{aligned}
&\textit{During Red Period} \\
&\quad q = 0 \\
&\textit{During Green Period} \\
&\quad \textit{if } CP_{demand}(t) > D(t) \\
&\qquad q = s \\
&\quad \textit{else} \\
&\qquad q = \frac{\partial CP_{demand}(t)}{\partial t} \\
&\textit{where : } CP_{demand}(t) = U(t - t_{ff})
\end{aligned}
\tag{3.6}
$$

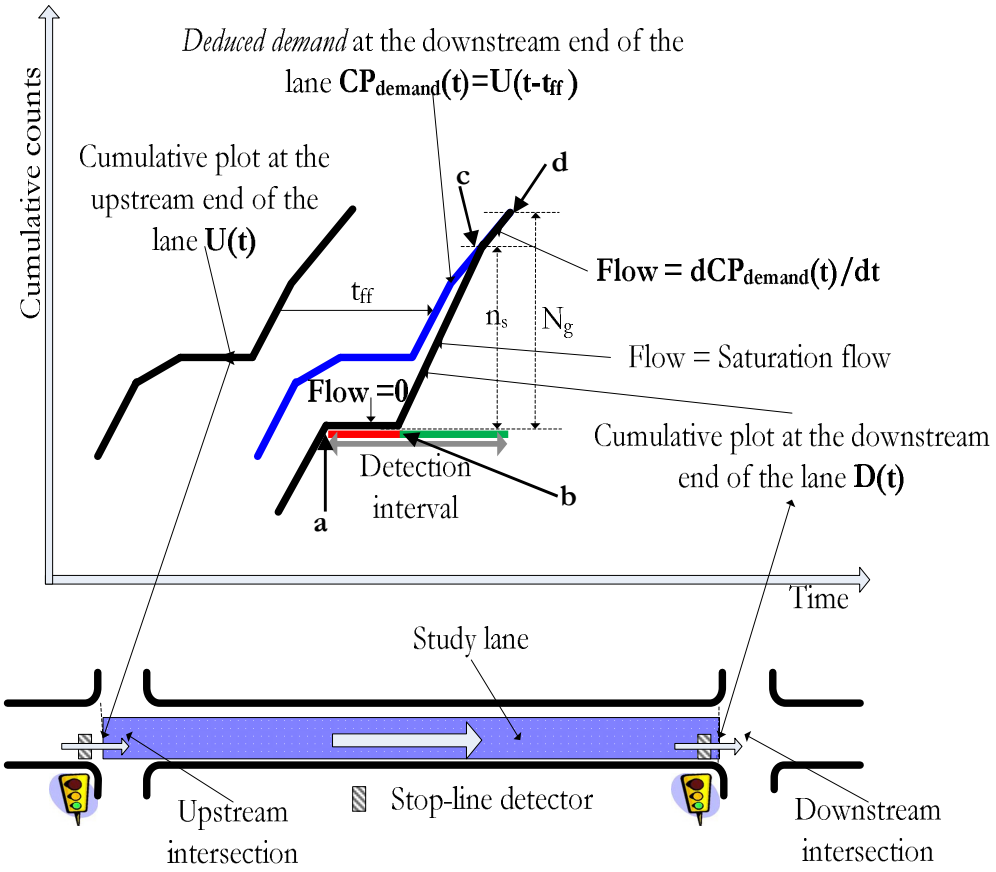

Figure 3-6: Estimation of D(t) for Case-DSS with *deduced demand* from U(t).

In Figure 3-6, the known parameters are:

i. the upstream cumulative plot, U(t);

ii. reference position for the D(t) (position *a* in the figure);

iii. signal timings at downstream intersection; and

iv. counts from the downstream end of the link (N_g).

Flow pattern at downstream intersection for the current detection interval is unknown. This is obtained by:

i. no flow during red period (*a* to *b*);

ii. during green period, the flow is at saturation flow until $CP_{demand}(t)$ is greater than D(t) (*b* to *c*); and thereafter flow follows the demand pattern (*c* to *d*).

Note: The flow pattern is estimated for each detection interval (Case-D and Case-DS) or for each signal cycle (Case-DSS) and the polyline for the cumulative plots is generated by cumulating the profiles from each estimation interval taking into account the residual queue from the last interval.

3.3 Model testing

The model is tested using a microscopic traffic simulator, AIMSUN (Barceló et al., 2005) (Refer to Appendix C). The use of simulation software for research is increasing, as they can efficiently represent the real world situation and reproduce its behavior. For realistic representation of the network and reproduction of the network behavior, the parameters for simulation model need to be calibrated. For a calibrated network, different scenarios can be simulated and the methodology can be tested for each scenario.

The three different AIMSUN API modules (*see* Figure 3-7) developed are for extraction of: a) signal controller data (i.e., signal phases and its corresponding time); b) detector data (i.e., detector counts for each detection interval); and c) individual vehicle travel data (i.e., time when vehicle is observed at upstream and downstream location). Detector data and signal data are inputs to the model for travel time estimation, which estimates average travel time for different intervals. Finally, the model is verified by comparing the average travel time estimated with the actual average travel time obtained from the individual vehicle API module.

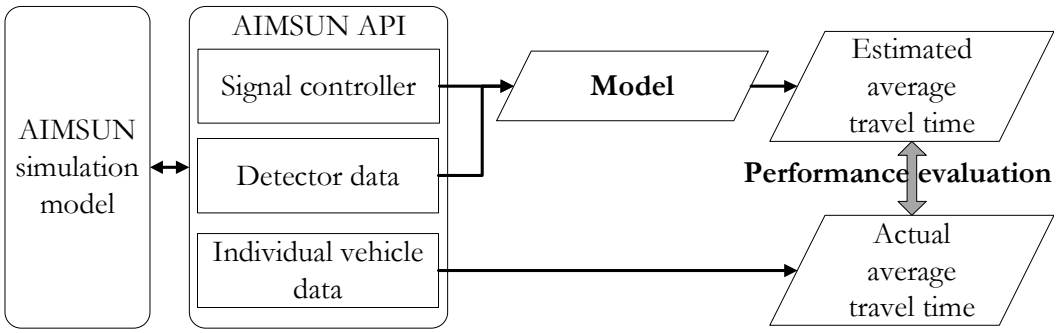

Figure 3-7: Architecture for model testing using AIMSUN.

The model is applied on a single lane link between two consecutive signalized intersections (*see* Figure 3-8). In the current analysis, flow from three different directions at upstream intersection and a through movement at downstream intersection is considered. Scenarios for different degrees of saturation in the range of 0.5 to 1.2 at downstream intersection are simulated.

The performance of the model, defined in terms of accuracy (%) (3.8), is evaluated for different detection intervals from 10 s to 360 s.

$$MAPE = \frac{\sum_{i=1}^{N} \frac{\left| actual_i - estimated_i \right|}{actual_i}}{N} \tag{3.7}$$

$$Accuracy(\%) = (1 - MAPE) * 100 \tag{3.8}$$

Where: N is the total number of time intervals;

$Actual_i$ and $estimated_i$ are the average actual travel time and average estimated travel time for each time interval, respectively;

The results presented here are from simulation with signal cycle time of 120 s and green split of 0.5 at both upstream and downstream intersection. Average travel time for 6 min (three times the signal cycle time) is estimated from simulation of one hour for each scenarios mentioned above.

For oversaturated situation if links are short then the queues are likely to extend to the upstream end of the link. Such situation will affect the saturation flow rate at the upstream intersection and therefore for Case-DSS, the saturation flow rate has to be appropriately corrected. It should not affect the estimation for Case-D and Case-DS. The aim of the current analysis for Case-DSS is to test the methodology for a given saturation flow rate and therefore

a constant saturation flow rate is considered for study link of around a kilometer in length. It makes sure that queue on the study link does not extend to the upstream end of the link.

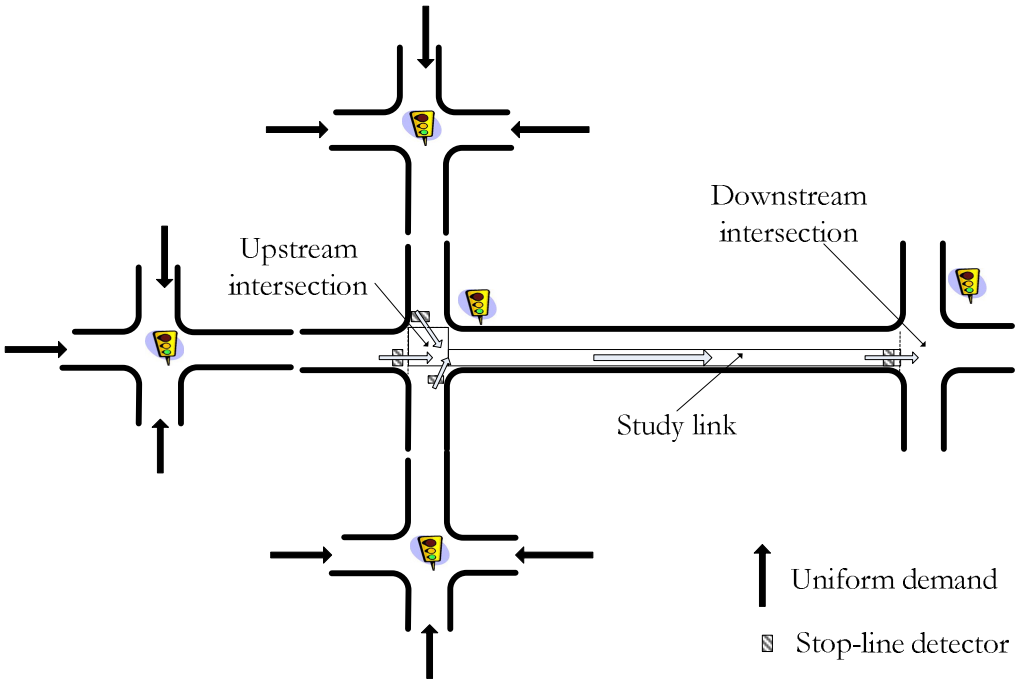

Figure 3-8: Test bed for model testing on a single link between two consecutive signalized intersections.

Figure 3-9 represents the graphs for detection intervals versus accuracy for the three cases. Each point on the graph represents the average of the accuracies obtained from different degree of saturation for a given detection interval. As expected, short detection intervals have higher accuracy levels irrespective of the cases and for detection intervals less than 30 s the estimation is very accurate. Detection interval is not critical if signal timings are available. Comparable accuracy can be obtained from:

i. Detector data from larger detection intervals with signal timings; and

ii. Detector data from shorter detection intervals without signal timings.

If detection interval is short, then signal timings and saturation flow rate are not required. For Case-D, the performance is not consistent for different detection intervals and in the present analysis the accuracy drops significantly to 80% when detection interval is close to integral multiple of signal cycle for instance 120 s, 240 s and 360 s. This inconsistency in the performance for Case-D is analyzed in the next section.

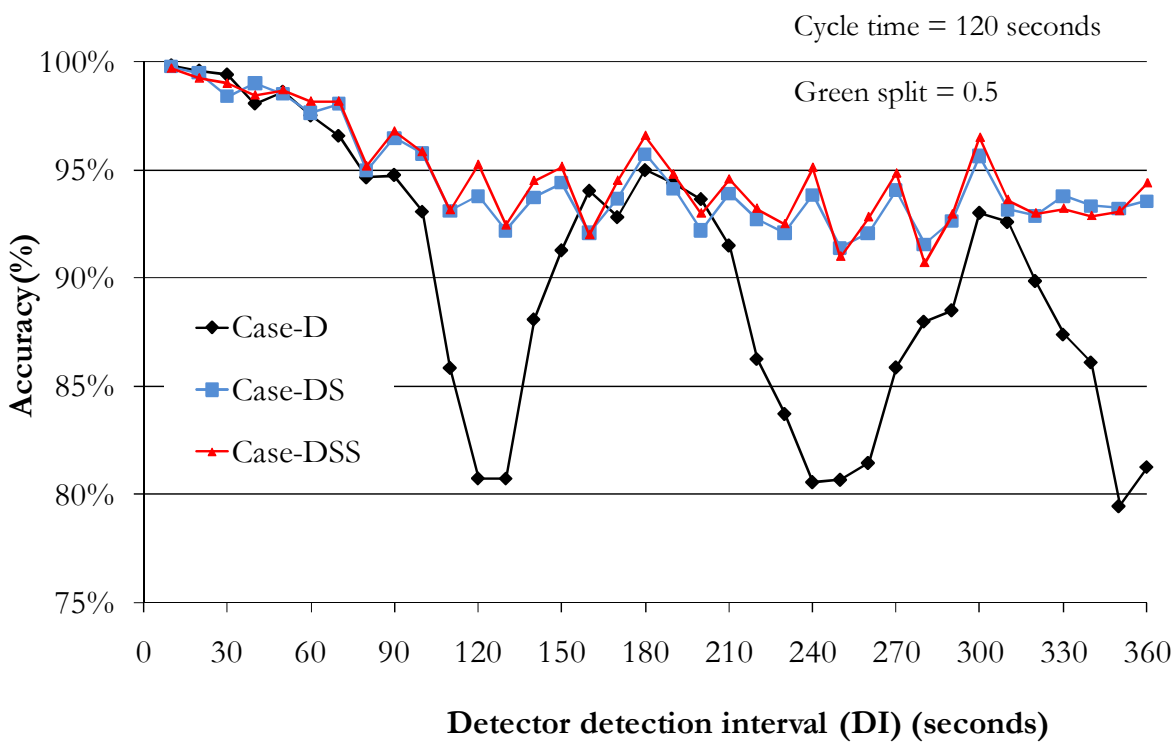

Figure 3-9: Comparative overview of the performance evaluation of the three cases (Case-D, Case-DS and Case-DSS).

3.3.1 Discussions on the results for Case-D

Fluctuations in the flow from certain combinations of signal phases in the detection interval can result in significant error in the travel time estimation from the cumulative plots generated under Case-D. To study this, let us consider a detection interval equal to signal cycle time. Four different combinations of signal phases in the detection interval are possible:

i. RG combination: red period followed by green period;

ii. GR combination: green period followed by red period;

iii. RGR combination: green period between two red periods; and

iv. GRG combination: red period between two green periods.

In Figure 3-10, for Case-D, the U(t) estimated for: a) RG combination has tendency to overestimate travel time; and b) GR combination has tendency to underestimate travel time. Whereas, in Figure 3-11 the U(t) estimated based on: a) RG combination has tendency to underestimate travel time; and b) GR combination has tendency to overestimate travel time. For RGR combination, the estimation for both U(t) and D(t) profiles can be either underestimated, overestimated or exact.

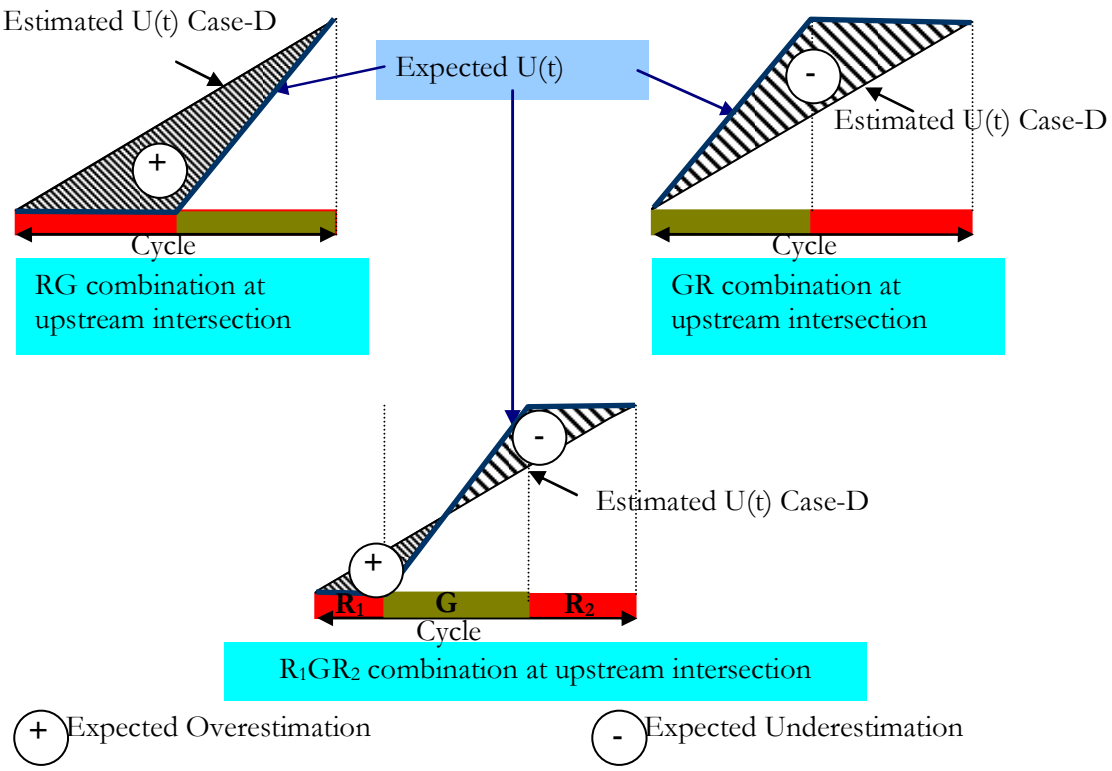

Figure 3-10: Upstream flow profile with detector detection interval equal to signal cycle at upstream intersection.

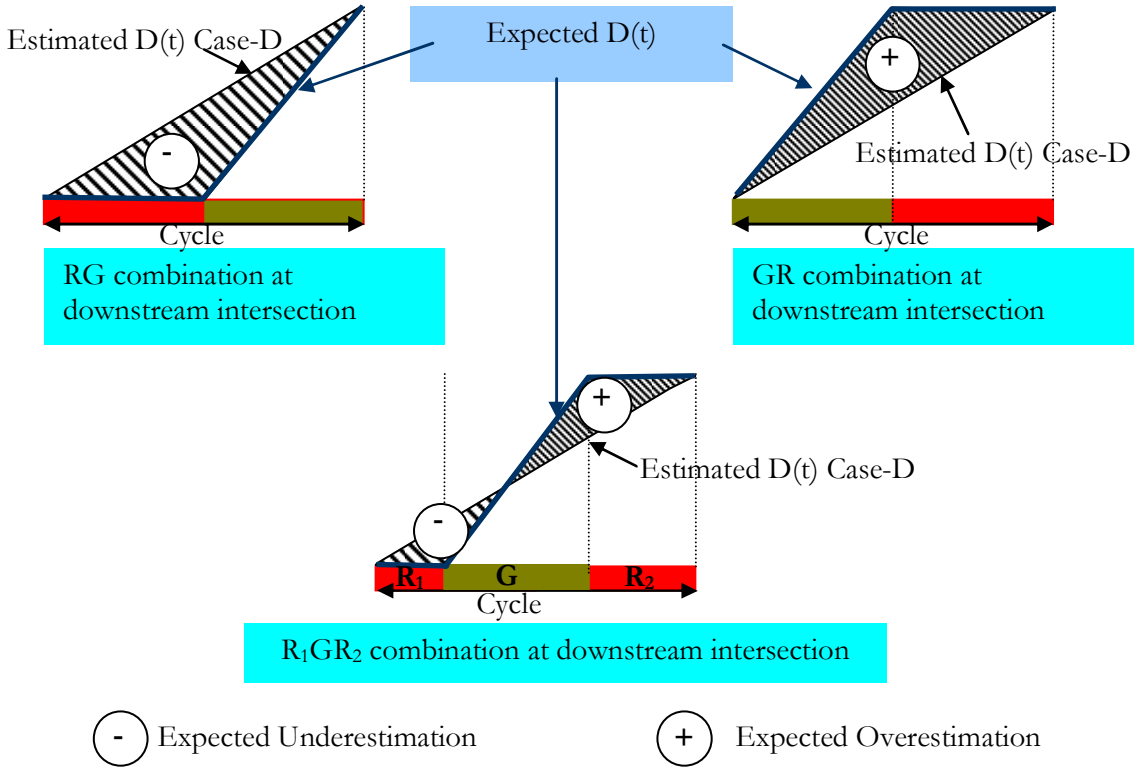

Figure 3-11: Downstream flow profile with detector detection interval equal to signal cycle at upstream intersection.

Figure 3-12 represents graph of actual average travel time versus estimated average travel time obtained from simulating following four different combinations of signal phases in the detection interval: a) RG_GR (++) combination; b) GR_RG (--) combination; c) GR_GR (-+) combination; and d) RG_RG (+-) combination. Here, RG_GR (++) combination represents red phase followed by green phase in the detection interval at upstream intersection whereas, green phase followed by red phase in the detection interval at downstream intersection and so for others.

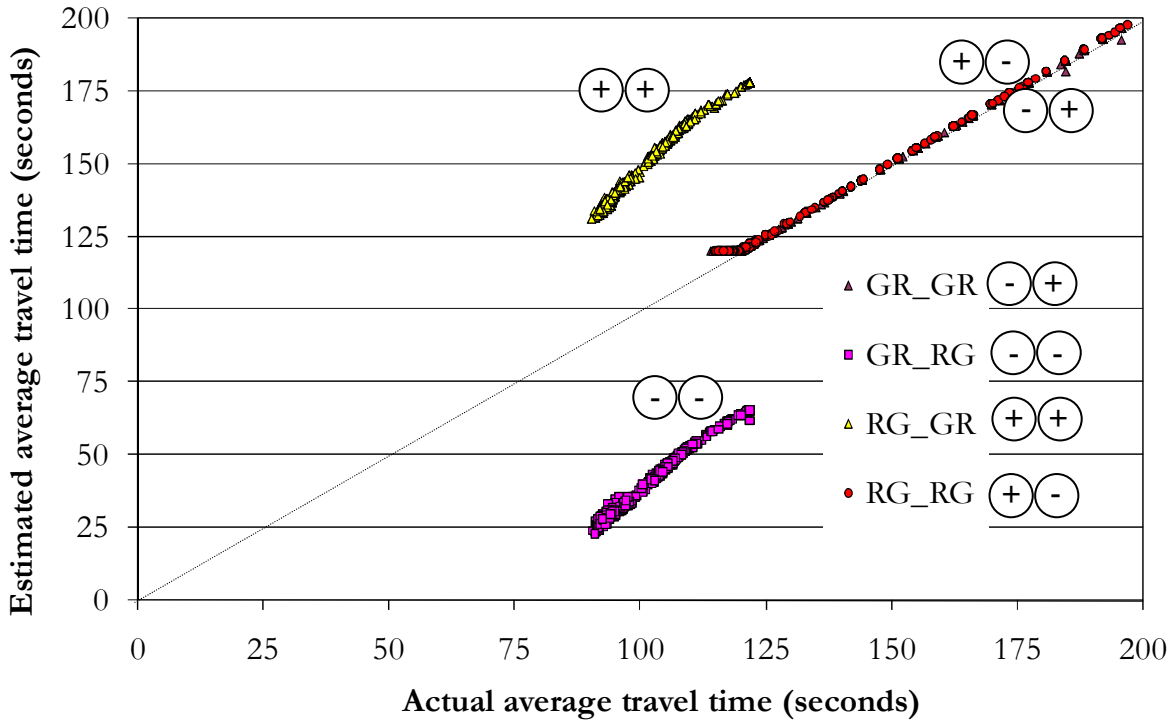

Figure 3-12: Performance for Case-D under different combination of signal phases in the detection interval.

The RG_GR (++) combination has the tendency to highly overestimate travel time. Conversely, GR_RG (--) combination has the tendency to highly underestimate travel time. In the present example, the GR_GR (-+) and RG_RG (+-) combinations results in exact estimation because the underestimate travel time at upstream is compensated by the overestimate travel time at downstream and vice versa.

The results presented in Figure 3-9 are from GR_RG (--) combination. Therefore when detection interval is integral multiple of signal cycle (120 s, 240 s and 360 s) then there was decrease in accuracy. We run the simulation for GR_GR (-+) combination (*see* Figure 3-13). In this case when detection interval is integral multiple of signal cycle time then the accuracy is good. The performance for Case-D is highly sensitive to the signal phases in the detection interval. When detection interval is integral multiple of signal cycles then there is huge

inconsistency in travel time estimation for Case-D. This means that when only detector data is available, detection interval should be carefully chosen in order to provide reliable travel time information from this data.

The performance for Case-DS and Case-DSS is consistent and is not sensitive to the signal phases in the detection interval. The accuracy is generally more than 95% and is within the acceptable limits. The integration of detector data with signal controller has the potential to improve the accuracy with better confidence in estimation.

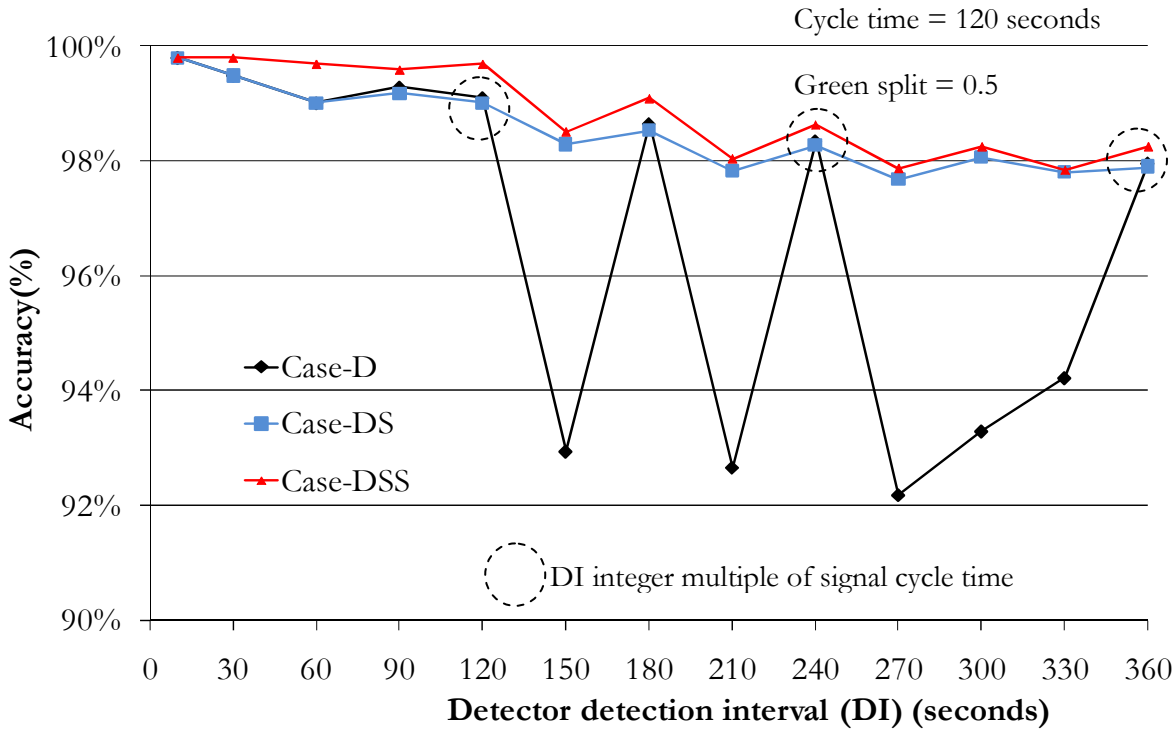

Figure 3-13: Accuracy versus detector detection interval graphs for three different cases on data availability with GR_GR (-+) combination.

These findings are further confirmed by sensitivity analysis of the model with respect to different parameters in the following section.

3.4 Sensitivity analysis

The cumulative plots generated for Case-DSS are realistic and accurate (*see* Figure 3-14), whereas for Case-D they are simplest but with inconsistency in the performance for travel time estimation.

The sensitivity analysis for Case-D and Case-DS is performed, considering Case-DSS as a reference, and with a goal to determine:

i. the parameters which contribute to the inconsistency; and

ii. the values of the parameters for which the model is most accurate and reliable.

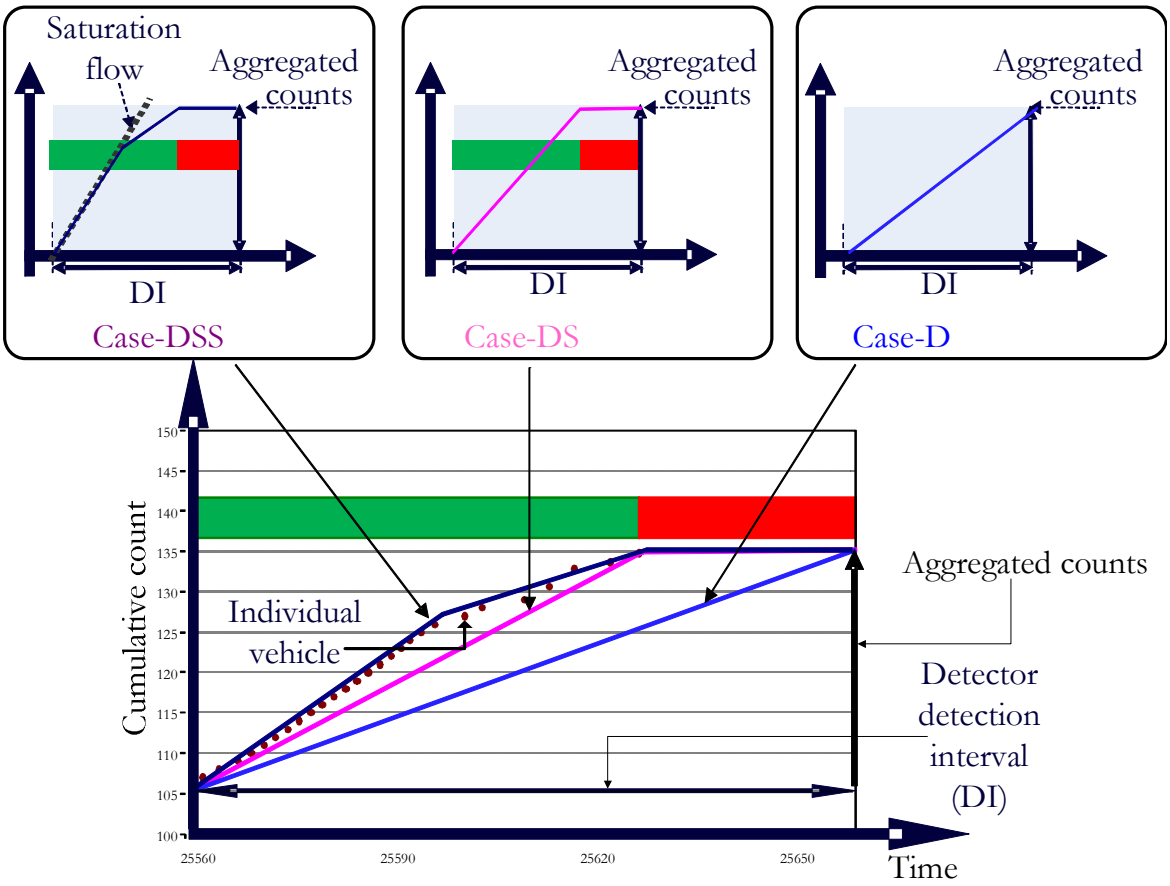

Figure 3-14: Illustration of cumulative plots for different cases and individual vehicle identification.

Following parameters are considered for the analysis:

i. Detection Interval: defined by variables β*c, where β is a rational number and c is signal cycle time.

ii. Signal green time: defined by variable g. It can be shown that as the green split (g/c) increases Case-D and Case-DS approaches Case-DSS.

iii. Sequence of signal phases in the detection interval defined by variables α*c ($0 \leq \alpha \leq 1$) which is the time from the start of the detection interval to the start of the green period within the detection interval or in other words it is the offset of the green with respect to detection interval.

For a given detection interval and signal timings there can be different patterns of signal timings within the detection interval. Figure 3-15*a*, represents different patterns of signal timings within a detection interval. These patterns determine the shape of the cumulative plot for Case-DSS. For consecutive detection intervals these patterns will change from one detection interval to another, except for detection interval which is integral multiple of signal cycle. However, for fixed signal cycle with rational value of β, the pattern will repeat itself after certain time. For instance, in Figure 3-15*b* where β = 1.5 third pattern is similar to first pattern.

iv. Degree of saturation (X): The degree of saturation determines the proportion of counts in the saturation flow rate and hence the shape of plots for Case-DSS.

To make the analysis valid for any cycle time the above defined variables are normalized with signal cycle time (c).

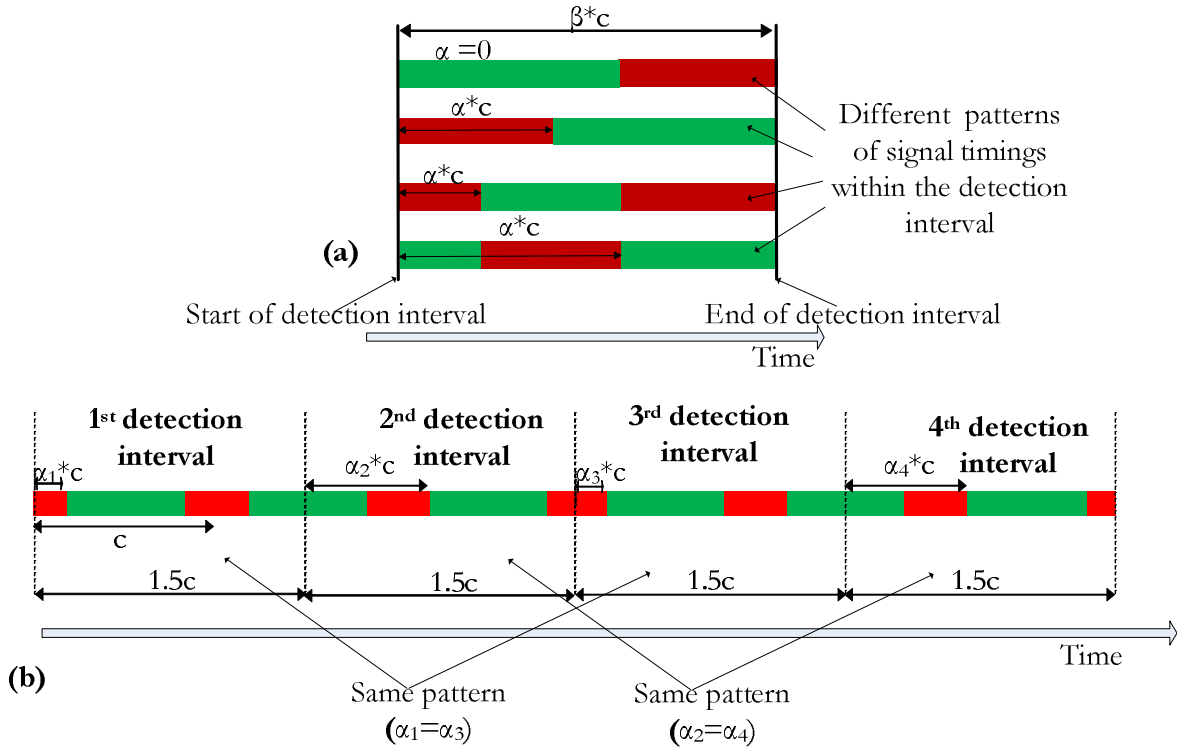

Figure 3-15: Illustration of (a) several patterns of signal timings within a detection interval; and (b) patterns for consecutive detection intervals with β = 1.5.

For model testing, the performance was evaluated by comparing the estimated and actual travel time using traffic simulation on a network. In this section for sensitivity analysis, we evaluate the deviation of cumulative plot for Case-D (Case-DS) from that of Case-DSS

(assuming uniform demand) and estimate the corresponding accuracy in the travel time estimation by simple geometry. To explain the methodology for sensitivity analysis we consider an example (*see* Figure 3-16). For travel time estimation one is interested in the area between the cumulative plot for upstream (U(t)) and downstream (D(t)). The shape of the plot is defined by the parameters: β, g/c, α and X. In the figure, the performance for U(t), is evaluated for a scenario where (($\alpha + g/c \leq 1$) and (($1 + \alpha + g/c$) $< \beta \leq 2$) and ($X < 1$)).

The accuracy for a combination of the parameters is defined as follows:

$$Accuracy(\%) = \left(1 - \frac{\left|Area_{Case\text{-}DSS} - Area_{Case\text{-}D}\right|}{Area_{Case\text{-}DSS}}\right) * 100 \qquad (3.9)$$

Where: $Area_{Case\text{-}DSS}$ and $Area_{Case\text{-}D}$ are the areas under the plots for Case-DSS and Case-D, respectively as presented in the figure.

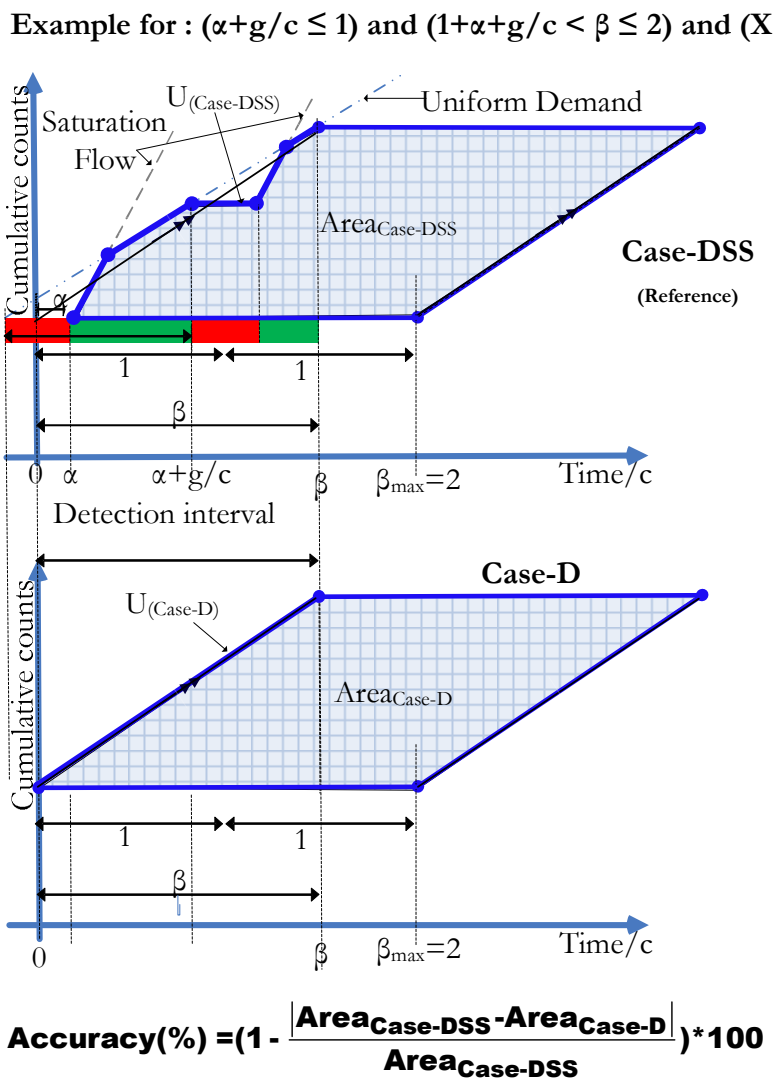

Figure 3-16: Example for evaluation of Case-D with Case-DSS as a reference.

The analysis is performed for $0< \beta \leq 2$; $0.5 \leq g/c \leq 0.9$; $0 \leq \alpha \leq 1$ and $0.5 \leq X \leq 1.2$. The performance of the model is defined in terms of accuracy (%) and standard deviation (σ^2). The accuracy (standard deviation) presented for a parameter (say β) is the 5^{th} percentile (standard deviation) of the accuracies (3.9) obtained from different scenarios considering all possible combinations with other parameters (g/c, α and X). So, accuracy is the minimum accuracy for 95% of the scenarios and standard deviation is an indicator for the relative reliability of the model. Higher standard deviation indicates lower reliability and vice versa.

3.4.1 Sensitivity analysis: Case-D

3.4.1.1 Sensitivity with respect to β

Case-D is highly sensitive to detection interval and β is identified as a critical parameter. Figure 3-17*a* and Figure 3-17*b* represent graphs for accuracy and σ^2 versus β, respectively. The accuracy decreases from more than 95% to less than 85% with increase of β from 0 to 1, respectively and thereafter it increases(> 90%) till β = 1.5 and decreases again to less than 85% for β close to 2. On the contrary, σ^2 monotonically increases for $0 < \beta < 1$ and $1.5 < \beta < 2$ and decreases for $1.5 < \beta < 2$ (Figure 3-17*b*). This indicates that the Case-D is least reliable when β is close to an integer (1 and 2) and for $1 \leq \beta \leq 2$ the Case-D is most accurate and reliable when β is close to 1.5.

3.4.1.2 Sensitivity with respect to g/c

Figure 3-17*c* and Figure 3-17*d* represent graphs for accuracy and σ^2 versus g/c, respectively, for β equal to 1, 1.5 and 2. The graphs for β equal to 1 and 2 are the same. Accuracy increases and σ^2 decreases (reliability increases) with increase of g/c. For high g/c (> 0.85) Case-D is relatively insensitive to β and accuracy is more than 95% (Figure 3-17*c*). Whereas, for lower g/c (<0.4) Case-D is highly sensitive to β. Relatively higher value of σ^2 (Figure 3-17*d*) for β equal *1* and *2* is consistent with the results of the sensitivity analysis for β i.e., Case-D is least reliable for integer values of β and most reliable for β around *1.5*.

3.4.1.3 Sensitivity with respect to α

Figure 3-17*e* and Figure 3-17*f* represent graphs for accuracy and σ^2 versus α, respectively, for β equal to 1, 1.5 and 2. For β equal 1.5 (*see* Figure 3-17*e*), the accuracy is generally more than 90% whereas, for β equal 1 and 2, there is a significant fluctuation in the accuracy from less than 75% (for α around 0.85) to more than 90% (for α around 0.3). As said earlier, for consecutive detection intervals with fixed signal timings the pattern of signal timings (α) within a detection interval is constant for integral values of β. The sensitivity of Case-D to α for integral values of β, makes it unreliable for such values of β. However, if tuned properly by choosing an appropriate α (e.g. $\alpha = 0.3$) it can give good estimations.

3.4.1.4 Sensitivity with respect to X

Figure 3-17*g* and Figure 3-17*h* represent graphs for accuracy and σ^2 versus *X*, respectively, for β equal to 1, 1.5 and 2. Relatively Case-D is less sensitive with respect to X and the accuracy increases by 2% for increase in X from 0.5 to 1. The relatively higher value of σ^2 (Figure 3-17*h*) for β equal to 1 and 2 is due to low reliability of Case-D for integer β.

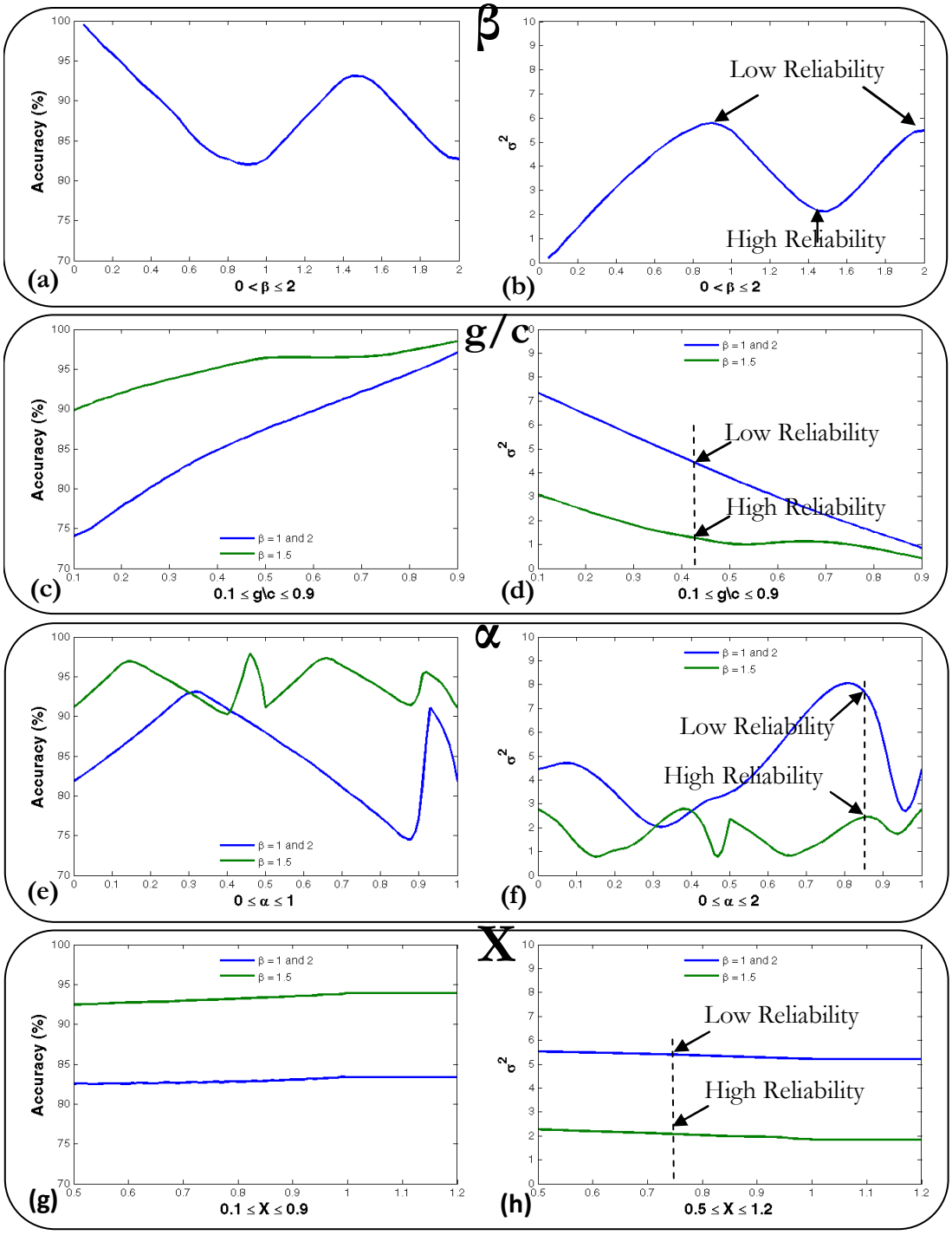

Figure 3-17: Results of the sensitivity analysis for Case-D with Case-DSS as reference.

3.4.2 Sensitivity analysis: Case-DS

The difference between Case-DSS and Case-DS is that Case-DSS considers saturation flow rate, and its flow profile depends on demand pattern, green split and degree of saturation. Similarly to the sensitivity analysis for Case-D, the sensitivity analysis for Case-DS is performed considering Case-DSS as reference and the results are presented in Figure 3-18. It

is found that the accuracy for Case-DS is generally higher than 94% (σ^2 < 2%) and is slightly sensitive to the parameters.

Similarly to Case-D, for $1 \leq \beta \leq 2$ the highest accuracy and reliability are for β close to 1.5 (Figure 3-18*a* and Figure 3-18*b*). For $0.1 \leq g/c \leq 0.5$ the accuracy drops from more than 99% to 96% and for $0.5 \leq g/c \leq 0.9$ the accuracy increases back to 99%. Case-DS is almost insensitive to α and there is slight decrease in accuracy and reliability for $0.75 \leq \alpha \leq 0.85$. Accuracy and reliability of the Case-DS actually increases with the increase in the degree of saturation (Figure 3-18*g* and Figure 3-18*h*). For X ≥1, all the counts are in saturation flow and Case-DS is same as Case-DSS (100% accuracy).

As the accuracies are generally more than 94% with σ^2 less than 2%, it is reasonable to conclude that Case-DS is generally consistent with Case-DSS and even in the absence of saturation flow rate information one could obtain travel time with reasonable accuracy by integrating detector data with signal controller data.

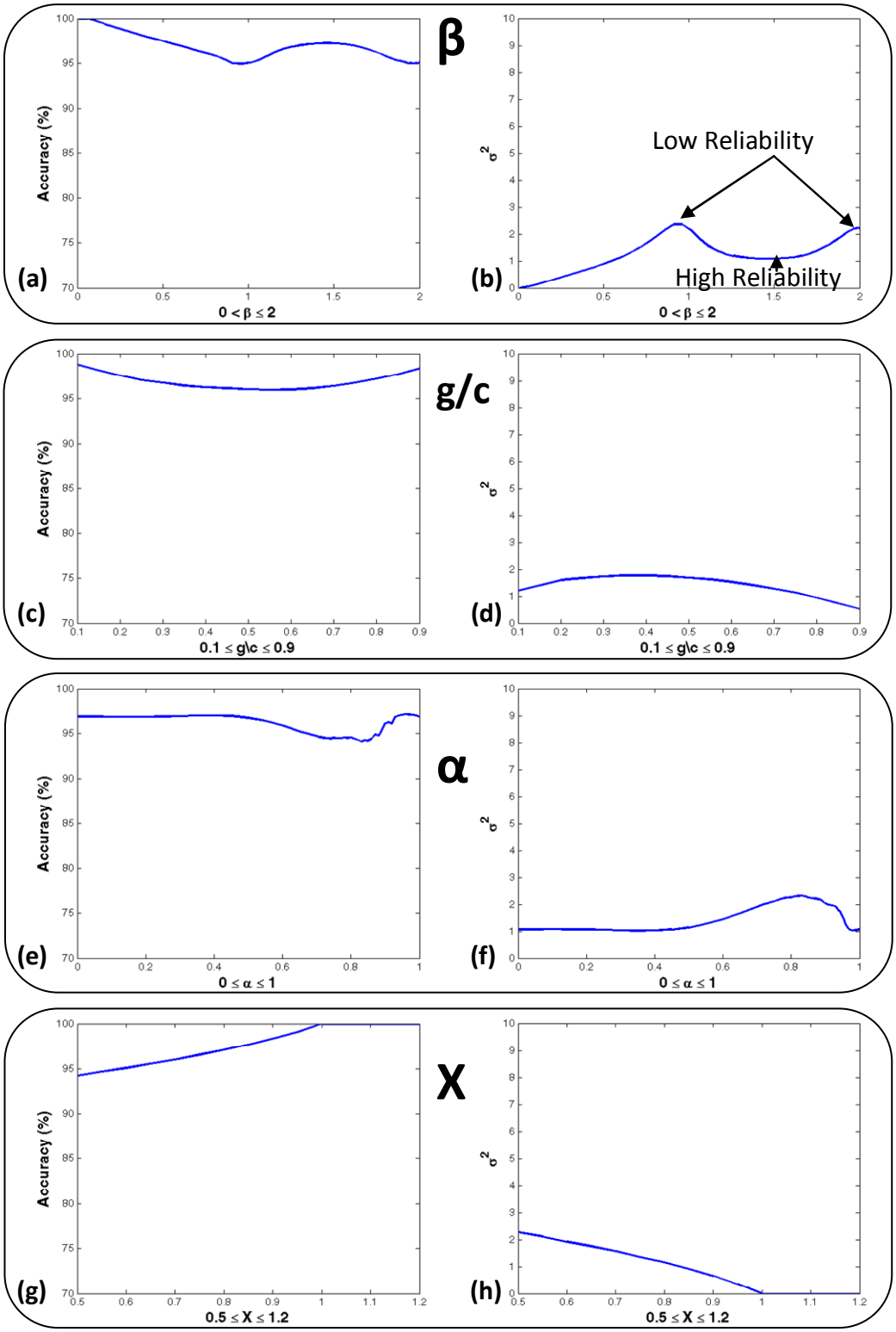

Figure 3-18: Results of the sensitivity analysis for Case-DS with Case-DSS as reference.

3.4.3 Explanation for the findings

The reason for low reliability at integer values of β and high accuracy for β around 1.5 can be explained with a help of an example.

Let us consider $\beta = 1.5$ (*see* Figure 3-19*a*) with different patterns of signal timings ($\alpha = 0$, *g/c, 0.5*(1-g/c), (1-0.5*g/c))* and compare deviation of the areas for travel time estimation from flow profiles under Case-D and Case-DS. Then, for Case-D, there is always a counter balance for underestimation or overestimation of area, which explains the improvement in accuracy.

However, for $\beta = 1$ (*see* Figure 3-19*b*), with $\alpha = 0$ and $\alpha = g/c$ there is either underestimation or overestimation with no counter balance area (lowest accuracy) and for $\alpha = 0.5*(1-g/c)$ and *(1-0.5*g/c)* there is a perfect balance of areas (highest accuracy). Therefore, for integer values of β, the estimation can range from perfect to worst which accounts for its low reliability.

In the above qualitative comparison we have considered Case-DS as a reference instead of Case-DSS due to simplicity in illustration of flow profiles. Consideration of flow profiles for Case-DSS will not affect the above qualitative comparison.

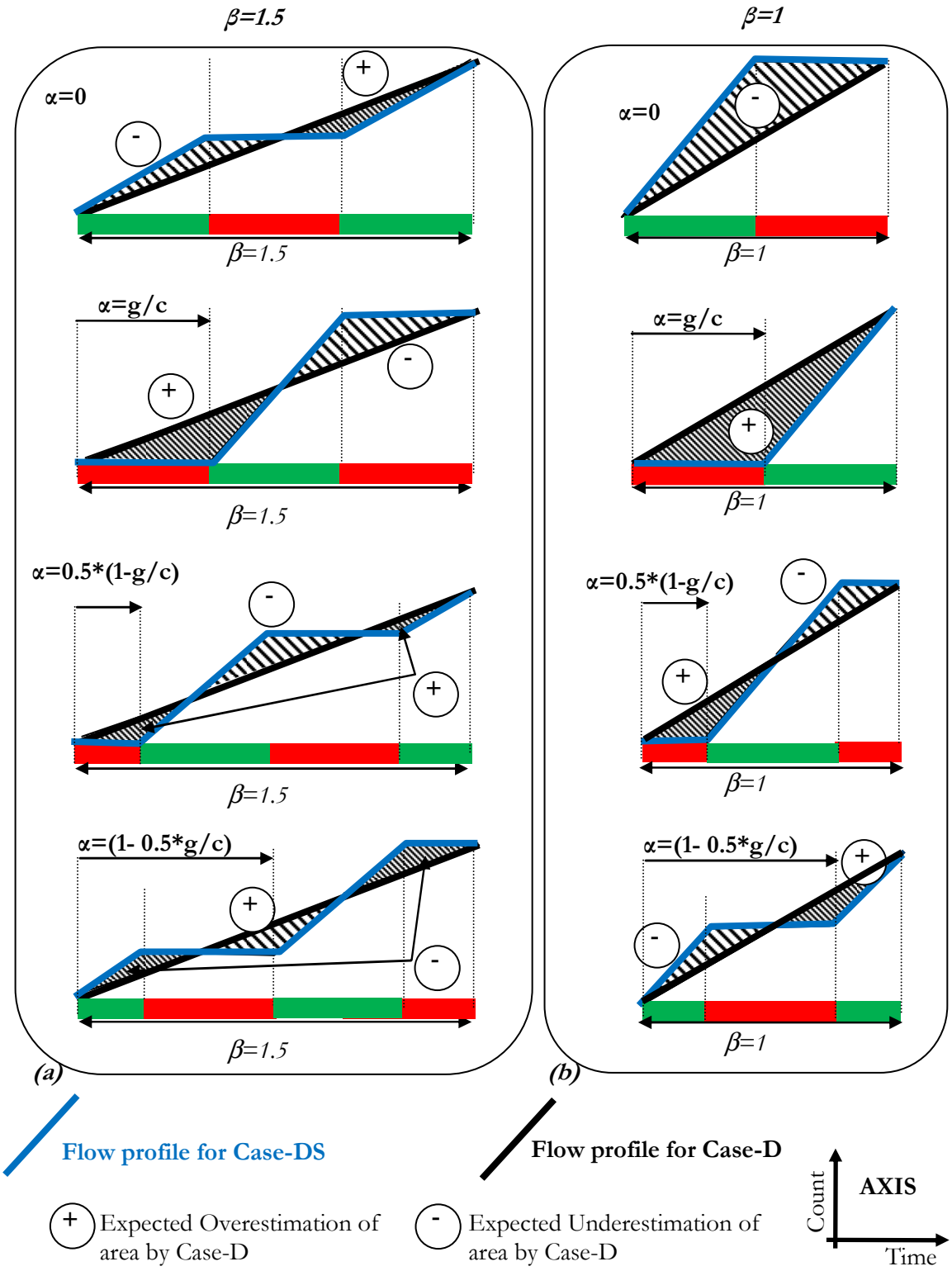

Figure 3-19: Deviation in area for travel time estimation of Case-D from Case-DS under different values of α and for (a) β=1.5 and (b) β=1 (assuming area to the right of cumulative plot is of interest).

3.5 Concluding remarks

This chapter explores three models for generation of cumulative plots: a) Case-D, when only detector data is available; b) Case-DS, when detector data and signal timings are available; and c) *Case-DSS*, when detector data, signal timings and saturation flow rate are available.

It can be concluded that theoretically if: a) stop-line detectors are present on all the lanes that contribute to cumulative plots; b) detectors provides accurate counts and mid-block source and sinks are absent; c) real turning proportions are known, then the integration of detector data with signal controller data provides accurate cumulative plots for travel time estimation.

When signal timings and saturation flow rate are available (Case-DSS), the estimation is very accurate and can be used as a reference. For the other cases, sensitivity in accuracy is tested depending on four parameters ((1) β, for the detection interval, (2) g/c, for the green split, (3) α, for offset between detection interval and green period, and (4) X, for degree of saturation).

When signal timings are available (Case-DS), the accuracies are generally more than 94% with σ^2 less than 2%, so it is reasonable to conclude that even in the absence of saturation flow rate information one should obtain travel time with reasonable accuracy by integrating detector data with signal timings.

In fact, with small values of β, accuracy is close to perfection in Case-D also. Yet, the sensitivity analysis for $1 \leq \beta \leq 2$ indicates that Case-D is highly sensitive to detection interval. For β around 1.5, the model is most accurate with high reliability, whereas, for β close to 1 and 2, the model is least accurate with low reliability. For Case-D, what matters is not how frequent the data is collected, but how the detection interval is related to signal timings. For instance, if signal cycle is two minutes and data is collected for four minutes interval then one can argue that for better confidence in travel time estimation one can collect the data for five minutes instead of four minutes which is twice the signal cycle.

X has relatively little impact on the sensitivity of Case-D. As for g/c and α, they are the two secondary most important factors for the sensitivity of Case-D; that is when β is close to 1 or 2.

The explanations for these findings are also provided, which enable us to generalize the results when only detector data is available. For $\beta > 2$, detection interval should be chosen such that β is close to the half of an odd number (e.g., 2.5, 3.5, 4.5, etc.), because of high accuracy and more stability. On the contrary, integral values of β should be avoided because

of its low reliability. If β is close to an integer, then accuracy and reliability can still be improved with high *g/c* or choosing α = 0.3. This generalization is consistent with the simulation results presented in model testing section for $1/12 \leq \beta \leq 3$, *g/c* = 0.5 and α = 0.

The performance of the model is encouraging and the extension of the model to consider presence of *relative deviation amongst cumulative plots* is presented in the next chapter.

4 CUPRITE development and testing

In the previous chapter, methodology to estimate cumulative plots by integrating detector data with signal timings was introduced. In this chapter, the methodology is further extended and cumulative plots are integrated with probe vehicle data with the aim to reduce the *relative deviation amongst the cumulative plots*. The developed methodology is also thoroughly tested for different scenarios.

4.1 Issue: Relative deviation amongst cumulative plots (RD)

The issue of relative deviation amongst the cumulative plots (also termed as "drift") is critical in the application of cumulative plots as can be figured out from the following section.

4.1.1 Effect of mid-link sinks and sources on cumulative plots

An urban link can have different mid-link infrastructures such as, a side street, parking etc. Depending on the time of the day and day of the week, these mid-link infrastructures can act as sink, source or both. A parking can acts as both source and sink, whereas, one way side street is either a source or a sink. A significant proportion of the flow can be from a mid-link source or to a mid-link sink. This proportion is a dynamic entity i.e., varies with time, and one can easily observe, on average, around 10% loss (or gain) of flow (or from) a side street.

Figure 4-1, illustrates an example where 300 vehicles are observed at upstream and 10% of the vehicles are lost in the mid-link sink (one-way side street) resulting in only 270 vehicles observed at downstream. By integrating the detector data with signal controller data one can obtain the cumulative plots at both upstream, $U_o(t)$, and downstream, $D(t)$, location. The counts at upstream are also contributed by the vehicles which are lost in the mid-link sink. Assuming that one can obtain $U_r(t)$- the revised cumulative plot at upstream based on the vehicles which traverses the whole link i.e., excluding the vehicles which are lost in the sink. The area between $U_r(t)$ and $D(t)$ represents the true actual total travel time for the vehicles that depart at downstream. However, practically $U_r(t)$ is unknown (The vehicles lost in the

mid-link sink are random and unknown.) and the area between $U_o(t)$ and D(t) is estimated, this leads to the error in total travel time estimation which is represented by the shaded area in the figure. Comparing $U_r(t)$ with $U_0(t)$, we can say that $U_o(t)$ is overestimated resulting in relative deviation from D(t). If relative deviation is left unchecked, then the error can exponentially grow with time.

For a mid-link source, there will be more counts at downstream than that at upstream, i.e. $U_o(t) < D(t)$. In such situations area between the plots is negative and hence travel time cannot be obtained.

In this dissertation the above mentioned issue of **relative deviation amongst the cumulative plots is referred as RD.**

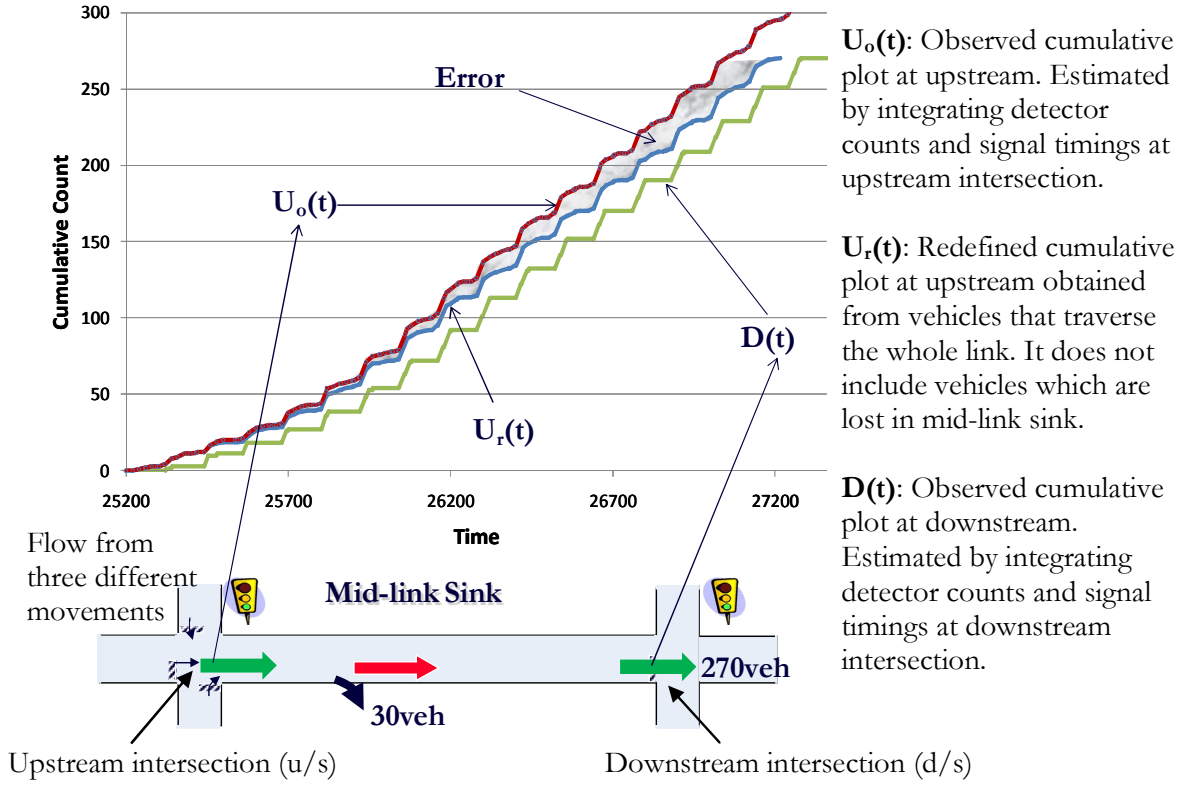

Figure 4-1: Illustration of the effect of mid-link sink on classical analytical procedure.

4.1.2 Detector counting error

The counts from the detector are not always accurate. These errors are mainly due to: a) Cross-talk; b) Pulse break up; c) Closely spaced vehicle; and d) Detector hanging (Refer to Appendix A, Section A.1.1.). These errors are random and its effect on cumulative plots is analogous to that of mid-link sinks and sources. For instance, say upstream detector on

average is overcounting by 10%, then the error represented in Figure 4-1 is analogous to what one would observe from detector counting.

4.2 CUPRITE development

4.2.1 Probe vehicle data and cumulative plots

Here probe vehicle is defined as the vehicle which can provide time stamp when at the intersection (position where cumulative plots are generated). Generally probe vehicle, such as taxi fleets, is equipped with GPS and can provide data for its position and time. There are issues related with probe vehicle such as frequency of data, map-matching of data, urban cannon etc. To address such issues is beyond the scope of this dissertation. We assume that the time when probe vehicle is at upstream (t_u) and downstream (t_d) intersection can be accurately obtained.

CUPRITE integrates the data from the probe with the cumulative plots (*see* Figure 4-2). Under FIFO traffic discipline the horizontal distance between the plots provides travel time for the i^{th} vehicle and the time when it is at upstream (t_U) and downstream (t_D). If we fix the probe information to the downstream cumulative plot i.e., $t_D = t_d$, then the probe vehicle is the i^{th} vehicle in the plots and we define $\Delta t = t_u - t_U$.

If there is no RD then for FIFO discipline Δt should be zero (*see* Figure 4-3*a*) and for non-FIFO discipline (*see* Figure 4-3*b*) Δt may or may not be zero. However, if we sum Δt for all the vehicles in the cumulative plots, then the summation ($\sum \Delta t$) should be zero, as presented in the example given in the figure. **Due to this property the area between the plots represents total travel time, as long as all the vehicles represented in U(t) are also represented at D(t).**

The above property of $\sum \Delta t = 0$ is when the summation is performed for all the vehicles (populations) represented in the cumulative plots. However, probe vehicles are only a random sample from the population. The objective here is to reduce the RD due to mid-link sinks and sources, and detector counting error etc. We make a hypothesis that RD can be reduced by fixing the probe information to D(t) (or U(t)) and redefine U(t) (or D(t)) such that property of $\sum \Delta t = 0$ is satisfied.

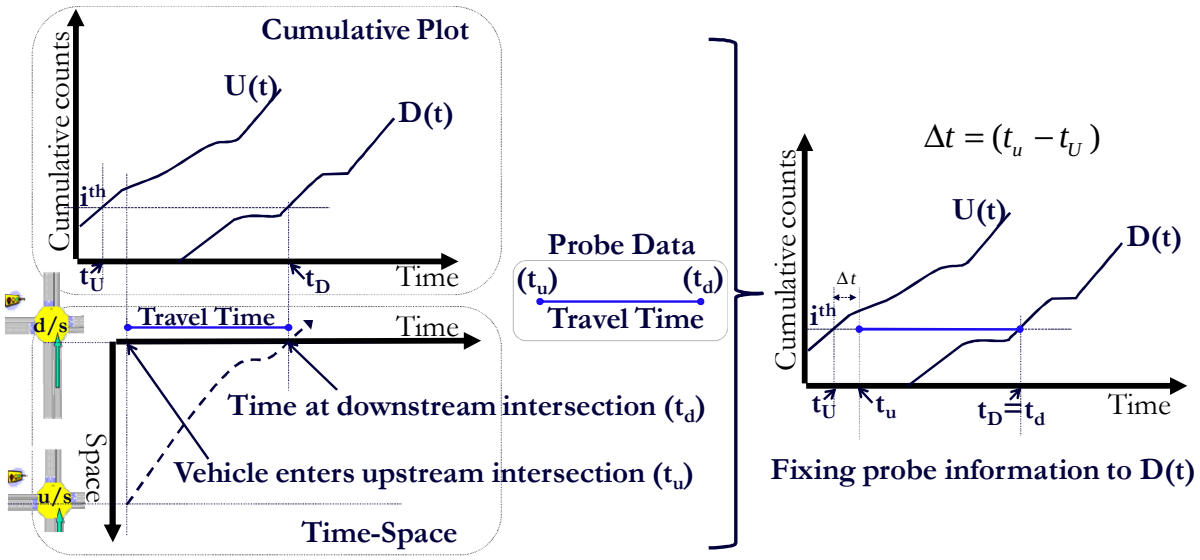

Figure 4-2: Probe vehicle and cumulative plots. Fixing probe information to D(t).

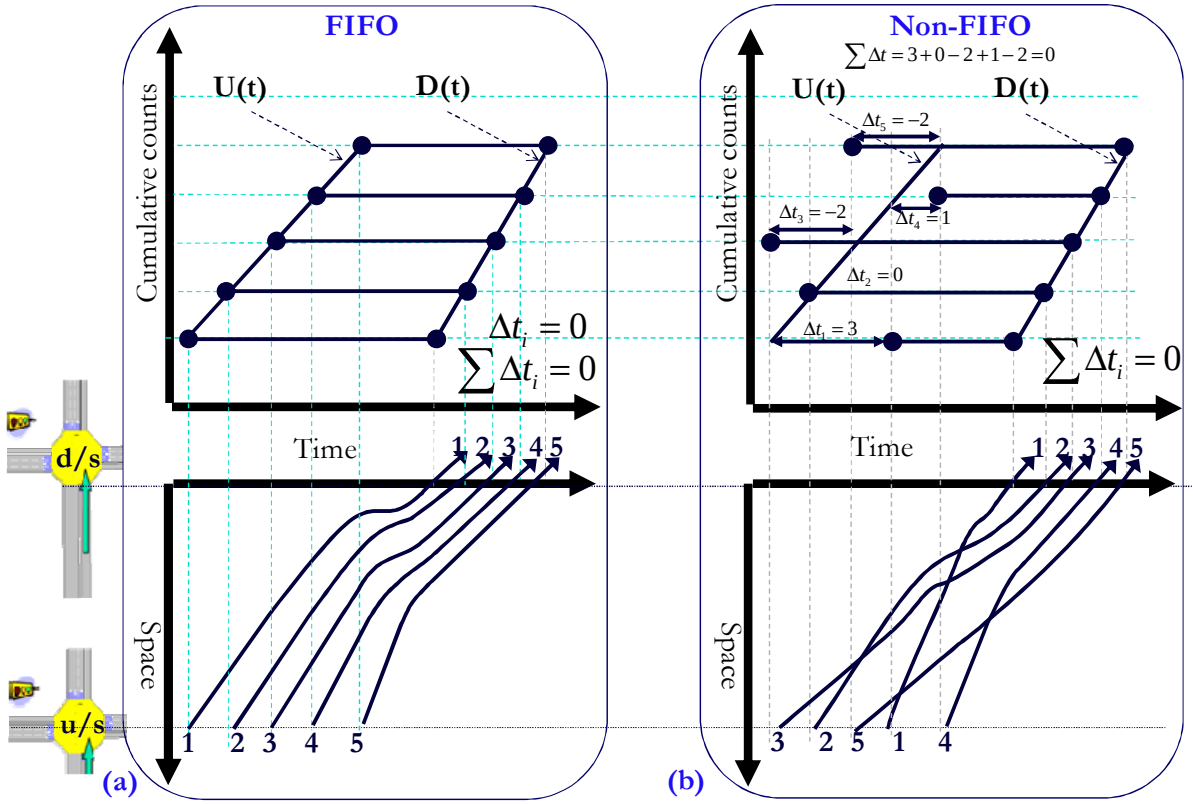

Figure 4-3: Relation between probe data (vehicle space-time trajectory) and cumulative plots for FIFO and non-FIFO situation.

Ideally, both U(t) and D(t) should be redefined to reduce the RD for instance, a scenario where downstream detector has counting error in addition to mid-link sink. However, simultaneous correction of the both is complicated. Here, the cumulative plots are obtained from stop-line detectors hence we are more confident in D(t) than in U(t) because the

estimation of U(t) depends on the link configuration at upstream intersection (This is discussed further in Section 5.1.). We only have a pair of cumulative plots at upstream and downstream and do not know which of the plot is responsible for RD. **To be consistent, in this dissertation we fix the probe to D(t) and redefine U(t) by defining the set of points through which U(t) should pass.**

4.2.2 How to redefine U(t)?

U(t) is redefined by:

i. First, integrating it with probe data (Section 4.2.2.1); and

ii. Finally making sure that *constrain in the cumulative plots* are satisfied (Section 4.2.3).

4.2.2.1 Integrating with probe data

The information from the probe is utilized to define points through which U(t) should pass. Say, we have: a) a reference point (t_{Ref}, U(t_{Ref})), i.e., the point in which we have confidence that it is a correct point on the plot; and b) point (t_p, Y_p) through which U(t) should pass. Then, (Refer to equations (4.1), (4.2) and (4.3); *see* Figure 4-4) we redefine U(t) by applying correction on it such that all points on the plot:

iii. Before time t_{Ref} have no correction;

iv. Between t_{Ref} to t_p are scaled vertically; and

v. Beyond t_p are shifted vertically so that the redefined curve is parallel to U(t) and is continuous with the points before time t_p.

$$U(t) = U(t) + Correction \tag{4.1}$$

$$Correction = \begin{cases} 0 & \forall\ t \le t_{Ref} \\ (scale - 1) * (U(t) - U(t_{\text{Ref}})) & \forall\ t_{Ref} < t < t_p \\ (scale - 1) * (U(t_p) - U(t_{\text{Ref}})) & \forall\ t \ge t_p \end{cases} \tag{4.2}$$

$$scale = \begin{cases} \dfrac{Y_p - U(t_{\text{Ref}})}{U(t_p) - U(t_{\text{Ref}})} & if\ U(t_p) \ne U(t_{\text{Ref}}) \\ 1 & if\ U(t_p) = U(t_{\text{Ref}}) \end{cases} \tag{4.3}$$

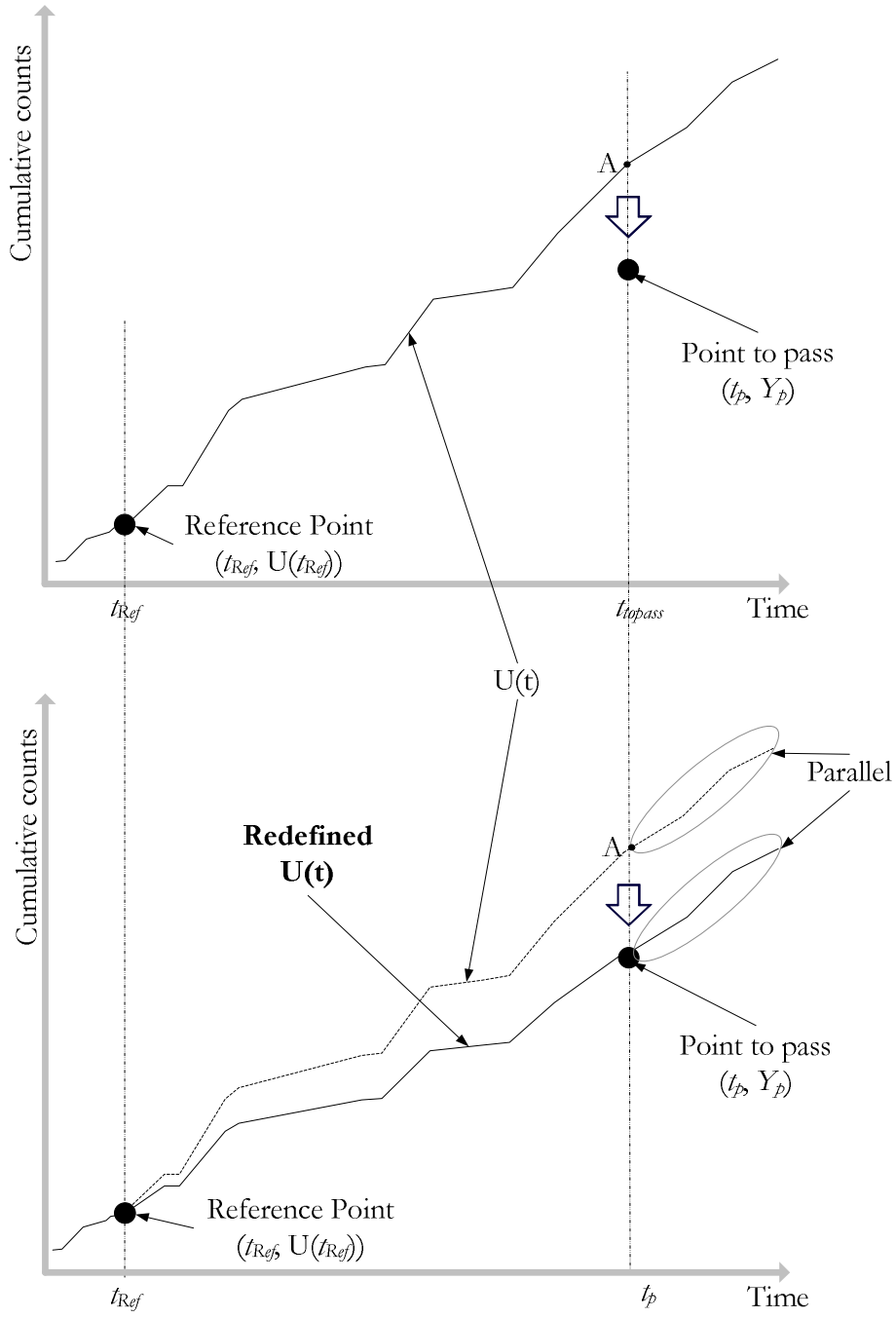

Figure 4-4: Redefining U(t) based on vertical scaling and shifting technique.

The concept behind above *vertical scaling and shifting* of the U(t) can be explained by an example. Refer to Figure 4-5*a*, has seven vehicles (*A* to *G*) detected at upstream (U(t)) and two of them (*C* and *D*) are for mid-link sink therefore, at downstream (D(t)) only five vehicles are detected. For simplicity assuming FIFO discipline. The rank of vehicles *E*, *F* and *G* are 5, 6 and 7 at U(t) and the 3, 4 and 5 at D(t), respectively. The presence of mid-link sink or mid-link source or detector counting error, only affects the rank of the vehicle in the plots which results in RD. In Figure 4-5*b*, the information for departing vehicle is fixed to D(t) and

thereafter U(t) is redefined. Before point *B* there is no change; between *B* and *E* it is scaled vertically; and after *E* it is shifted vertically. The vertical distance defines the magnitude of RD; hence the correction is applied only on the vertical axis (Cumulative counts) and not on the horizontal axis (Time).

The slope of the cumulative plot defines traffic flow. During signal red phase there is no flow and slope of the plot is zero (flat shape). The flat shape during signal red phase is conserved after vertical scaling and shifting. However, if horizontal shifting was made then the flat shape during signal red phase is not conserved.

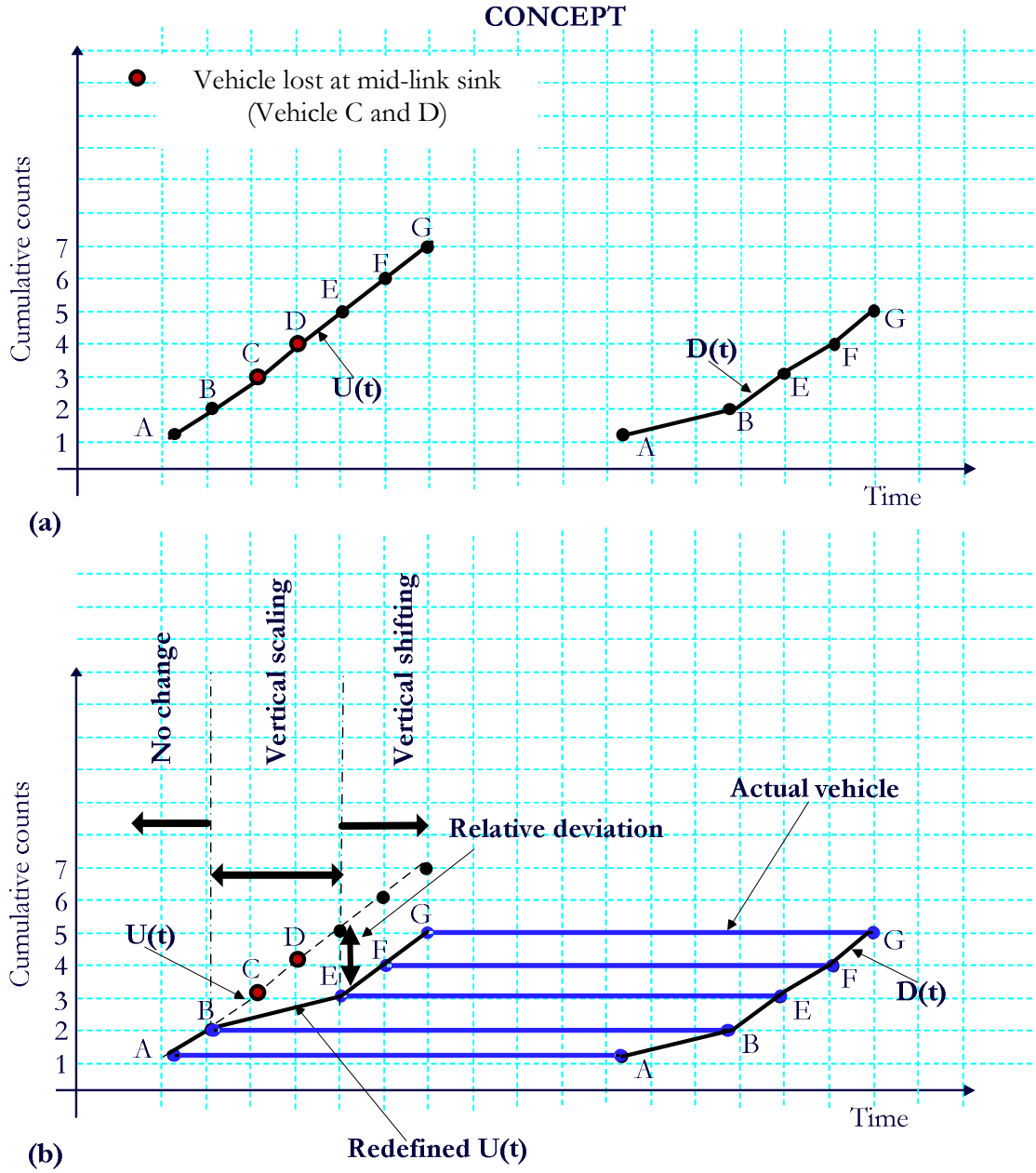

Figure 4-5: Concept of vertical scaling and shifting technique.

To define the points from where U(t) should pass, CUPRITE considers the probe vehicle data. In addition, if *conditions for virtual probe* (defined in Section 4.2.2.2.1) are satisfied then the information is also incorporated to define the required points.

4.2.2.2 Virtual probe

Virtual probe is defined as a virtual vehicle that, during undersaturated traffic flow, departs from the downstream at the end of signal green phase (i.e., it is the last vehicle that departs the signal green phase) and its travel time is free-flow travel time of the link. The probe is not real and is defined with the aim of reducing RD.

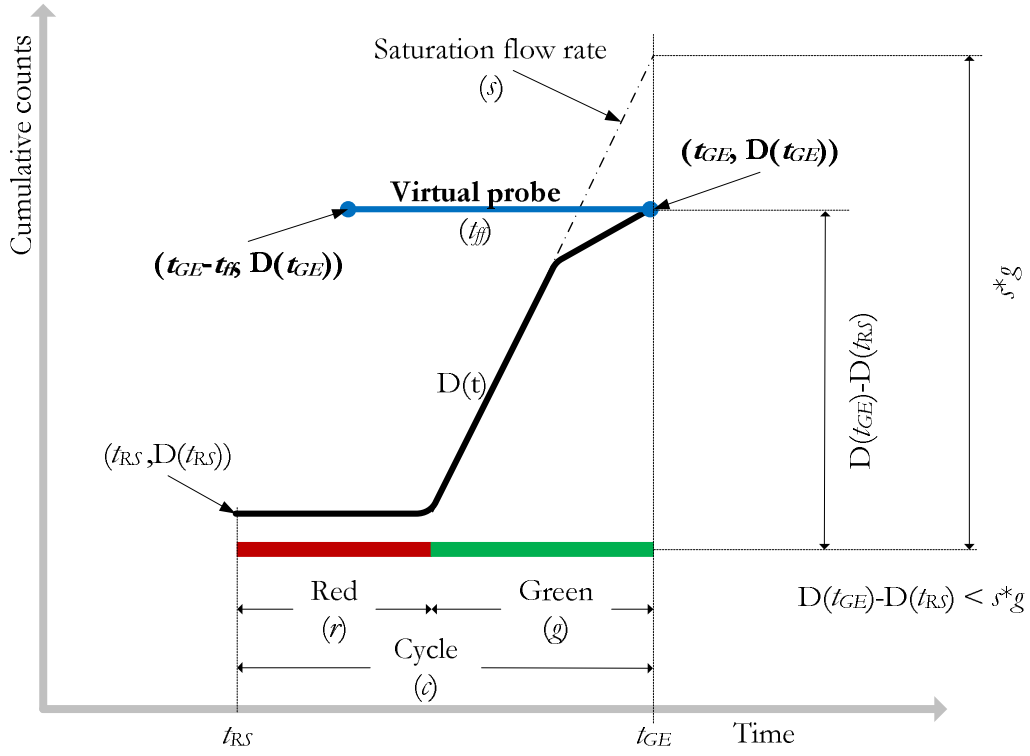

Figure 4-6: Illustration of virtual probe, fixed to D(t) at the end of signal green phase.

We define traffic signal control cycle as time since the start of effective red phase (t_{RS}) to end of effective green phase (t_{GE}). For undersaturated traffic conditions vehicle queue should vanish at the end of each signal cycle and travel time for the vehicle entering the intersection during the end of signal cycle should be close to free-flow travel time (t_{ff}) of the link. Therefore, during undersaturated traffic conditions we can define virtual probe such that it is observed at upstream and downstream at time t_{GE} - t_{ff} and t_{GE}, respectively (i.e. for virtual probe $t_u = t_{GE} - t_{ff}$ and $t_d = t_{GE}$.) (*see* Figure 4-6).

It is to be noted that the virtual probe is only defined if the following *conditions for virtual probe* are satisfied:

i. Absence of source for significant mid-link delay;

ii. No-leftover-queue; and

iii. Presence of RD.

4.2.2.2.1 Conditions for virtual probe

Absence of source for significant mid-link delay

As the travel time of a virtual probe is defined as free-flow travel time of the link, therefore on the study link the following sources for significant mid-link delay should be absent:

i. *Mid-link intersection*: U(t) and D(t) should be for stop-line locations of two consecutive intersections. If the intersections are not consecutive then unknown delay at mid-link intersection(s) results in non free-flow condition.

ii. *Mid-link on-street bus stop*: On-street bus stop blocks the flow of vehicles following the bus therefore; there should not be any mid-link on street bus stop on the study link.

No-leftover-queue

Virtual probes are defined only for undersaturated conditions with logic of zero queue length at the end of signal green phase. Traffic condition is defined as undersaturated if counts during the signal cycle (or more specifically during signal green time) are less than the corresponding capacity i.e.,

$$D(t_{GE}) - D(t_{RS}) < s*g \tag{4.4}$$

To take into account the error in estimation of capacity we can rewrite the above equation as:

$$s*g - \left[D(t_{GE}) - D(t_{RS})\right] > \Delta \tag{4.5}$$

Where: D(*t*) is the cumulative count at time *t*; *s* and *g* are saturation flow rate and effective signal green time, respectively; *s*g* is the capacity and Δ is a calibration parameter.

To define the above equation it is assumed that there is no spill-over from downstream link. If there is spill-over, then vehicles are restricted to flow resulting in low counts at stop-line

detector. Capacity is generally not corrected to account for the spill-over from downstream link. Due to which the above equation is satisfied and system can falsely indicate undersaturated situation for spill-over cases. Though under such situation the queue may not vanish and hence virtual probe should not be defined.

Presence of RD

With above conditions, theoretically RD exists if:

$$t_{GE} - U^{-1}(D(t_{GE})) \neq t_{ff} \tag{4.6}$$

As t_{ff} is a statistical estimator and its actual value can vary from driver to driver. Moreover, practically there can be presence of minor mid-link delays such as interaction with the vehicles from the mid-link source or mid-link sinks or pedestrian, etc. Therefore, certain confidence should be taken into account to define if there is a presence of RD. Hence to define virtual probe the following equation should be satisfied:

$$U^{-1}(D(t_{GE})) - t_{GE} \notin [t_{ff} - \delta, t_{ff} + \delta] \tag{4.7}$$

Where δ is a calibration parameter taking into account the variation in the estimation of t_{ff}. It can be considered equal to the standard deviation of the estimate of t_{ff}.

4.2.2.3 How to define the points from where U(t) should pass?

Say, we have *n* probe vehicles and the database for the probe is defined as list of [t_u] and list of [t_d] where the size of each list is *n*. The value of j^{th} element in the list represents the data from the j^{th} probe.

The list [t_u] and [t_d] can be appended with additional elements satisfying the *conditions for virtual probe*. If the conditions are satisfied, then for each undersaturated signal cycle: a) time corresponding to the end of the green time (t_{GE}) is appended to the list [t_d]; and b) (t_{GE} - t_{ff}) is appended to the list [t_u].

Following are the steps to be followed to define the points from where U(t) should pass:

Step 1 Sort list [t_d] in ascending order of its values. This is required as the probe information is fixed to D(t).

Step 2 Sort list [t_u] in ascending order of its values. This is required to make sure that the redefined U(t) is monotonically increasing and satisfies the property of $\sum \Delta t = 0$.

Step 3 The required points through which U(t) should pass are (t_{uj}, D(t_{dj})); where t_{uj} and t_{dj} are j^{th} value in the sorted list of [t_u] and [t_d], respectively.

For better understanding an example is presented in Figure 4-7, where we have four probes and corresponding list of [t_u] and [t_d]. The example is for non-FIFO discipline with $t_{d1} < t_{d2} < t_{d3} < t_{d4}$ and $t_{u2} < t_{u1} < t_{u4} < t_{u3}$.

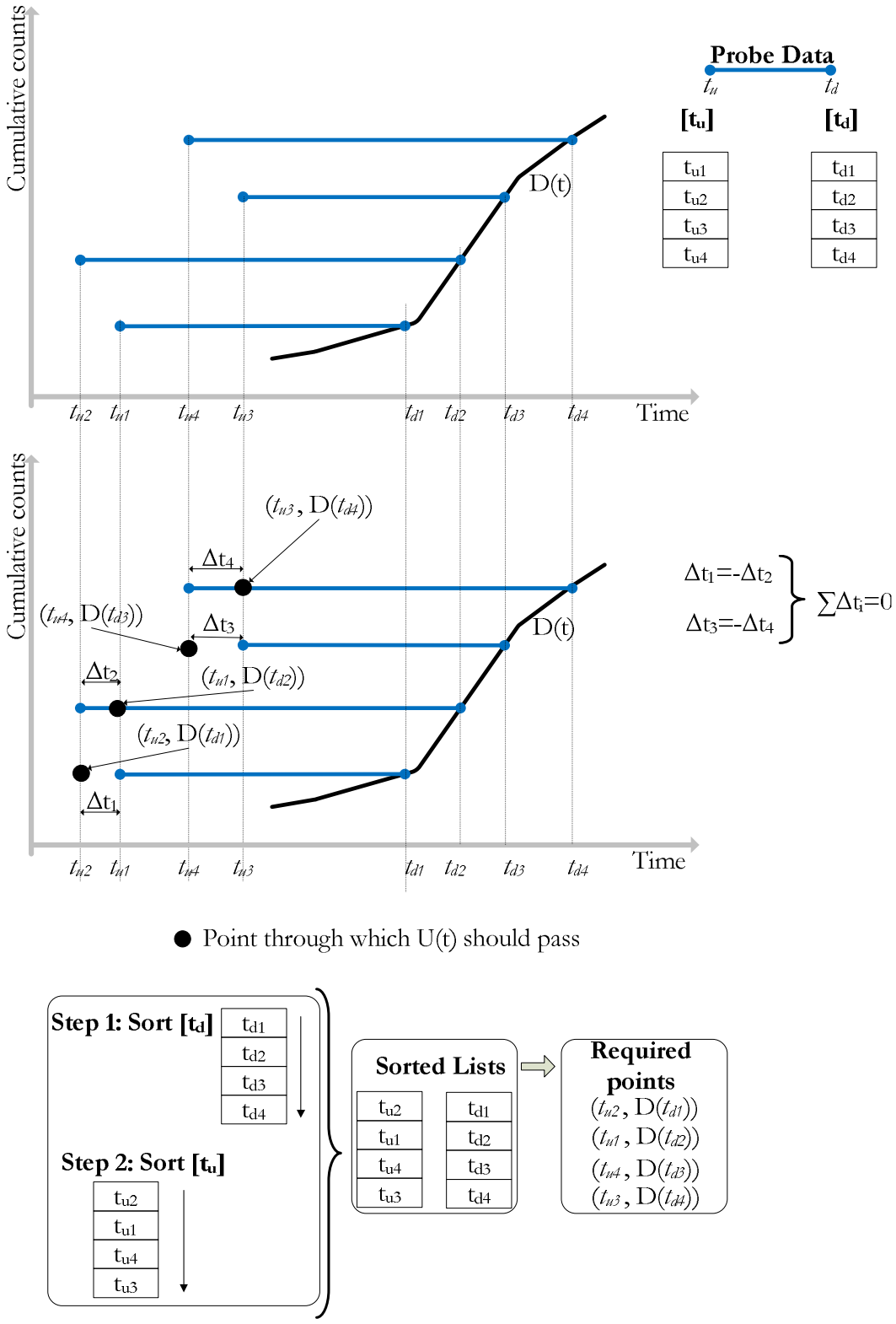

Figure 4-7: Example for estimating point from where U(t) should pass.

4.2.2.4 How to define the reference points?

U(t) and D(t) are initially two independent cumulative plots. When the traffic condition is free-flow (for instance during night) then counts for cumulative plots can be initialized to

zero. This is the initial reference point (P_0). Say [P_1, P_2, P_3, …, P_n] is the list of n points from where U(t) should pass then for redefining U(t) for point P_i, the reference point is P_{i-1}.

4.2.3 Constrain in the cumulative plot

Ideally, the counts at downstream (D(t)) should not exceed the expected demand (U(t-t_{ff})) at downstream. Here we are assuming that the downstream cumulative plot is accurate and we redefine upstream cumulative plot, therefore we define the following constrain (4.8) (A lower bound for U(t).).

$$U(t - t_{ff}) \geq D(t) + \Delta \tag{4.8}$$

Where, Δ is a calibration parameter.

If for an estimation interval, a virtual or real probe is used then equation (4.8) will definitely be satisfied. However, if virtual or real probe is not used then there are scenarios where the equation (4.8) is not satisfied. For instance:

i. Downstream intersection is oversaturated: and upstream detector is undercounting or there is presence of mid-link source;

ii. Downstream intersection is undersaturated and downstream detector is overcounting.

If the equation (4.8) is not satisfied, then we redefine U(t) such that:

$$\begin{aligned} &if\ U(t_{GE} - t_{ff}) < D(t_{GE}) + \Delta \\ &\quad then U(t) = U(t) + Correction \end{aligned} \tag{4.9}$$

$$Correction = \begin{cases} 0 & \forall\ t \leq t_{Ref} \\ (scale - 1) * (U(t) - U(t_{\mathrm{Ref}})) & \forall\ t_{Ref} < t < t_{GE} - t_{ff} \\ (scale - 1) * (U(t_p) - U(t_{\mathrm{Ref}})) & \forall\ t \geq t_{GE} - t_{ff} \end{cases} \tag{4.10}$$

$$scale = \begin{cases} \dfrac{D(t_{GE}) - U(t_{\mathrm{Ref}})}{U(t_{GE} - t_{ff}) - U(t_{\mathrm{Ref}})} & if\ U(t_{GE} - t_{ff}) \neq U(t_{\mathrm{Ref}}) \\ 1 & if\ U(t_{GE} - t_{ff}) = U(t_{\mathrm{Ref}}) \end{cases} \tag{4.11}$$

Where t_{Ref} is the time corresponding to the last "point-to-pass" defined using virtual or real probe.

The above correction is analogous to defining a virtual probe when equation (4.8) is not satisfied. If we define $t_p = t_{GE}\text{-}t_{ff}$ and $Y_P = D(t_{GE})$, then the equations (4.2) and (4.3) is same as the equations (4.10) and (4.11), respectively.

The rational for virtual probe is that during undersaturated traffic condition, the last vehicle departing at end of green phase should have travel time close to free-flow travel time of the link. Virtual probe is applicable even if equation (4.8) is satisfied (For instance, if upstream is overcounting or there is mid-link sink, then during undersaturated traffic conditions equation (4.8) should be satisfied.) whereas, the above correction is only applied when equation (4.8) is not satisfied. It only checks the lower bound for the U(t).

4.2.4 Summary of the algorithm

The summary of the algorithm is as follows (*see* Figure 4-8):

Step 1 Cumulative plots are defined by integrating signal controller data with detector data.

Step 2 Probe vehicle data (list of $[t_u]$ and $[t_d]$) is defined:

a. Fixing real probe data with D(t).

b. Only if the *conditions for virtual probe* are satisfied then the list $[t_u]$ and $[t_d]$ is appended with additional elements corresponding to the virtual probe i.e., $t_u=t_{GE}\text{-}t_{ff}$; $t_d=t_{GE}$, where t_{GE} is the time corresponding to the end of signal green interval.

Step 3 Points through which U(t*)* should pass are defined.

Step 4 U(t) is redefined by a) first vertical scaling and shifting the plots so that it passes through the above defined points (Step 3) and b) thereafter, making sure that the constrain in the cumulative plots (equation (4.8)) are satisfied.

Step 5 Finally, for each estimation interval, average travel time is estimated using classical analytical procedure (Average travel time is the ratio of the area between the plots and number of vehicles departing.).

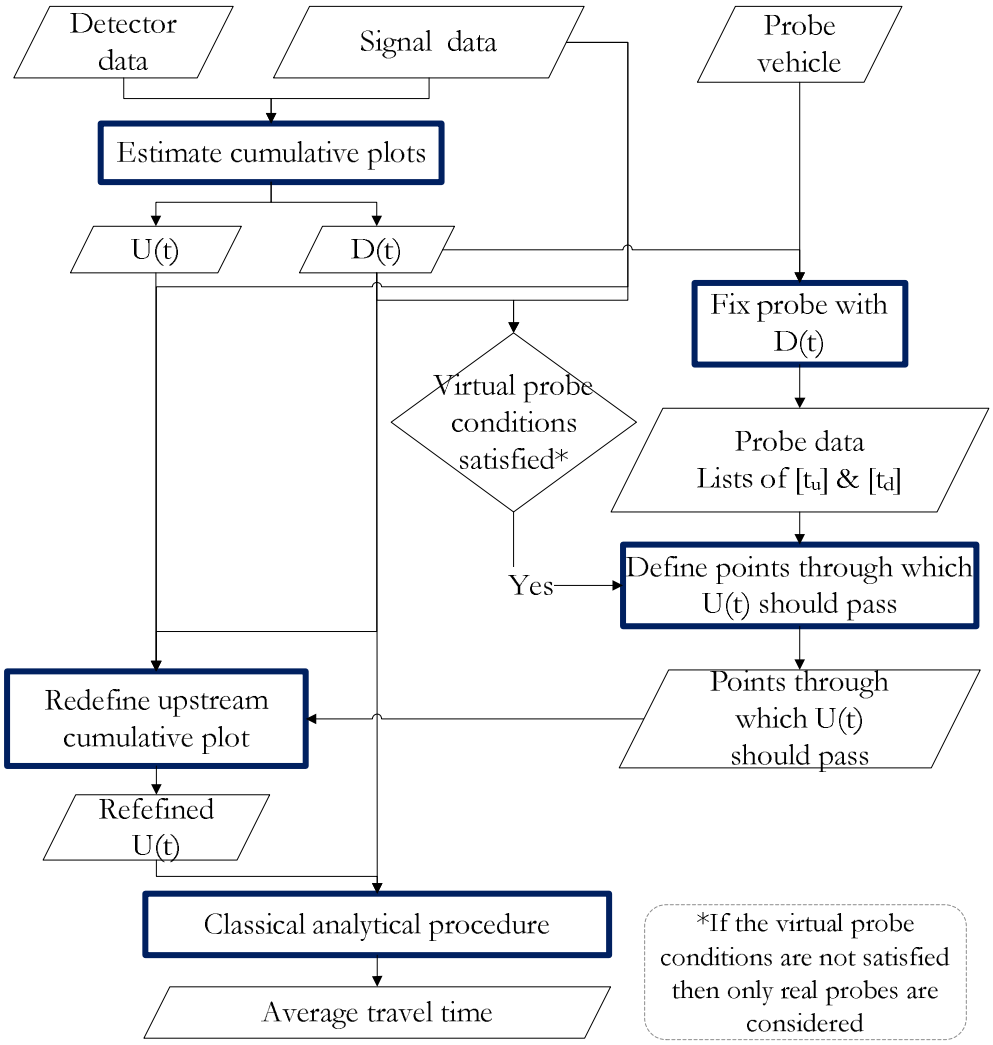

Figure 4-8: CUPRITE basic architecture.

CUPRITE can be applied both online and offline. For online, the cumulative plots are generated in real time and travel time is estimated which captures the most recent travel time for real time applications. Whereas, for offline the plots are generated with the complete set of inputs and travel time is estimated for each estimation interval. Offline application includes development of accurate database for historical travel time. The database can be used by the operators to analyze the performance of the network. Note: the basic algorithm, as developed in this section, is the same for both online and offline applications. However, for online application as the plot is defined in real time therefore, the accuracy of the previously defined points from where the curve should pass is also checked.

4.3 Online and Offline application

"*In computer science, an online algorithm is the one that processes its inputs piece-by-piece without having the entire input available from the start. In contrast, an offline algorithm is given the whole problem data from the beginning and is required to output an answer which solves the problem at hand.*"

Source: Wikipedia (*http://en.wikipedia.org/wiki/Online_algorithm*)

Here, the problem to solve is: "how to define the points from where U(t) should pass?" Input are cumulative plots -U(t) and D(t); and probe data- list of [t_u] and [t_d].

***Online* application:** Say we are interested to know the average travel time for all the vehicles that depart downstream during the last five minutes interval. And we need to update this information after each five minutes. For instance, the information is required at 7:00, 7:05, 7:10…. For this, cumulative plots are estimated piece-by-piece based on the data available until the end of current time interval.

In Figure 4-9, the points from where the curve should pass are defined based on the data available till the current time t_c.

i. In Figure 4-9*a*, $t_c = t_1$. Three points *P1*, *P2* and *P3* are defined and redefined cumulative plots at upstream ($U_1(t)$) is also presented. Here *P3* corresponds to time t_{u3}.

ii. In Figure 4-9*b*, $t_c = t_2$. The data indicates that third and fourth probe are in non-FIFO discipline due to which the point *P3* defined earlier (in Figure 4-9*a*) is corrected and now *P3* corresponds to time t_{u4}. The curve $U_2(t)$ is considered for online travel time estimation for the current estimation interval illustrated in the Figure 4-9*b* .

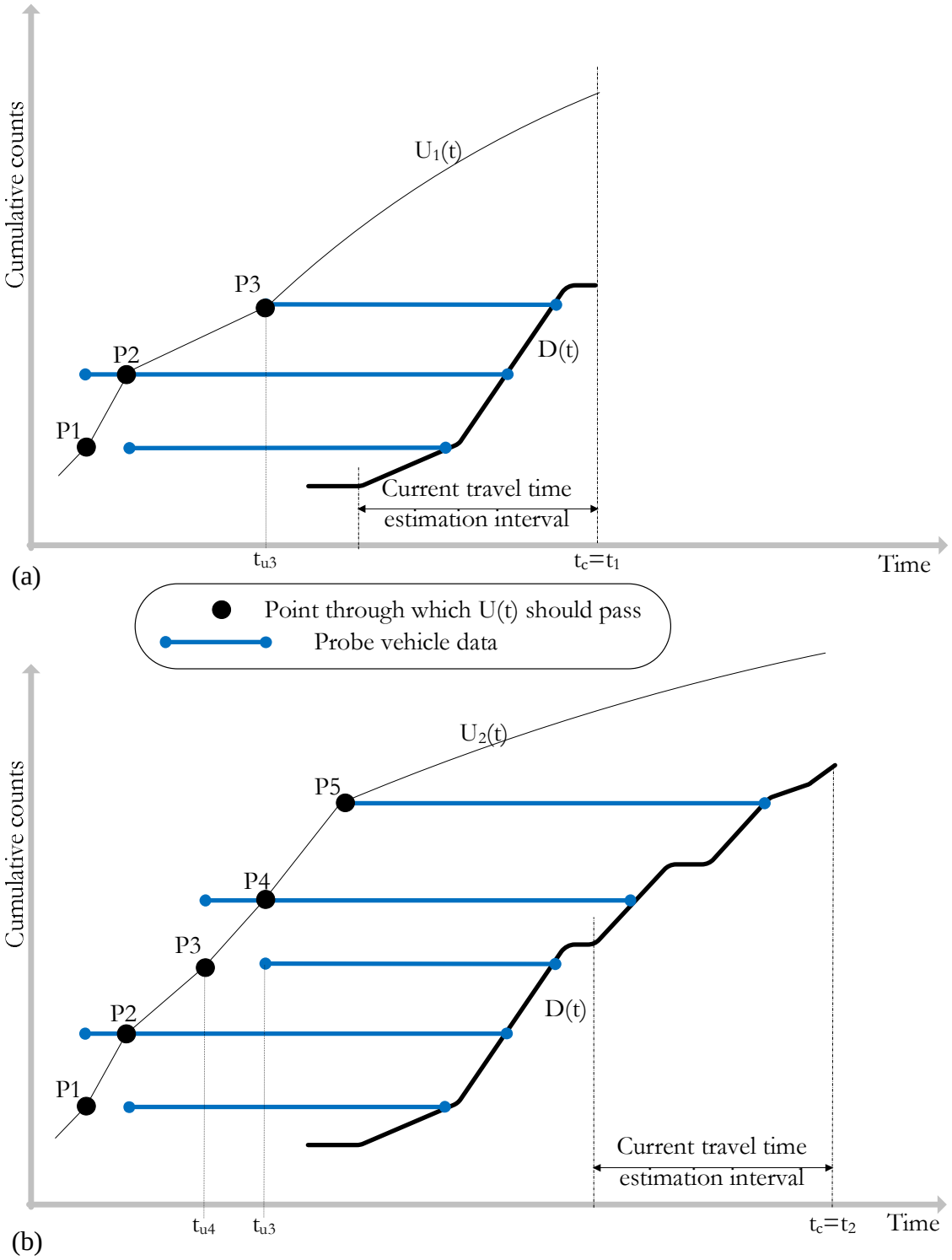

Figure 4-9: Example for defining the points from where the U(t) should pass for online application: a) at time t_1; b) at time t_2.

***Offline* application**: Say at the end of the day a traffic operator is interested to know how the network had performed during the day. In this case, detector counts and probe data for the complete day are utilized to define the cumulative plots.

Let us consider an example. Figure 4-10 represents the cumulative plots (U(t) and D(t)) estimated till the current time (t_c) indicated in the figure. The plots are for a 10% sink case. Actual cumulative plots are the accurate cumulative plots to be used for travel time estimation. They are obtained from individual simulated vehicles traversing the complete link. In Figure 4-10 *a, b* and *c* are for *online* application and *d* is for *offline.*

i. Figure 4-10*a*: t_c = 7:18:00. Traffic condition is undersaturated therefore, virtual probe is used and we can see that redefined U(t) is close to actual U(t).

ii. Figure 4-10*b*: t_c = 7:24:00. Oversaturated traffic condition with no probe data. There is a deviation in redefined U(t) from that of actual U(t). (Refer zoomed portion of the figure).

iii. Figure 4-10*c*: t_c = 7:30:00. Oversaturated traffic condition with probe data. Here, there are actually two probes observed at upstream, but only one of them has departed from the downstream. Therefore, for the current period only the first probe is considered to redefine U(t). Note: as U(t) is redefined, the error in the previous estimation interval (7:18:00 to 7:24:00) is also corrected (Refer zoomed portion of the figure). For online application to estimate travel time for estimation interval from 7:18:00 to 7:24:00, the plots represented in Figure 4-10*b* are considered. However, if time series modeling is to be performed and one is interested in time series of travel time then the errors performed in the previous intervals can be corrected.

iv. Figure 4-10*d,* is an example for *offline* estimation. U(t) is redefined with all the probes and travel time for each estimation intervals are estimated. It can be seen that redefined U(t) is close to actual U(t) hence, *offline* estimation should have better accuracy than that of *online*.

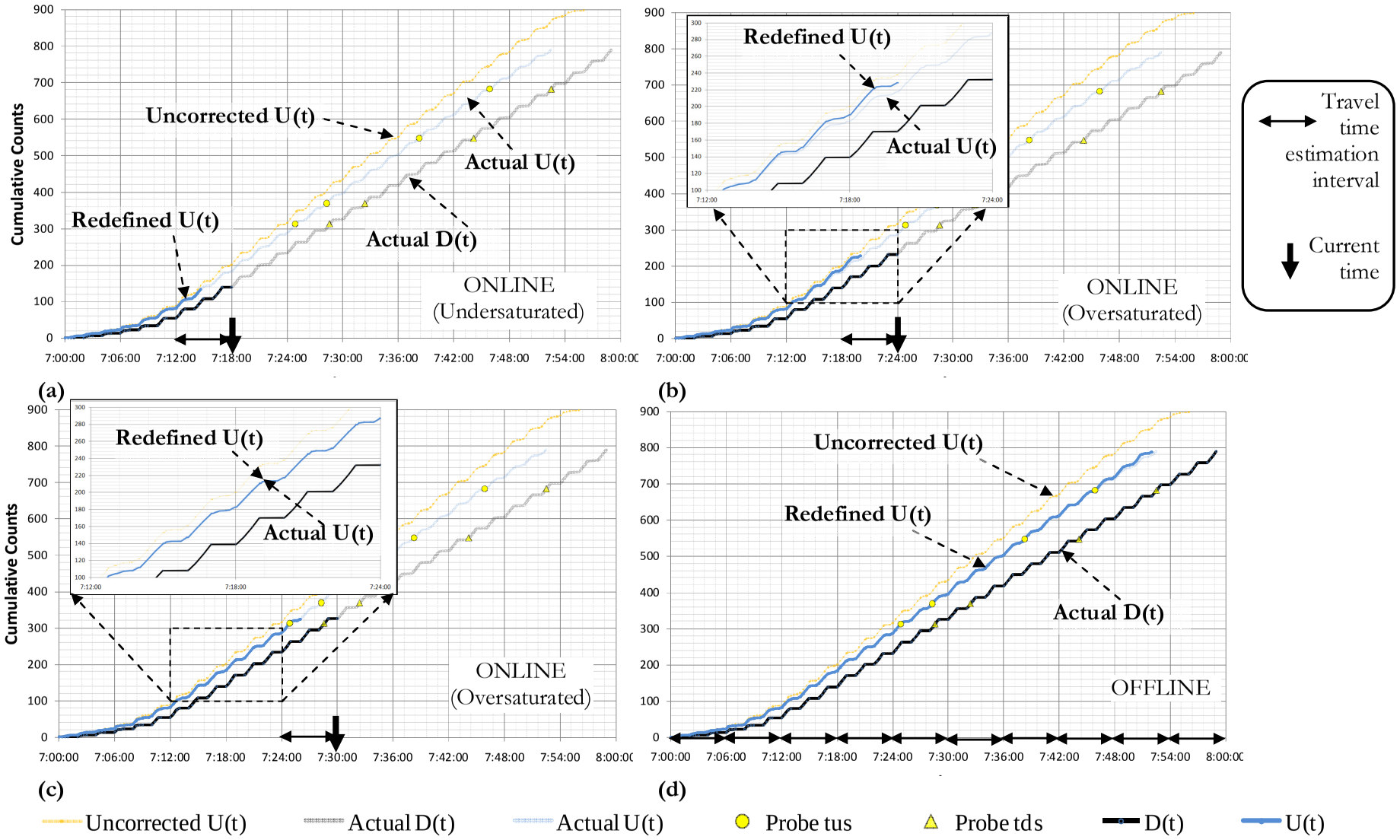

Figure 4-10: Example for *online* and *offline* applications.

4.4 CUPRITE testing

The architecture for CUPRITE testing is provided in Figure 4-11. Detector and signal controller data are input to CUPRITE. The required probes are randomly selected from individual simulated vehicle data.

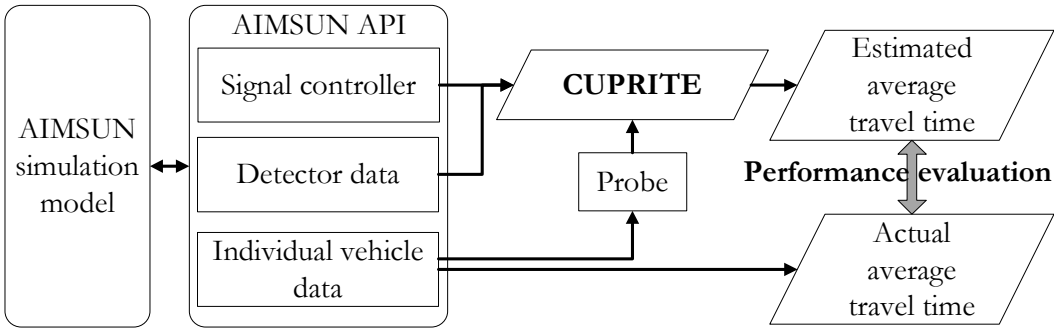

Figure 4-11: Architecture for CUPRITE testing using AIMSUN.

4.4.1 Performance indicators

The performance of CUPRITE is evaluated terms of:

i. Accuracy (Section 4.4.1.1).

ii. Sensitivity with respect to number of probes (Section 4.4.1.2).

iii. Comparing with *Probe-Only* method (Section 4.4.1.3).

iv. Comparing with HCM 2000 model during undersaturated traffic conditions (Section 4.4.1.4).

4.4.1.1 CUPRITE estimation accuracy

Following two different accuracy indicators are considered:

i. A_M: (4.15) Accuracy defined in terms of Mean Absolute Percentage Error (MAPE (4.14)) which is most common performance statistic indicator used in literature. It indicates the overall average CUPRITE performance.

ii. A_5: (4.17) Accuracy defined in terms of 95th percentile of errors ($Error^{95th}$ (4.16)) obtained from each estimation interval. This indicator also covers the confidence in the estimate i.e., 95% of the times the observed accuracies should be higher than or equal A_5.

$$Error_i = \left(\frac{\left|actual_i - estimated_i\right|}{actual_i}\right) \tag{4.12}$$

$$Accuracy_i = (1 - Error_i) * 100 \tag{4.13}$$

$$MAPE = \frac{\sum_{i=1 to N} Error_i}{N} \tag{4.14}$$

$$A_M(\%) = (1 - MAPE) * 100 \tag{4.15}$$

$$Error^{95th} = 95th\ percentile\ of\ Error_i\ \ for\ i = 0\ to\ N \tag{4.16}$$

$$A_5(\%) = (1 - Error^{95th}) * 100 \tag{4.17}$$

Where, N is the total number of estimation intervals. $Actual_i$, $estimated_i$, $Error_i$, and $Accuracy_i$ are the average actual travel time, average estimated travel time, absolute relative error and accuracy for i^{th} estimation interval, respectively.

4.4.1.2 CUPRITE sensitivity (S_n and S_p) with respect to number of probes

The performance of CUPRITE is evaluates for minimum number of probes required for accurate travel time estimation as:

i. **S_n**: Fixed number, S_n, of probe vehicles during each estimation interval.

ii. **S_p**: Fixed percentage, S_p, of all vehicles traversing the link as probe vehicles. This percentage is a proxy for the market penetration of probes in vehicles traversing the link during certain time periods.

4.4.1.3 CUPRITE comparison with "Probe-Only" method

While presenting the results, comparison of CUPRITE with model solely based on probe data here referred as *Probe-Only* is also provided. *Probe-Only* (4.18) method assumes that probe represents a random sample from all the vehicles (population) and average of the travel time from the probes (t_i) is the representative of the population, given that the sample size (n_p) is at least a minimum value.

$$Average\,travel\,time = \frac{\sum_{i=1}^{n_p} t_i}{n_p};\quad n_p \geq 1 \qquad (Probe\text{ - }Only\ \text{method}) \tag{4.18}$$

4.4.1.4 CUPRITE comparison with Highway Capacity Manual 2000 during undersaturated traffic conditions

Travel time (*TT*) can be simply defined as sum of free-flow travel time (t_{ff}) and average control delay per vehicle (*d*) (4.19). We expect that during undersaturated traffic condition, a standard delay formula such as, Highway Capacity Manual 2000 (HCM 2000) should provide good estimate of travel time. Equation (2.22) is the delay formula defined in HCM 2000 (Refer to Section 2.2.2.2.2 for discussion on HCM 2000 method).

$$TT = t_{ff} + d \tag{4.19}$$

In the present analysis following parameters are considered (Refer to equation (2.22) to equation (2.27) for parameter definition):

C = 120 s;

g = 30 s;

PF =0.7735 is considered. Refer to Exhibit 16-12 of HCM 2000 for: *g/C* = 0.25 and the highly favorable progression quality (arrival type 5 defined in Exhibit 16-11.);

c = s*g/C = (0.533*2*30/120*3600 = 960 veh/h); where *s* is saturation flow rate (=0.533*number of lanes);

T = 3*120/3600 = 0.1 h;

X = *v*/*c*. Vehicle flow rate (*v*) is obtained from the downstream stop-line detector counts. The flow rate during each estimation interval is the detector counts during the estimation interval divided by the time length of the estimation interval;

k = 0.5 for fixed signal as defined in HCM 2000;

X_u: the degree of saturation at upstream intersection. It is approximated as *v*/*c* ratio of upstream through movement. Here, it is obtained from the detector counts at upstream intersection;

Q_b: initial queue at start of period *T* (vehicle). Here, the analysis is for undersaturated traffic condition; and start of each travel time estimation interval is end of signal

green phase. Therefore, Q_b can be assumed to be zero. As $Q_b = 0$ therefore, $d_3 = 0$. Note: for oversaturated traffic Q_b is positive and is difficult to estimate, hence here HCM is not applied for oversaturated traffic condition;

t: the duration of unmet demand in *T* (hour). Here, Q_b=0 therefore this value is not required;

u: the delay parameter. Here, $Q_b = 0$ therefore this value is not required.

The delay defined by HCM 2000 is the delay experienced by all vehicles that arrive during the analysis period. The travel time we estimate using CUPRITE is for all vehicles that depart during the analysis period (travel time estimation interval). Here, the analysis is performed for undersaturated traffic condition so queue should vanish at end of each signal cycle. The analysis period is integer multiple (three times) of signal cycles with fixed signal parameters. Therefore, the vehicles arriving and departing during the analysis period must be same. Hence, travel time estimates from CUPRITE can be compared with that from HCM 2000.

4.4.2 Framework for CUPRITE testing

CUPRITE is tested thoroughly for: a) different traffic flow conditions (undersaturated and oversaturated); and b) potential causes of RD (sink/source/detector error). In Figure 4-12, the framework for CUPRITE testing is illustrated. In this chapter, CUPRITE is tested for travel time estimation between two consecutive intersections (single link). In the next chapter (Chapter 5), the application of CUPRITE for route travel time estimation is discussed followed by its testing on multiple links route.

For oversaturated traffic condition, sensitivity in terms of S_n and S_p is performed. For undersaturated traffic condition only S_n is considered. As virtual probe can be defined only for undersaturated traffic flow condition therefore, for such traffic condition the importance of the virtual probe is also demonstrated through following cases:

i. Case R: Here, S_n, number of real probes is considered and virtual probe is not considered. $S_n \geq 1$ because we are considering real probes only.

ii. Case V+R: Here, if the *conditions for virtual probe* are satisfied, then virtual probe is considered in addition to, S_n, number of real probes. S_n=0 corresponds to situation when only virtual probe is considered. Similarly, $S_n = 1$, indicates that one real probe in addition to virtual probe is considered.

Table 4-1 and Table 4-2 present different combinations of cases tested for undersaturated and oversaturated traffic condition, respectively.

Probe information is only available when it has departed the downstream intersection. Hence, the results for *online* and *offline* applications are also differentiated.

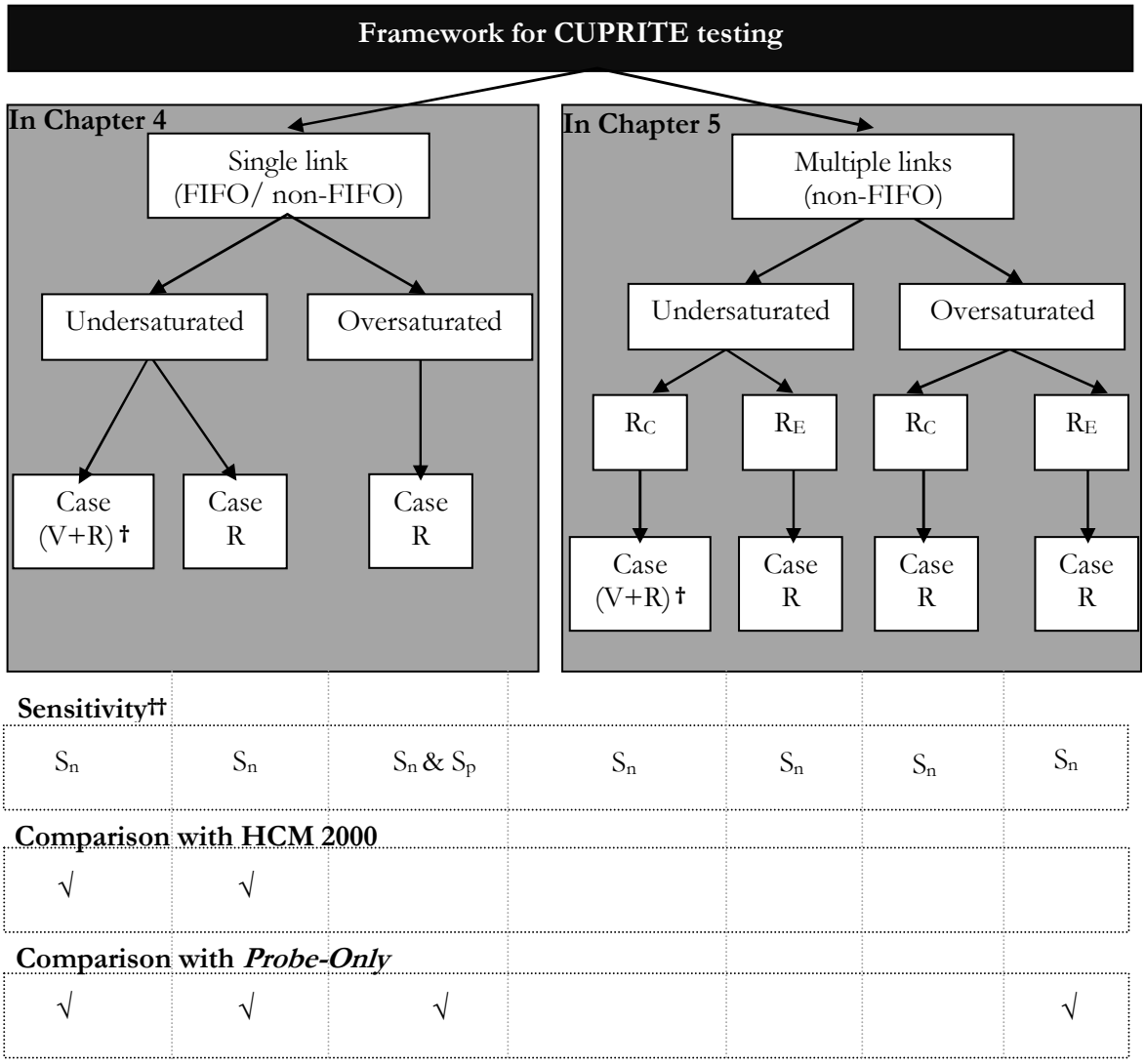

Case V+R: Virtual and Real probe.
Case R: Real probe.
R_C: *Component* based route travel time (Chapter 5).
R_E: *Extreme* based route travel time (Chapter 5).

† When real probes are zero then the case is only virtual probe.
†† S_n: Fixed number of probes per estimation interval.
S_p: Fixed percent of vehicles traversing as probe.

Figure 4-12: Framework for CUPRITE testing.

Table 4-1: Different cases considered for CUPRITE testing for undersaturated traffic flow conditions (↑: detector overcounting; ↓: detector undercounting)

Case Study	Discipline (FIFO/non-FIFO)	Sink (%)	Source (%)	Detector Error (%)				Comments
				Upstream		Downstream		
				↑	↓	↑	↓	
A1	Both	10						Model performance for FIFO and non-FIFO discipline. (Virtual Probe Only)
A2.1	Non-FIFO	10						Virtual probe is not considered. Results presented for scenarios with at least one real probe in each estimation interval. (Case: R)
A2.2			10					
A2.3				10				
A2.4					10			
A2.5						10		
A2.6							10	
A3.1		10						Both virtual and real probe are considered. (Case: V + R)
A3.2			10					
A3.3				10				
A3.4					10			
A3.5						10		
A3.6							10	

Table 4-2: Different cases considered for CUPRITE testing during oversaturated traffic condition (↑: detector overcounting; ↓: detector undercounting)

Case Study	Discipline (FIFO/non-FIFO)	Sink (%)	Source (%)	Detector Error ((%)				Comments
				Upstream		Downstream		
				↑	↓	↑	↓	
B1	Both	10						Model performance for FIFO and non-FIFO results.
B2.1	non-FIFO	5, 10, 15, 20						Provides comparative overview of model performance for different independent sink and source percentages. (non-FIFO discipline)
B2.2			5, 10, 15, 20					
B3.1				10				Analyses the impact of detector error. (non-FIFO discipline)
B3.2					10			
B3.3						10		
B3.4							10	
B4.1		20	10					Net:10 Source — Analyses the impact of net effective relative deviation due to mid-link sink and sources, and detector error. (non-FIFO discipline)
B4.2		10	20					Net:10 Sink
B4.3		10	10					Net: 0
B4.4		20	20					Net: 0
B4.5		50	50					Net: 0
B4.6		90	90					Net: 0
B4.7		10	10		10		10	Net: 0
B4.8		10	10	10		10		Net: 0

Note: Case B4.3 to B4.6 are analogous to travel time estimation on multiple links route using cumulative plot at upstream and downstream of the route. Case B4.3 and B4.4 are analogous to a route with major road; Case B4.5 and B4.6 are analogous to a route with minor road

4.4.3 Definition of sink and source percentage

Sink percentage is defined as the ratio of vehicles lost in the sink to the vehicles observed at upstream. Source percentage is defined as the ratio of vehicles gained from the source to the

vehicles departing from downstream (Figure 4-13). In the present analysis 5%, 10%, 15% and 20% of sink and source are considered.

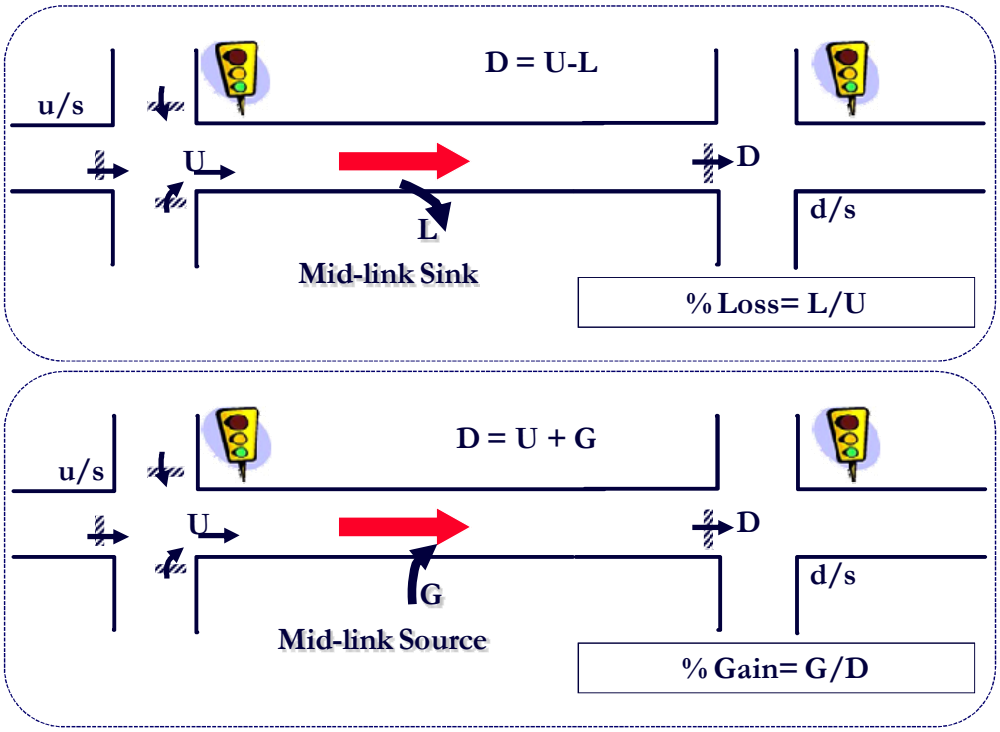

Figure 4-13: Definition of percentage loss to mid-link sink and percentage gain from mid-link source.

4.4.4 Single link testing

The aim here is to test the performance of CUPRITE with respect to RD. Therefore, CUPRITE is applied on a link between two consecutive signalized intersections (similar to the network illustrated in Figure 3-8). The testing of CUPRITE on a single link is the foundation for further CUPRITE applications such as route travel time (discussed in Chapter 5).

Two different networks, one with single lane link and another with double lane link, are considered. Traffic flow on a single lane link follows FIFO queueing discipline. Testing CUPRITE on FIFO discipline defines the maximum accuracy that can be obtained and hence demonstrates the potential of CUPRITE. Traffic flow on double lane link follows non-FIFO queueing discipline and is better representative of the real world.

The flow is from three different directions at upstream intersection (*see* Figure 3-8). Only through movement at downstream intersection is considered. Bottleneck is at downstream

intersection. Vehicles for the mid-link sink/source are random vehicles traversing the network.

The results presented here are from the simulations with:

i. Signal cycle time (C) of 120 s; green split (g/C) for through movement at downstream intersection are 0.5 and 0.25 for single lane FIFO network and double lanes non-FIFO network, respectively. Signal parameters define the shape of the cumulative plot.

ii. Scenarios for different degree of saturation (X) in the range of 0.5 to 1.2 at downstream intersection.

iii. Average travel time estimation interval (T_{EI}) of 360 s i.e. three times of signal cycle time.

In the following sections, the performance for undersaturated and oversaturated traffic conditions is separately presented.

4.4.4.1 Undersaturated traffic condition

Here first the result for use of virtual probe for FIFO and non-FIFO networks is presented, followed by comparative overview of different undersaturated ($0.5 \leq X < 1$) cases for non-FIFO network.

4.4.4.1.1 Virtual probe for FIFO and non FIFO networks

Figure 4-14 represents the data from simulation with no real probe consideration from 10% mid-link sink case. Virtual probe is defined for undersaturated traffic condition resulting in consistent accuracy of more than 97% for both FIFO and non-FIFO networks. The graph also differentiates the accuracies obtained for three different traffic conditions: a) non-congested (undersaturated); b) shoulder (congestion build-up and dissipation); and c) congested (oversaturated). In the present analysis travel time estimation interval is three signal cycle. Therefore, an estimation interval can have a maximum of three virtual probes, each corresponding to the end of each signal green phase. For undersaturated traffic condition the number of virtual probes per estimation interval should be three. During congestion build-up and dissipation process there are estimation intervals with either one or two virtual probes. For oversaturated traffic condition there should not be any virtual probe. This means that

during congestion build-up and dissipation process RD can be partially corrected and during congested situation there is no correction applied resulting in low accuracy in the latter case.

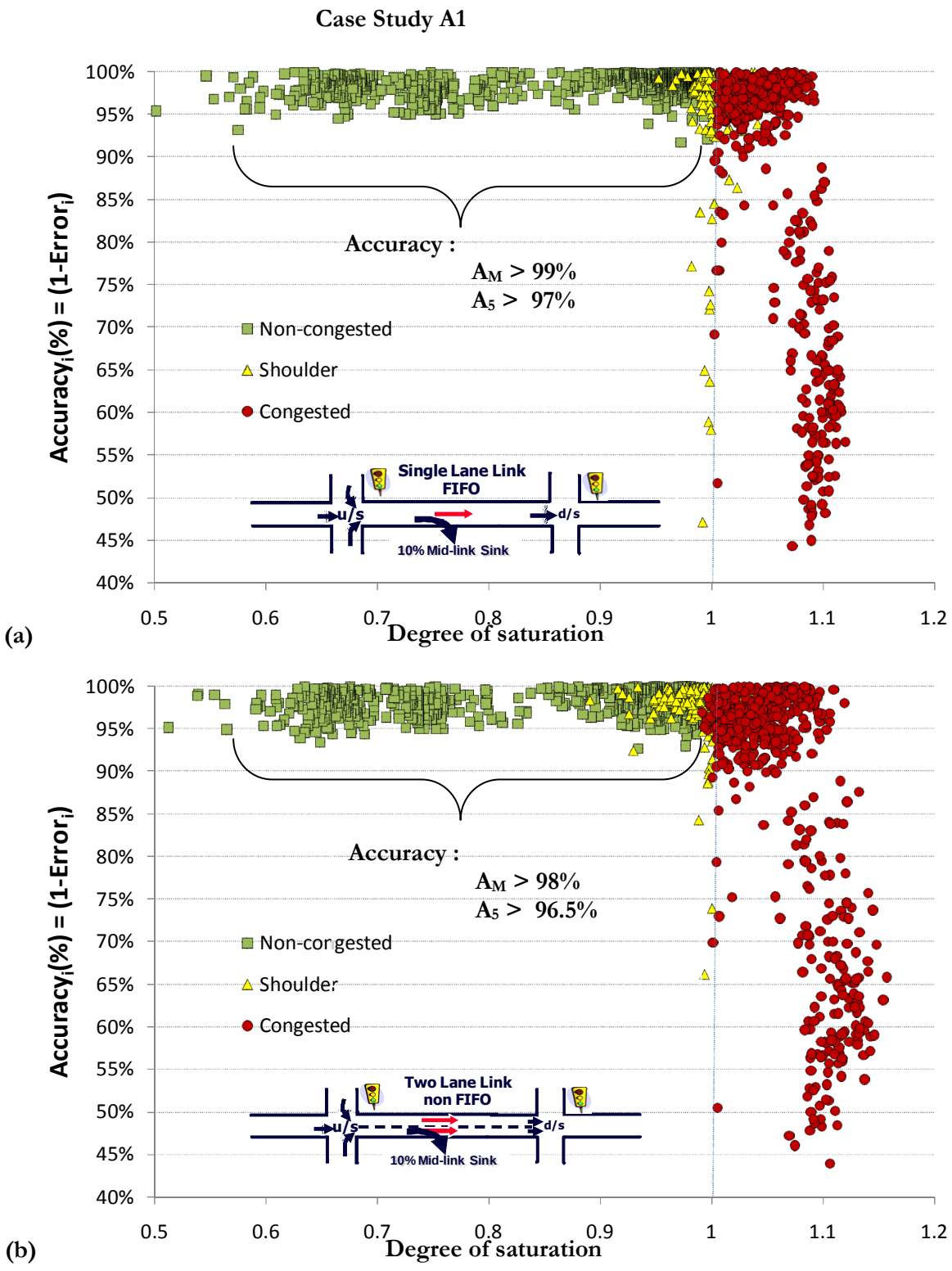

Figure 4-14: Simulation for different traffic flow conditions with no real probe: a) FIFO network and b) non-FIFO network. (Case A1).

4.4.4.1.2 Comparative overview of different undersaturated cases for non-FIFO

Here, first the results for Case R and its comparison with *Probe-Only* are presented followed by results for Case V+R and its comparison with HCM. The results of the graphs for 10% sink case (A2.1 and A3.1) and 10% downstream detector overcounting (A2.5 and A3.5) are illustrated in this chapter. The graphs for the other cases are in Appendix D (Figure D-1 to Figure D-4).

Case R and comparison with Probe-Only

For case R (case A2.1 to case A2.6), where virtual probes are not considered, the accuracy of CUPRITE increases with increase in S_n and is consistent with all the cases (*see* Figure 4-15 and Figure 4-16; and Figure D-1 to Figure D-4). If S_n is small (only one or two probes) then there is significant benefit of integrating cumulative plots with probe vehicle data. For instance for $S_n = 1$ the CUPRITE estimates are higher than *Probe-Only* by around 15% in A_5 accuracy and 5% in A_M accuracy. Though, not much benefit if S_n is large. This is because large number of probes per estimation interval is good representative of all the vehicles in the estimation interval.

Case V+R and comparison with HCM

Case V+R

In all the cases (case A3.1 to case A3.6), it is observed that consideration of only virtual probe ($S_n = 0$) is most accurate. In fact, the consideration of real probes in addition to virtual probes generally decreases the accuracy by 3%. The reason for which is explained below.

The correction based only on virtual probe assumes uniform relative deviation throughout the signal cycle. Hence, after the vertical scaling, general shape of the upstream cumulative plot is preserved (i.e., there is no distortion). The magnitude of relative deviation is random and it can result in overestimation, underestimation or perfect estimation. Therefore, the assumption of uniform relative deviation can result in effective balance of the relative deviation values.

The consideration of real probe requires fixing the probe with downstream cumulative plot. The error in the estimation of downstream cumulative plot can result in wrong estimation of rank of the probe vehicle in the cumulative plot. Moreover, non-FIFO queueing discipline does not necessarily guarantee the conservation of rank at upstream cumulative plot.

Resulting in distortion in the general shape of the upstream cumulative plot and hence lower accuracy compared to case with only virtual probe.

The above explanation is supplemented with the following example. Figure 4-17 represents an example from a scenario from 10% sink case (case A3.1). The dots in the figure correspond to the vehicles observed at both upstream and downstream. In the figure: D(t) is downstream cumulative plot; $U_0(t)$ observed cumulative plot at upstream; $U_r(t)$ is redefined upstream cumulative plot, defined from the vehicles traversing the complete link. In Figure 4-17*b*, virtual probes are considered and $U_{r1}(t)$, redefined cumulative plots considering the virtual probe, is obtained. The shaded area in the figure represents the overestimation and underestimation of travel time. It can be seen that $U_{r1}(t)$ is close to $U_r(t)$ and error is low, i.e., overestimation and underestimation balance each other. In Figure 4-17*c* real probe is considered in addition to virtual probe, and the redefined cumulative plot $U_{r2}(t)$ is presented. It can be seen that $U_{r2}(t)$ is quite far away from $U_r(t)$, and there is overestimation of travel time. However, the real probe considered in Figure 4-17*d*, provides better estimates. Thus, the consideration of real probe can sometimes provide better estimates and sometimes can provide worse estimate compared to that of scenarios where only virtual probe is considered.

Most of the time, the consideration of real probes ($S_n \geq 1$) has lower accuracy than from only virtual probe case ($S_n=0$). In Figure 4-19, the accuracies from $S_n \geq 1$ versus $S_n=0$ are presented (The values are from 10% sink case.). It can be seen that most of points are below the 45° line, indicating that most of the time $S_n=0$ have better accuracy. Figure 4-19*a* and Figure 4-19*b* define the frequency distribution for three cases, where A_5 accuracy for $S_n = 0$ is: more than; close to; or less than, that for case with at least one real probe ($S_n = 1$or $S_n = 2$). Note: "close to" means the absolute difference of the accuracies is less than or equal to 0.1%; "more than" means the difference is more than 0.1%; and "less than" means the difference is less than 0.1%. It can be seen that $A_5(S_n = 0) > A_5(S_n = 1)$ and $A_5(S_n = 0) > A_5(S_n = 2)$ are most frequent.

It is observed that overcounting of downstream detector further decreases the accuracy from CUPRITE. Refer to case V+R in Figure 4-16 for $S_n = 0$: $A_M = 97.8\%$ and $S_n = 1$: $A_M = 95\%$. Detector overcounting results in overestimation of degree of saturation. In the case A3.5 approximately 25% of the undersaturated estimation intervals are falsely considered as oversaturated due to overcounting at downstream and hence in these intervals virtual probe is not defined. These 25% of the cases are actually equivalent to Case R that accounts for the drop in accuracy.

Note: Here S_n=0 has better accuracy even if virtual probe is not defined for 25% of the cases. This is because, in such situations the *constrains in the cumulative plots* are generally not satisfied, and while redefining U(t) we make sure that the constrains are satisfied resulting in better estimates (Refer to Section 4.2.3).

Comparison with HCM 2000

HCM 2000 method is independent of the number of probes per estimation interval. Here, we use calibrated HCM (with *PF* =0.7735, *k* =0.5) which provides best estimates for travel time. It makes sense if we compare HCM with Case V+R, as the application of HCM assumes that there is no mid-link intersections; on-street bus stops etc. i.e., situations identical to *conditions for virtual probe* (Refer to section 4.2.2.2). The performance of HCM (*see* Figure 4-15 and Figure 4-16; and Figure D-1 to Figure D-4) is generally good with A_5 > 90% and A_M > 95% and is only slightly lower than CUPRITE (with consideration of virtual probe).

The delay from HCM depends on the estimates of degree of saturation. Here, degree of saturation is estimated based on the detector counts. The error in the detector counts results in wrong estimate for degree of saturation. Overcounting and undercounting by detector results in overestimation and underestimation of the degree of saturation, respectively.

Figure 4-20 illustrates HCM delay estimates using equations (2.22) to (2.25). The slope of the curve is the rate of change in delay with respect to degree of saturation. The curve is monotonically increasing with rather gentle slope for low degree of saturation and steep slope once traffic becomes congested. Detector overcounting can result in higher error in travel time estimation than detector undercounting. For instance, (*see* Figure 4-20) for X= 0.9, 10% overcounting results in 6 s error in delay whereas, 10% undercounting results in 3.5 s error in delay estimation. This is confirmed by the results obtained from the case studies on overcounting (*see* Figure 4-16). Comparing with other cases, HCM accuracy is lowest for overcounting case (case A3.5). For instance, the A_5 accuracy from HCM for overcounting case is 86.7% whereas from undercounting case is 94.1%. The A_M accuracy is 94.2% and 97.2%, respectively.

Note: The error in estimation of degree of saturation during oversaturated traffic condition can result in significant error in delay estimates from HCM. For instance (*see* Figure 4-20) 10% overestimation in degree of saturation at X=1.05 can result in 13.6 s error in the delay estimate.

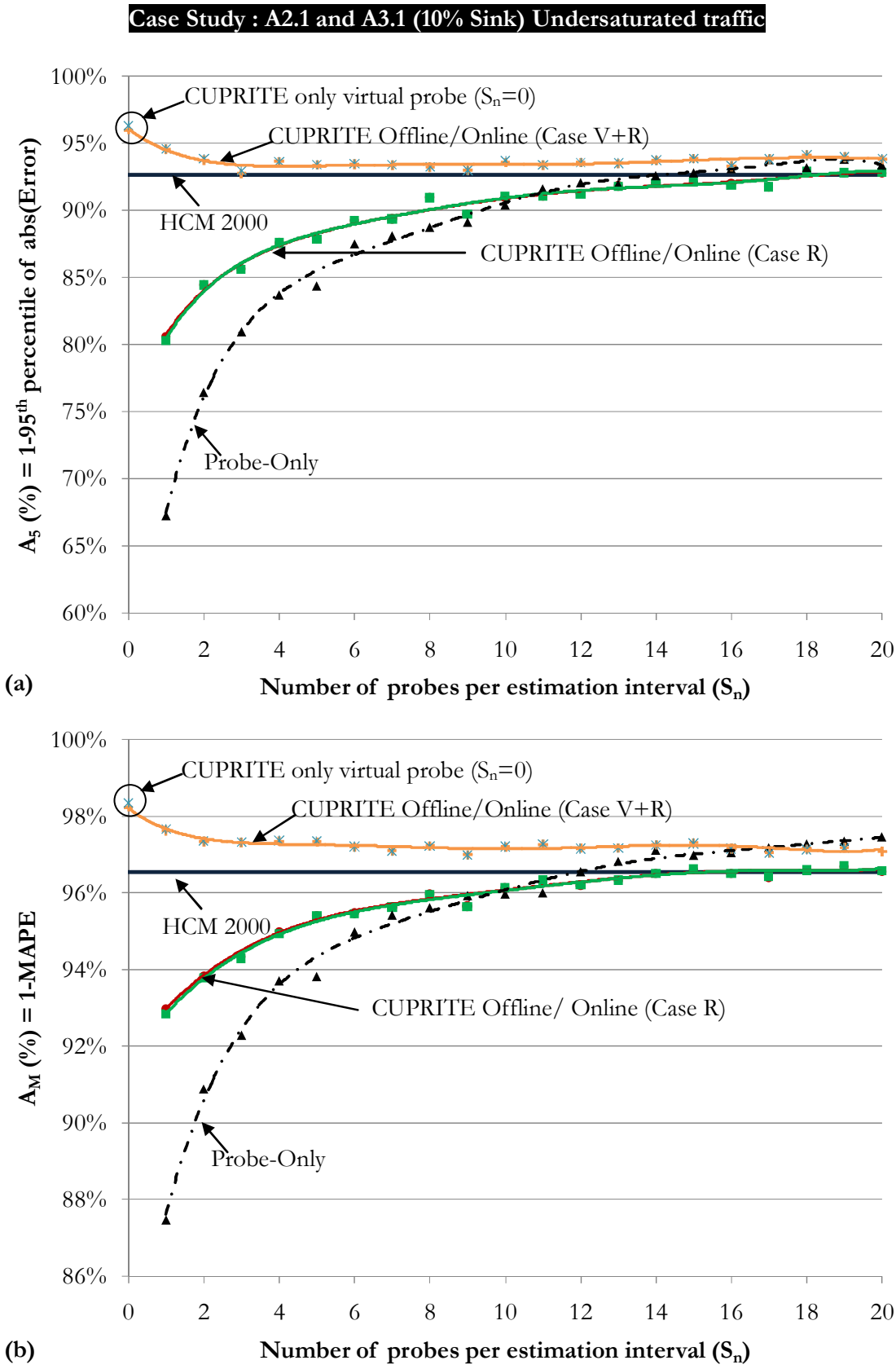

Figure 4-15: Comparative results for 10% mid-link sink case during undersaturated traffic condition. (a) Results for accuracy: A_5 and (b) Results for accuracy: A_M.

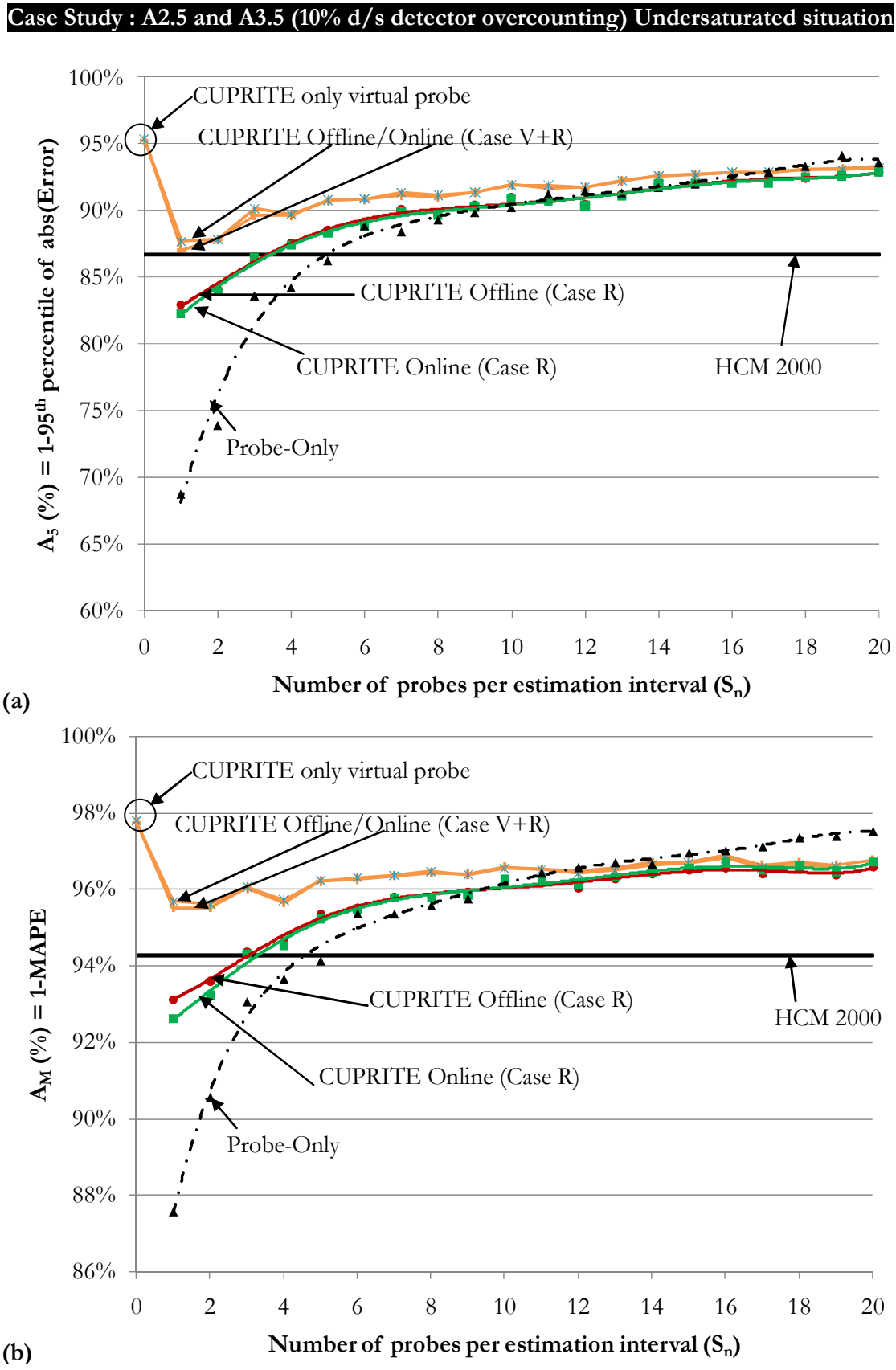

Figure 4-16: Comparative results for 10% downstream detector overcounting case during undersaturated traffic condition. Results for accuracy :(a) A_5 and (b) A_M.

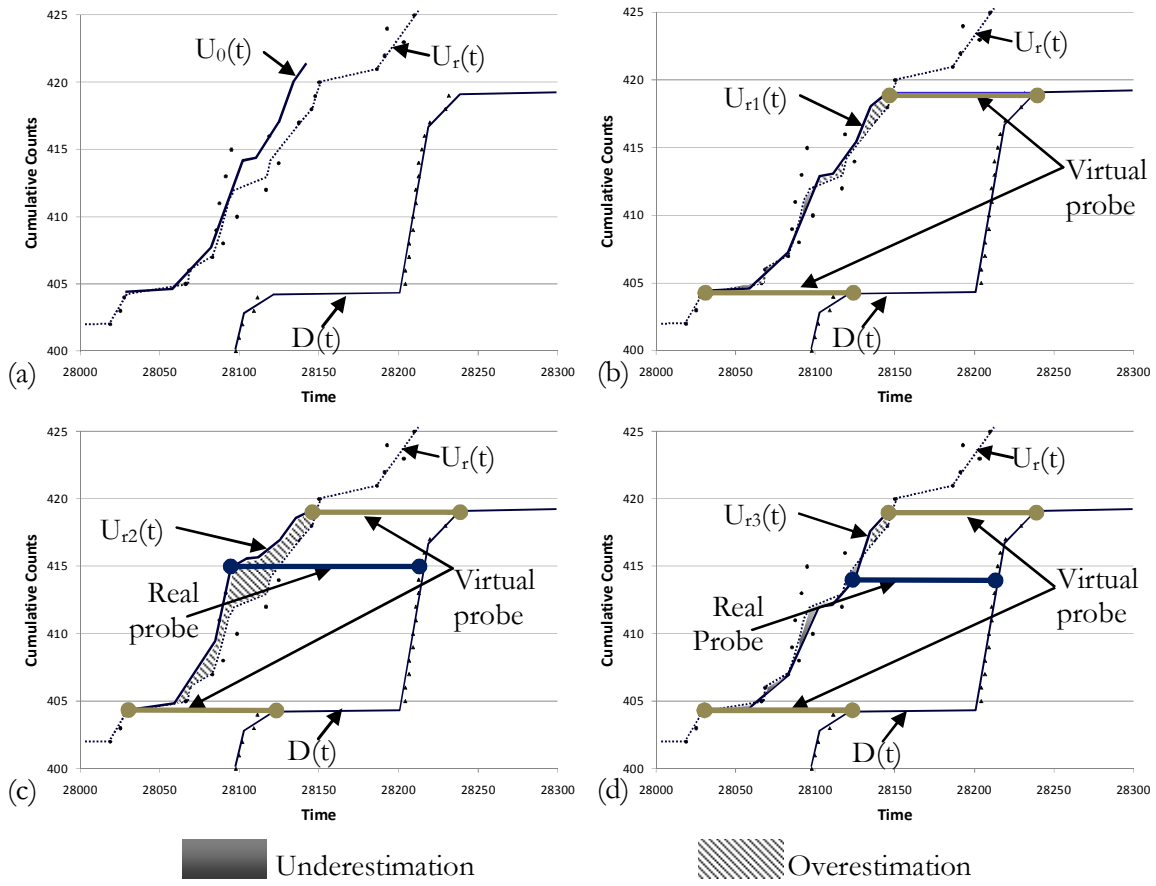

Figure 4-17: An example from 10 % mid-link sink case with different probe consideration.

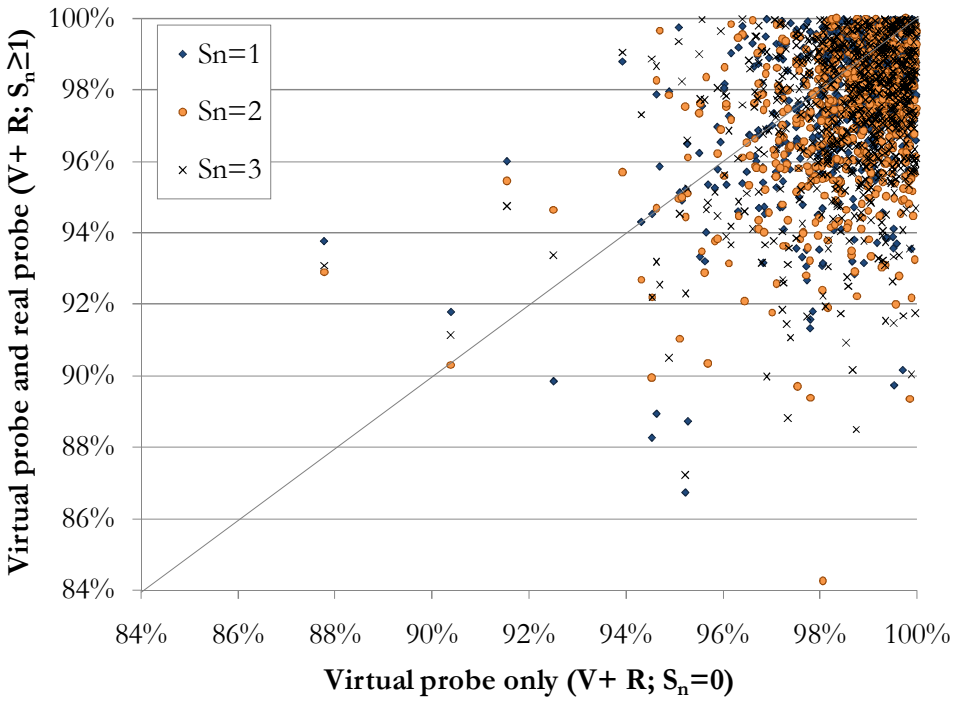

Figure 4-18: Accuracy estimates (A_5) from V+R case with S_n= 1, 2 and 3 probes versus S_n= 0 from 10% mid-link sink (case A3.1).

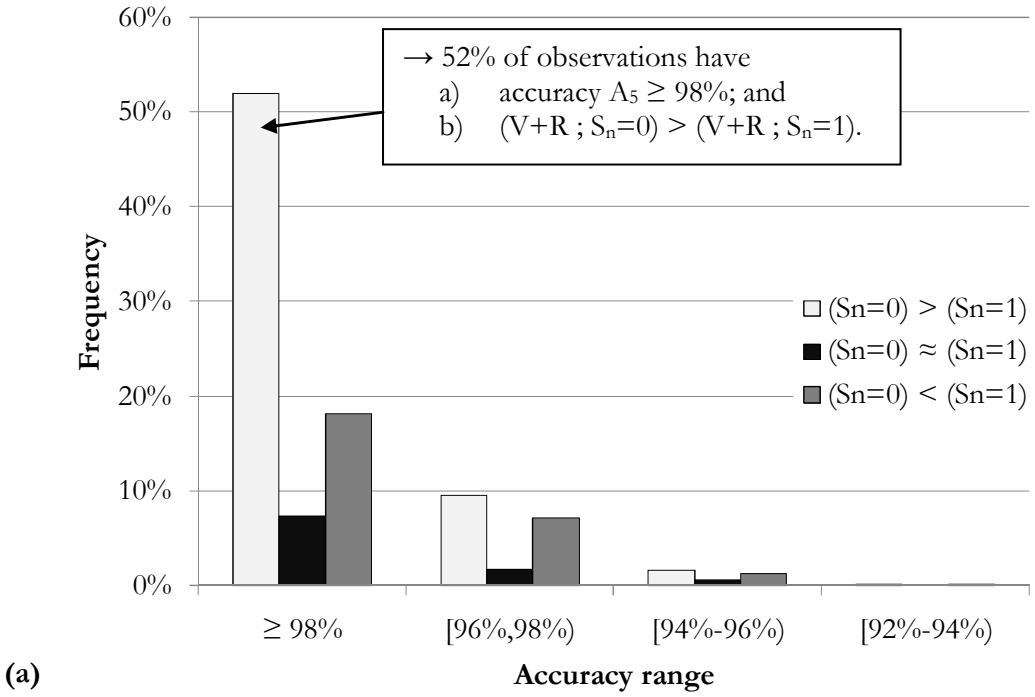

(a)

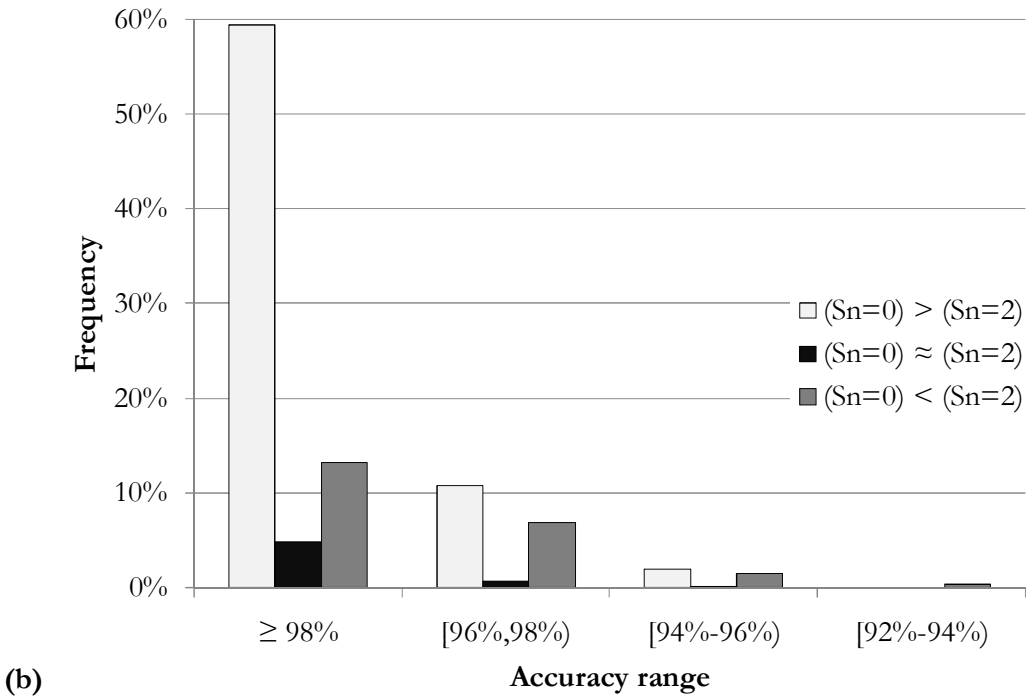

(b)

Figure 4-19: Case with 10% mid-link sink (case A3.1): a) and b) are frequency distribution of the accuracies (A_5) for different scenarios where estimates from only virtual probes are better than, close to or less than those from virtual and real probes.

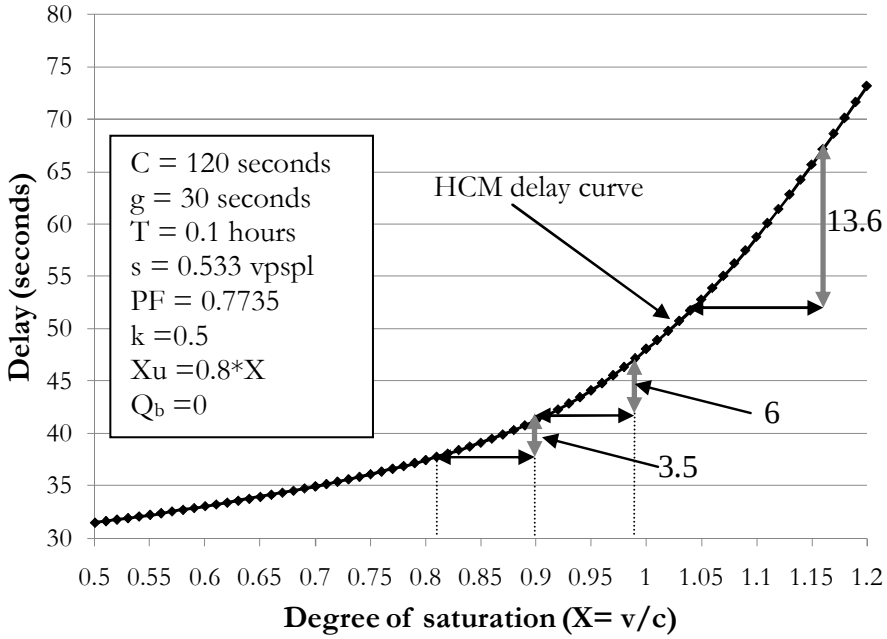

Figure 4-20: HCM 2000 delay versus degree of saturation at downstream intersection.

If the delay is mainly from the signal control at intersection then travel time estimates during undersaturated traffic condition with fixed signal controller can be satisfactorily obtained from HCM 2000 method by defining its parameters from stop-line detector counts. The application of CUPRITE slightly improves the accuracy, though not much benefit. However, the application of CUPRTIRE during undersaturated traffic condition maintains consistency in the travel time estimation methodology for both undersaturated and oversaturated traffic conditions.

If virtual probe is not considered and less number of real probes are available then CUPRITE guarantees better estimates than that from *Probe-Only*.

For oversaturated condition virtual probe does not exist, and only real probes are considered as discussed in next section.

4.4.4.2 Oversaturated traffic condition

Here, the results of the simulation for scenarios with $1 \leq X \leq 1.2$ are presented in following order:

i. Discussion on fixed number of probes per estimation interval (S_n)

   a. 10% sink, both FIFO and non-FIFO networks (Case B1).

b. Comparative results for different sink and source percentage (Case B2.1 and case B2.2).

c. Detector counting error (Cases B3.1, B3.2, B3.3 and B3.4).

d. Simultaneous presence of different sources of RD (Case B4.1 to case B4.9).

e. Discussion on reliability of estimates.

ii. Discussion on percentage of vehicles traversing as probe (S_p).

4.4.4.2.1 Fixed number of probes per estimation interval (S_n)

10 per cent sink both FIFO and non-FIFO networks (Case B1)

The result for FIFO is illustrated in Figure D-5 and for non-FIFO is illustrated in Figure 4-21. It is observed that:

i. The performance of CUPRITE with at least one probe per estimation interval with respect to: a) A_M accuracy is close to 98% and 95% for FIFO and non-FIFO networks, respectively; and b) A_5 accuracy is close to 95% and 90% for FIFO and non-FIFO networks, respectively. This demonstrates that on an average CUPRITE estimate is more than 95% accurate; and 95 percent of the time the accuracy is more than 90%.

ii. If we have only a few probes per estimation interval ($S_n < 5$) then there is significant benefit of integrating probes with cumulative plots. If the number of probes per estimation interval is large ($S_n > 10$) then the probes are good representative of the population of the vehicles and there is little benefit of integrating probes with cumulative plots.

iii. As expected, o*ffline* application performs better than *online* application. The difference is mainly when $S_n = 1$ or $S_n = 2$.

iv. Accuracy increases with increase in number of probes for both CUPRITE and *Probe-Only*.

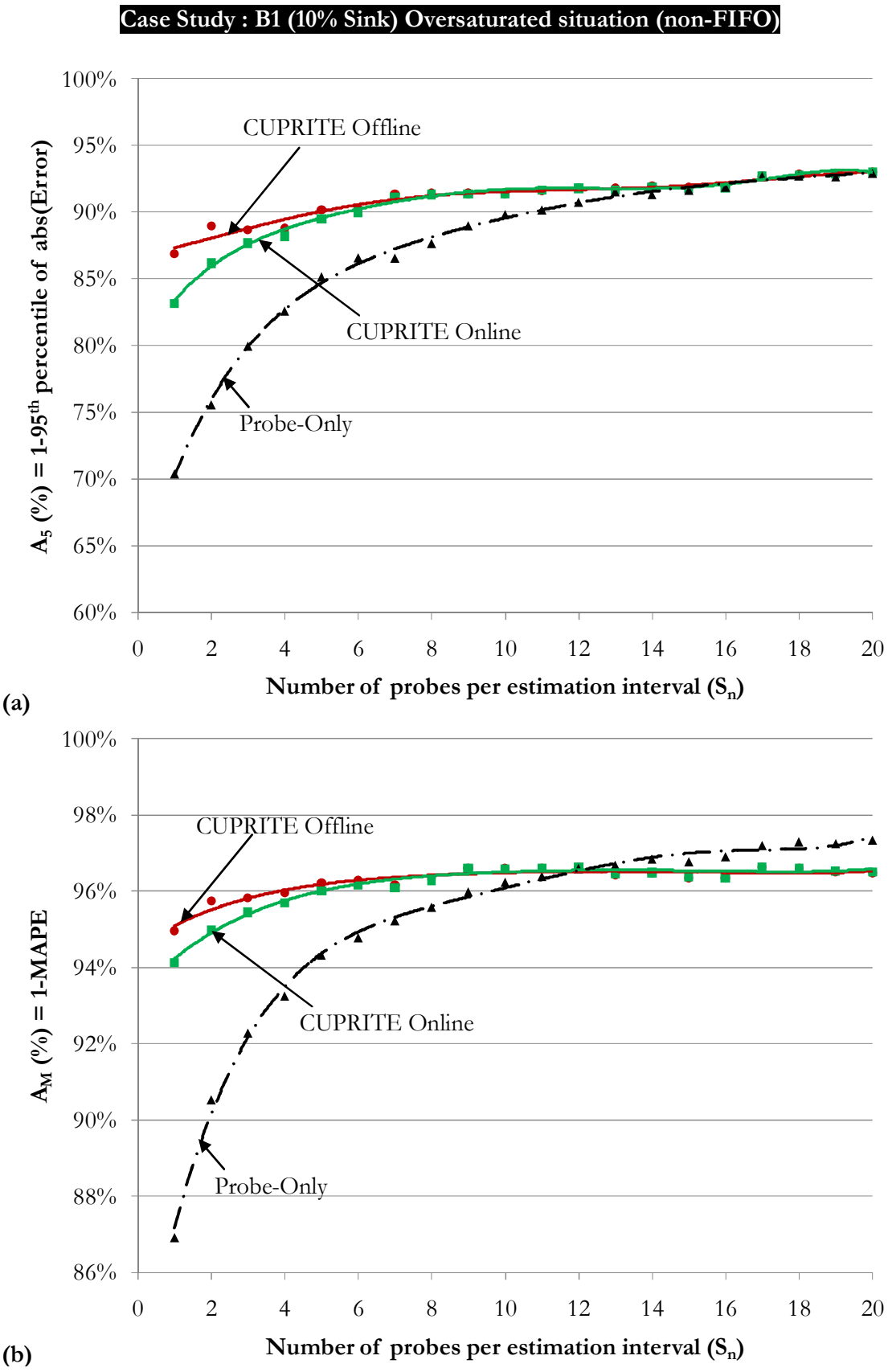

Figure 4-21: Case B1 (10% sink) oversaturated traffic condition for non-FIFO discipline. Results for accuracy: a) A_5 and b) A_M versus S_n.

Comparative results (Case B2.1 and case B2.2)

Figure 4-22 and Figure 4-23 illustrate comparative results of the accuracy versus S_n for non-FIFO network under 5%, 10%, 15% and 20% sink cases (case B2.1) for CUPRITE offline and online application, respectively. The result for different source percentages (case B2.2) is illustrated in Figure D-6 and Figure D-7. It can be observed that:

i. *For offline application with $S_n = 1$ (both sink and source case)*: The A_5 accuracy ranges from 84.6% to 86.4% and A_M accuracy ranges from 94.1% to 94.8%. Hence we can say that CUPRITE offline application is insensitive to the magnitude of mid-link source and sink.

ii. *For online application with $S_n = 1$ (both sink and source case)*: The A_5 accuracy decreases with increase in the sink and source percentage, whereas, the decrease in A_M accuracy is not much. The A_5 accuracy ranges from 75.1% (20% sink) to 84.3% (5% sink) and A_M accuracy ranges from 93.4% to 94.1%. However, if $S_n > 1$ then CUPRITE is insensitive to magnitude of mid-link source and sink.

iii. For *Probe-Only* with $S_n = 1$ the A_5 accuracy is around 60% and A_M is around 85%.

It can be concluded that CUPRITE average performance (A_M) is insensitive to the mid-link source and sink percentage. Though for online application if percentage of sink is high then for $S_n = 1$, the A_5 accuracy ranges from 75.1% (20% sink) to 84.3% (5% sink) but still much higher than *Probe-Only*.

For online application: If the probe departs at the start of the estimation interval then the relative deviation is corrected until the start of the estimation period. The relative deviation within the estimation period is not corrected. However, if the probe is the one that departs at the end of the estimation period, then the relative deviation for the complete estimation period is corrected. Thus depending on the position of probe within the estimation interval, the online estimation can vary from worse to best estimation and hence lowers A_5 accuracy. As the magnitude of relative deviation depends on the sink/source percentage therefore, the drop in the accuracy also depends on the sink/source percentage. For $S_n = 1$ there is equal chances of probe to be in the first half or second half of the estimation interval. For $S_n > 1$, one can observe probes in both first half and second half of the estimation interval therefore with $S_n > 1$ there is generally insensitive to the magnitude of sink/source.

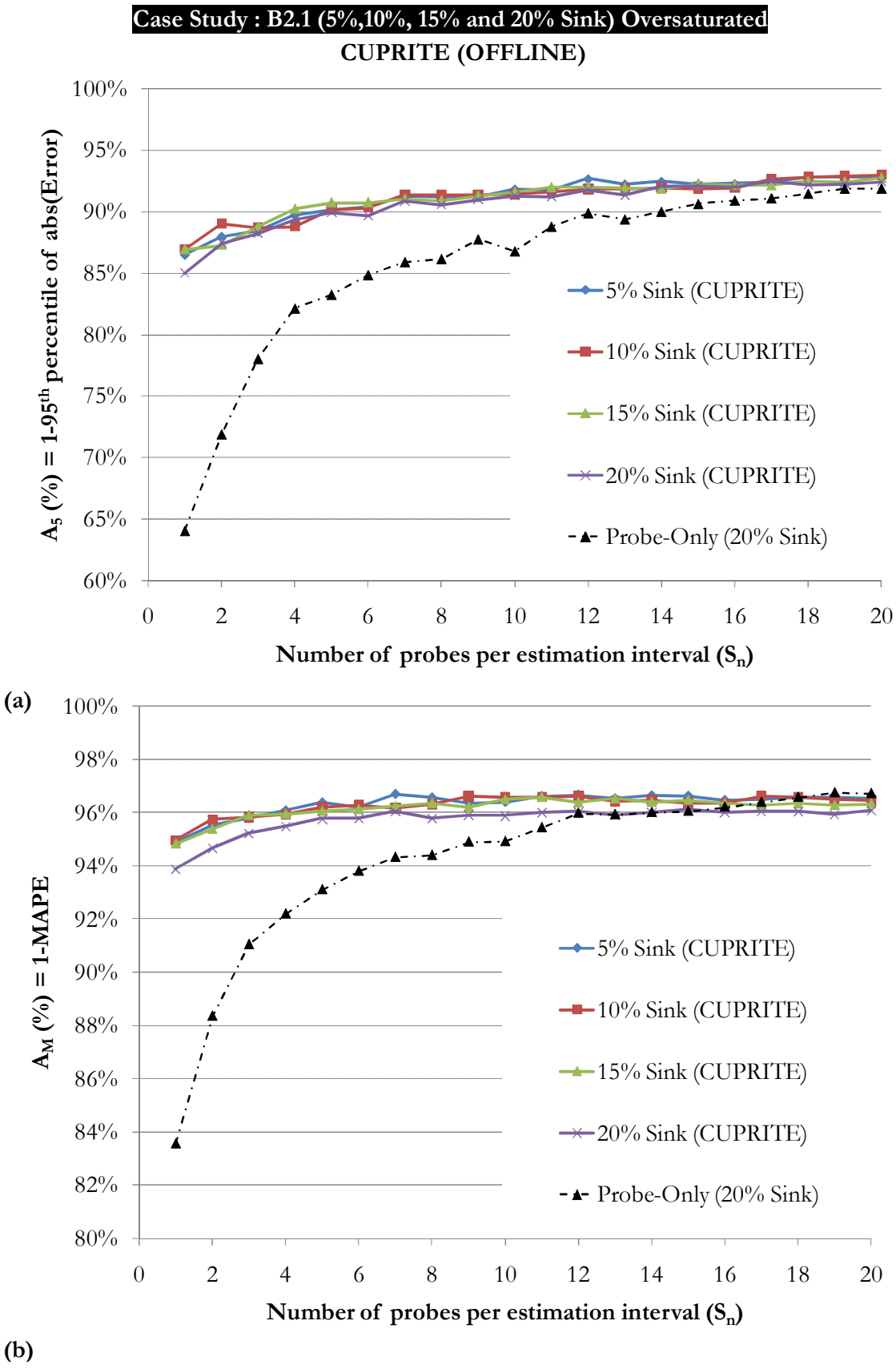

Figure 4-22: CUPRITE Offline application for different sink percentages (5%, 10%, 15% and 20%); oversaturated traffic condition; non-FIFO discipline. Results for accuracy: a) A_5 and b) A_M versus S_n.

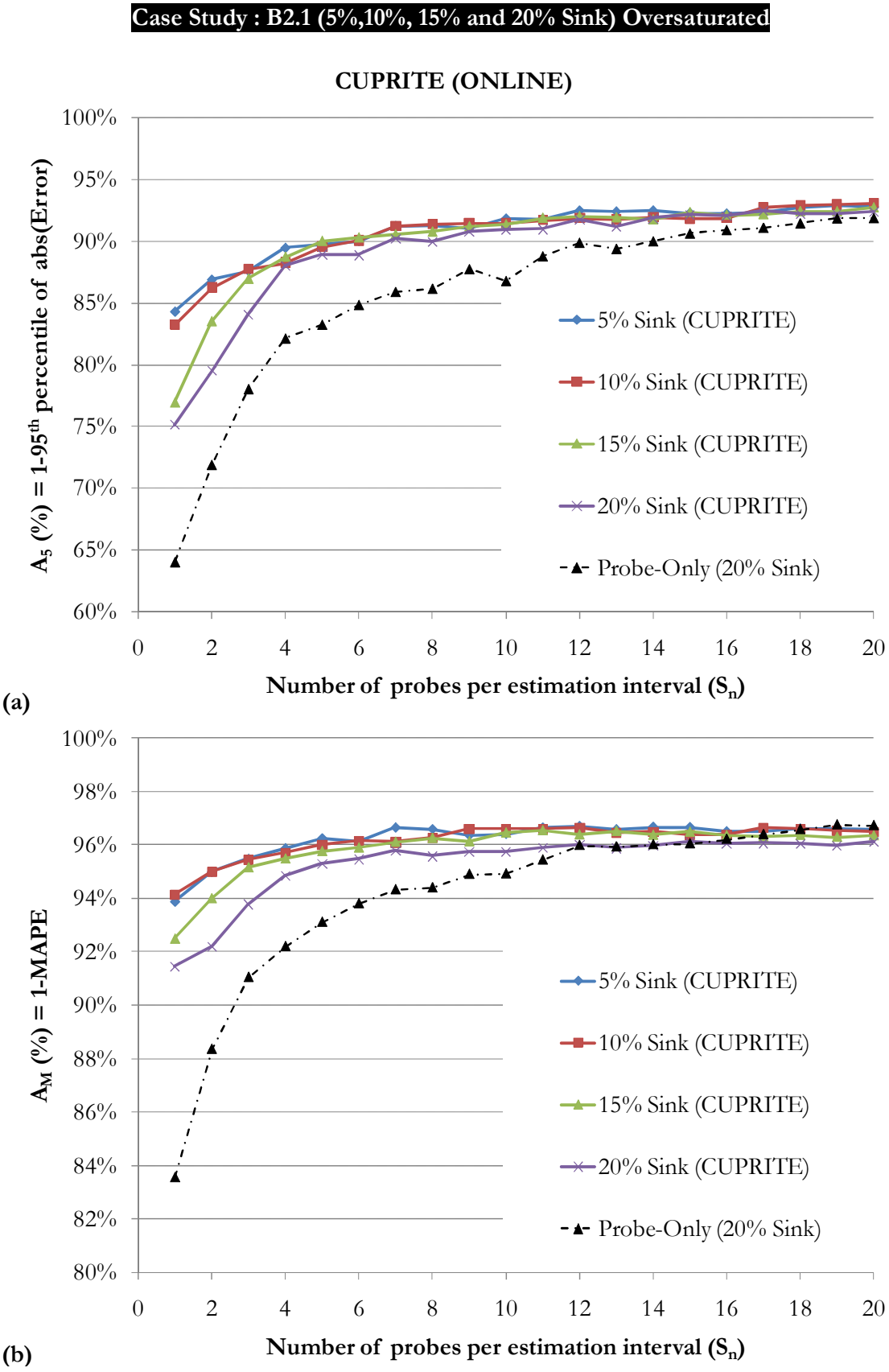

Figure 4-23: CUPRITE Online application for different sink percentages (5%, 10%, 15% and 20%); oversaturated traffic condition; non-FIFO discipline Results for accuracy: a) A_5 and b) A_M versus S_n.

Detector counting error (Case study B3.1, B3.2, B3.3 and B3.4)

Here CUPRITE is tested for 10% error in detector counting: upstream detector overcounting (case B3.1); upstream detector undercounting (case B3.2); downstream detector overcounting (case B3.3) and downstream detector undercounting (case B3.4). The results with respect to S_n are presented in Figure 4-24 and Figure D-8 for online and offline application, respectively. The accuracy for CUPRITE is close to 95% and 90% with respect to A_M and A_5, respectively. These results are consistent with that of 10% mid-link source and 10% mid-link sink case studies i.e., the effect of overcounting at downstream is equivalent to mid-link source; or the effect of undercounting at downstream is equivalent to mid-link sink etc. This confirms our hypothesis in section 4.1.2 that RD from detector counting error is analogous to that from mid-link sink/source case.

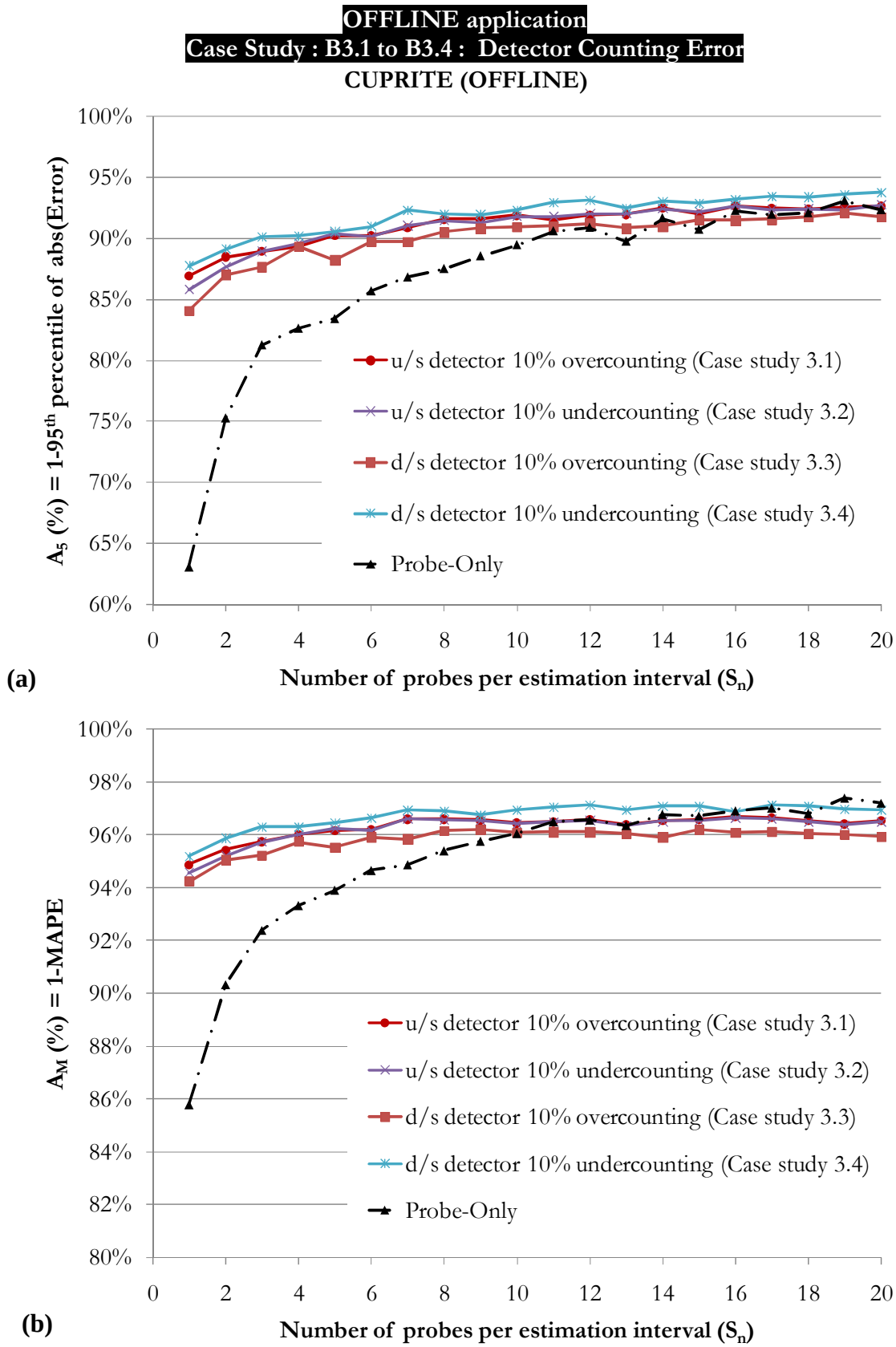

Figure 4-24: Detector counting error with fixed number of probes per estimation interval (S_n) for offline application: Cases B3. 1 to B3.4: Results for accuracy: a) A_5 and b) A_M versus S_n.

Discussion on simultaneous presence of different sources of RD

The above testing is for two independent conditions of sink, source, and detector counting error. A mid-link infrastructure can simultaneously act as both source and sink. For instance parking or two independent side streets, one acting as source and other acting as sink, etc.

If the net loss of vehicles to sink and gain of vehicles from source is zero then the issue of RD should not exist. In practice, source and sink percentage are dynamic in nature and for a larger time period such as one hour or so they may balance each other. Nevertheless, for each travel time estimation interval the effect of RD exits and integration of probe vehicles with cumulative plots have potential to improve the accuracy.

The above argument is supported through the following case studies:

i. *Net non-zero RD:* Figure 4-25 represents the results from 20% sink and 10% source case. This results in effective 10% sink. The results are consistent with that obtained from 10% sink case. The A_5 accuracy increases from 80% to 91% and A_M accuracy increases from 93% to 96% with increase in S_n. Similar results are obtained for 10% sink and 20% sources (Refer to Figure D-10).

ii. *Zero RD: 10% sink and 10% source case.* Figure 4-26 represents results from A_M accuracy and A_5 accuracy, respectively versus S_n. The performance of CUPRITE is consistent with A_5 accuracy close to 96% with at least one probe per estimation interval. In the present case, of 10% sink and 10% source, the net RD during the simulation period is zero. However, the vehicle lost in sink and gained from the source are random (with exponential arrival distribution in the simulation settings) due to which for each estimation period there exists RD and hence the performance can be enhanced by consideration of real probe. Refer to improvement in accuracy from $S_n = 0$ to $S_n > 0$. Similar results are obtained for: *a)* Case B4.4 20% sink and 20% source (Figure D-14); *b)* Case B4.5- 50% sink and 50% source (Figure D-15); *c)* Case B4.6- 90% sink and 90% source (Figure D-16); *d)* Case B4.7- 10% sink, 10% source, both upstream and downstream detector undercounting by 10% (Figure D-17) ; and *e)* Case B4.8- 10% sink, 10% source, both upstream and downstream detectors overcounting by 10% (Figure D-18).

   Note: If the loss and gain of vehicles are uniform throughout the simulation then, the net RD is also zero for each estimation interval. During such

condition, $S_n = 0$ should provide accurate results. Refer to Figure D-13 for results from uniform sink and source. There is slight decrease (by around 2%) in the accuracy when we move from $S_n = 0$ to one or two probes per estimation interval. This indicates that in absence of RD, there is significantly high accuracy during no probe condition. Then presence of one or two probes per estimation interval can induce slight error. However, for practical application it is unknown if the loss and gain of vehicles balance each other. Nevertheless, presence of probe vehicles provides confidence in the estimation.

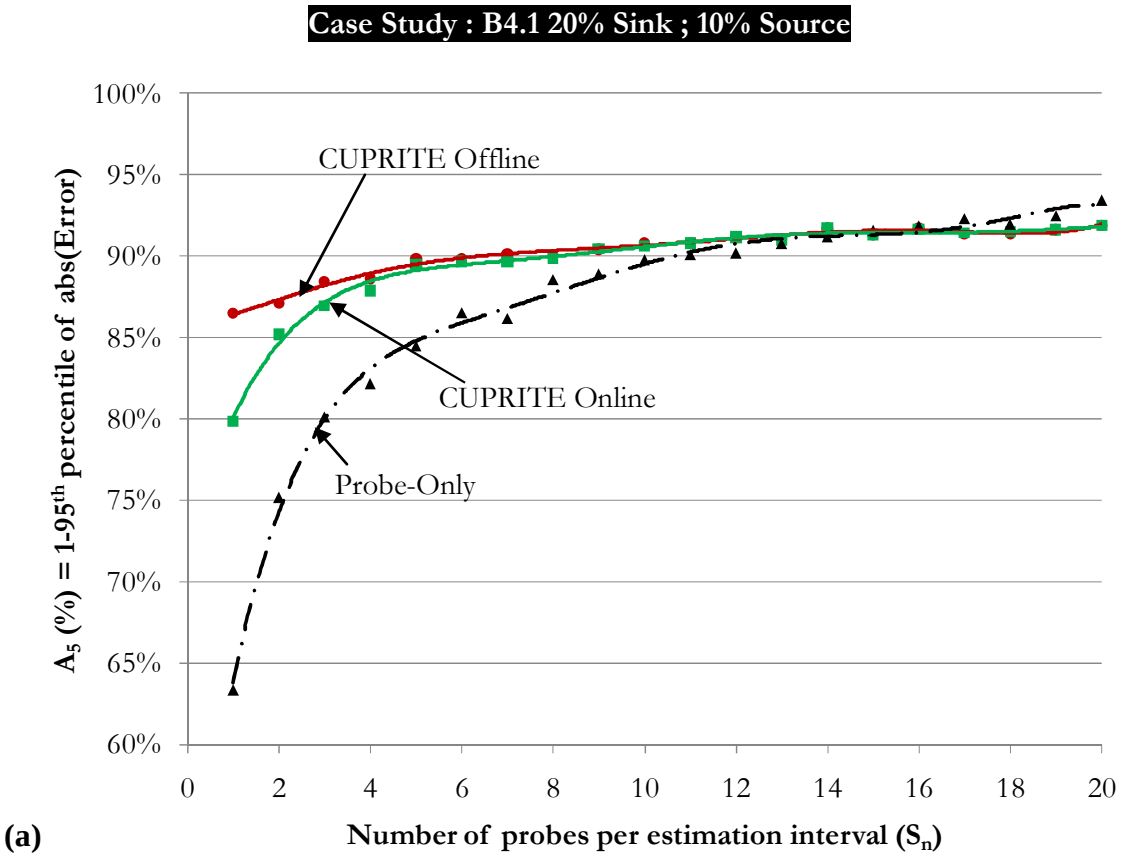

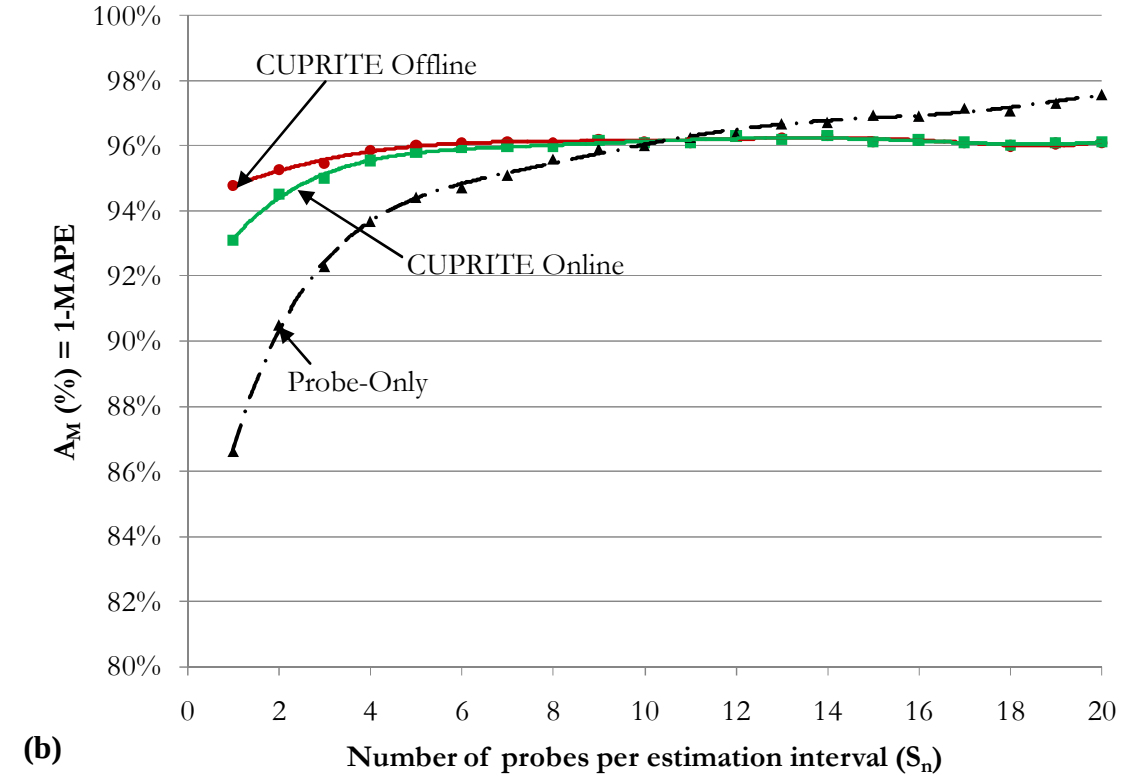

Figure 4-25: Simultaneous presence of both sink and source. Case B4.1 (20% sink and 10% source). Results for accuracy: a) A_5 and b) A_M versus S_n.

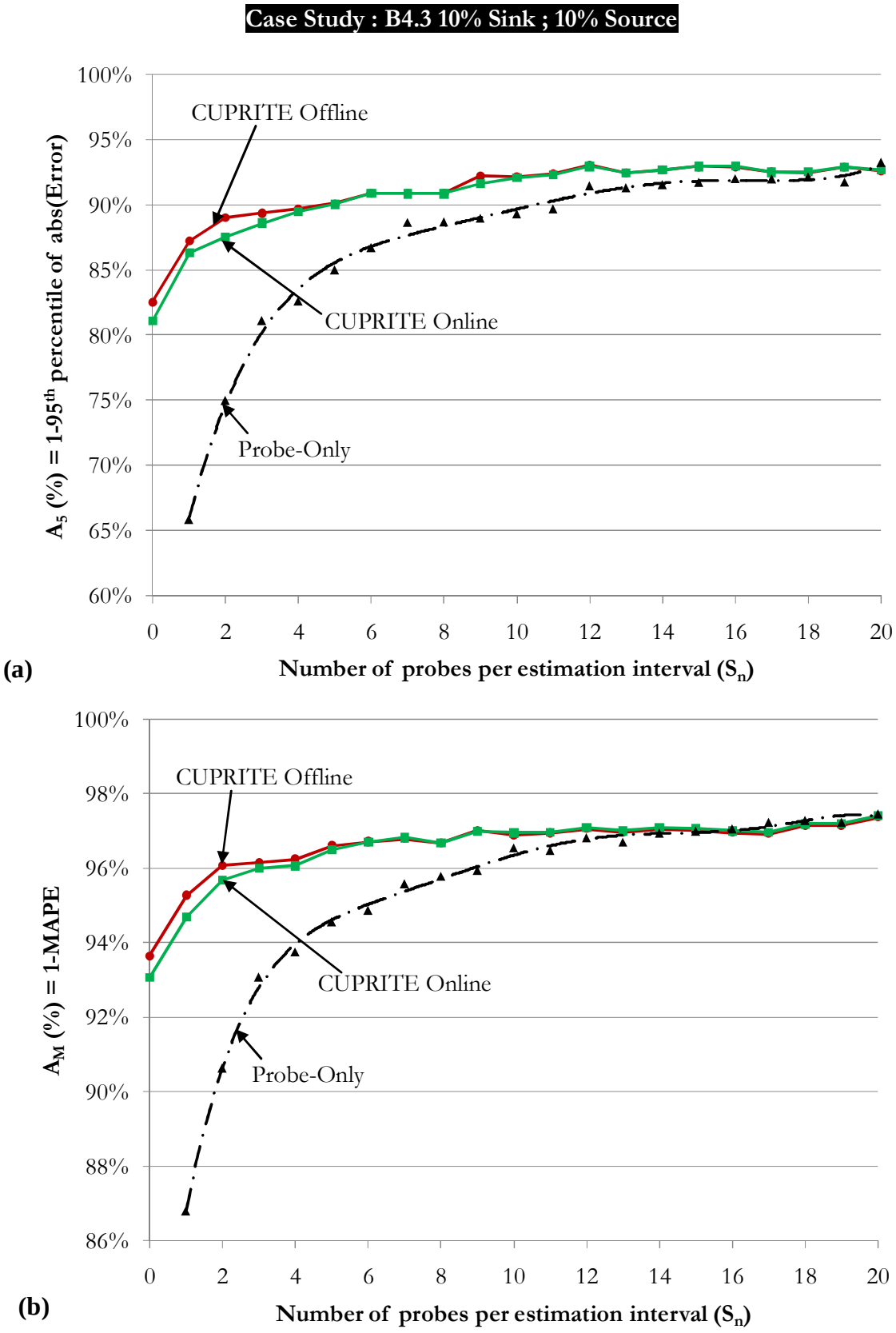

Figure 4-26: Simultaneous presence of both sink and source. Case B4.3 (10% sink and 10% source). Results for accuracy: a) A_5 and b) A_M versus S_n.

Reliability of the estimates

Figure 4-27 represents standard deviations (σ) of accuracies versus S_n for non-FIFO network. It can be said that higher the standard deviation, lower is the reliability of the accuracy estimate and vice versa. It is observed that the reliability of the CUPRITE increases (σ decreases) with increase in S_n and CUPRITE is more reliable than *Probe-Only*. In fact, when we have only one or two probes, then estimates from *Probe-Only* is uncertain, it can vary from perfect to worst estimate. Hence, integration of cumulative plots and probe not only increases the robustness of the travel time estimates using cumulative plots but also overcomes the issue of uncertainty in the estimates from the use of probe vehicles.

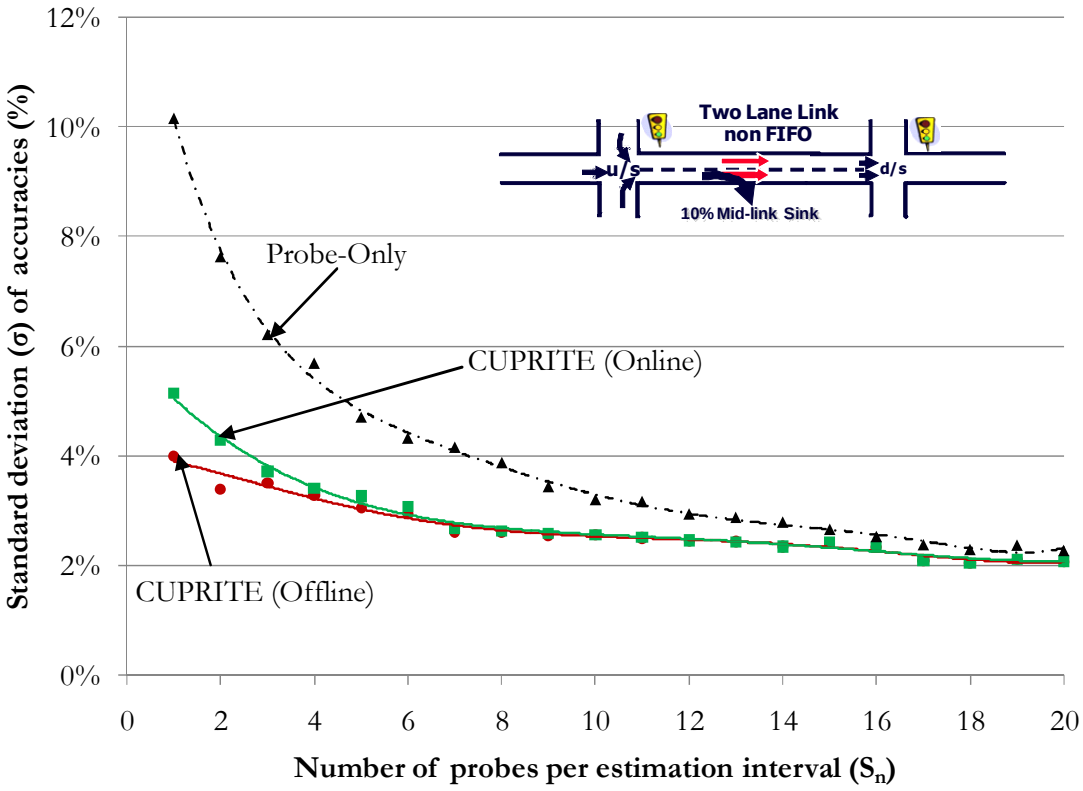

Figure 4-27: Standard deviation of accuracy versus number of probes per estimation interval.

4.4.4.2.2 Probe as percentage of all vehicles traversing the link (S_p)

Here, a fixed (S_p) percent of the vehicles is randomly selected from all the vehicles traversing the link during the complete simulation period. There may be certain estimation intervals with no probe data. Figure 4-28 illustrates the frequency distribution of estimation interval versus S_n. The data is from 10% sink case and non-FIFO network. It is observed that $S_P \geq 5\%$ can cover all the estimation intervals with $S_n \geq 1$, whereas, for $S_p \leq 3\%$ there can be significant

number of estimation intervals with no probe ($S_n = 0$). For instance, $S_P = 1\%$, can have more than 30% of estimation intervals with no probe.

Note: For *Probe-Only* (4.18) travel time cannot be estimated if there is no probe. Therefore, travel time for estimation interval with no probe is assumed to be equal to the travel time of the previous estimation interval with at least one probe.

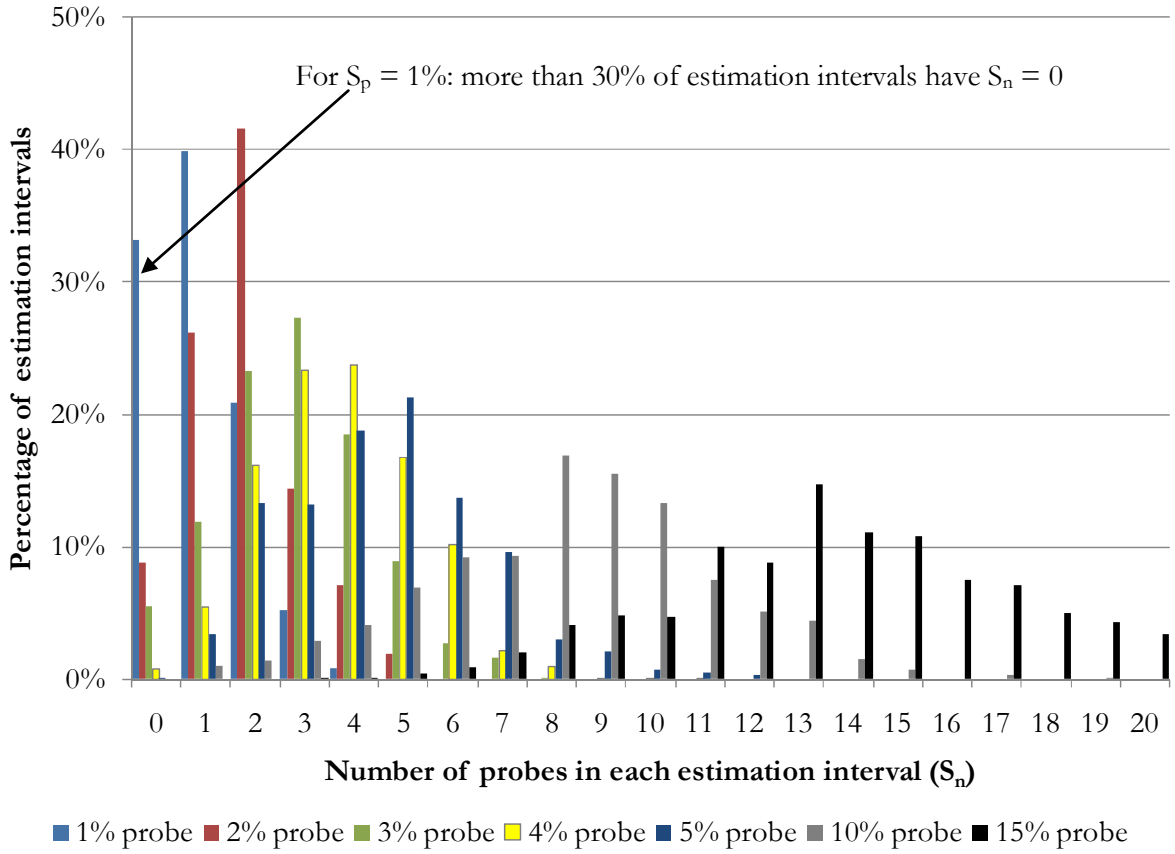

Figure 4-28: Percentage of estimation intervals with different number of probes per interval.

Figure 4-29 represents the results for 10% sink case (Case B1, non-FIFO) with probes as percentage of vehicles traversing the link. Each of the estimation interval considered may not have a probe. It is observed that:

i. For *offline* application: The performance is consistent and A_5 accuracy is more than 86% and A_M accuracy is more than 95%, respectively. As expected *offline* performs better than *online*.

ii. For *online* application: there is increase in A_5 accuracy from 70% to 86% for increase in probe from 0% to 3%. A_M accuracy increases from 90% to 95% for increase in probe from 0% to 3%.

iii. Accuracies for *Probe-Only* increases with increase in probe percentage. For low probe percentage (S_P < 5%) significant large number of estimation intervals is with no probe or a few number of probes which accounts for low accuracy. Integration of probe with cumulative plots for low probe percentage significantly enhances the accuracy. As percentage of probe increases, the number of probes per estimation interval also increases resulting in better accuracy. For instance, S_P = 15% probes generally provide S_n = 10. For such cases, probes are good representative of the population of the vehicles and there is little benefit of integrating probes with cumulative plots.

The results consistent with the above are obtained for other cases. Refer to Figure D-11 and Figure D-12. It can be concluded that 3% of the vehicles traversing the link as probes have the potential to provide accurate travel time for online application. For offline application even 1% of probe can provide accurate results.

The percentage of vehicles traversing as probes highly depends on the route, time of the day and day of the week. There are greater chances of obtaining probes on the link heavily traversed then on links with minor flow. The current market penetration of probe is very low and one does not expect more than 3% to 4% of vehicles as probes on heavily traversed route. With this limited number of probes, CUPRITE can significantly enhance the accuracy of travel time estimates on urban network.

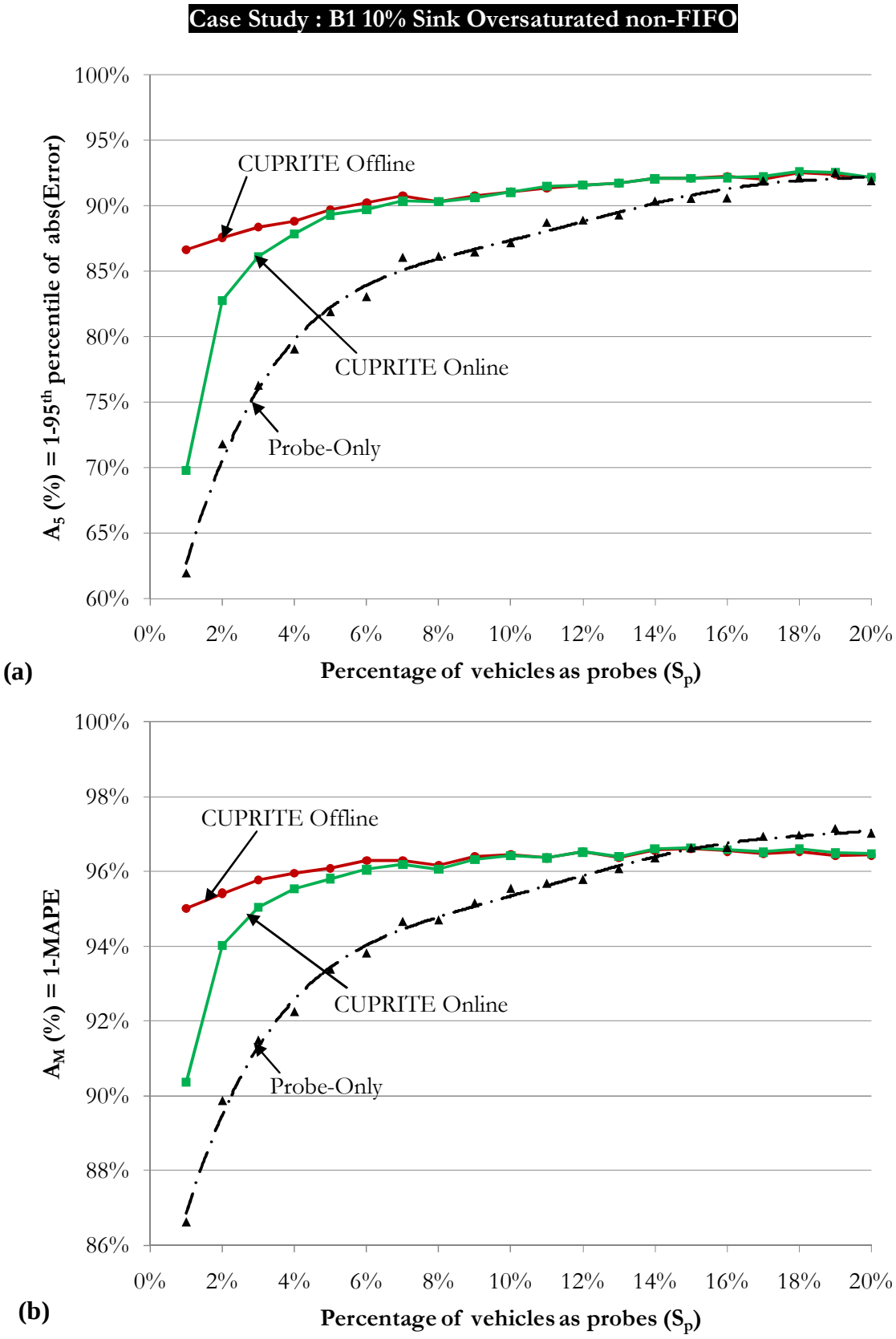

Figure 4-29: 10% sink case results for accuracy: a) A_5 and b) A_M versus S_p.

4.5 Concluding remarks

The methodology, CUPRITE, developed and tested in this chapter provides encouraging results for travel time estimation by integrating data from different sources: detectors and signal controller data at different locations on the network and probe vehicles. The exhaustive testing of CUPRITE indicates that the integration of different data sources provides better performance than method based on single data source only. It overcomes the issue of relative deviation amongst cumulative plots and uncertainty of travel time estimates from a few probes (sample size of one or two vehicles). It can provide accurate travel time for successive estimation intervals for both *offline* and *online* applications.

For undersaturated traffic condition, the concept of virtual probes is introduced and accurate estimates (Accuracy > 95%) can be obtained without consideration of real probe. It is observed that the use of real probes in addition to virtual probes can slightly decrease the accuracy by around 3% compared to the case when only virtual probe is considered. However, the real probe data is a real data and its use provides confidence in correction of relative deviation amongst the plots.

For oversaturated traffic condition, real probe significantly enhances the accuracy. Only one probe per estimation interval or three percent of vehicles traversing as probe is sufficient for accurate estimates for different magnitude of sink, source or detector counting error. For *Probe-Only* significantly large numbers of probes are required to obtain accuracy comparable to that from CUPRITE. The current market penetration of probe vehicle is quite low, especially in urban network and a large number of probes per estimation interval are rare. With current few numbers of probes, CUPRITE can significantly enhance the accuracy of travel time estimation.

In this chapter, CUPRITE is tested on a link between two consecutive intersections which forms the foundation of the CUPRITE application. In the next chapter, the application of CUPRITE for movement specific and route travel time estimation is discussed.

5 Discussions on route travel time estimation

In this chapter a methodology for exit movement specific travel time is recommended, followed by the discussion on the travel time estimation for a route using *Component* based and *Extreme* based estimation technique.

5.1 Exit movement specific link travel time

5.1.1 Significance

The flow on an urban link can be from different entrance links at upstream and towards different exit links at downstream. For instance in Figure 5-1 there are three exit movements at downstream: *Lft*, *Thru* and *Rt*. The entrance flow on the link is also from three different directions at the upstream: *A*, *B* and *C*. In all, there can be nine different combinations of flows: *A* to *Lft*, *A* to *Thru*, *A* to *Rt*, *B* to *Lft*, *B* to *Thru*, … ,*C* to *Rt*. Based on the delay experienced by a vehicle at upstream intersection and at downstream intersection there can be nine different combinations of travel time from an upstream link to the downstream link. For route specific travel time one is interested in one of these combinations based on the flow associated with the route.

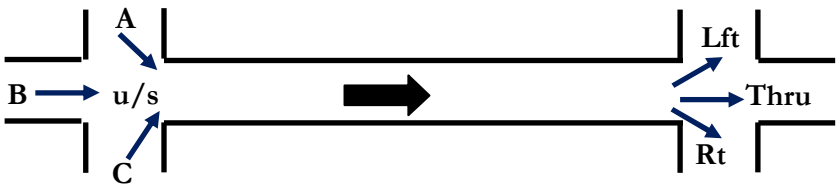

Figure 5-1: Different turning movements associated with a link.

We define travel time on a link as the time required to travel from the entrance of upstream intersection to the entrance of downstream intersection. Therefore, here we can define total entrance flow at upstream (*u/s)* as combination of flow from *A*, *B* and *C* and focus on the estimation of travel time from *u/s* to *Lft*, *u/s* to *Thru* and *u/s* to *Rt* (i.e., travel time associated with different exit turning movements of the link.).

Figure 5-2 is real individual vehicle travel time for two different movements on one of the urban signalized link in Lucerne city, Switzerland[14]. It can be seen that travel time from *u/s* to *Lft* movement is significantly higher than that from *u/s* to *Thru* movement. And the average travel time (*u/s* to *d/s*) is not a true representative of different movements. Hence it is worth analyzing travel time for different movements associated with link.

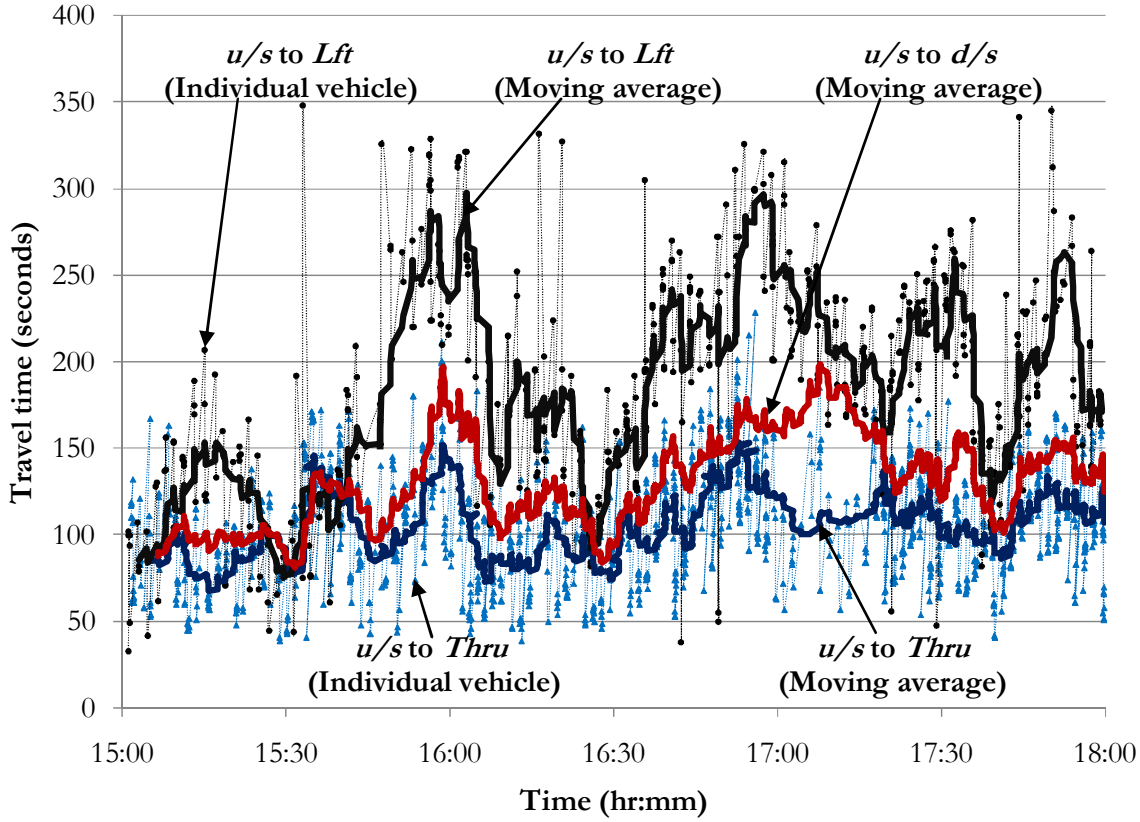

Figure 5-2: Example for actual travel time for different exit movements associated with a link.

5.1.2 Issue

CUPRITE can be applied for the above discussed link exit movement specific travel time estimation. For this we need to estimate accurate upstream (arrival) and downstream (departure) cumulative plots for each exit movement. Assuming detectors at stop-line location: one can accurately obtain departure cumulative plot for each exit movements. The stop-line detector at upstream intersection provides total upstream cumulative plot i.e.,

[14] The data is from intersection A (Kasernenplatz) to intersection D (Pilatusplatz) (Refer to Figure 6-7) of the study site discussed in the next chapter on CUPRITE validation with real data.

cumulative plot based on the total flow at the upstream entrance of the link. What is unknown is the upstream cumulative plot for each exit movement.

Note: For simplicity of discussion here we use the term exit moments. To be precise we consider the combination of different movements, based on the link geometry and signal phases. For instance: for downstream intersection in Figure 5-3*a* travel time for all the movements is to be differentiated (Here downstream cumulative plot for *Rt*, *Lft* and *Thru* movements are obtained from detector d_{a1}, d_{a2} and d_{a3}, respectively.) whereas, for downstream intersection in Figure 5-3*b* travel time for right movement is to be differentiated from combination of the through and left movement (Here, downstream cumulative plot for *Rt* movement is obtained from detector d_{b1} and for *Thru+Lft* movement is obtained from sum of counts from d_{b2} and d_{b3}.).

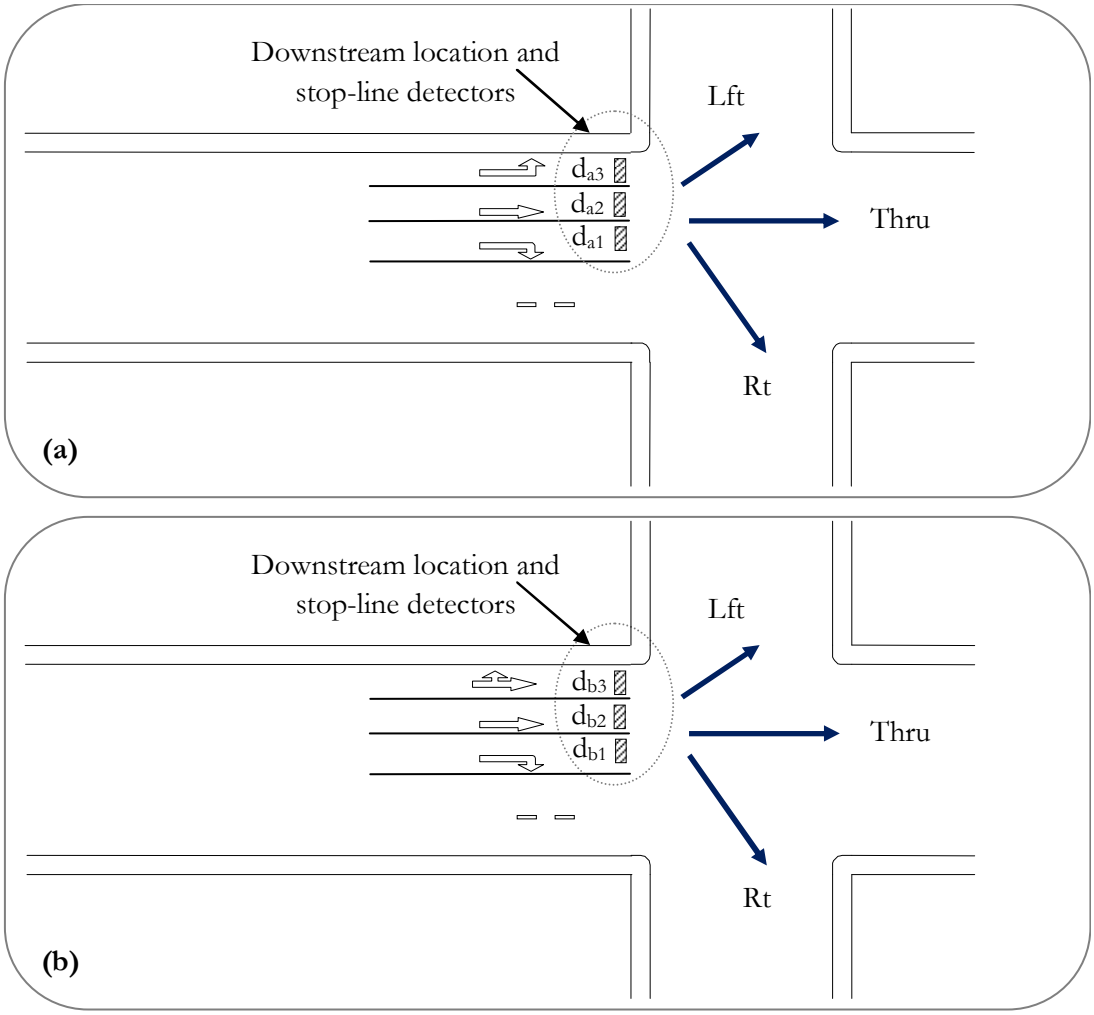

Figure 5-3: Example for two different downstream exit movement combinations based on link geometry.

5.1.3 Vertical scaling technique to define the upstream cumulative plot for each exit movement

Let us consider an example. Figure 5-4 illustrates a study link with flow from three different directions at upstream intersection and exit flow towards three different movements at downstream intersection. In the example, at upstream intersection: Detector *A* and detector *C* are on shared-used lane with proportion of counts η_A and η_C, respectively towards the study link. One can obtain total cumulative plot at upstream (U_T) of the study link as a linear combination of cumulative plots from each upstream detector, scaled with respect to the counts proportions:

$$U_T = \eta_A CP_A + \eta_B CP_B + \eta_C CP_C \tag{5.1}$$

Where: η_A, η_B and η_C are proportion of counts observed at upstream detectors *A*, *B* and *C*, respectively towards the study link. Here, η_B is unity as detector *B* is not on a shared-use lane.

To estimate the arrival cumulative plot for each movement we consider *vertical scaling technique* on U_T. Here we define *scaling factors*: S_{Lft}, S_{Thru} and S_{Rt} as the factors used to vertically scale U_T to define upstream cumulative plot for each movements.

$$U_{Lft} = f(S_{Lft}, U_T);\ U_{Thu} = f(S_{Thru}, U_T);\ U_{Rt} = f(S_{Rt}, U_T) \tag{5.2}$$

Say variables *d*, *p*, and *m*, represent day of the week, time period of the day, and m^{th} exit turning movement, respectively. The variable $\hat{S}_{m,p,d}$ represents the scaling factor for m^{th} exit movement, p^{th} period of d^{th} day of the week. For instance: $\hat{S}_{Lft,7:00-7:15am,Monday}$ is the scaling factor for left exit movement, from 7:00 a.m. to 7:15 a.m. on Monday. The cumulative plot for m^{th} movement ($U_m(t)$) can be defined as follows:

$$U_m(t) = U_m(t_{s,p}) + \hat{S}_{m,p,d}[U_T(t) - U_T(t_{s,p})] \quad \forall Time\ Periods\ and\ \forall t \in [t_{s,p}, t_{e,p}] \tag{5.3}$$

Where: $t_{e,p}$ and $t_{s,p}$ is the time corresponding to the start and end of the p^{th} time period.

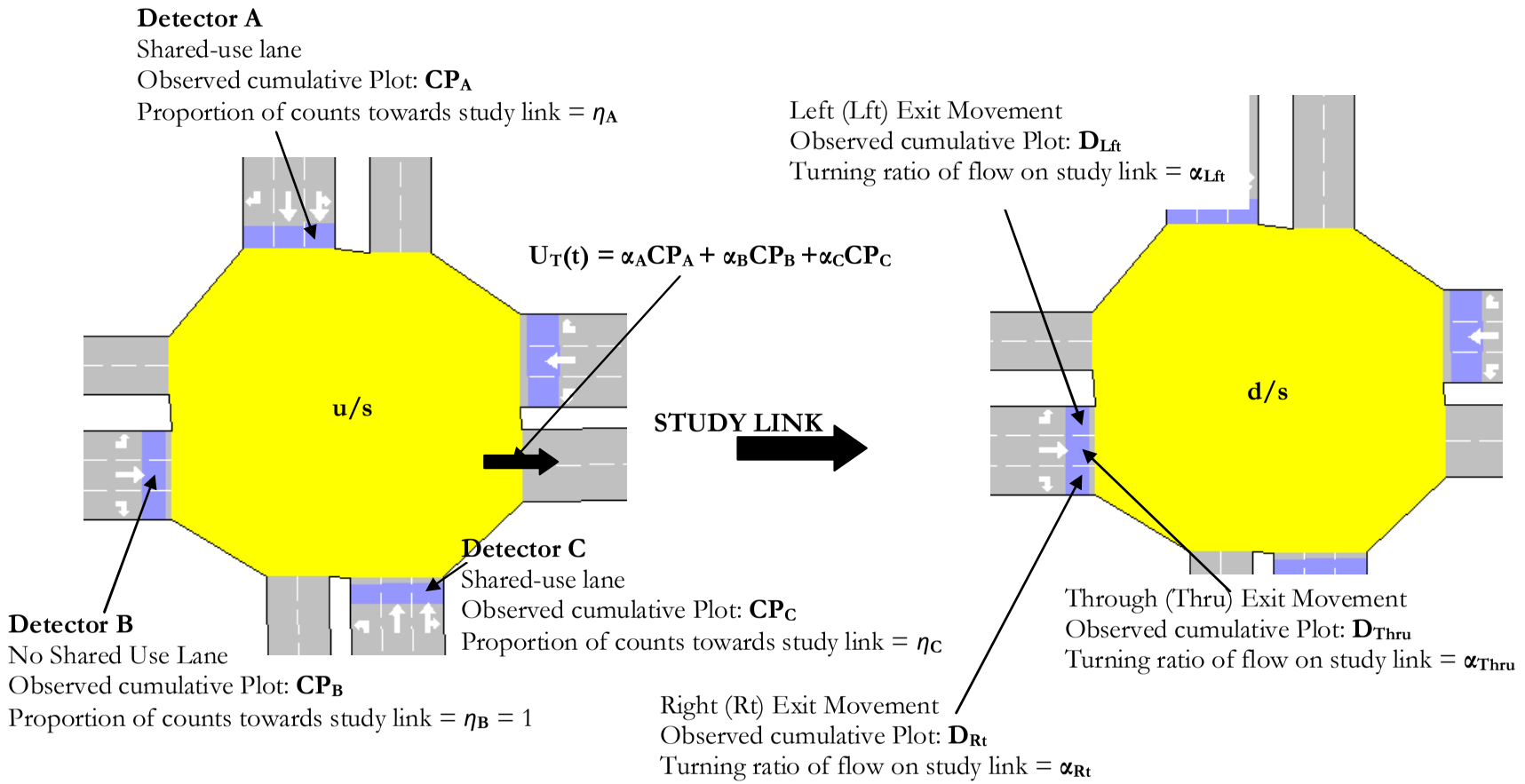

Figure 5-4: Example of a study link with flow from three different directions at upstream intersection and exit flow towards three different movements at downstream intersection.

5.1.3.1 How to define the scaling factor

Here we consider two different approaches to define the scaling factor based on: historical average turning ratios; and historical effective scaling factor. Both are defined in terms of time of the day and day of the week.

5.1.3.1.1 Average turning ratios

As U_T is the total counts observed at the upstream entrance of the link, therefore it is obvious that the initial estimate for the scaling factor should be the actual real time exit turning ratio of the link.

In practice, travelers traversing on a link, decides its movement based on its destination and route choice for that destination. Turning ratios are random variables and vary with time. For instance, Figure 5-4 illustrates real turning ratio, measured on a particular day, on a link at Ikegami Shinmachi Intersection, Kawasaki city, Japan. It can be seen that there is significant variation in the turning ratio for different peak periods and different time of the period (For instance, *Thru* movement turning ratio for morning peak period varies from 60% to 85% with average of 78% whereas, during evening peak period the average for *Thru* movement is 83% with relatively less variation.). Turning ratio is a stochastic (random) parameter, and different observations for same time of the day and day of the weak have different values. However, one can obtained the best estimate for the expected turning ratio based on the past (historical) observations.

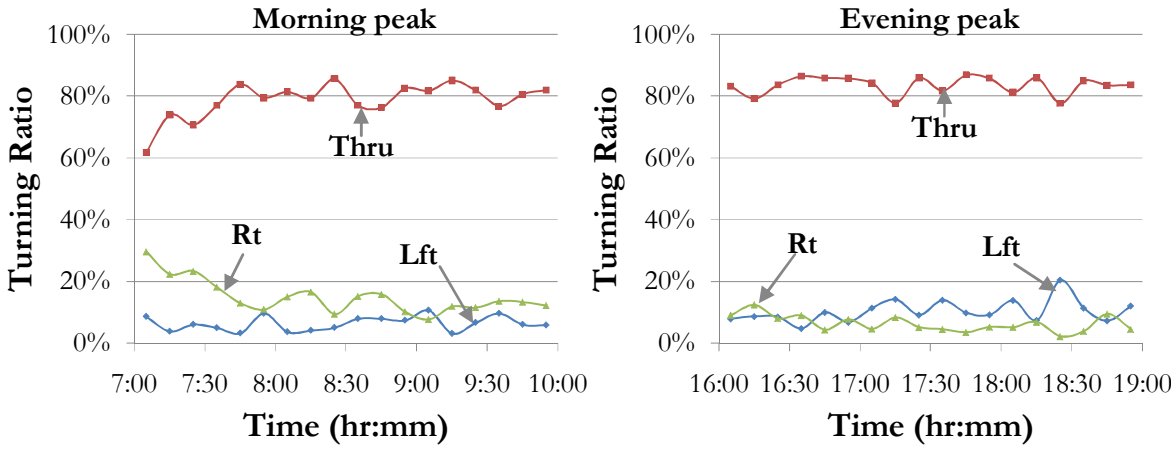

Figure 5-5: Example for real turning ratios for three different directions from one of the link at Ikegami Shinmachi intersection, in Kawasaki City, Japan.

Estimating turning ratios is mathematically a non-deterministic problem with infinite number of solutions. Models for both static and dynamic (real time) applications are developed to estimate the "most likely" solution. For instance, Martin (1997) has applied Linear programming for real time turning ratio estimation. Lan and Davis (1999) used non linear least square approach and quasi maximum likelihood approach using Markovian traffic flow model. The models in literature can be applied for developing the historical database for average turning ratios values for different time of the day and day of the week and hence the scaling factor can be define based on the most appropriate value.

Say variable $\alpha_{m,p,d}$ represents the historical average turning ratio for m^{th} exit movement, during p^{th} time period and d^{th} day of the week. Then we can define scaling factor as:

$$\widehat{S}_{m,p,d} = \alpha_{m,p,d} \tag{5.4}$$

The above consideration of the average turning ratio defines the expected cumulative plot at upstream of the link for each movement. This is the initial upstream cumulative plot and is to be further redefined to take into account the effect of mid-link sinks and sources, and detector counting error.

5.1.3.1.2 Effective scaling factor

The testing result in the previous chapter gives confidence in the accurate estimation of travel time for offline application of CUPRITE. Hence, the offline redefined cumulative plot at upstream with probe data can be utilized for developing a historical database of effective scaling factor for different time of the day and day of the week. The effective scaling factor incorporates the scaling required for exit turning ratio and also due to probable loss/gain of vehicles to/from mid-link sinks/sources.

To develop the database, at the end of each day, the total cumulative plot observed at upstream (U_T) and the offline cumulative plot for m^{th} movement (U_m) should be integrated to define the effective scaling factor for time periods with at least one probe vehicle

Say variable $s_{m.p,d}$ (5.5) represents the scale for a record of m^{th} exit movement, p^{th} time period of d^{th} day of the week:

$$s_{m,p,d} = \frac{Y_{T,d,p} - Y_{m,d,p}}{Y_{T,d,p}}$$

$$Where: \quad Y_{T,d,p} = U_T(t_{e,p}) - U_T(t_{s,p}) \qquad (5.5)$$

$$Y_{m,d,p} = U_m(t_{e,p}) - U_m(t_{s,p})$$

Where:

$U_T(t)$ and $U_m(t)$ is the total upstream cumulative counts observed and cumulative count for m^{th} movement, respectively at time t;

$t_{e,p}$ and $t_{s,p}$ is the time corresponding to the start and end of the p^{th} time period;

$Y_{T,d,p}$ and $Y_{m,d,p}$ is the total counts observed, and counts for the m^{th} movement observed during the p^{th} time period, respectively (see Figure 5-6*e*).

The database consists of the values of the effective scaling factor $s_{m,p,d}$ properly classified in corresponding time of the day and day of the week. The database is daily self updated, with the new values defined at the end of the day. The required scaling factor $\hat{S}_{m,p,d}$ can be defined as the median of values of effective scaling factor defined in the historical database:

$$\hat{S}_{m,p,d} = Median\ of\ s_{m,p,d} \qquad (5.6)$$

5.1.3.2 Example of the methodology

Say we have a historical database of the scaling factor, either defined in terms of turning ratios or effective scaling factor. For each of the periods shown in the Figure 5-6, first the scaling factor from historical database is obtained and initial estimate of the upstream cumulative plot for movement *m i.e.*, $U_m(t)$ is defined using equation (5.3). Thereafter, $U_m(t)$ is redefined as discussed in Section 4.2 by integrating with probe vehicle data. Finally, the redefined $U_m(t)$ is utilized to self update the historical database using equation (5.5).

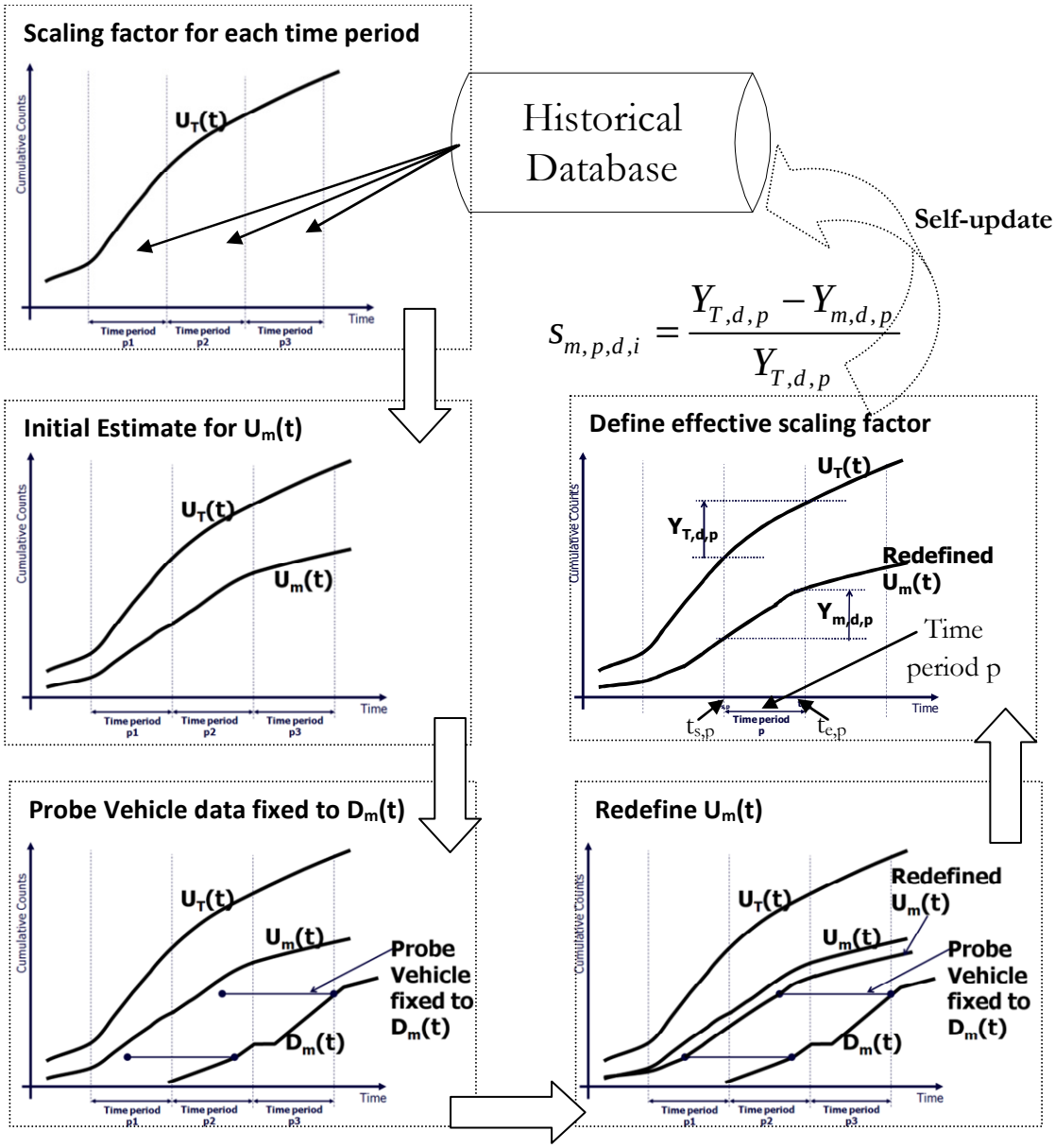

Figure 5-6: Example of the methodology for estimation of upstream cumulative plot for each exit turning movement.

5.1.4 Architecture for exit-movement specific link travel time

The architecture for the CUPRITE to take into account the exit-movement specific travel time estimation is provided in Figure 5-7:

i. Initial upstream cumulative plot for a movement is defined by *vertically scaling* the total upstream cumulative plots with *scaling factor* defined with historical database;

ii. Downstream cumulative plot for the movement is defined by integrating the downstream detector with signal timings;

iii. Probe vehicle data is fixed to downstream cumulative plots;

iv. Thereafter, upstream cumulative plot is redefine; and

v. Finally, travel time for the movement is estimated as ratio of area between the cumulative plots and the number of vehicles departing from the exit movement.

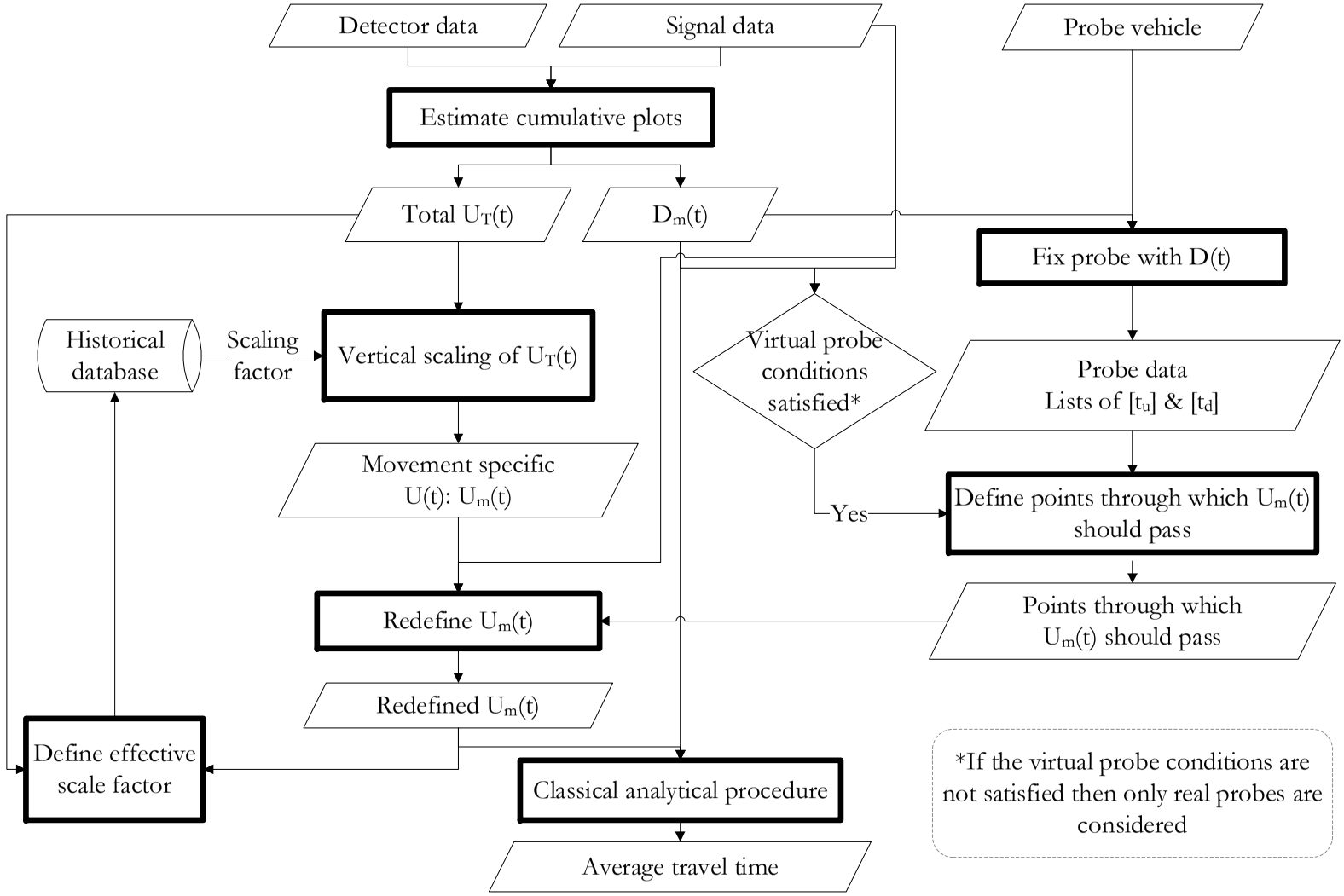

Figure 5-7: CUPRITE architecture for link-movement specific travel time estimation.

In next chapter (section 6.2.1) to validate the CUPRITE on real data we apply scaling factor defined in terms of average turning ratio. The thorough testing of the above recommendation for developing a database for effective scaling factor is beyond the scope of this dissertation.

5.2 Route travel time

A route can be divided into different components. The route (from *S* to *E*) shown in Figure 5-8 can be divided into five components: a) left movement from *S* to *A*; b) through movement from *A* to *B*; c) left movement from *B* to *C*; d) right movement from *C* to *D*; and e) right movement from *D* to *E*. The travel time for the route is the sum of the travel time on each component.

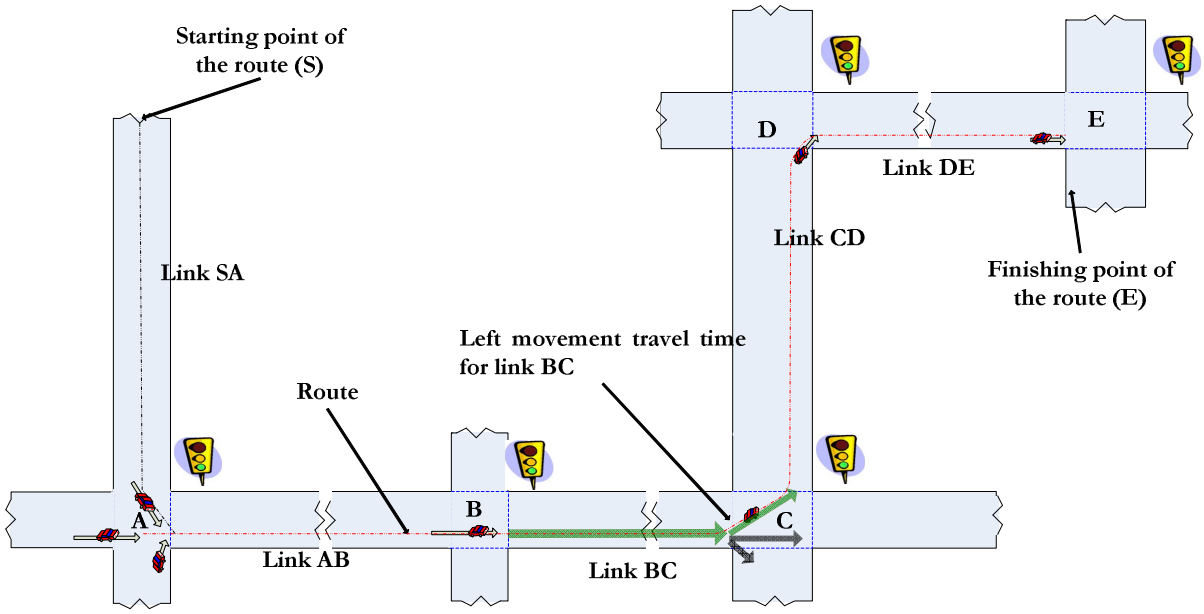

Figure 5-8: Example for route travel time.

Say, a vehicle starts its journey at time t_{start} to cover the above route and travel time on i^{th} component at time t be $TT_i(t)$. Then in order to obtain route travel time following two methods can be applied:

i. *Instantaneous method:* This is the sum (5.7) of travel time of each component of the route at time t_{start} i.e.

$$\text{Instantaneous } TT_{Route} = \sum_{\forall Route\ Components} TT_i\ (t_{start}) \tag{5.7}$$

ii. *Time-slice method:* This is the sum (5.8) of travel time of each component of the route at time when vehicle is expected to be at that component. That is,

travel time of first component is $TT_1(t_{start})$; travel time of second component is $TT_2(t_{start} + TT_1(t_{start}))$; travel time for third component is $TT_3(t_{start} + TT_1(t_{start}) + TT_2(t_{start} + TT_1(t_{start}))$ and so on.

$$\text{Time-Slice } TT_{Route} = \sum_{\forall Route\ Components} TT_i(t_{start} + \sum_{j=1}^{i-1} TT_j) \quad (5.8)$$

5.2.1 CUPRITE for route travel time estimation

CUPRITE can be applied for route travel time estimation in following two approaches:

i. *Extreme* Based (R_E): Here we estimate route travel time by directly considering the area between the cumulative plots at extreme points of the route i.e., upstream entrance and downstream exit of the route; and

ii. *Component* Based (R_C): Here we add movement specific travel time of each component of the route.

5.2.1.1 Extreme based route travel time (R_E)

Here the route travel time is estimates using the cumulative plots at upstream entrance and downstream exit of the route. At downstream exit all the vehicles departing during the travel time estimation interval are considered. A proportion of these departing vehicles are those that traverse the complete route and are randomly distributed throughout the estimation period. Due to this random distribution the area between the plots is a representative of travel time for the vehicles that traverses the complete route.

This approach is quite simple to apply. The detectors are required only at upstream and downstream of a route, all other components of the route do not need to have detectors. However, the required probes should be those which traverse the complete route. Note: Here virtual probe cannot be considered as mid-link intersections are source of significant mid-link delay even during undersaturated situation (Refer to Section 4.2.2.2 in Chapter 4).

5.2.1.2 Component based route travel time (R_C)

Here, we consider the pairs of cumulative plot at upstream and downstream for each component. Each pair of cumulative plot is independent from the other pair in the network as relative deviation amongst each pair is corrected independently. Say $U_{l,m}(t)$ and $D_{l,m}(t)$

represents a pair (the upstream and downstream cumulative plot) for m^{th} movement of link (component) *l*.

Consider the Figure 5-8, say one is interested to know the travel time from point *S* to start of the link *CD* i.e., average travel time for the vehicles departing from left movement of link *BC* during time interval from t_1 to t_2. For each of the components: link *SA*, link *AB* and link *BC* we have separate cumulative plots. Figure 5-9 and Figure 5-10 represents the methodology for instantaneous and time-slice travel time, respectively.

For instantaneous travel time (Figure 5-9), we consider the average travel time of all vehicles departing during time interval t_1 to t_2 for a) left movement of link *SA*; b) through movement of link *AB*; and c) left movement of link *BC*.

For time-slice travel time (Figure 5-10) we consider average travel time of the vehicles departing during time interval a) t_1 to t_2 from left movement of link *BC*; b) t_3 to t_4 from through movement of link *AB*; and d) t_5 to t_6 from left movement of link *SA*. Where t_3, t_4, t_5 and t_6 are time obtained based on the vehicles represented in the upstream cumulative plot of the downstream link i.e.,

$$\begin{aligned} t_3 &= U_{BC,Lft}^{-1}(D_{BC,Lft}(t_1)); \quad t_4 = U_{BC,Lft}^{-1}(D_{BC,Lft}(t_2)) \\ t_5 &= U_{AB,Thru}^{-1}(D_{AB,Thu}(t_3)); \quad t_6 = U_{AB,Thru}^{-1}(D_{SA,Lft}(t_4)) \end{aligned} \tag{5.9}$$

Note: Here, we are interested in estimating the travel time, i.e., the experienced travel time for the trip. Therefore, the above analysis starts from the downstream component (link *BC*) and move toward the upstream component (link *SA*). “Instantaneous travel time” is a good estimator for real time application as it is more close to the expected travel time in the next interval. “Time-slice travel time” is a good estimator for offline applications as it provides accurate estimates for experienced travel time. In the present analysis we are interested in experienced travel time hence we apply time-slice analysis using component based approach. For real time application instantaneous travel time can be applied using component based approach for better estimates for expected travel time.

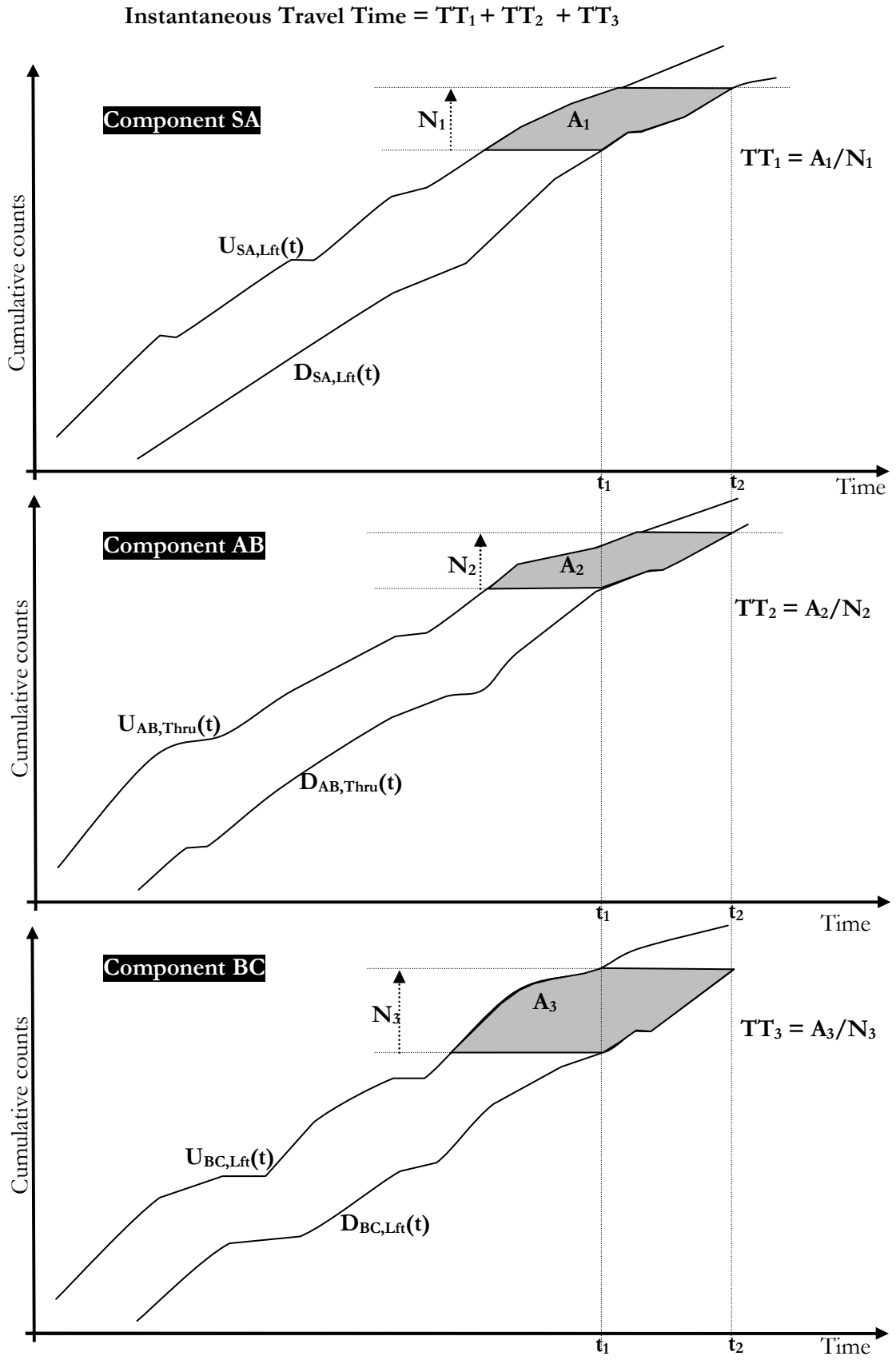

Figure 5-9: Example for instantaneous route travel time.

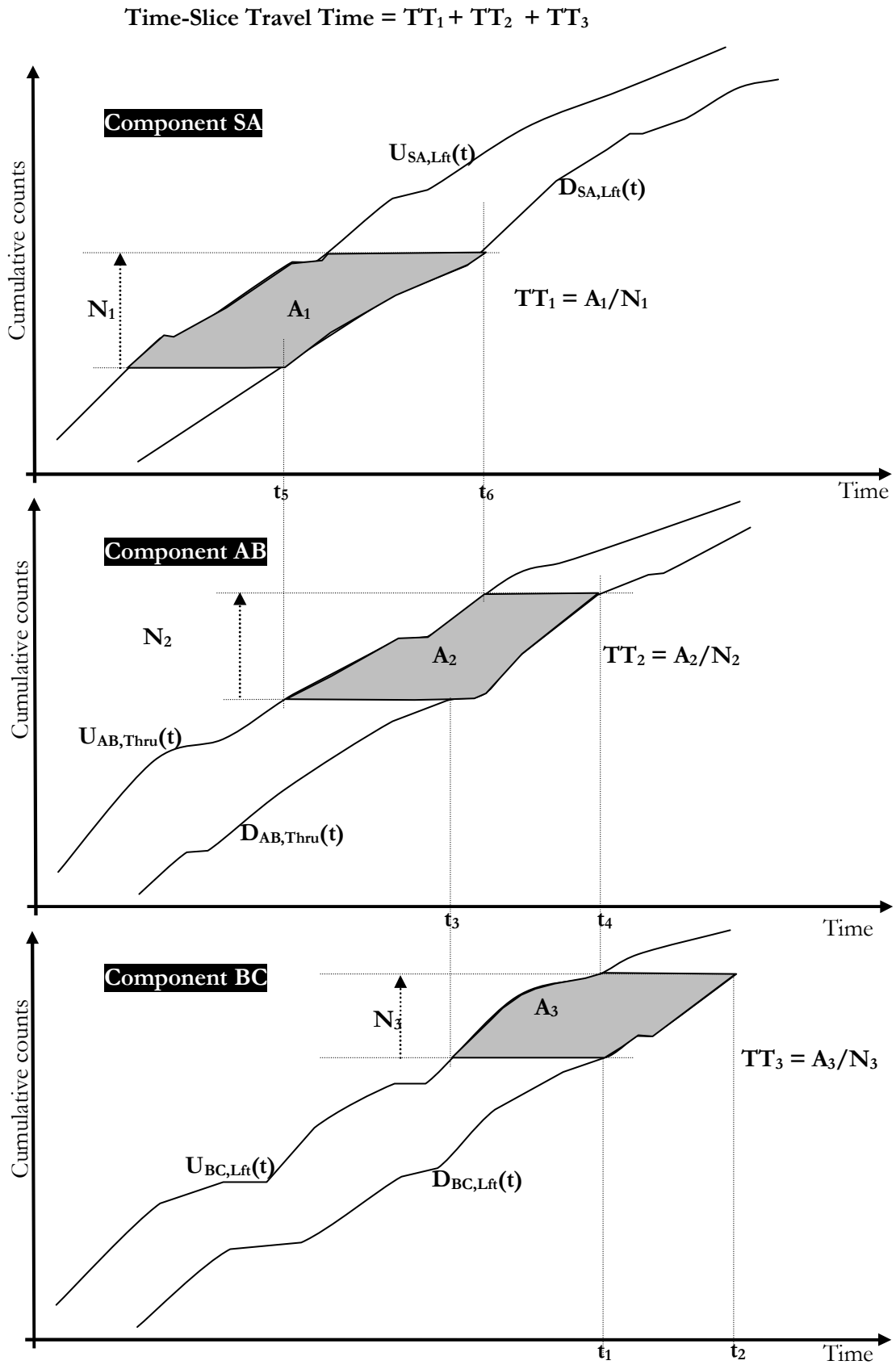

Figure 5-10: Example for time-slice route travel time: *Component* based (R_C).

5.2.2 CUPRITE testing for route travel time

In the previous chapter CUPRITE was tested on single link between two consecutive intersections. In this chapter CUPRITE is tested to estimate travel time for multiple links route. A network of five consecutive signalized intersections, with stop-line detectors is considered for the testing (*see* Figure 5-11) and we define a route from intersection *A* to intersection *E*.

First the R_E and R_C estimation techniques are compared for flow F1 (where 90% of the flow at upstream traverses the route). Thereafter, the result of R_E application is provided for following flow values:

i. F2: 50% of the flow at upstream traverses the route.

ii. F3: 20% of the flow at upstream traverses the route.

The Origin-Destination matrix for the network is randomly defined so that the above mentioned flow conditions are satisfied. Due to random selection, for case study F1 and F3, the counts at upstream (intersection *A*) are 5% more than that at downstream (intersection *E*) i.e., there is effective 5% sink. Similarly, for case study F2, there is effective 10% source.

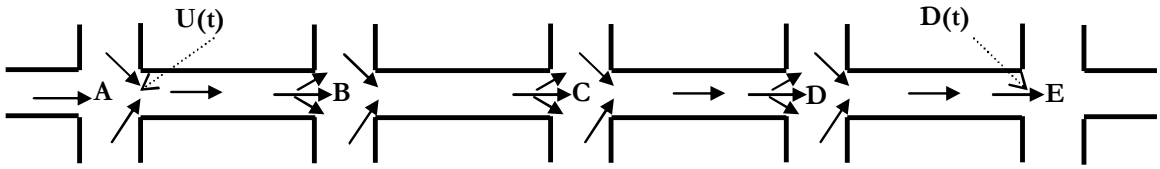

F1 : 90% of the vehicles in U(t) are also in D(t)
F2 : 50% of the vehicles in U(t) are also in D(t)
F3 : 20% of the vehicles in U(t) are also in D(t)

- All intersections are signalized
- All links are two lanes, with separate left and right movement lane.
- Length of each link is approx 500 m

Figure 5-11: Network for CUPRITE testing for route travel time estimation.

Figure 5-12 illustrates the framework for the testing. Two different case studies are performed:

i. Case M1: Here the comparison between R_C and R_E technique is performed for flow combinations F1 and for: undersaturated (Case M1.U); and oversaturated traffic condition (Case M1.O).

ii. Case M2: Here different flow combinations (F1, F2 and F3) are analyzed for R_E technique.

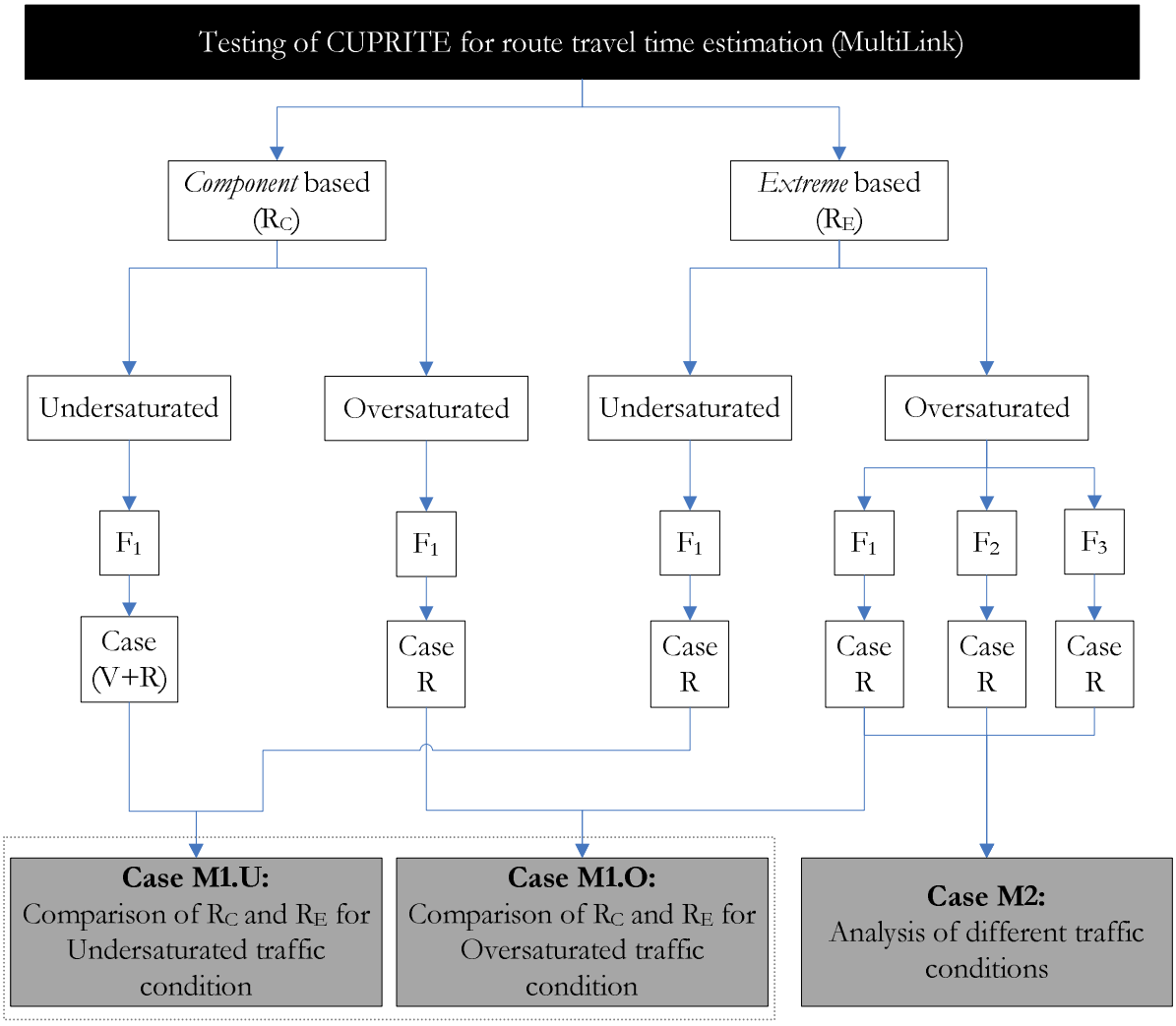

Case V+R: Virtual and Real Probe.
Case R: Real probe.

F1: 90% flow at upstream traverses the route.
F2: 50% flow at upstream traverses the route.
F3: 20% flow at upstream traverses the route.

Figure 5-12: Framework for testing of CUPRITE for route travel time estimation.

For R_C the components defined are through movements from *A* to *B*; *B* to *C*; *C* to *D*; and *D* to *E*. For R_E cumulative plots at upstream entrance (U(t)) at intersection *A* and downstream exit (D(t)) at intersection *E* are considered.

5.2.2.1 Case M1

The results for undersaturated (case M1.U) and oversaturated (case M1.O) traffic conditions are presented in Figure 5-13 and Figure 5-14, respectively.

During undersaturated traffic condition, virtual probe can be defined for each component and hence even in the absence of real probe accurate travel time can be obtained for R_C ($A_M > 96\%$ and $A_5 > 94\%$, for $S_n = 0$) (*see* Figure 5-13). The presence of probes slightly decreases the accuracy this is consistent with the results for single link (Refer to Section 4.4.4 and example in Figure 4-17. Due to randomness in the vehicle arrival and other reasons, the consideration of real probes provides distortion in the U(t) resulting in low accuracy compared to that of virtual probe case.).

During oversaturated traffic condition, virtual probes are not considered and the accuracy for R_C increases with increase in S_n (*see* Figure 5-14).

Both A_5 and A_M for R_C is slightly higher than that from R_E. This indicates that R_C provides better estimates in terms of average performance and consistency in performance.

Though R_C is more accurate but detectors data and signal timings are required for each component. There are higher chances of getting probe for each component than one traversing the complete path. R_E is simple to apply and data only at upstream and downstream of the route is required but the required probe should traverse the complete route, which could be less frequent.

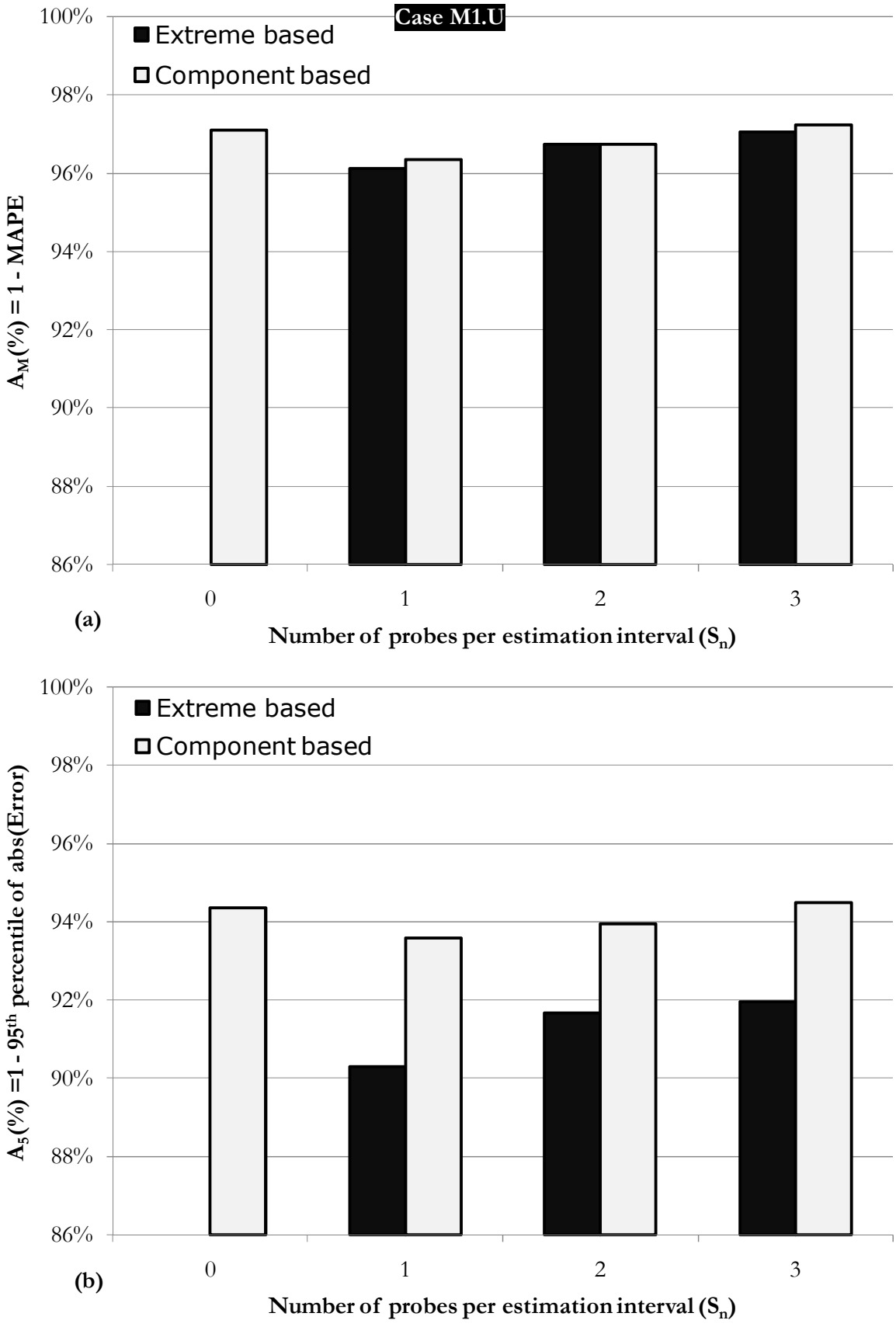

Figure 5-13: Case Study M1.U, Flow = F1, Accuracy (a) A_M and (b) A_5 versus S_n.

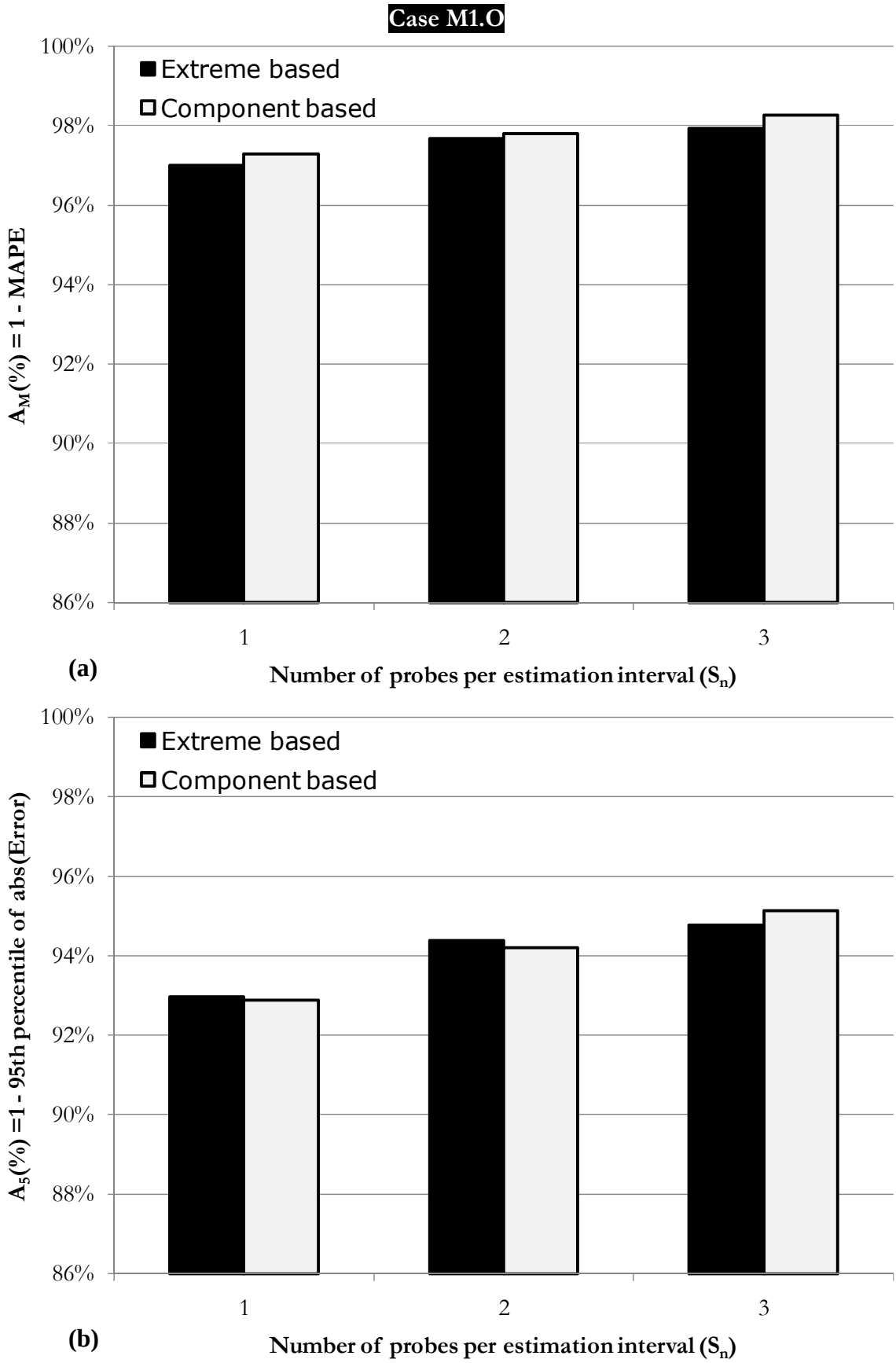

Figure 5-14: Case Study M1.O, Flow = F1, Accuracy (a) A_M and (b) A_5 versus S_n.

5.2.2.2 Case M2

In the previous section it is demonstrated that R_C has better performance than R_E. Therefore, in this section we perform further testing using R_E. This provides lower bound for the performance as the approach R_C can slightly improve the accuracy. The results for the three different flows F1, F2 and F3 are presented in Figure 5-15, Figure 5-16 and Figure 5-17, respectively. The results are consistent with the previous case studies on a single link (Subsection 4.4.4) i.e.,

i. With at least one probe per estimation interval the performance of CUPRITE in terms of A_M and A_5 is generally more than 95% and 85%, respectively. Whereas, significantly large number of probe vehicles are required to obtain comparable accuracy from *Probe-only* method.

ii. Online application performs better than offline application.

iii. With less number of probes there is significant benefit of integrating detector data, signal timings and probe vehicle.

For the above analysis the "true" average travel time for the route is obtained by all the vehicles that traverse the complete route. For F3 (*see* Figure 5-17) only 20% of the vehicles traverse the complete route. Therefore, for large S_n (>15) the accuracy from *Probe-only* method is significantly higher.

The above analysis indicates that CUPRITE can be applied for route travel time estimation for different flow combination with implicit consideration of mid-route delay due to presence of mid-route intersections or other sources for delay.

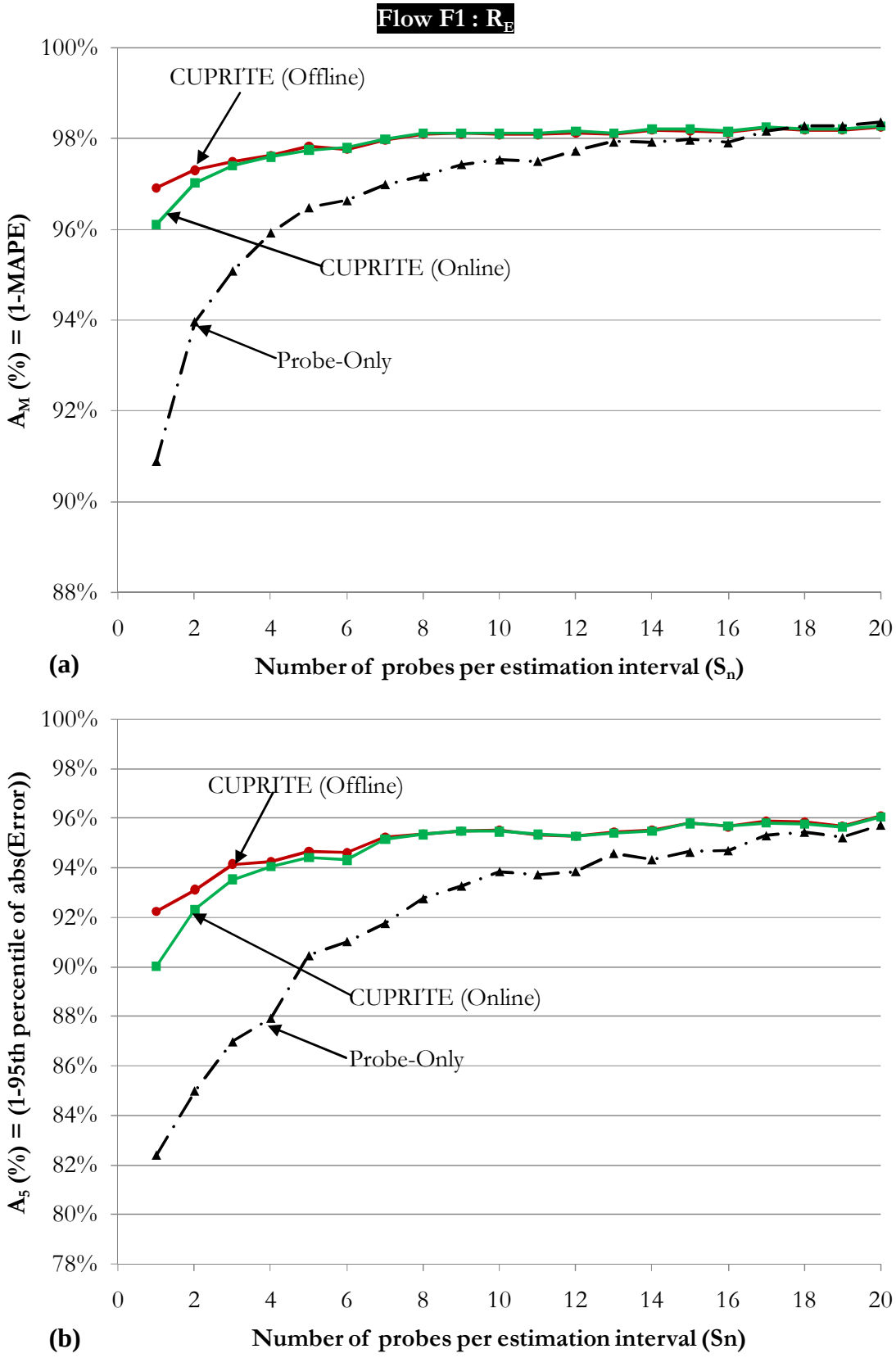

Figure 5-15: Case F1 90% of demand goes through the route (Effective 5% sink). Results for accuracy: (a) A_M and (c) A_5 versus S_n.

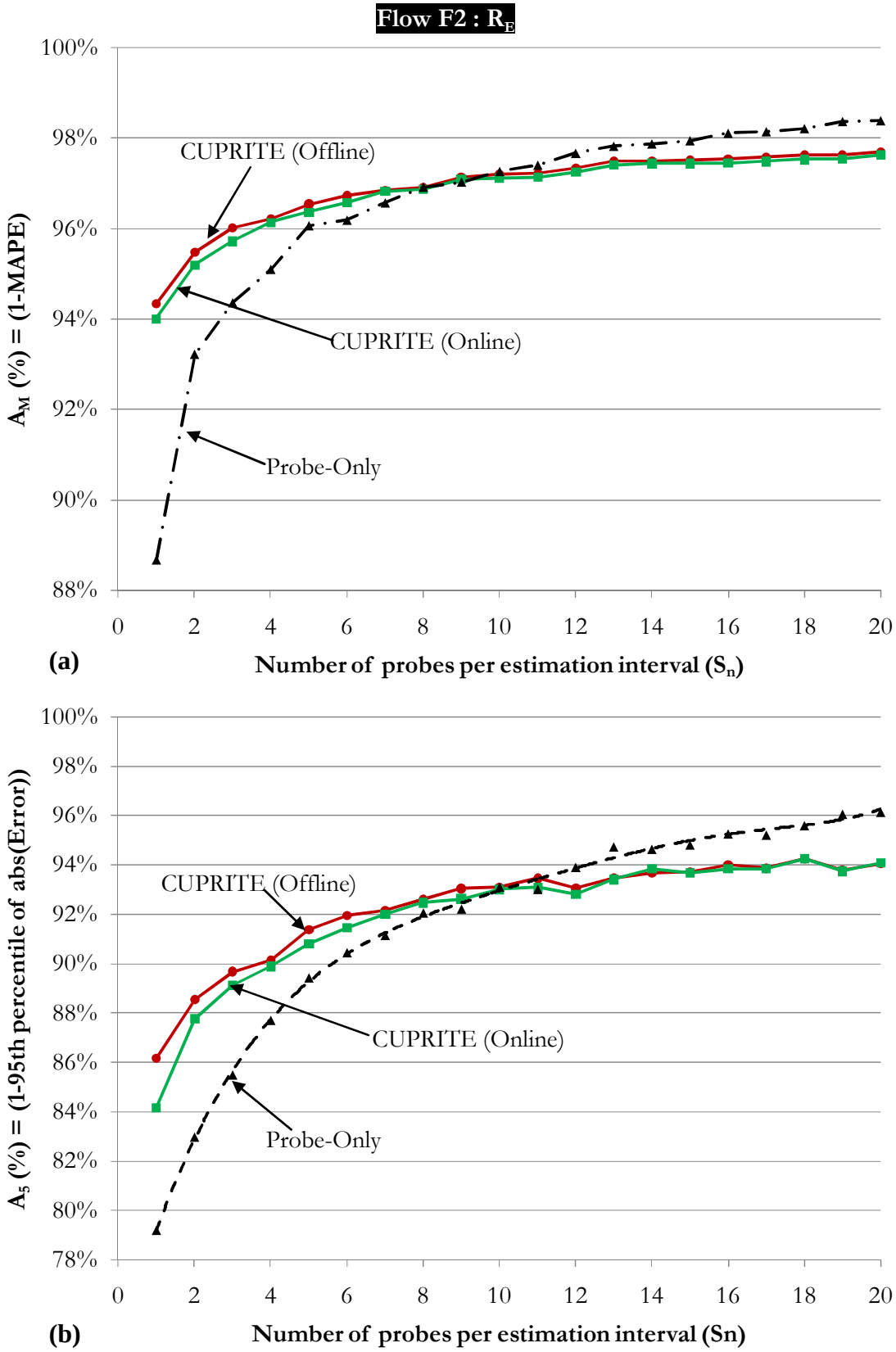

Figure 5-16: Case F2 50% of demand goes through the route (Effective 10% source). Results for accuracy: (a) A_M and (c) A_5 versus S_n.

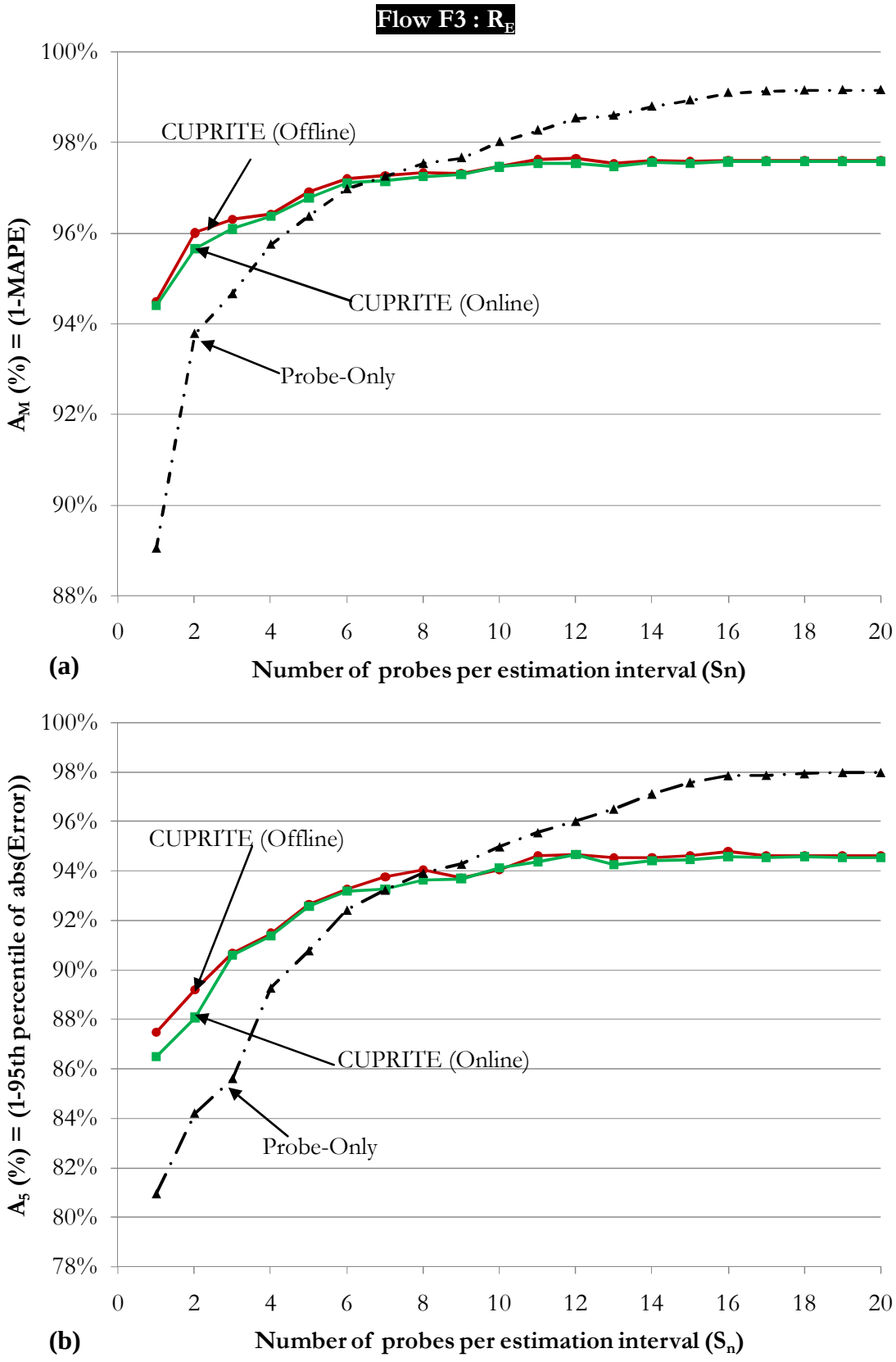

Figure 5-17: Case F3 20% of demand goes through the route (Effective 5% sink). Results for accuracy: (a) A_M and (c) A_5 versus S_n.

5.3 Concluding remarks

As discussed in the literature review chapter (Chapter 2) one of the major limitations of the existing travel time estimation models is that the travel time provided is average for the whole link. Generally to estimate movement specific link travel time, penalties (s) are added to the average link travel time. For ITS applications more robust and accurate movement specific travel time is required. This chapter discusses about the application of the CUPRITE for estimation of movement specific travel time for a link followed by the discussion on the route travel time estimation. Two different approaches: a) *Component* based; and b) *Extreme* based, are discussed. Both the approaches provide similar results. Component based is more reliable with greater chances of probe vehicle in each interval, though additional data from each component is required. *Extreme* based is simple, and only requires data from upstream and downstream of the route but chances of obtaining a probe that traverses the entire route might be low. The *Component* based and *Extreme* based approaches discussed here are also validated with real data in the next chapter.

6 Validation on real data

Having obtained encouraging results from CUPRITE testing on controlled environment, we move on to validate the methodology on real data. This chapter describes the framework for the CUPRITE validation followed by site description and results.

6.1 Framework

6.1.1 Validation methodology

CUPRITE is validated on real data collected at Lucerne city, Switzerland. The signal control at the site is equipped with VS-PLUS signal controller (VS-PLUS). The signals are controlled centrally and the data from the controller is logged and stored by the Lucerne City Transport Authority (StadtLuzern). The detector counts and signal timings for CUPRITE are obtained from VS-PLUS data.

Ground truth, individual vehicle travel time, is obtained from manual number plate (license plate) survey. It was performed on 15th April, 2008 (Tuesday, working day) from 3:00 p.m. to 6:00 p.m. The survey period captures both undersaturated and oversaturated traffic conditions. The required probe vehicles for CUPRITE were randomly selected from the survey data.

Figure 6-1 systematically illustrates the steps involved in the validation procedure. Prior to the application of the CUPRITE, both VS-PLUS data and number plate survey data need to be cleansed (Section 6.1.2). The cleaned data is the input to CUPRITE and it provides estimated average travel time (Section 6.1.3) which is finally, statistically validated with ground truth average travel time obtained through survey (Section 6.1.5).

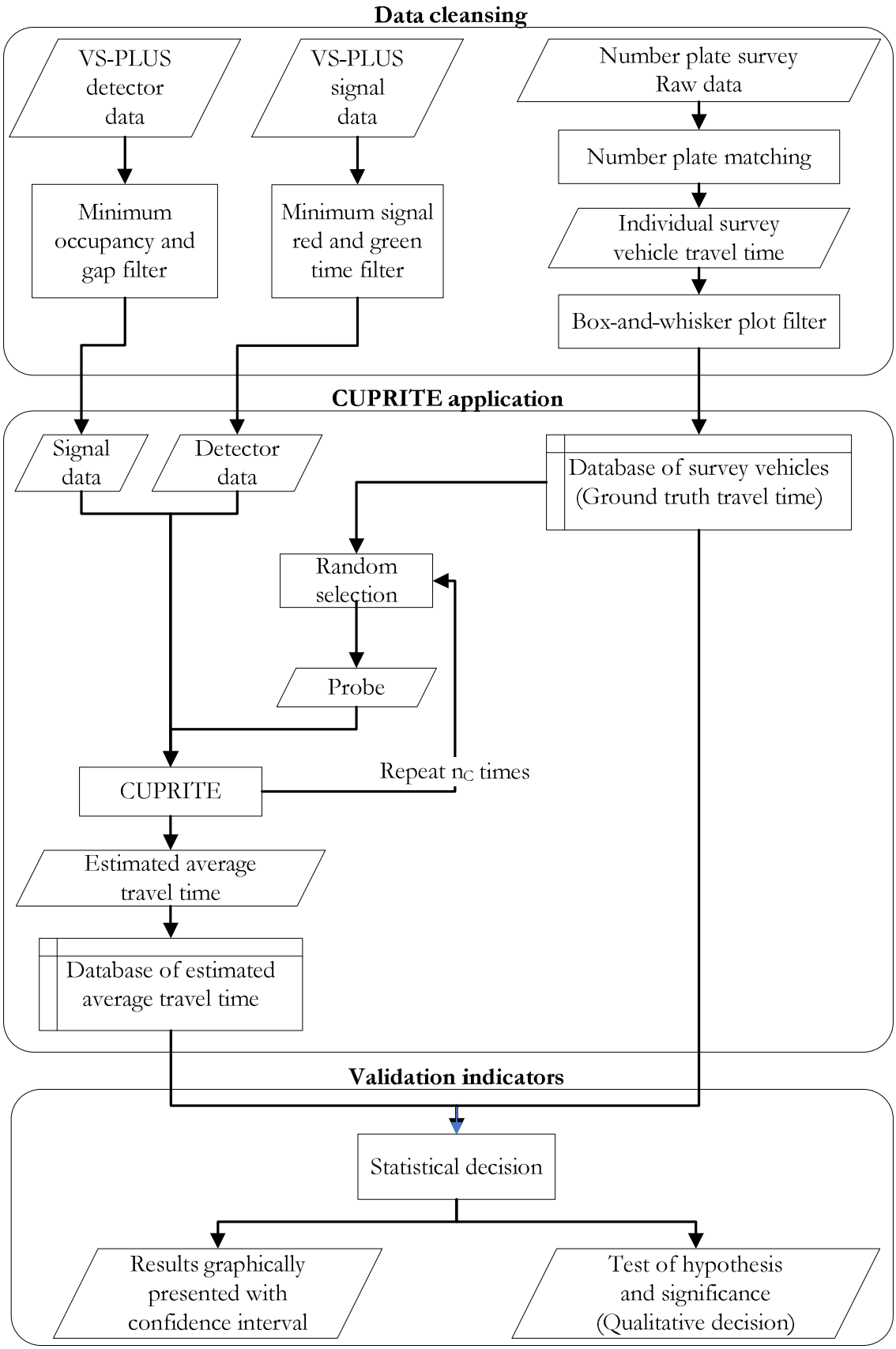

Figure 6-1: Framework for CUPRITE validation.

6.1.2 Data cleansing

6.1.2.1 Number plate survey data

A manual number plate survey was performed and first four digits of the vehicle number plate and the corresponding time stamp when the vehicle enters the intersection were obtained. For details refer to Appendix E. Travel time of a vehicle between two survey stations is the time difference when it is observed at two stations. The number plate at upstream and downstream stations is matched and individual vehicle travel time is obtained. Due to human error or two vehicles having similar first four digits of the number plate or other reasons, there may be observed travel time much different from the neighboring traversing vehicles. These deviant travel time values are considered as outliers and are not be considered for the validation procedure. Here, the *box-and-whisker plot technique* is employed to filter the outlier travel time values.

6.1.2.1.1 Filtering the outlier using box-and-whisker plot technique

In the *box-and-whisker plot technique* a set of data is represented in: *a)* median (M), separating the data in two parts; *b)* lower quartile (LQ) i.e., the median of the lower part of data or 25^{th} percentile; and *c)* upper quartile (UQ) i.e., median of the upper part of data or 75^{th} percentile. The difference between the upper quartile and lower quartile is Inter Quartile Range (IQR) and it defines the scatter of the data. The Lower Bound Value (LBV) and Upper Bound Value (UBV) are:

$$LBV = LQ - 1.5 * IQR \tag{6.1}$$

$$UBV = UQ + 1.5 * IQR \tag{6.2}$$

$$IQR = UQ - LQ \tag{6.3}$$

Any point lying below LBV or above UBV is regarded as an outlier and is disregarded.

Figure 6-5 represents an example. Figure 6-5*a* represents the raw date. To filter the outlier, a 10 min time window (5 min before and 5 min after) around the *data point under consideration* is defined. Box-and-whisker plot is obtained for all the data points within the time window. If the *data point under consideration* (*see* Figure 6-5*b*) is below LBV or above UBV then it is defined as outlier. The process is repeated for all the data points. Note: all the points (including those earlier defined as outliers) within the time window are considered for

defining box-and-whisker plot. Figure 6-5*c* represents the final cleansed data with outliers removed.

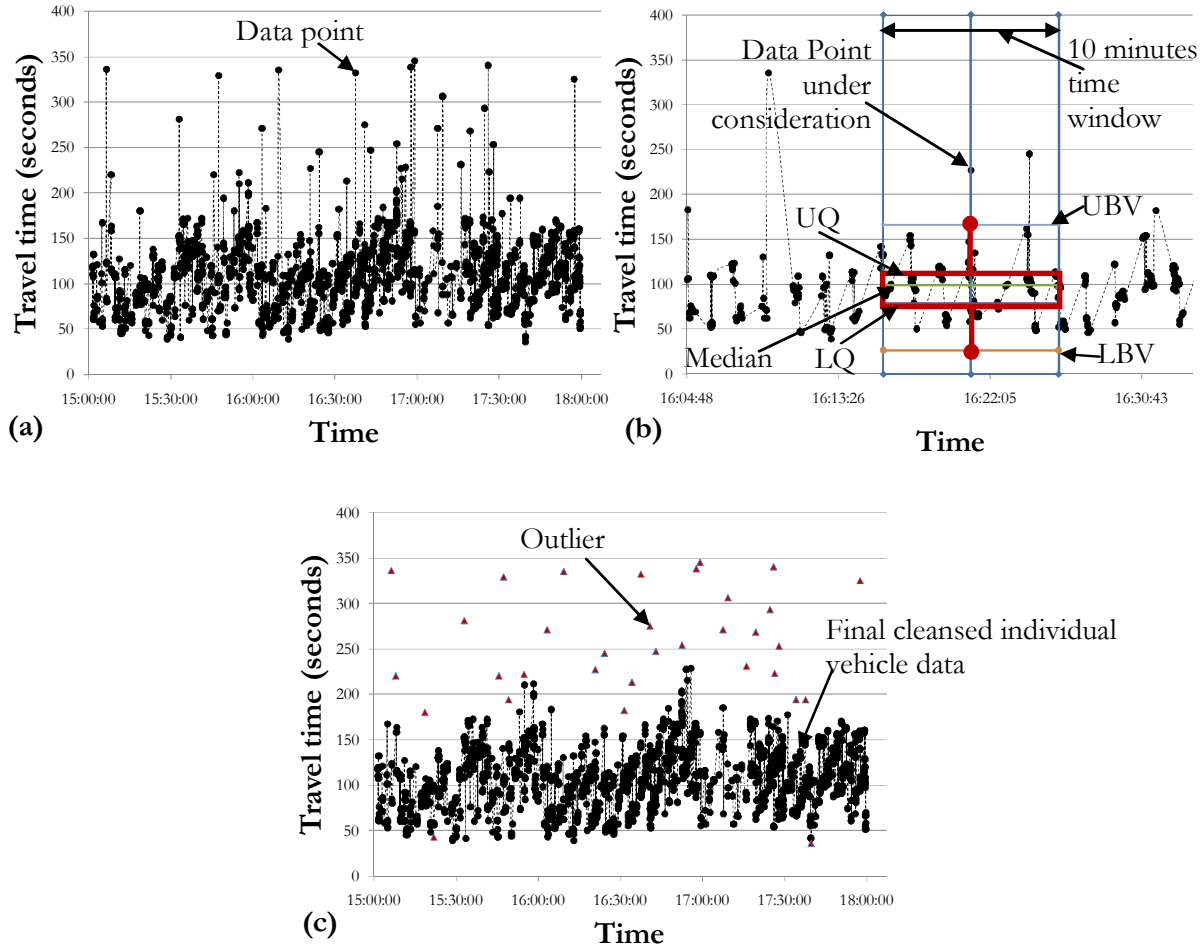

Figure 6-2: Example of filtering the outlier using box-and-whisker plot.

6.1.2.2 VS-PLUS data

VS-PLUS provides pulse data for each detector and signal phase, i.e., value '1' or '0' and corresponding time stamp. If we plot the values versus time, then a pulse can be defined as the portion of the graph represented by value of one (*see* Figure 6-3). Due to different reasons, sometimes there is noise in the pulses (unexpected fluctuations) which need to be filtered out. The noise can be due to due to pulse breakup (Refer to Section A.1.1 in Appendix A).

6.1.2.2.1 Filter for VS-PLUS detector data

The values of '1' and '0' indicate the presence and non-presence of a vehicle on the detector, respectively. Therefore: a) the time length for a pulse represents the occupancy time (OT) of the vehicle on the detector; b) the time difference between the end of the leading pulse and

start of the following pulse is represents of the gap (G) between the vehicles; and c) the time difference between the start of two consecutive pulses is the representative of the headway between vehicles (*see* Figure 6-3). Ideally, a pulse should correspond to a vehicle and hence the vehicle by vehicle count can be obtained. However, due to noise in the pulse there can be overcounting of vehicles. To avoid this we define minimum accepted occupancy time (OT_{min}) and minimum accepted gap (G_{min}). The filter is applied such that: a) if the gap between two consecutive pulses is less than G_{min} then both the pulses are merged, representing only one count for two pulses; and b) if the occupancy time is less than OT_{min} then pulse is disregarded. The value of OT_{min} and G_{min} used in the present analysis is 0.3 s, each.

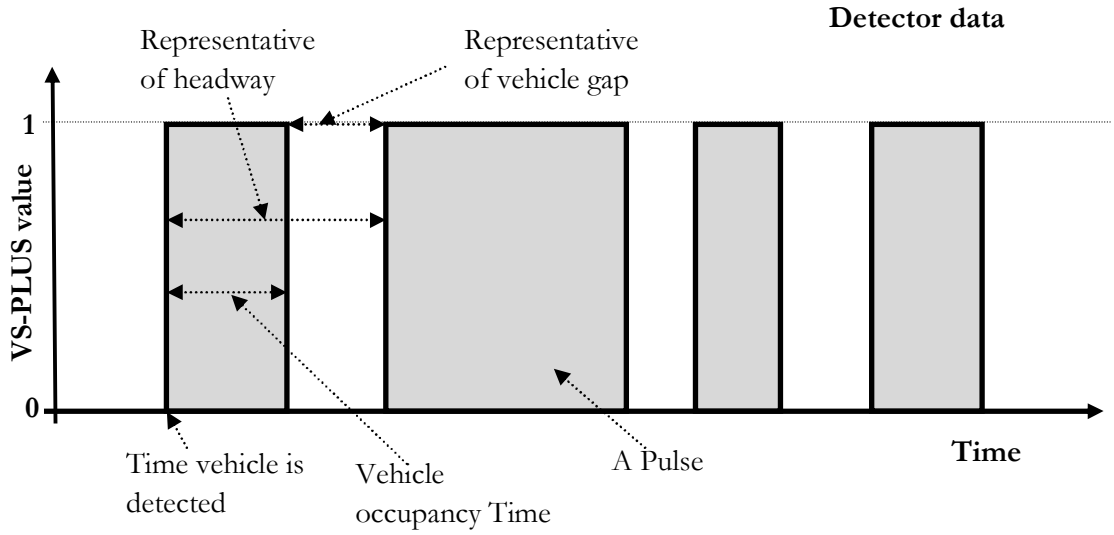

Figure 6-3: Pulse data representation for VS-PLUS detector data.

The above filter of minimum occupancy and minimum gap can only remove noise in the pulse. This does not resolve the problem of detector counting error due to closely spaced vehicles, cross-talk etc. For instance, if the gap between vehicles is small and detector is not able to differentiate two consecutive vehicles then a long pulse, instead of two pulses is obtained. This results in undercounting. CUPRITE addresses this issue of detector counting error (Refer to Chapter 4).

6.1.2.2.2 Filter for VS-PLUS signal data

The values of '0' and '1' indicate the start of display red light and display green light for the signal phase, respectively (*see* Figure 6-4) and hence the corresponding displayed signal red time and displayed signal green time. Ideally, a displayed green or red should be more than some minimum value but due to noise in the data there are periods where we have pulses

close to each other. Analogous to the previous filter for VS-PLUS detector data, we consider the minimum red and green time to be 3 s and pulse or gaps less than 3 s are ignored.

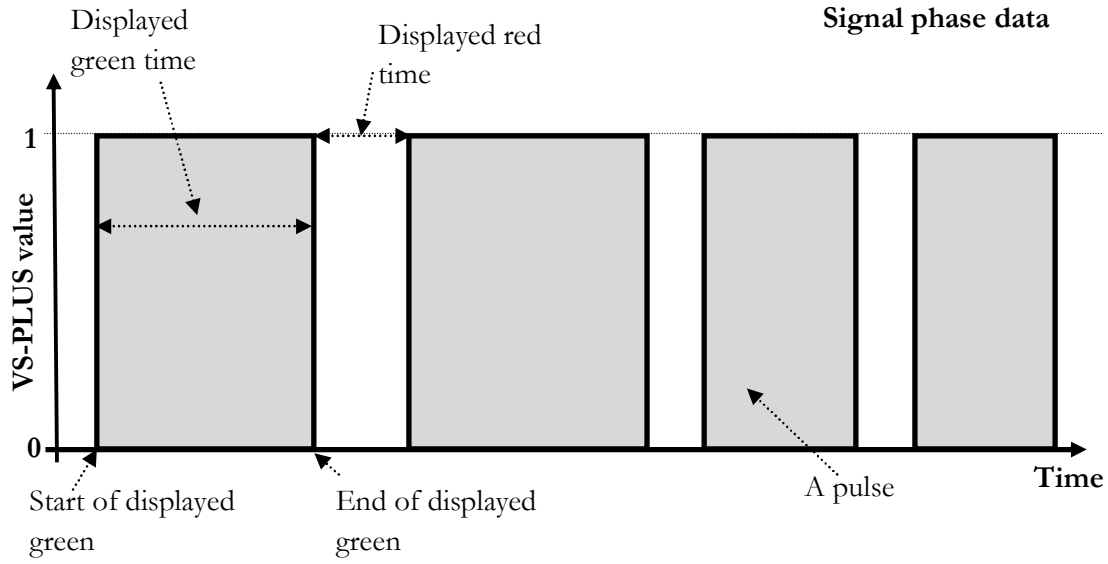

Figure 6-4: Pulse data representation for VS-PLUS signal data.

6.1.3 CUPRITE application

As the survey vehicle data is available for a fixed time period and the probe data required for CUPRITE application is randomly selected from the survey vehicle data. Therefore, for each estimation interval CUPRITE is applied for n_C times (6.5) with different values of the seed for random number generator to randomly selecting probe vehicles. Hence, the application of CUPRITE provides different travel time estimates for a given estimation interval. Say for an estimation interval the mean and standard deviation of the estimates be $\overline{X}_C$ and S_C, respectively. Then we apply the sampling theory and confidence bounds for the travel time estimate by CUPRITE are defined by:

$$\bar{X}_C - t_{\alpha/2,n_C-1}\frac{S_C}{\sqrt{n_C}} \le \mu_C \le \bar{X}_C + t_{\alpha/2,n_C-1}\frac{S_C}{\sqrt{n_C}} \qquad (6.4)$$

Where:

μ_C is the mean of the population of estimates from CUPRITE application;

$t_{\alpha/2,n_C-1}$ is the *t*-statistic at α level of significance and n_C-*1* degrees of freedom;

n_C is defined as follows:

$$n_C = Min(\frac{n_s!}{N!(n_s - N)!}, 20); \qquad \text{assuming } n_s \geq N \tag{6.5}$$

n_s is number of survey vehicles in the estimation interval.

This means that, for an estimation interval, if *N* number of probe vehicles is required, then CUPRITE is applied by randomly selecting different combinations (without repetition of same combination) of *N* probe vehicles, or for 20 times, whichever is the minimum. For instance, say 2 (=N) probe vehicles in an estimation interval are required. If number of survey vehicles are 10, then there can be 45 different combinations of two probe vehicles. In this case, CUPRITE is applied 20 times by randomly selecting (without repetition) a combination each time. However, if there are 5 survey vehicles then only 10 combinations of two probe vehicles is possible. In this case, CUPRITE is applied 10 times and all the combinations are considered.

6.1.4 Ground truth travel time

The number plate survey captures the sample of vehicles traversing the link (*see* Figure 6-5). We are interested in actual average travel time for all the vehicles departing the link during travel time estimation interval. Say the mean and standard deviation of the travel time obtained from the survey be $\overline{X}_s$ and S_s, respectively. We apply the sampling theory to estimate the confidence bounds in the actual average travel time (μ_s) of the vehicles as:

$$\bar{X}_s - t_{\alpha/2,n_s-1}\frac{S_s}{\sqrt{n_s}} \leq \mu_s \leq \bar{X}_s + t_{\alpha/2,n_s-1}\frac{S_s}{\sqrt{n_s}} \tag{6.6}$$

Where: $t_{\alpha/2,n_s-1}$ is the *t*-statistic with α level of significance and n_s-*1* degrees of freedom; n_s is number of survey vehicles in an estimation interval.

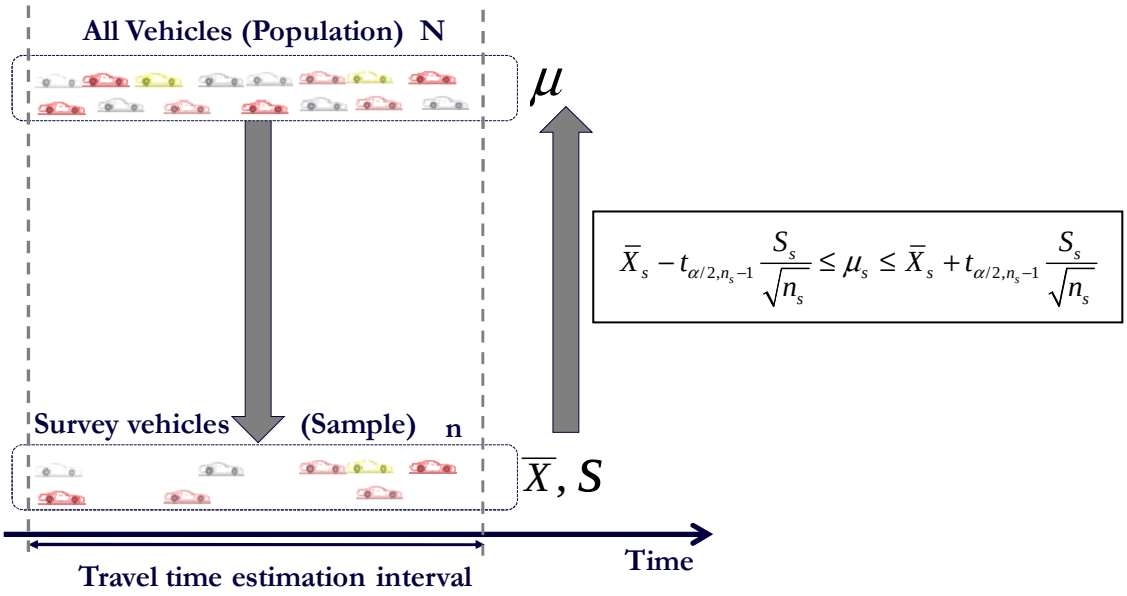

Figure 6-5: Systematic representation of the sample of vehicles captured from the population; and confidence in the estimate of population from that of the sample.

6.1.5 Validation indicator

We present the results: graphically by overlapping the time series of travel time from survey and CUPRITE application; and qualitatively as statistical test of hypothesis and significance.

6.1.5.1 Graphical presentation of results

Figure 6-6 illustrates an example for the presentation of results. For each estimation interval, the black box represents the confidence bounds for the ground truth average travel time (*see* Figure 6-6*a*) and the orange box represents the confidence bounds for the travel time estimates from the CUPRITE (*see* Figure 6-6*b*).

Accuracy of the estimates from CUPRITE is defined as following:

$$Error_i = \left(\frac{\left|\bar{X}_{s_i} - \bar{X}_{C_i}\right|}{\bar{X}_{s_i}}\right) \tag{6.7}$$

$$MAPE = \sum_{i=1 to n} \frac{Error_i}{n} \tag{6.8}$$

$$Accuracy(\%) = 1 - MAPE \tag{6.9}$$

Where: $Error_i$ is the absolute percentage error for i^{th} estimation interval; $\bar{X}_{s_i}$ and $\bar{X}_{C_i}$ are the mean of survey travel time and mean of travel time estimates from CUPRITE application

during i^{th} estimation interval, respectively; n is the number of estimation intervals; and *MAPE* is the Mean Absolute Percentage Error obtained from the CUPRITE application for different estimation intervals during survey period.

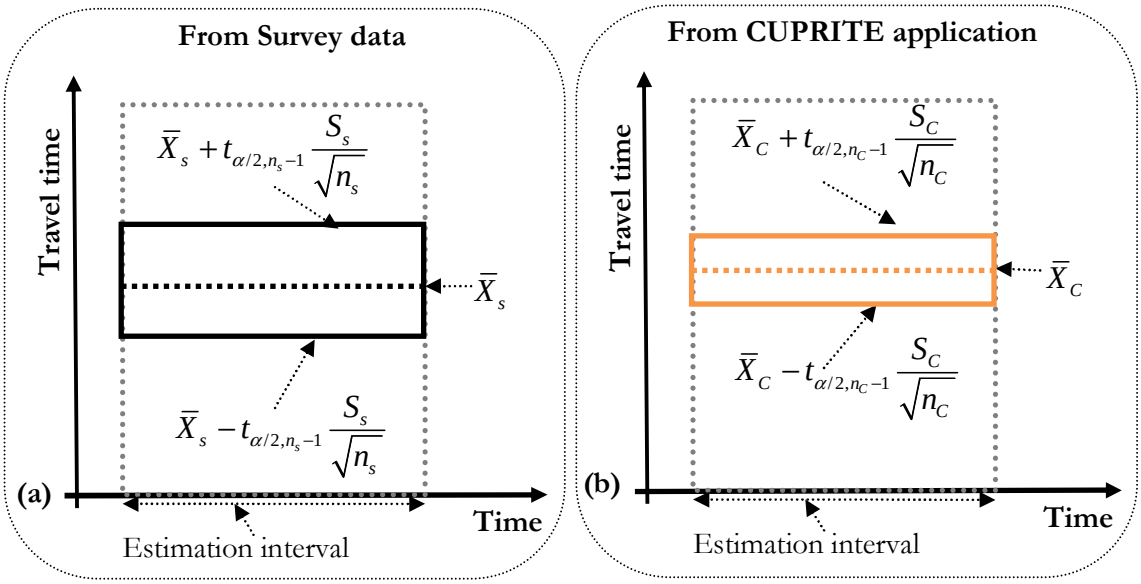

Figure 6-6: Systematic representation of the results for CUPRITE validation.

6.1.5.2 Statistical test

We perform statistical test so as to make qualitative decisions about the CUPRITE validation. The intension is to determine whether there is enough evidence to "reject" a (null) hypothesis about the CUPRITE validation. Here, two different processes: a) number plate survey and b) CUPRITE application; provide dataset for average travel time. We are interested to know if these two processes provide statistically similar results, i.e., the mean of the two processes are the same.

We make a null hypothesis H_0 (6.10): that the true mean[15] of the first process (μ_s) is equal to the true mean of the second process (μ_C). Or in other words the two sets of data (number plate and CUPRITE) with sample means $\overline{X}_s$ and $\overline{X}_C$, respectively are both part of the same population so that their population means are equal. Null hypothesis is tested against the alternate hypothesis (H_a) that the two means are not equal (6.11).

$$Null\ Hypothesis\ (H_0):\ \mu_s = \mu_C \tag{6.10}$$

[15] Mean of the population from which the process is a sample. μ_s is the mean of the population of vehicles traversing the link. μ_C is the mean of all possible estimates from CUPRITE application using different probe vehicles drawn from the population of vehicles traversing the link.

$$Alternative\ Hypothesis\ (H_a):\ \mu_s \neq \mu_C \tag{6.11}$$

If we "do not reject" the null hypothesis (H_0), then we are saying that despite the fact that the travel time estimates come from two different processes there is not enough evidence to say that they are not part of the same overall population.

The statistical test to make the above decision is *t-test to compare two sample means (two-tailed t-test)*. We form the test statistics assuming that the true standard deviations for the two processes are not equivalent (Interested readers can refer to any standard statistic book or chapter 7 of online engineering statistic handbook (NIST).).

The degree of freedom (*df*) is estimated using the Welch-Satterthwaite approximation (6.12).

$$df = \frac{(\frac{s_1^2}{n_1} + \frac{s_2^2}{n_2})^2}{(\frac{s_1^4}{n_1^2(n_1-1)} + \frac{s_2^4}{n_2^2(n_2-1)})} \tag{6.12}$$

$$t_{test\ statistics} = \frac{X_1 - X_2}{\sqrt{\frac{s_1^2}{n_1} + \frac{s_2^2}{n_2}}} \tag{6.13}$$

Where: X_i, s_i and n_i is the mean, standard deviation and number of observations, respectively for the two processes. $X_1 = \overline{X}_s$; $X_2 = \overline{X}_C$; $s_1 = S_s$ and $s_2 = S_C$; $n_1 = n_s$ (number of survey vehicles during the estimation interval); $n_2 = n_C$ (6.5).

For α level of significance we reject the null hypothesis Ho, if:

$$\left|t_{test\ statistics}\right| \geq t_{\alpha/2,df} \tag{6.14}$$

Else we do not reject the null hypothesis and reject the alternate hypothesis.

Where: $t_{\alpha/2,df}$ is the upper critical value of the Student's-t distribution at α level of significance with *df* degree of freedom.

"Do not reject H_0" indicates there is not enough evidence to reject the assumption that: *CUPRITE estimates are statistically equivalent to the real travel time from the number plate survey*.

Note: Statistically, both the indicators defined in the previous subsections are connected. If the confidence bounds of the CUPRITE application (defined in Section 6.1.5.1) contain the mean of the survey travel time then we do not reject the null hypothesis (defined in Section 6.1.5.2).

6.2 Site description

The data is collected on eleven consecutive signalized intersections (intersections *A* to *K*) as shown in the Figure 6-7. It consists of three legs:

i. Intersection *A* to intersection *D* in which the flow is from a freeway (E35) with minor mid-link sinks and sources;

ii. Intersection *D* to intersection *I*, which passes through the city centre and the bottleneck mainly at intersection *F* and intersection *I*. This leg also carries traffic to the railway station; and

iii. Intersection *I* to intersection *K*, where there is no mid-link sink or source, but significant amount of mid-link delay due to pedestrians. Link from intersection *I* to intersection *K* is along the lake side with significant number of tourists.

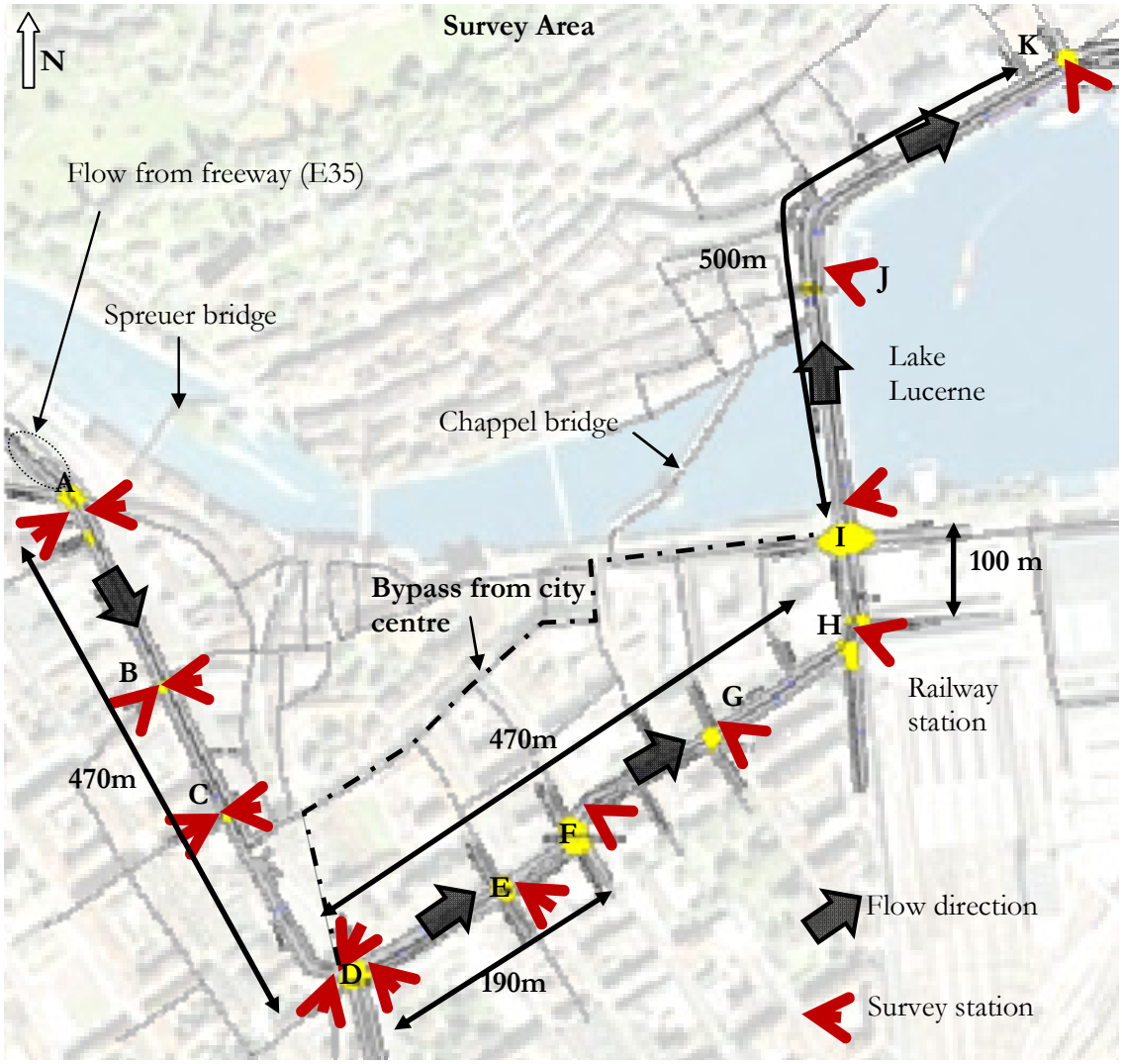

Figure 6-7: Number plate survey site.

6.2.1 Leg 1: Route A→D

Intersection *A* to intersection *D* is quite interesting (*see* Figure 6-8). From *A* to *B*, there is minor side street acting as both source and sink; from *B* to *C* there is on-street bus stop; and from *C* to *D*, there are two different movements (left and through) associated with the link, in addition to significant loss in the side street. Following are the detailed characteristics.

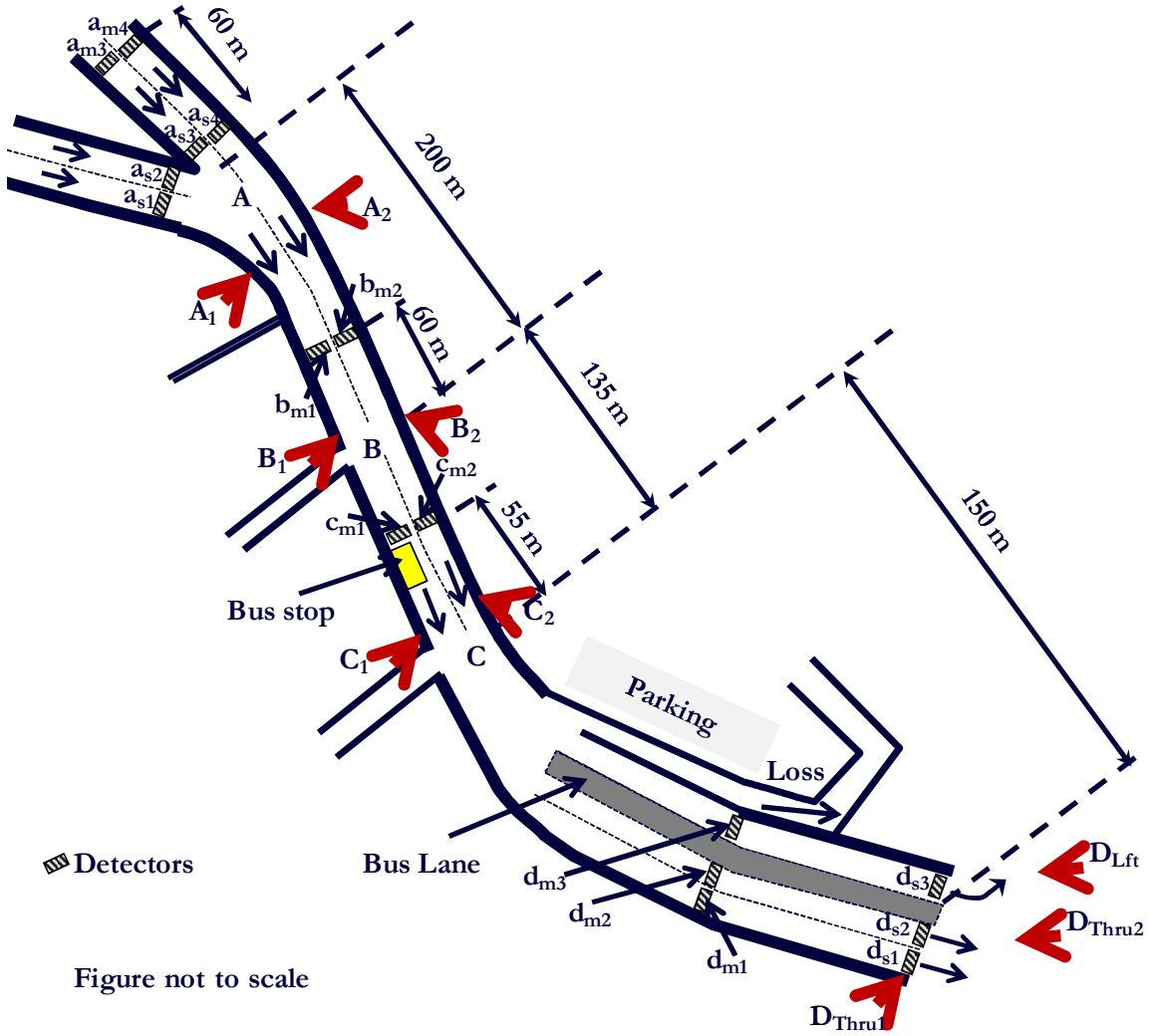

Figure 6-8: Illustration of the link characteristics between intersections *A* and *D*.

6.2.1.1 Link AB

For link A to B, there are four stop-line detectors (a_{s1},a_{s2}, a_{s3}, a_{s4}) at the upstream end and two mid-link detectors (b_{m1},b_{m2}) at 60 m upstream of intersection *B*. Comparing the counts from the detectors, we found that there is approximately 2% difference between the counts from the pair of detectors (*see* Table 6-1). There can be different reasons for this difference in the counts: a) either detectors at *A* are undercounting; and/or b) detectors at *B* are overcounting; and/or c) there are vehicles from/to the minor street between intersection *A* and intersection *B*.

Left link at the entrance of intersection *A*, has a pair of detectors (a_{m3},a_{m4}) 60 m upstream of the stop-line. Comparing the counts between detectors (a_{s3}, a_{s4}) and (a_{m3}, a_{m4}) it is found that there is approximately 1.6% difference during the survey period and 3.8% difference during

the survey day. Either detectors (a_{s3}, a_{s4}) are overcounting or detectors (a_{m3}, a_{m4}) are undercounting (see Table 6-2) or both.

Table 6-1: Detector counts between intersections *A* and *B*

Time period	u/s detectors (a_{s1},a_{s2}, a_{s3}, a_{s4})	d/s detectors (b_{m1},b_{m2})	Absolute percentage difference
3:00 p.m. – 6:00 p.m.	6'123	6'250	2.1 %
Daily	21'744	22'164	1.9%

Table 6-2: Detector counts for left entrance link of intersection *A*

Time period	u/s detectors (a_{m3},a_{m4})	d/s detectors (a_{s1},a_{s2})	Absolute percentage difference
3:00 p.m. – 6:00 p.m.	3'213	3'264	1.6 %
Daily	11'034	11'465	3.8%

6.2.1.2 Link BC

For link from intersection *B* to intersection *C*, there is on-street bus stop on the left lane of the road. If the bus stops at the stop then it blocks the lane. Due to which there is additional mid-link delay for the flow of vehicles on the link *BC*. Here we have mid-link detectors (c_{m1},c_{m2}) at 55 m upstream of the stop-line at intersection *C*.

6.2.1.3 Link CD

Comparing (Table 6-3) the counts for link between intersections *C* and *D*, we have three detectors (d_{s1}, d_{s2} and d_{s3}) at stop-line and corresponding three detectors (d_{m1}, d_{m2} and d_{m3}) at 60 m upstream of the stop line. It is found (*see* Table 6-3) that detectors (d_{s1}, d_{s2} and d_{s3}) have approximately 4% higher counts than (d_{m1}, d_{m2} and d_{m3}).

Table 6-3: Detector counts from detectors between intersections *C* and *D*

Time period	u/s detectors (d_{m1},d_{m2}, d_{m3})	d/s detectors (d_{s1},d_{s2}, d_{s3})	Absolute percentage difference
3:00 p.m. – 6:00 p.m.	5'050	5'232	3.5%
Daily	17'447	18'180	4.0%

The above comparison clearly indicates that detectors are not perfect and have counting error.

For link from *C* to *D*, the flow from intersection *C* is distributed into flow towards a) through movement (D_{Thru}) b) turning left (D_{Lft}) towards city centre and c) loss (Loss) towards parking and side-street. The distribution of the flow on link from *C* to *D* towards the three movements is illustrated in the Figure 6-9. This distribution is obtained based on the ratio of the counts from (d_{s1},$d_{s2,}$ d_{s3}) and (c_{m1},c_{m2}). It can be considered that during the survey period, on average 55% of the flow from *C* is towards direction D_{Thru}; 29% is for direction D_{Lft} and 16% is *Loss*.

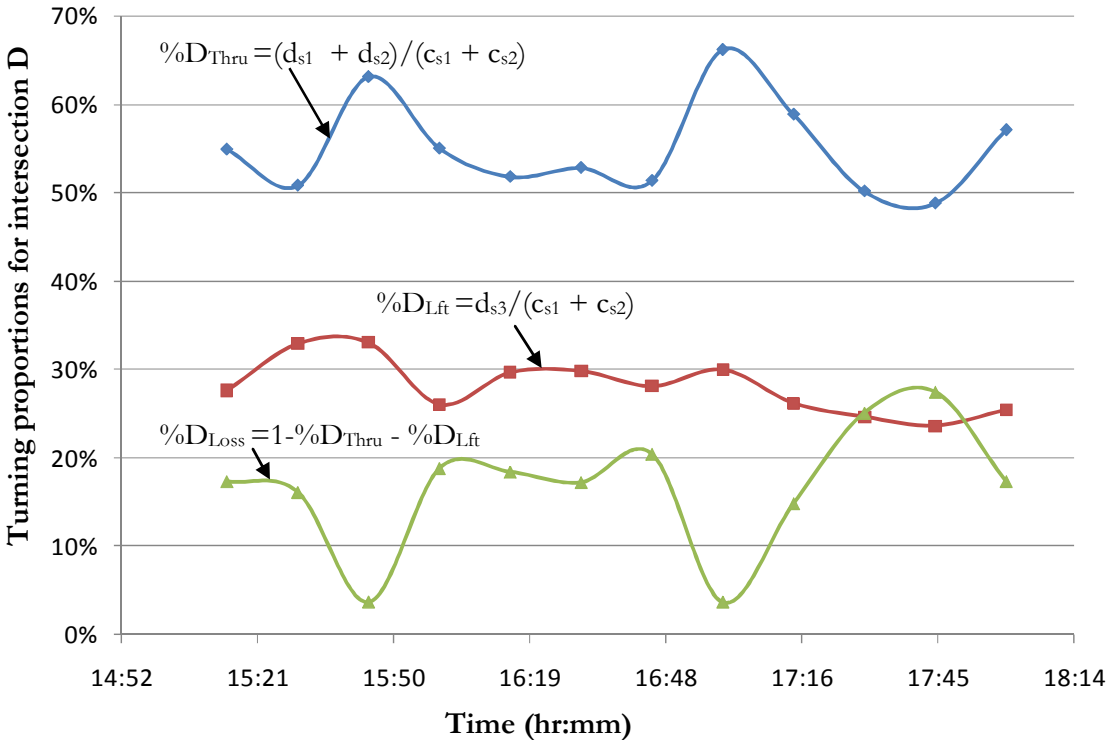

Figure 6-9: Turning proportions for different directions from *C* to *D*.

6.2.2 Leg 2: Route D→I

Route from intersection *D* to intersection *I* is approximately 570 m. The links are of two lanes of which the right lane from *D* to *G* is a bus lane. There is a detector d_d at the upstream of the route and two detectors i_{s1} and i_{s2} at stop-line of *I* (*see* Figure 6-10). During the survey period, effectively, 20% gain of vehicles is observed from *D* to *H* (*refer to* Table 6-4) and 64% gain of vehicles from *D* to *I*. 30% of the vehicles from *H* to *I* are lost towards direction *Y* (railway station).

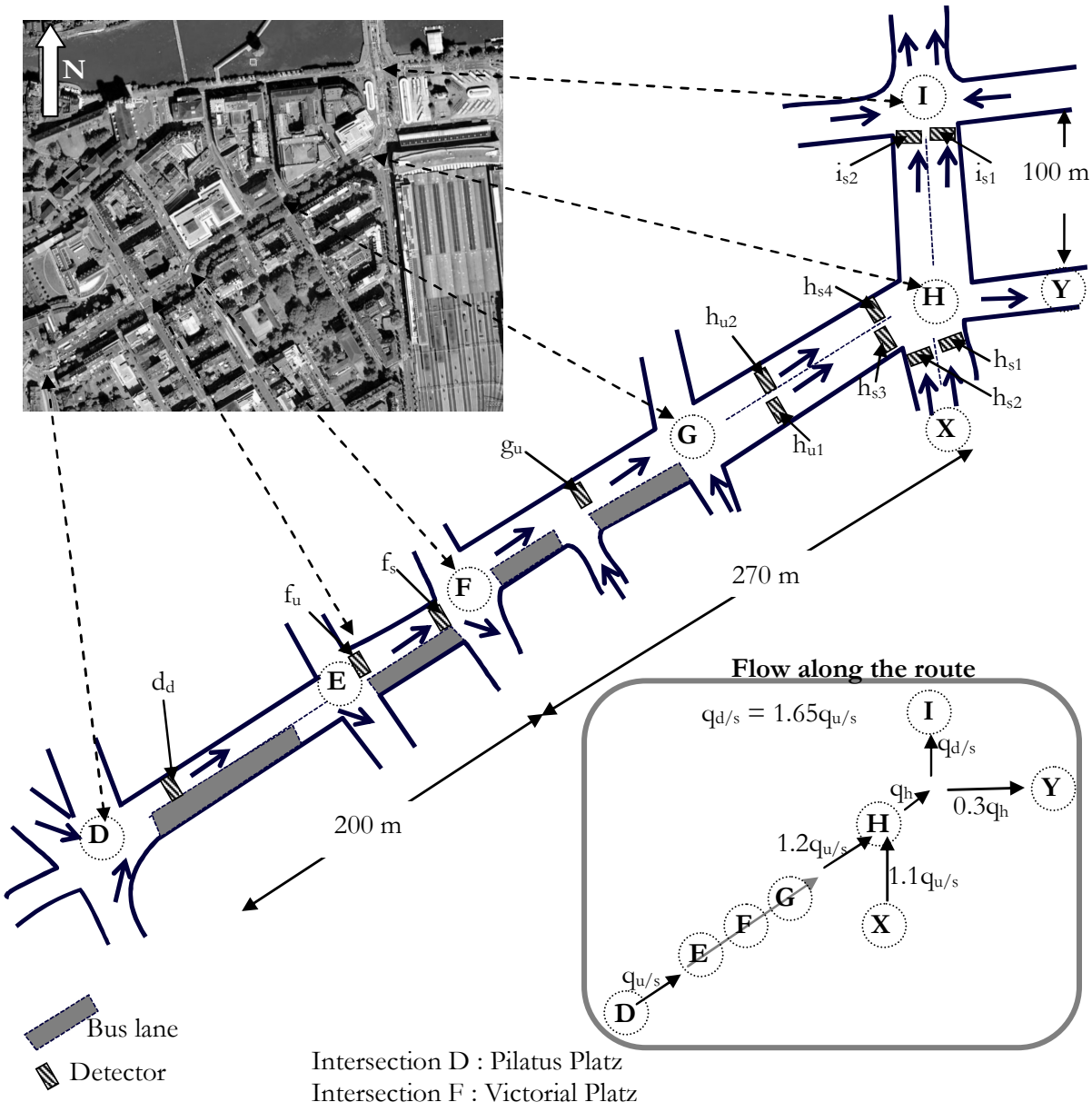

Figure not to scale and only one direction is systematically presented

Figure 6-10: Illustration of the link characteristics between *D* to *I*.

Table 6-4: Detector counts for intersections *D* to *I* (Leg 2)

Time period	Counts d_d	Counts hs_4+ hs_3	Effective gain from intersection D to H	Counts i_{s2} + i_{s1}	Effective gain from intersection D to I
3:00 p.m. – 6:00 p.m.	7,200	8,580	19%	11,808	64%
Daily	34,996	42,124	20%	53,012	51.5%

6.2.3 Leg 3: Route I→K

Link from intersection *I* to intersection *K*, is systematically illustrated in Figure 6-11. Though there is absence of mid-link source or sink, but there is significant mid-link delay due to

pedestrian crossing and on-street bus stop. Comparing the counts from detectors at nearby location, around 10% difference in the detector counts is observed. In the figure, we can see that counts from detector k_{s1} and k_{s2} differ by 10% from those of k_{m1} and k_{m2}. The link consists of two lanes with almost 50% vehicle split on both the lanes.

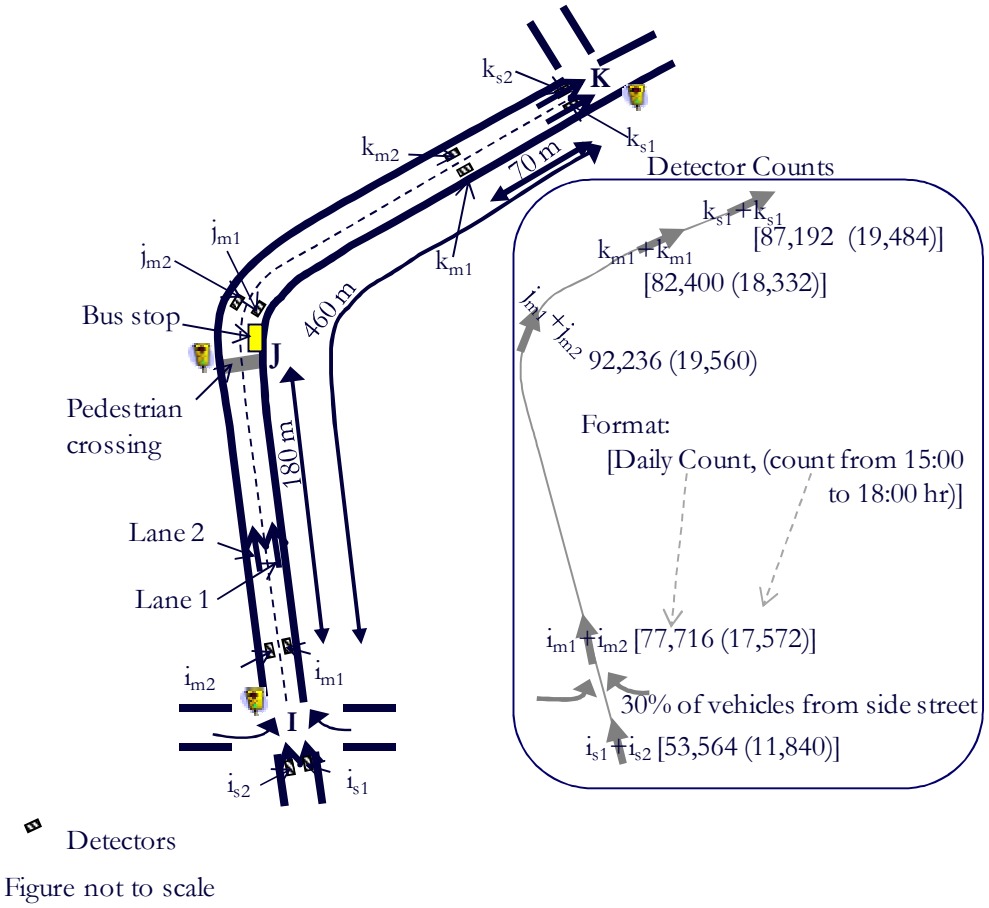

Figure 6-11: Illustration of the link characteristics between intersections I and *K* and corresponding detector count.

6.3 Validation results

Refer to section 6.1.5 (page 178) for the details of the how results are presented. Travel time estimation interval is for five signal cycles. As signals are adaptive therefore the cycle time is not fixed. Fixed number of probes per estimation interval is considered. Two tailed t-tests were considered significant at (α=) 0.05.

This means that we are 95 % confident that the: a) true travel time is within black box (Figure 6-6*a*); and b) travel time estimate from CUPRITE is within the orange box (Figure 6-6*b*).

CUPRITE is validated for both *Extreme* based and *Component* based travel time estimation approach. Table 6-5 presents different cases considered for validation.

Table 6-5: Different cases for CUPRITE validation

Case	Extreme based (R_E)	Component based (R_C)	Comments
Case Leg 1: (A→D)	A→D_{Lft}		Importance of movement specific travel time estimation.
	A→D_{Thru}		
Case Leg 2: (D→I)	D_{Lft}→I		City centre with flow for railway station.
Case Leg 3: (I→K)	I→K		Leg with mid link delay due to significant pedestrian volume.
Case R_E Vs R_C	A→F	A→D_{Lft}→F	Comparison between *Extreme* based and *Component* based travel time estimation.
	D_{Lft}→I	D_{Lft}→F→I	
	D_{Lft}→K	D_{Lft}→F→I→K	
Case S_p	A→D_{Lft}		Discussion on consideration of percentage of vehicles as probes.

The route from *A→I* and *A→K* is not considered. This is because there is a bypass from intersection *D* to intersection *I* (*see* Figure 6-7), which is used by drivers to avoid the congestion through the city centre. The vehicle observed at both *A* and *I* or *A* and *K* can be the one traversing through the bypass.

In the following subsections, the results of time series of travel time and statistical decision from t-tests are presented in the same figure. For each estimation interval:

i. Orange and black boxes are as defined in Section 6.1.5.1;

ii. Green circle represents, "not enough evidence to reject H_0"; and

iii. Red triangle represents "Reject H_o".

6.3.1 Case Leg 1: (A→D)

CUPRITE is applied for estimating travel time from intersection *A* to intersection *D*. The four stop-line detectors at *A* (a_{s1},a_{s2}, a_{s3}, a_{s4}) provide total cumulative plot at the upstream (U_T). The downstream cumulative plots for through movement (D_{Thru}) and left movement (D_{Lft}) are obtained from stop-line detectors (d_{s1},d_{s2}) and detector (d_{s3}), respectively. U_T is scaled vertically using the average turning ratio of 55% for through movement and 30% for left

movement to define the initial arrival cumulative plot for each movement (Refer to Section 6.2.1.3). CUPRITE is applied with fixed number of probes per estimation interval. For one, two and three probes per estimation interval the results obtained: a) For $A \rightarrow D_{Lft}$ are illustrated in Figure 6-12, Figure 6-13 and Figure 6-14; and b) for $A \rightarrow D_{Thru}$ are illustrated in Figure 6-15, Figure 6-16 and Figure 6-17, respectively.

In most of the estimation intervals, the null hypothesis cannot be rejected. Indicating that our initial assumption (Mean estimated from CUPRITE is statistically equivalent to that of number plate survey.) is not rejected at 0.05 level of significance.

The orange box overlaps with black box, indicating that the CUPRITE can estimate the true actual travel time. It can be seen that even the short term oversaturation in the system can be accurately estimated. For instance, in Figure 6-12: fourth, fifth, sixth and seventh estimation intervals (time from 15:30 hr to 16:00 hr) are congestion build up, and there is significant variation in average travel time between the three periods. This fluctuation is also captured accurately by CUPRITE.

For $A \rightarrow D_{Lft}$: the accuracy (6.9) of the CUPRITE model increases from 92.3% to 94.6% with increase in number of probes from one probe per estimation interval (*see* Figure 6-12) to three probes per estimation interval (*see* Figure 6-14), respectively.

For $A \rightarrow D_{Thru}$: the accuracy (6.9) of the CUPRITE model increases from 88% to 92% with increase in number of probes from one probe per estimation interval (*see* Figure 6-15) to three probes per estimation interval (*see* Figure 6-17), respectively.

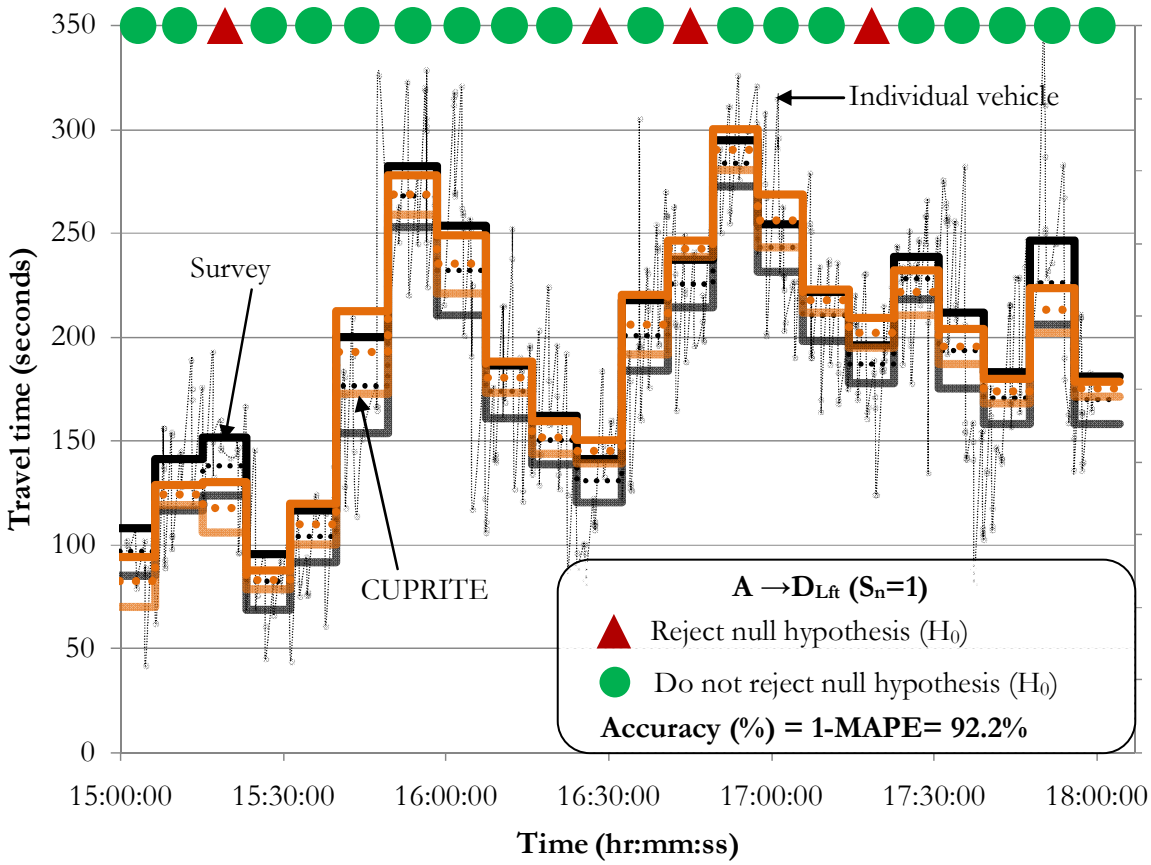

Figure 6-12: Results for A→D_{Lft} with S_n = 1.

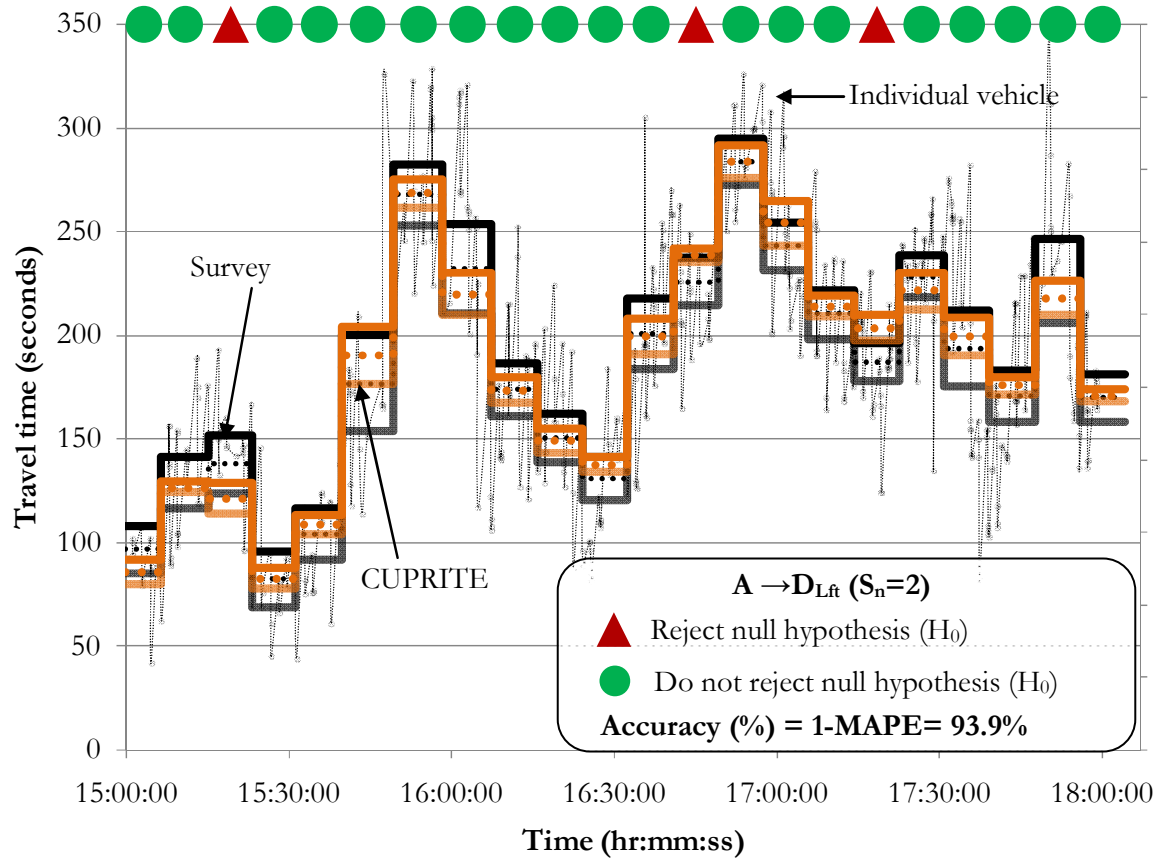

Figure 6-13: Results for A→D_{Lft} with S_n = 2.

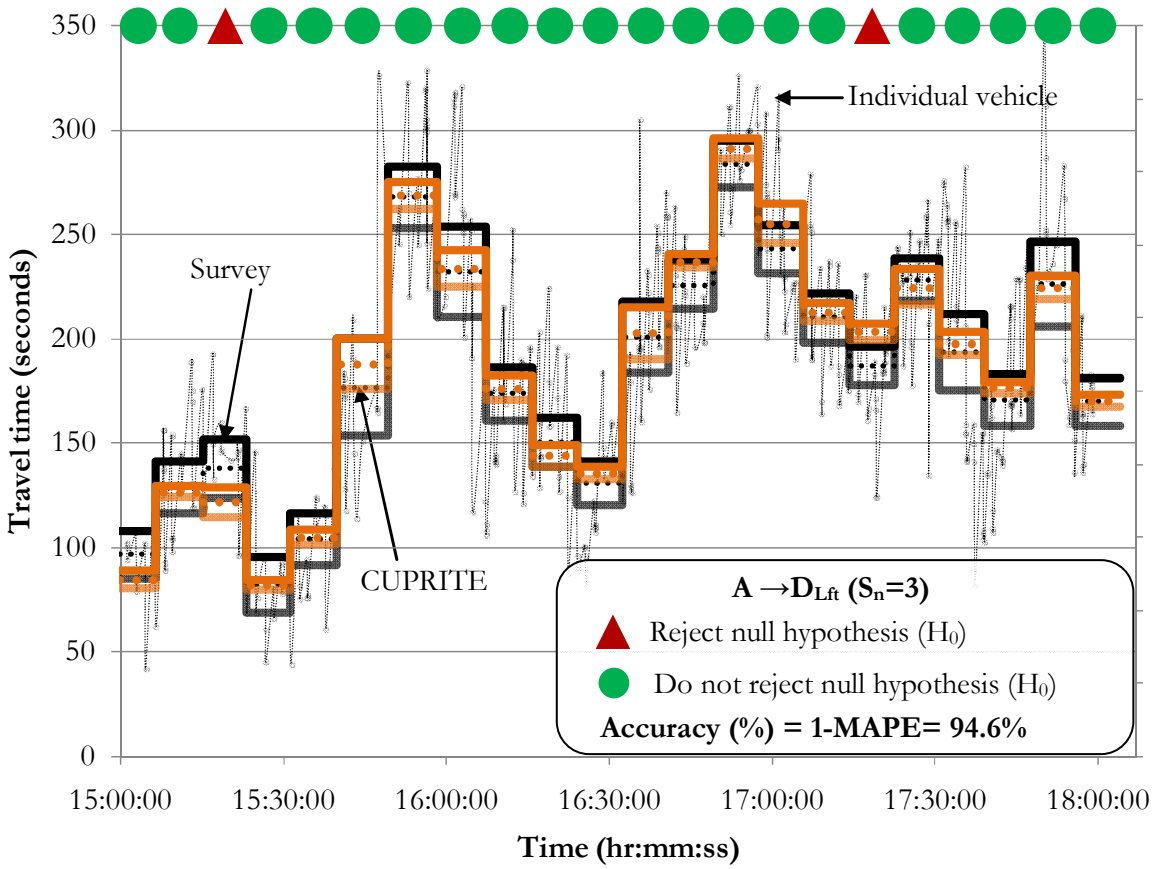

Figure 6-14: Results for A→D_{Lft} with S_n = 3.

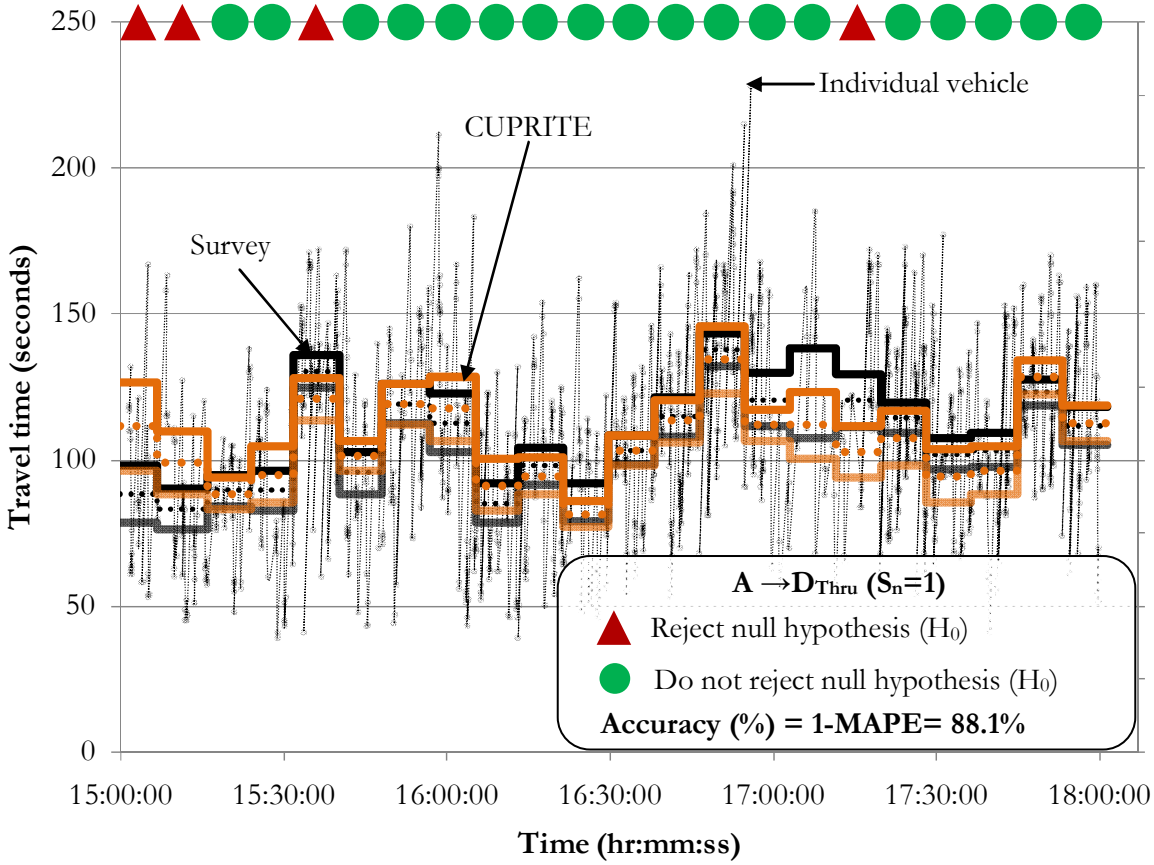

Figure 6-15: Results for A→D_{Thru} with S_n = 1.

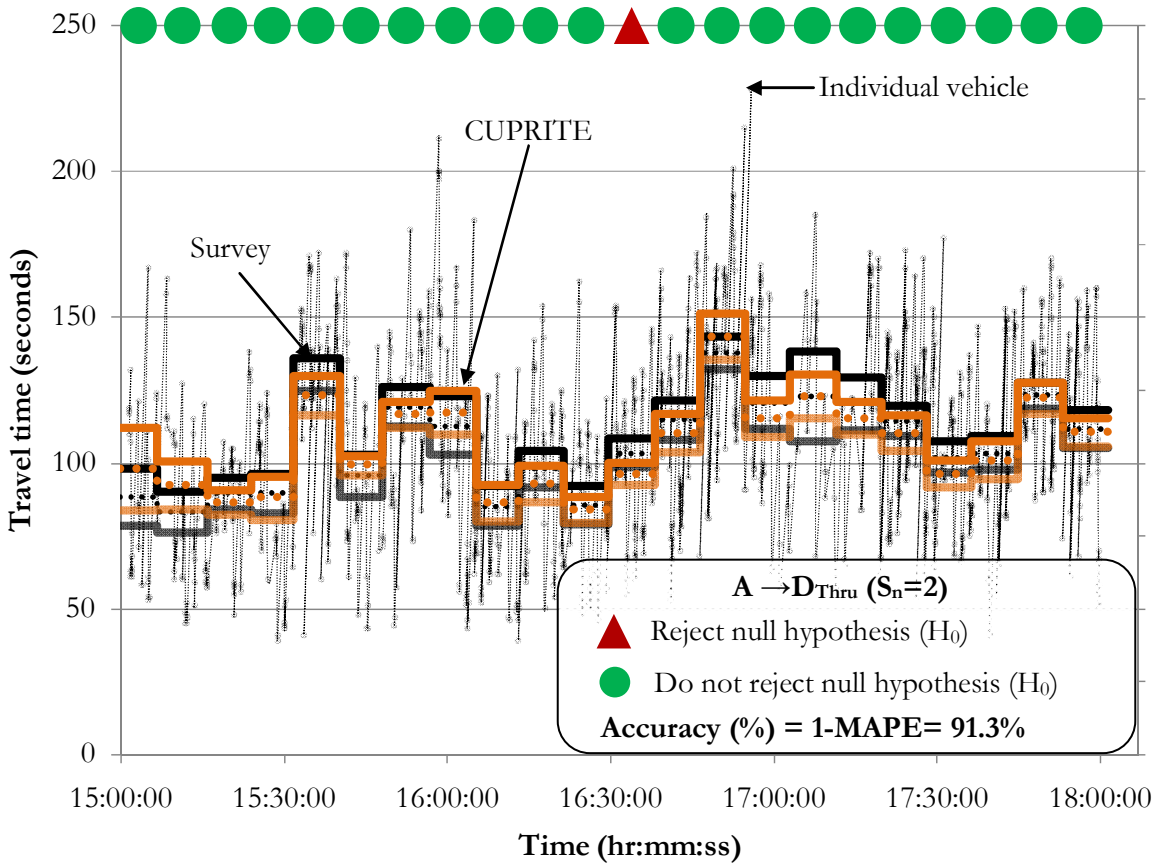

Figure 6-16: Results for A→D_{Thru} with S_n = 2.

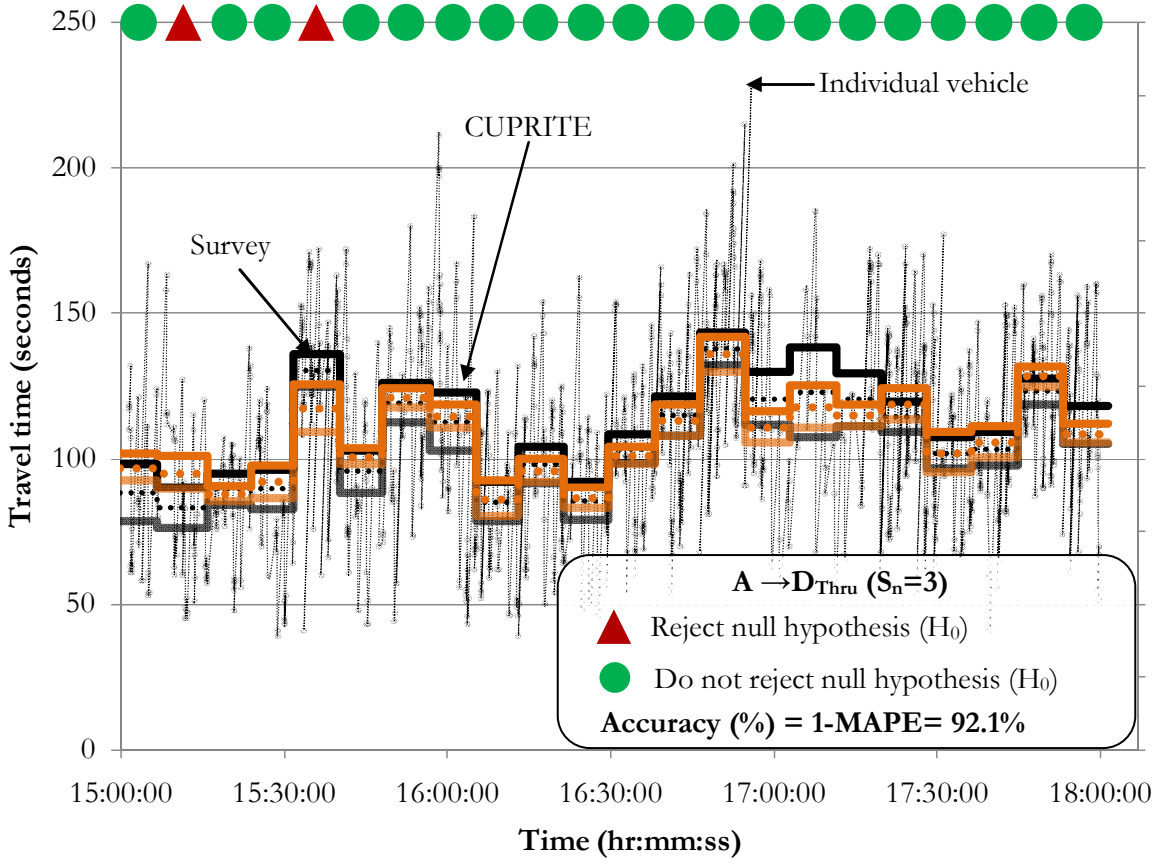

Figure 6-17: Results for A→D_{Thru} with S_n = 3.

6.3.2 Case Leg 2: (D→I)

For this route the number plate survey data corresponds to the vehicles observed at upstream detector d_d and downstream detector i_{s2} (*see* Figure 6-10). Hence, CUPRITE is applied with upstream cumulative plot defined by the counts from d_d and downstream cumulative plot defined by counts from i_{s2} and signal timings at intersection *I*. Route from *D* to *I* is equivalent to 65% mid-link gain of vehicles. Less than 35% of the vehicles are captured in the survey. The signal cycle time at intersection *I* is around 50 s and if we consider five signal cycles then only few number of survey vehicles are available in each estimation interval. Hence to represent the results we consider ten signal cycles as travel time estimation interval. The results for estimation interval of five signal cycles are presented in Appendix G. The survey results are available from 15:23:00 onwards. The results with consideration of one, two and three probes per estimation interval are illustrated in Figure 6-18, Figure 6-19 and Figure 6-20, respectively.

The accuracy from CUPRITE increases from 87.7% to 92 % with one to three probes per estimation interval, respectively. For more than one probe per estimation interval, the null hypothesis is not rejected in any of the estimation intervals. Individual vehicles captured from survey are also illustrated in the figures. It can be seen that not many vehicles are captured in each estimation interval, due to which there is higher inter quartile range for the confidence bounds for ground truth travel time from survey vehicles. Nevertheless, the fluctuations in time series of average travel time is well represented from the survey data and CUPRITE application could easily capture this behavior.

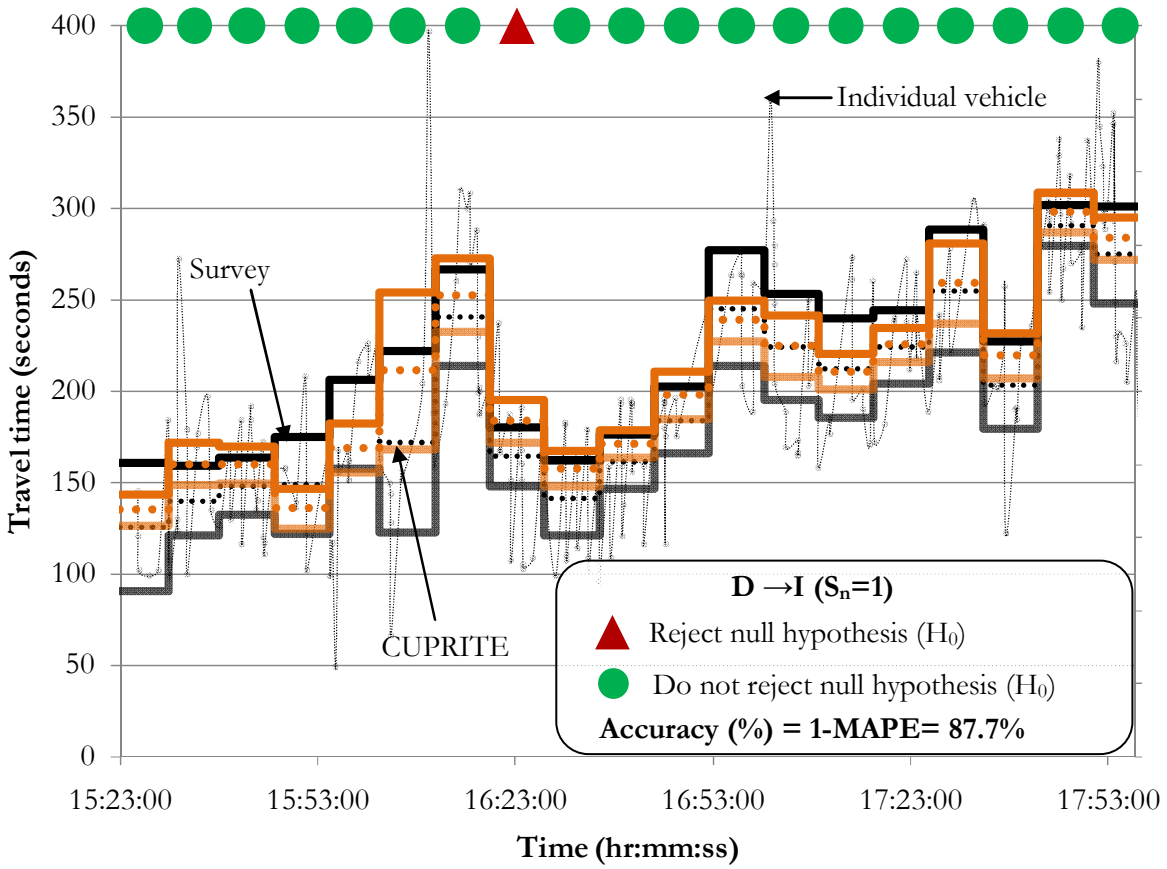

Figure 6-18: Results for D→I with S_n = 1.

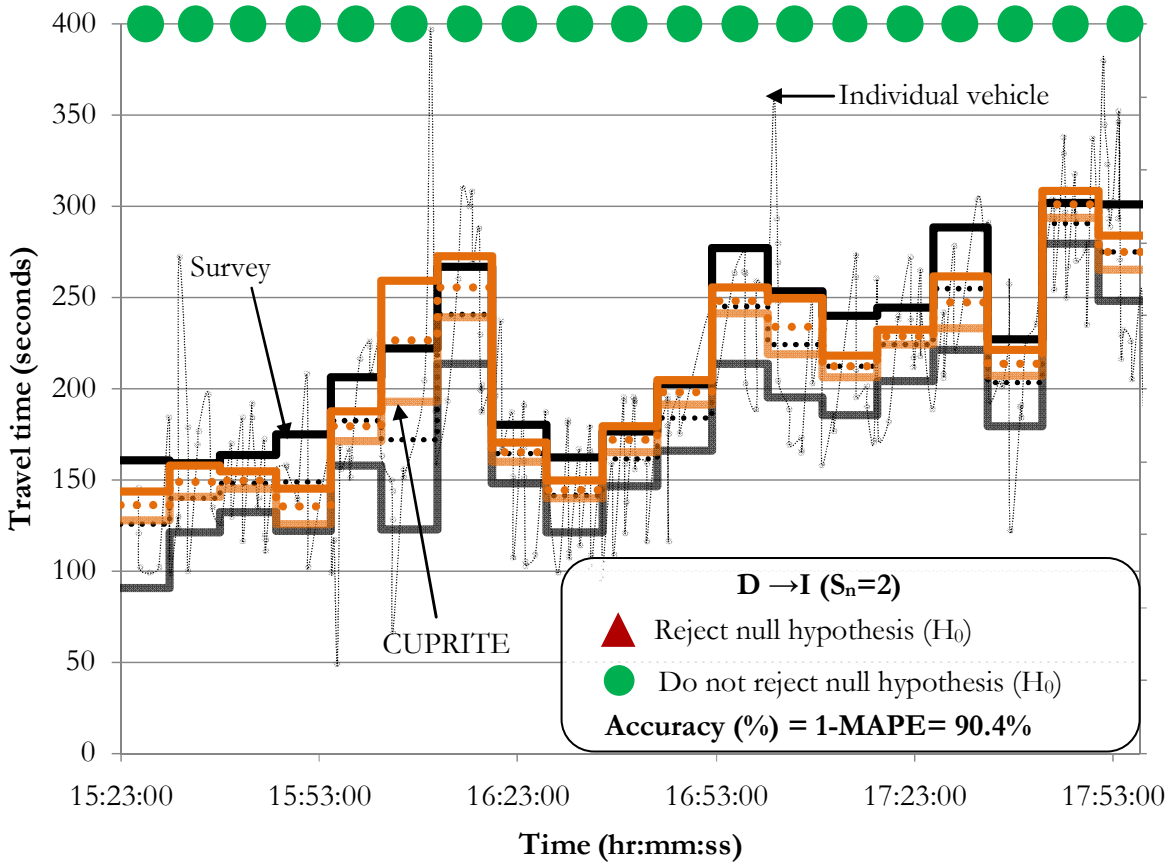

Figure 6-19: Results for D→I with S_n = 2.

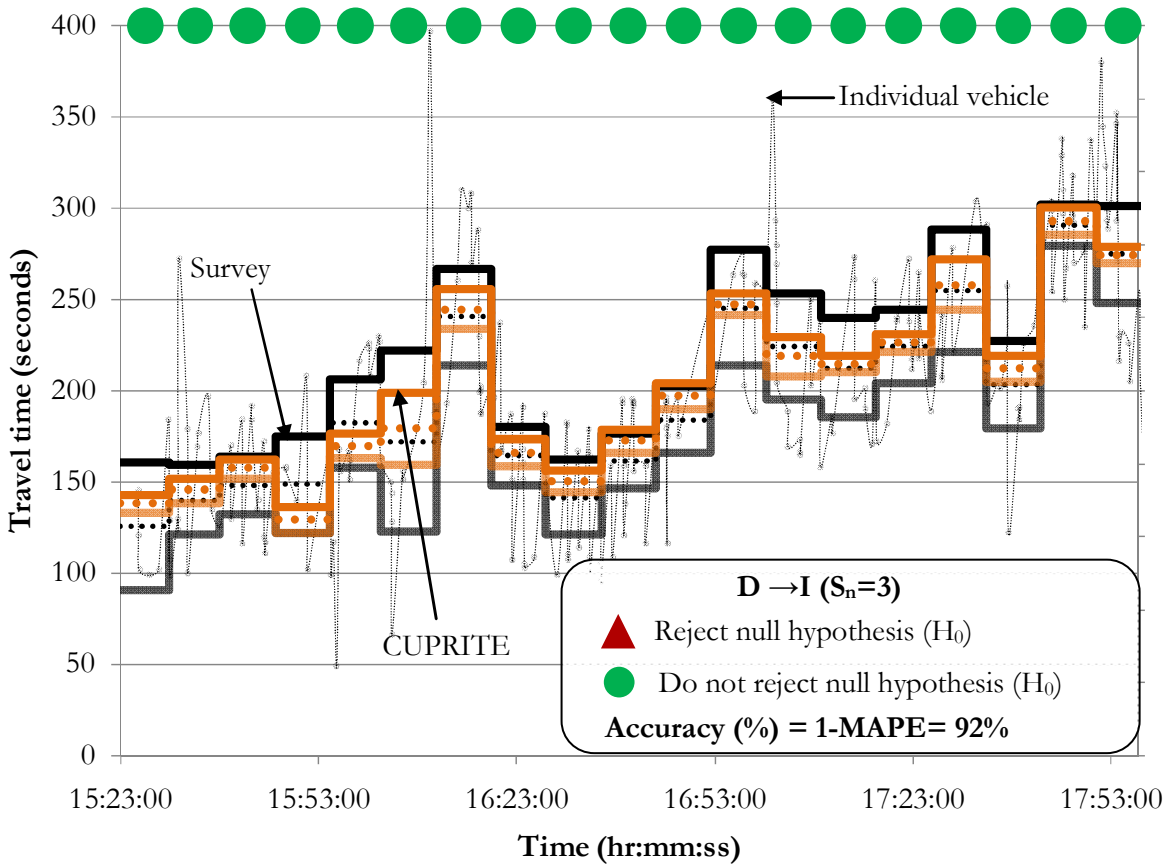

Figure 6-20: Results for D→I with S_n = 3.

6.3.3 Case Leg 3: (I→K)

The number plate survey is for vehicles which are traversing on lane 2 (*see* Figure 6-11) i.e., vehicles observed at detector i_{m2} at upstream and detector k_{s2} at downstream are surveyed. Hence, CUPRITE is applied with detector data from detectors i_{m2} and k_{s2} and the results presented here are travel time on lane 2 of the route I→K. The survey data is available from 16:19 hours to 18:00 hours.

The accuracy (6.9) of the CUPRITE increases from 83.5% to 92% with increase in number of probes from one probe (*see* Figure 6-21) to three probes (*see* Figure 6-23) per estimation interval, respectively. Consistent with the previous application, it also captures the micro travel time fluctuations amongst the estimation intervals. The null hypothesis is also not rejected in most of the estimation interval.

The validation of the model on this leg provides confidence that the model can be successfully applied to routes with significant mid-link delay.

Note: This case is analogous to configuration where detector is only on a representative lane, assuming lane 2 as representative lane. CUPRITE can accurately estimate travel time for each lane of the link.

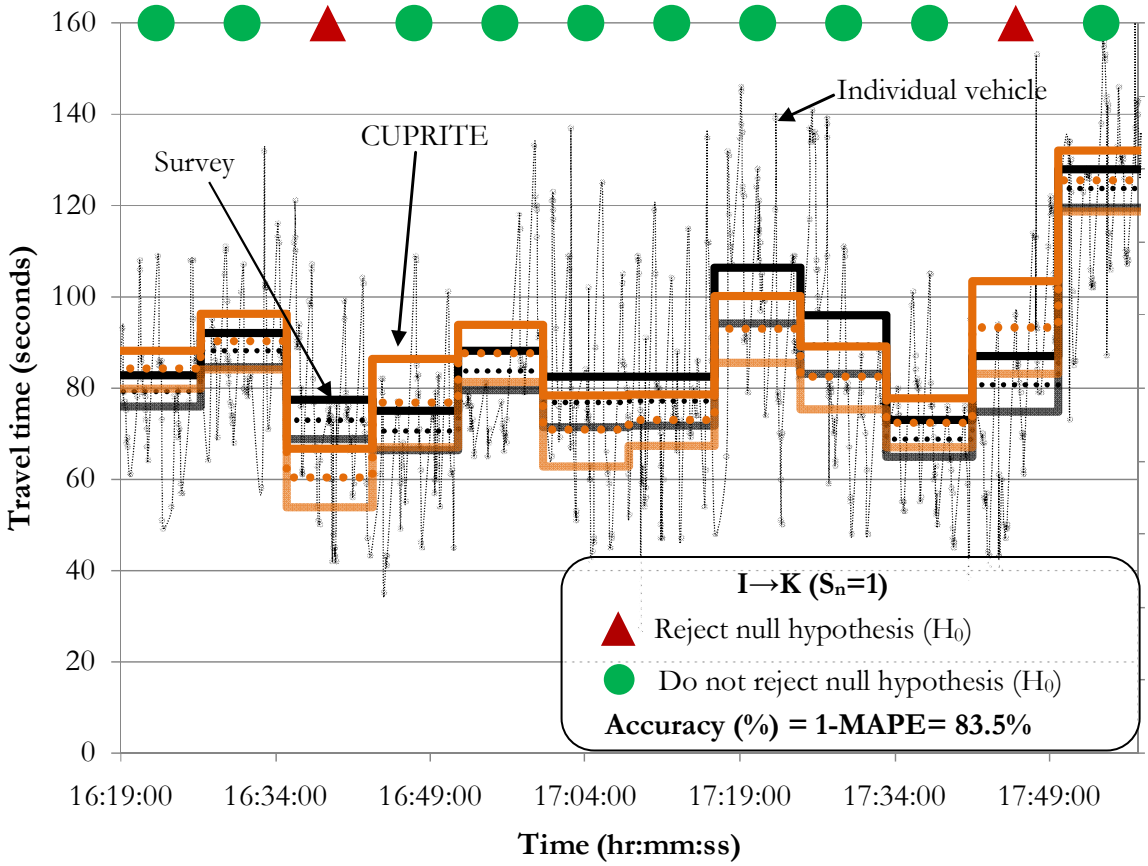

Figure 6-21: Results for I→K with S_n = 1.

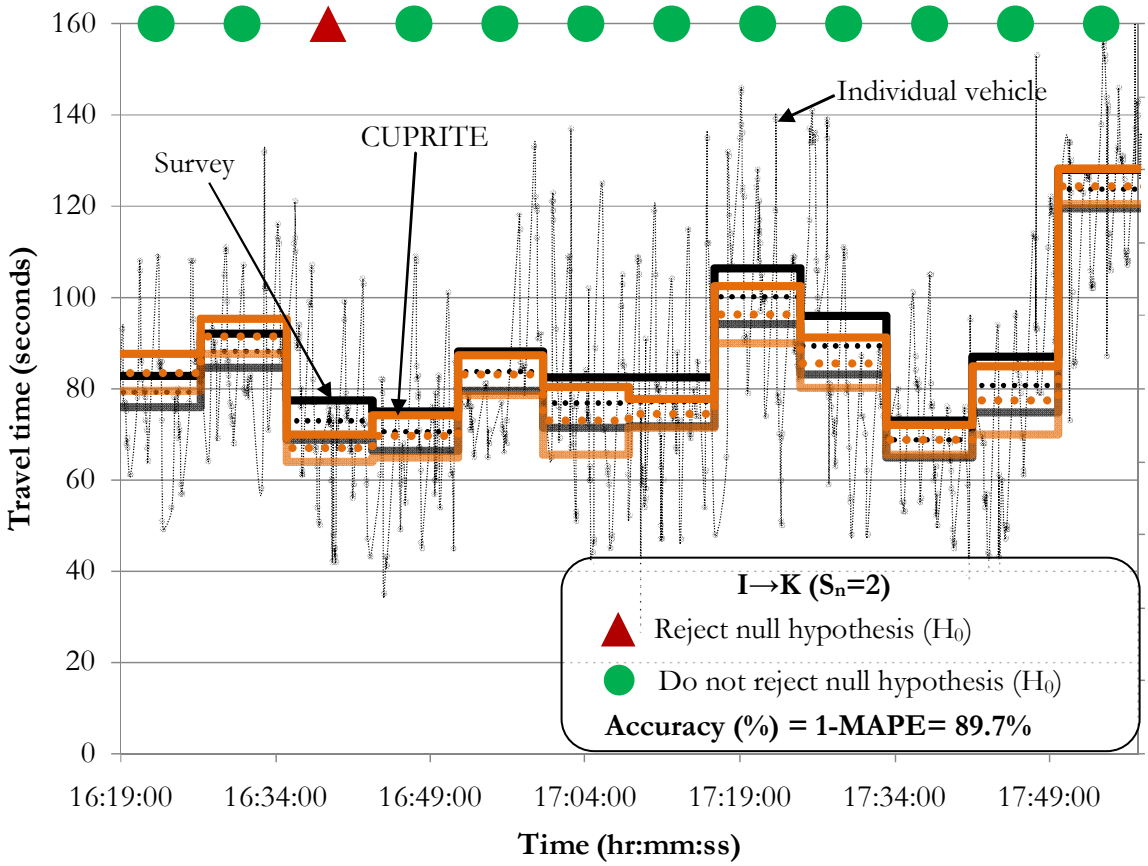

Figure 6-22: Results for I→K with S_n = 2.

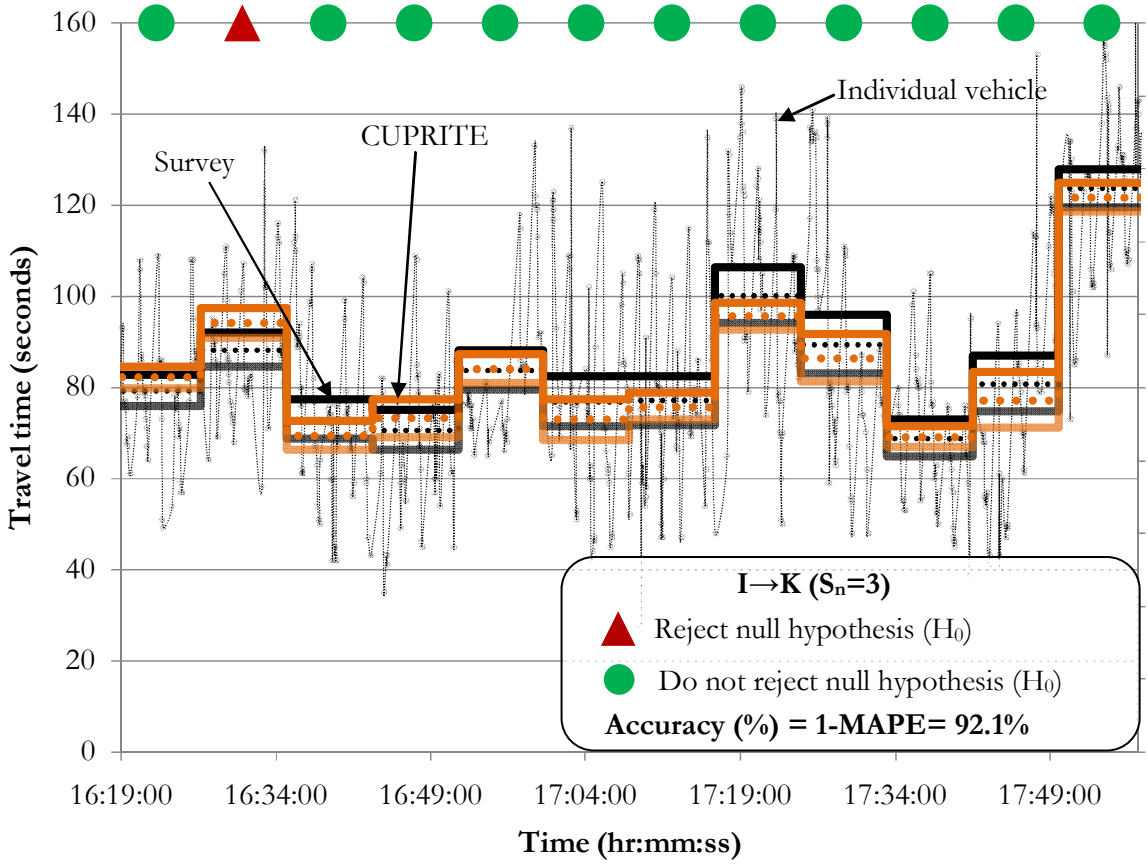

Figure 6-23: Results for I→K with S_n = 3.

6.3.4 Case R_E Vs R_C

Extreme based (Section 5.2.1.1) and *Component* based (Section 5.2.1.2) approaches are compared for route A→F; route D→I; and route D→K. For detail results refer to Appendix F, Appendix G and Appendix H. For *Component* based estimation, time-slice method (Section 5.2) is considered.

Figure 6-24, Figure 6-25 and Figure 6-26 summarize the accuracy for three routes for *Extreme* based and *Component* based estimation for one, two and three probes per estimation interval, respectively. It is observed that *Component* based estimation performs better than *Extreme* based though additional data corresponding to each component for the route is required.

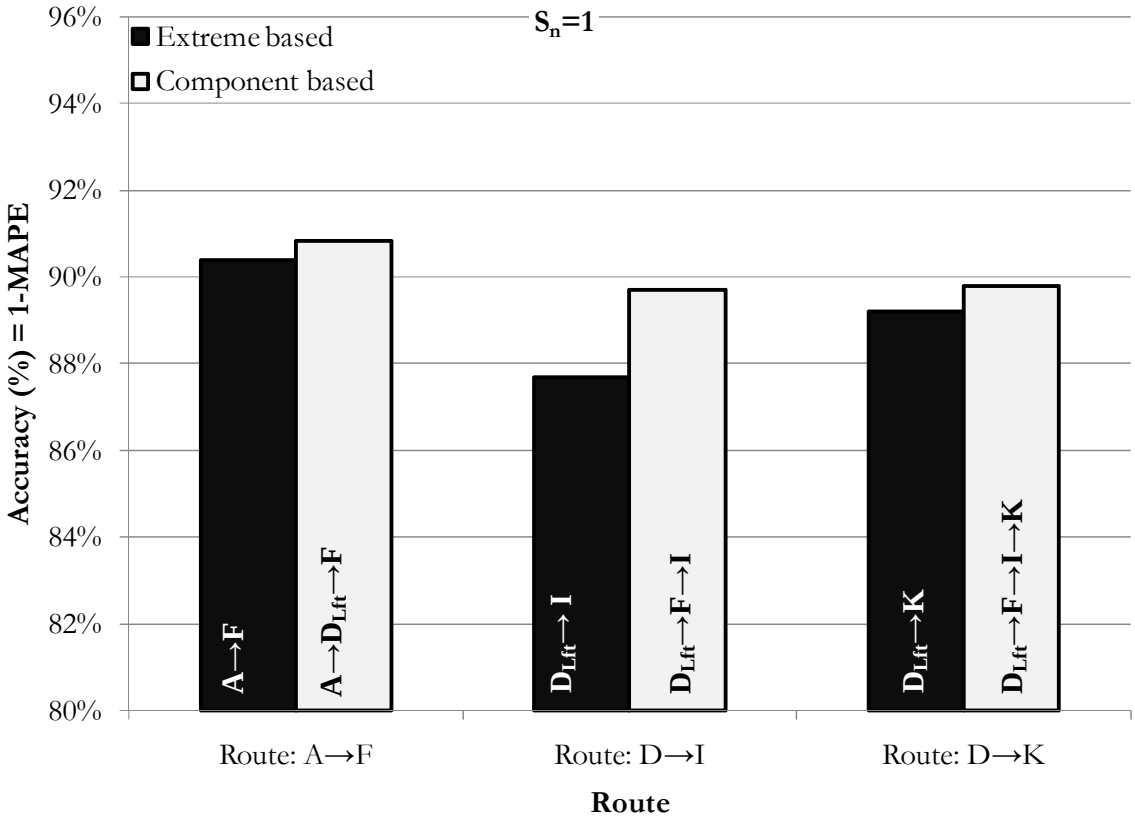

Figure 6-24: Results of *Extreme* based and *Component* based travel time estimation for different routes with S_n = 1.

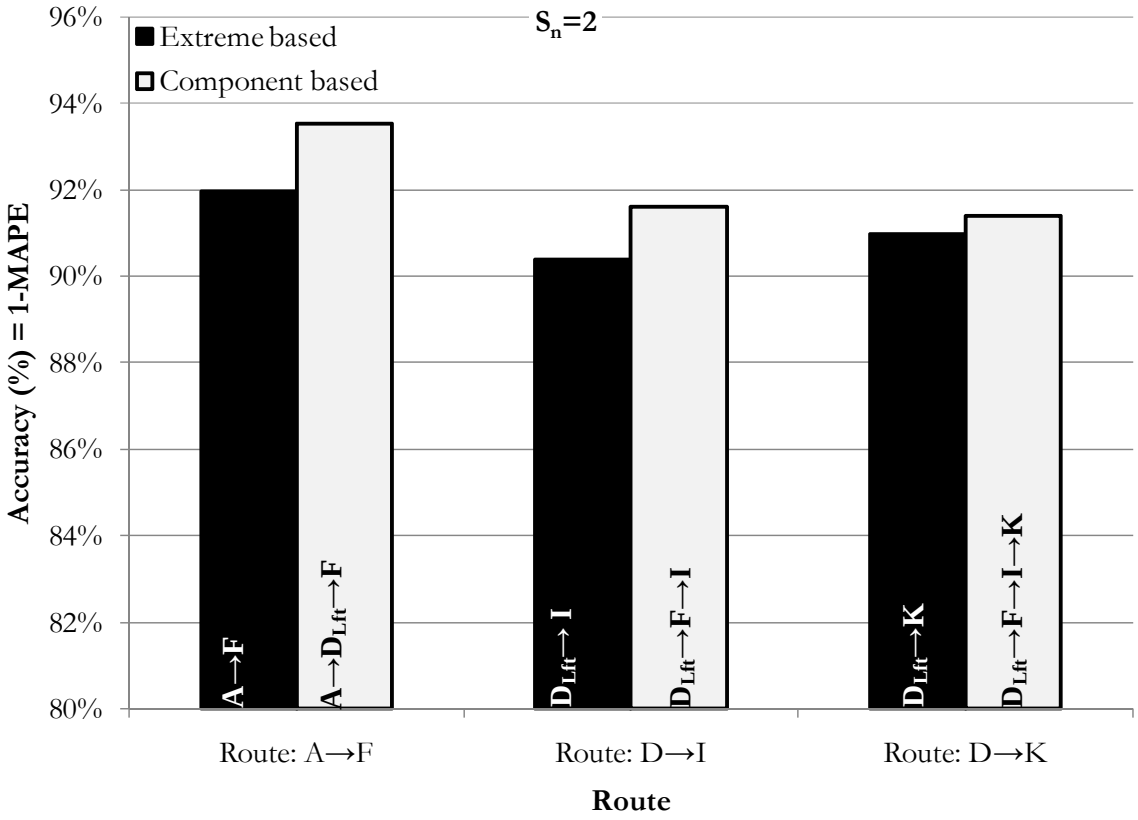

Figure 6-25: Results of *Extreme* based and *Component* based travel time estimation for different routes with S_n = 2.

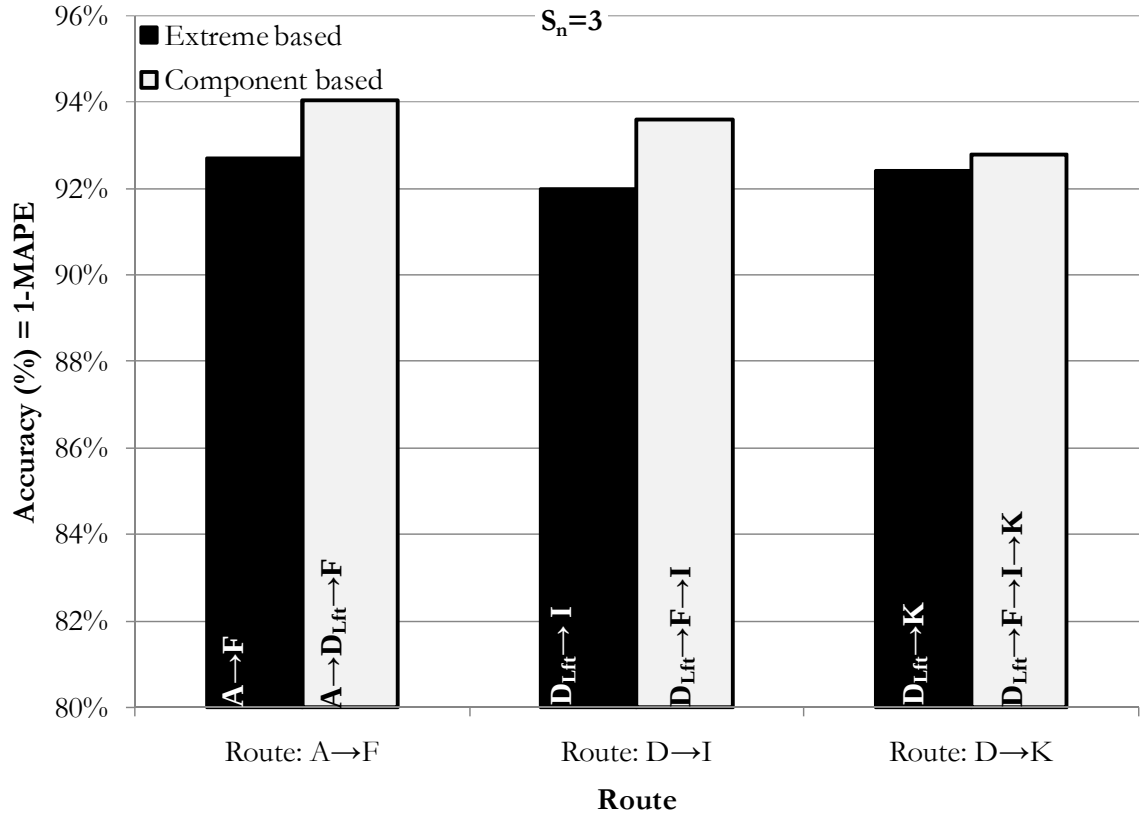

Figure 6-26: Results of *Extreme* based and *Component* based travel time estimation for different routes with S_n = 3.

6.3.5 Case S_p

The above cases consider fixed number (S_n) of probes per estimation interval. This section presents the results for CUPRITE application where probes are percentage (S_p) of vehicles traversing the route during three hour of survey period. Hence in an estimation period there can be no probe ($S_n = 0$) or at least one probe ($S_n > 0$). The results for route A→D_{Lft} with S_P equal to 1%, 2% and 3% are illustrated in Figure 6-27, Figure 6-28 and Figure 6-29, respectively. There is increase in accuracy from 83.5% to 92.3% with increase in S_p from 1% to 3%, respectively. Figure 6-30 illustrates the frequency distribution of estimation intervals versus S_n for different S_p values. For $S_p = 1\%$, more than 50% of the estimation periods have no probe ($S_n = 0$); and the percentage of estimation intervals with $S_n = 0$ decreases with increase in S_p. The results indicate that even with 1% of probes CUPRITE can capture the fluctuation in time series of travel time. In most of the estimation intervals for S_p equal to 2% and 3%, the null hypothesis is not rejected indicating that CUPRITE estimates are statistically equivalent to the number plate survey.

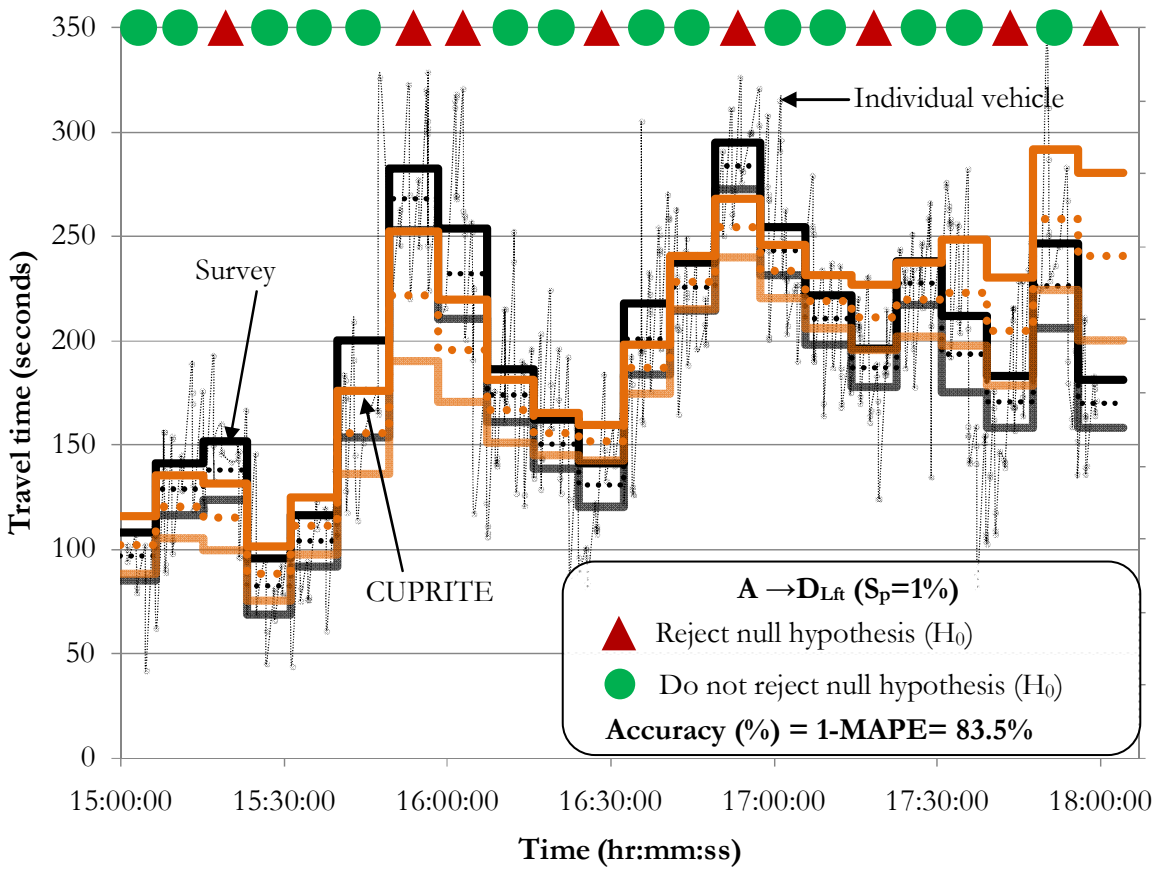

Figure 6-27: Results for A→D_{Lft} with S_p=1%.

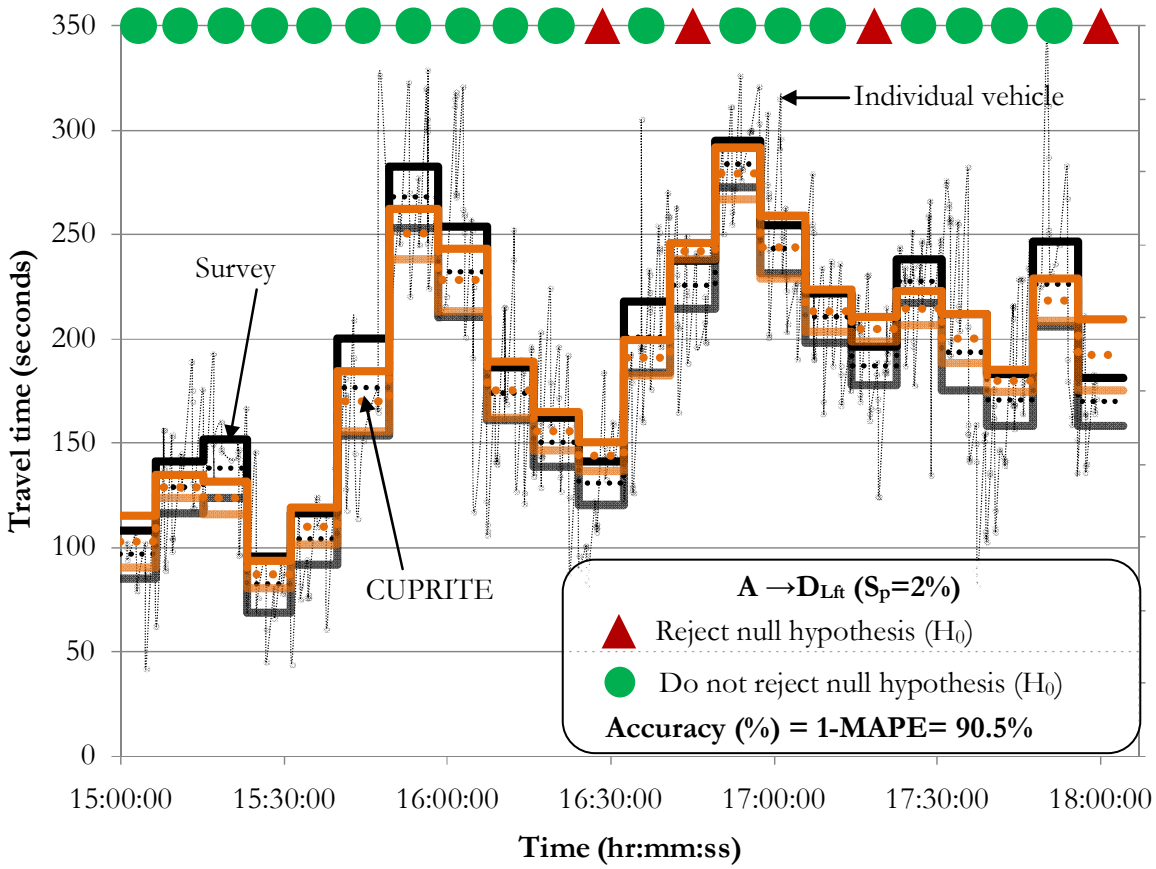

Figure 6-28: Results for A→D_{Lft} with S_p=2%.

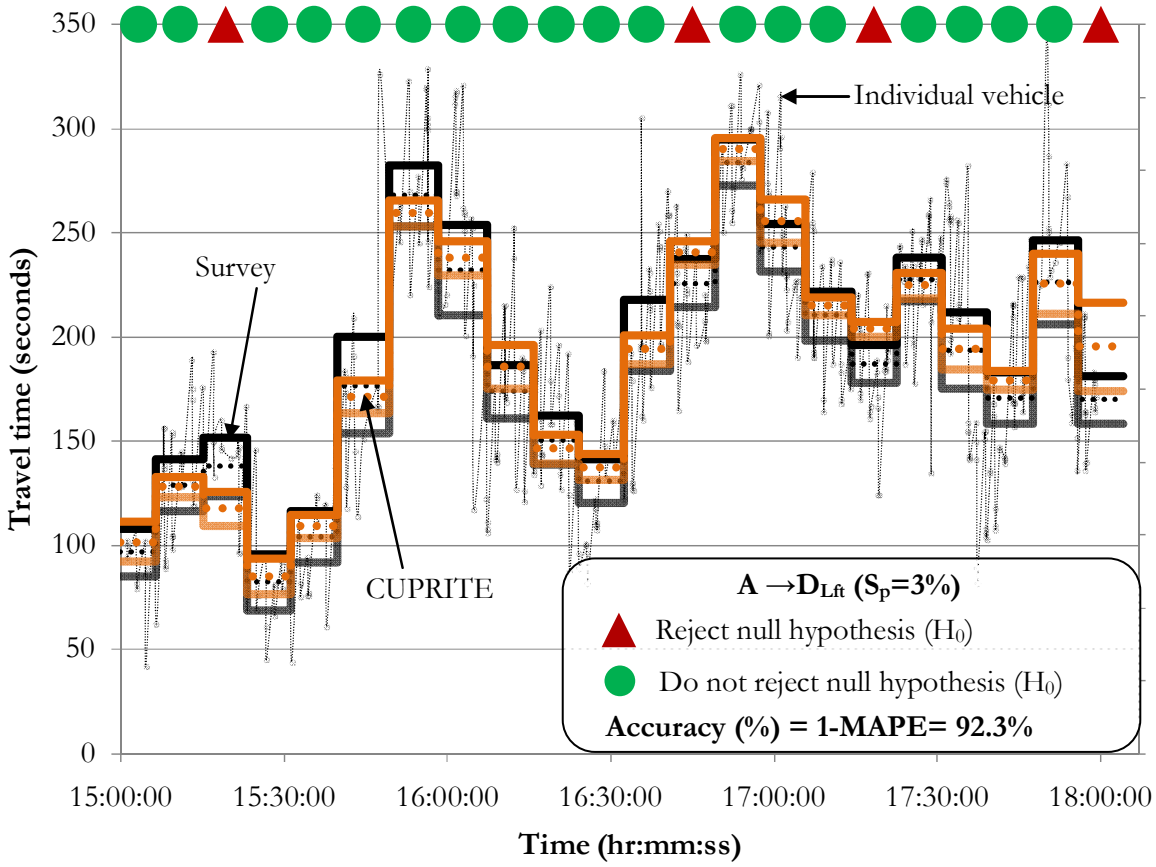

Figure 6-29: Results for A→D_{Lft} with S_p=3%.

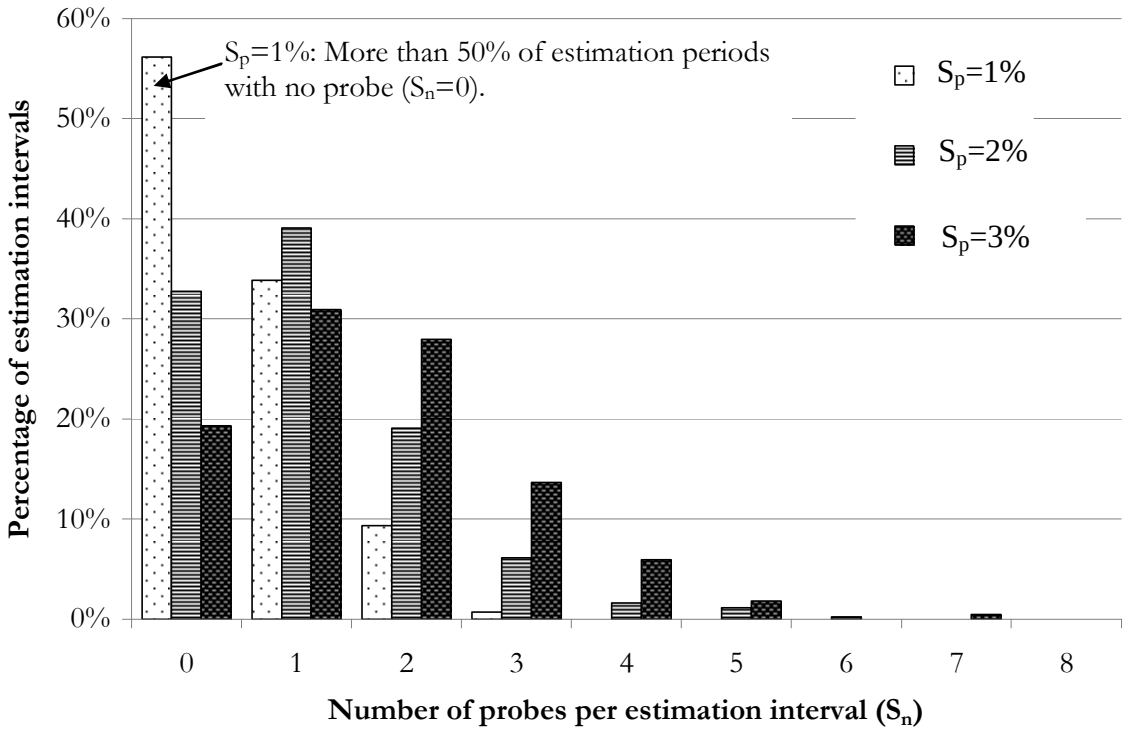

Figure 6-30: Percentage of estimation intervals versus S_n for route $A \rightarrow D_{Lft}$.

6.4 Concluding remarks

In this chapter, CUPRITE is validated on real data from number plate survey on signalized urban network at Lucerne, Switzerland. CUPRITE is applied on different routes with following characteristics:

i. detector counting error;

ii. mixed traffic (with buses);

iii. on-street bus stops;

iv. significant loss and gain from mid-link sinks and sources, respectively;

v. significant mid-link delay due to pedestrian crossing; and

vi. urban links passing through the city centre.

Travel time for different turning movements on a route is also considered.

Two tailed t-tests are computed to determine if difference exists between the real travel time from survey and CUPRITE application. The tests were considered significant at the 0.05 and

the result of the tests indicates that travel time estimates from CUPRITE are statistically equivalent to real estimates from number plate survey.

From this, we can conclude that CUPRITE can be successfully applied for travel time estimation on urban networks. It can accurately estimate travel time for different exit turning movements and route travel time. It can also accurately capture the short term oversaturation in the system.

The application of CUPRITE using *Extreme* based and *Component* based travel time estimation is also validated. The results indicate that the component based estimation has the potential to increase the accuracy. Though, additional data from each component of a route is required.

7 Conclusions

7.1 Research contributions

The methodology, CUPRITE, developed in this research addresses the following complexities for travel time estimation on urban networks:

i. Interruptions in traffic flow due to conflicting areas;

ii. Significant proportion of flow to/from mid-link sinks/sources;

iii. Detector counting error; and

iv. Travel time for different exit movements.

CUPRITE is based on classical analytical procedure for travel time estimation. The classical procedure is vulnerable to relative deviation amongst the cumulative plots due to mid-link sinks and sources, and detector counting error. These issues are addressed by integrating detector data, signal timings and probe vehicle data. First, detectors and signal timings are integrated to obtain cumulative plots at different locations on the network. Thereafter, probe vehicle data is utilized to enhance the accuracy of travel time estimation. The performance of the methodology during each step of its development is thoroughly tested using simulated data. Finally, it is validated with real data.

The testing is performed for both undersaturated and oversaturated traffic conditions. For undersaturated traffic condition, the concept of virtual probe is introduced and it provides accurate estimates (Accuracy more than 95%) without the need of real probe. For oversaturated traffic condition or situations where virtual probe cannot be used, the integration of real probe data with cumulative plots significantly enhances the accuracy. It is concluded that only one probe per estimation interval or three percent of vehicles traversing as probe can provide accuracy (overall average performance) of more than 95% irrespective of the magnitude of sink, source or detector counting error.

The methodology is also compared with a model solely based on probe data (*Probe-Only*). For *Probe-Only* significantly large numbers of probes (more than 10) are required to obtain accuracy comparable to that of CUPRITE. Moreover, if few probes per estimation interval are available then travel time estimates from *Probe-Only* are unreliable. For instance, with one probe per estimation period, the standard deviation of accuracies from *Probe-Only* is around 10% whereas, that from CUPRITE is around 4%. Hence it can be concluded that the integration of multisource data not only improves the accuracy but also the reliability of travel time estimates.

The real data for the validation is obtained through number plate survey at a site in Lucerne city, Switzerland. The study site is a typical urban network with following characteristics: *a)* mixed traffic (with buses); *b)* on-street bus stops; *c)* significant loss and gain from mid-link sinks and sources, respectively; and *d)* significant mid-link delays due to pedestrian crossing. The loop detectors on the site are not perfect.

CUPRITE is applied at the above site for estimating travel time for different movements on a link and travel time for different routes. Two tailed t-test (at 0.05 level of significance) results confirm that the travel time estimates from CUPRITE are statistically equivalent to real estimates from number plate survey data. Validation results also indicate that CUPRITE can accurately capture the time series of travel time and short-term oversaturation in the system.

The testing and validation of CUPRITE has demonstrated that it can be successfully applied for accurate and reliable travel time estimation on urban networks. Hence, the goals and objectives of this research defined earlier in Section 1.4 are achieved. The principal contributions of this research can be summarized as follows:

i. *A new methodology* for travel time estimation on urban networks. It exploits advantages of both traffic detector counts and probe vehicle data. It addresses the weakness of individual data sources, by integrating the data from different sources for accurate and reliable travel time estimation.

ii. The methodology provides exit movement specific travel time and hence *detailed understanding of the network performance*. For instance, excessive travel time for an exit movement can identify the critical movement at an intersection.

iii. The methodology is robust with respect to mid-link sinks and sources, and detector counting error. Hence, have *better network applicability*.

iv. It can capture accurate time series of travel time and also short-term oversaturated situations. Hence can be applied for *developing historical database*, which is the basic requirement for travel time prediction.

v. The methodology only needs one probe per estimation interval or less than 3% of vehicles traversing the link as probe for accurate travel time estimates. The current probe market penetration is low and therefore the requirement of few numbers of probes makes the *methodology directly applicable*.

vi. Though the development of methodology is based on urban networks, but it can be equally applied to freeway facilities. It can be easily *integrated with traffic monitoring system to simultaneously monitor both urban and freeway networks*.

7.2 Future research directions

In this research the plot of cumulative counts versus time for both U(t) and D(t) are represented in the same figure (two dimensional plot). Therefore, the probe data utilized is the time when it is at upstream and downstream intersection. For future research, it is recommended that three-dimension modeling should be considered. This includes *a)* cumulative counts; *b)* time; and *c)* location from upstream to downstream. The above three dimensional representation of cumulative plots should be integrated with trajectory of the probe vehicle for more detailed modeling. This should provide better understanding of the shock-wave propagation and traffic flow characteristics.

The aim for integrating cumulative plots with probe vehicle is to reduce RD. For this the downstream cumulative plot is considered as accurate and upstream cumulative plot is redefined. Practically, we do not know which cumulative plot is responsible for RD and considering D(t) as accurate and redefining U(t) approach works well as is evident from the testing and validation results in this dissertation. It is expected that further improvement in accuracy is possible if we simultaneously correct both U(t) and D(t) for reduction of RD. It should be worth extending the research further to

define approaches for simultaneous correction of errors in estimation of both U(t) and D(t).

CUPRITE provides average travel time, which is a standard indicator for network performance measure and an important input for number of transport analysis. Travel time on an urban link is bi-modal and hence different statists such as quartiles should also be explored. The application of CUPRITE for estimation of quartile of travel time is presented in Appendix J.

Furthermore, this research can be extended in the following avenues by integrating CUPRITE with:

1. Time series modeling tools for travel time prediction.
2. Public Transport Priority Systems (PTPS) to improve the PTPS efficiency and reliability.
3. Signal control algorithm to optimize its parameters.

7.2.1 Travel time prediction

The objective of this research is to accurately estimate travel time, which is the experienced travel time. Travel time estimates from CUPRITE are not predicted travel time i.e. it is not predicting the expected value of travel time in next five minutes or so. CUPRITE can be extended for travel time prediction because the basic requirement for any travel time prediction tool is accurate travel time estimation. Prediction tools such as time series analysis, pattern recognition etc. require accurate historical database for travel time. The development of database for urban network is challenging as most of the urban sites are not equipped with advance direct travel time measurement equipments such as AVI and the ground truth travel time is unavailable. Generally, it is recommended to use probe vehicle for development of database. However, a large number of probes per estimation interval are required for statistically accurate travel time estimation. CUPRITE provides accurate estimation of travel time with low number of probes. Hence, it has the potential to develop an accurate database of travel time. It can be extended by integrating with prediction tools for accurate travel time prediction.

7.2.2 Integration with Public Transport Priority Systems

A hybrid model can be developed by integrating CUPRITE with public transport (bus) vehicle data. The hybrid model should differentiate between vehicle travel time and bus travel time on the link. It should predict the time when the bus should be at the stop-line, taking into account the variability of travel time of the bus. The hybrid model should be useful for testing different strategies for Public Transport Priority Systems (PTPS) and should enhance the efficiency of PTPS.

7.2.3 Feedback to signal control algorithm

A feedback model from CUPRITE to signal control algorithm can be developed with the objective to optimize signal controller parameters. Such direct optimization method has never been used in practice due to difficulty in getting accurate performance measures in real-time. The optimization of the signal control parameters would enhance the performance of controller, resulting in reduced delay, less number of stops at intersection which in turn would reduce energy consumption and vehicle emissions.

References

AKÇELIK, R. (1978) A New Look at Davidson's Travel Time Function. *Traffic Engineering and Control,* 19**,** 459-463.

AKÇELIK, R. (1988) Highway capacity delay forumula for signaliyed intersections. *ITE Journal (Institute of Transportation Engineers),* 58**,** 23-27.

AKÇELIK, R. (1991) Travel time functions for transport planning purposes: Davidson's function, its time-dependent form and an alternative travel time function *Australian Road Research* 21**,** 49-59.

AKCELIK, R. & ROUPHAIL, N. M. (1993) Estimation of delays at traffic signals for variable demand conditions. *Transportation Research Part B: Methodological,* 27**,** 109-131.

AKCELIK, R. & ROUPHAIL, N. M. (1994) Overflow queues and delays with random and platooned arrivals at signalized intersections. *Journal of Advanced Transportation,* 28**,** 227-251.

ASANO, M. (2004) Adaptive Traffic Signal Control Using Real-Time Delay Measurement. *Department of Civil Engineering, Faculty of Engineers.* Tokyo, Japan, University of Tokyo.

BAJWA, S. I., CHUNG, E. & KUWAHARA, M. (2003) A travel time prediction method based on pattern matching technique *21st ARRB and 11th REAAA Conference.* Cairns, Australia,.

BAJWA, S. U. I., CHUNG, E. & KUWAHARA, M. (2004) An adaptive travel time prediction model based on pattern matching. *11th World Congress on ITS.* November, 2004.

BARCELÓ, J., CODINA, E., CASAS, J., FERRER, J. L. & GARCIA, D. (2005) Microscopic traffic simulation: A tool for the design, analysis and evaluation of intelligent transport systems. *Journal of Intelligent and Robotic Systems: Theory and Applications,* 41**,** 173-203.

BERKA, S., TARKO, A., ROUPHAIL, N. M., SISIOPIKU, V. P. & LEE, D.-H. (1995) Data fusion algorithm for ADVANCE Release 2.0. *Advance Working Paper Series, No. 48, University of Illinois at Chicago, Chicago, IL.*

BPR (1964) Bureau of Public Roads: Traffic Assignment Manual. IN U.S. DEPT. OF COMMERCE, U. P. D., WASHINGTON D.C (Ed.).

BRILON, W. & WU, N. (1990) Delays at fixed-time traffic signals under time-dependent traffic conditions. *Traffic Engineering and Control,* 31**,** 8.

CARDEN, P. J., HOUNSELL, N. B. & MCDONALD, M. (1989) SCOOT Model Accuracy. *Transport and Road Research Laboratory Contract report 153*

CATHEY, F. W. & DAILEY, D. J. (2001) Transit vehicles as traffic probe sensors. *IEEE Conference on Intelligent Transportation Systems, Proceedings, ITSC.* Oakland, CA.

CHAKROBORTY, P. & KIKUCHI, S. (2004) Using bus travel time data to estimate travel times on urban corridors. *Transportation Research Record.*

CHEN, H., GRANT-MULLER, S., MUSSONE, L. & MONTGOMERY, F. (2001) A study of hybrid neural network approaches and the effects of missing data on traffic forecasting. *Neural Computing and Applications,* 10**,** 277-286.

CHOI, K. & CHUNG, Y. (2002) A data fusion algorithm for estimating link travel time. *ITS Journal: Intelligent Transportation Systems Journal,* 7**,** 235-260.

CHUNG, E. & KUWAHARA, M. (2007) Mapping Personal Trip OD from Probe Data. *International Journal of ITS Research* 5**,** 11.

COIFMAN, B. (2001) Vehicle reidentification and travel time measurement, Part II: Uncongested freeways and the onset of congestion. *IEEE Conference on Intelligent Transportation Systems, Proceedings, ITSC.* Oakland, CA.

COIFMAN, B. & CASSIDY, M. (2001) Vehicle reidentification and travel time measurement, Part I: Congested freeways. *IEEE Conference on Intelligent Transportation Systems, Proceedings, ITSC.* Oakland, CA.

COIFMAN, B. & CASSIDY, M. (2002) Vehicle reidentification and travel time measurement on congested freeways. *Transportation Research Part A: Policy and Practice,* 36**,** 899-917.

COIFMAN, B. & ERGUETA, E. (2003) Improved vehicle reidentification and travel time measurement on congested freeways. *Journal of Transportation Engineering,* 129**,** 475-483.

COIFMAN, B. & KRISHNAMURTHY, S. (2007) Vehicle reidentification and travel time measurement across freeway junctions using the existing detector infrastructure. *Transportation Research Part C: Emerging Technologies,* 15**,** 135-153.

DAGANZO, C. F. (1997) *Fundamentals of Transportation and Traffic Operations,* Pergamon, Oxford.

DAILEY, D. J. (1993) Travel-time estimation using cross-correlation techniques. *Transportation Research,* 27 B**,** 97-107.

DAILEY, D. J. (1999) A statistical algorithm for estimating speed from single loop volume and occupancy measurements. *Transportation Research Part B: Methodological,* 33**,** 313-322.

DAILEY, D. J., HARN, P. & LIN, P.-J. (1996) ITS Data Fusion. *Research Project T9903, Task 9* *http://www.its.washington.edu/pubs/fusion_report.pdf.*

DAVIS, G. A., NIHAN, N. L., HAMED, M. M. & JACOBSON, L. N. (1990) Adaptive forecasting of freeway traffic congestion. *Transportation Research Record,* 1287**,** 29-33.

DIA, H. (2001) An object-oriented neural network approach to short-term traffic forecasting. *European Journal of Operational Research,* 131**,** 253-261.

DIAS, C. (2007) Self Learning Tool for Travel Time Estimation in Signalized Urban Networks Based on Probe Data. *Department of Civil Engineering.* Tokyo, Japan, University of Tokyo.

DOUGHERTY, M. (1995) A review of neural networks applied to transport. *Transportation Research, Part C: Emerging Technologies,* 3 C**,** 247-260.

EL FAOUZI, N. E. (2004) Data fusion in road traffic engineering: An overview. IN DASARATHY, B. V. (Ed.) *Proceedings of SPIE - The International Society for Optical Engineering.* Orlando, FL.

EL FAOUZI, N. E. (2006) Bayesian and evidential approaches for traffic data fusion: methodological issues and case study. *Presented at the 85th Transportation Research Board Meeting.*

ELANGO, C. & DAILEY, D. J. (2000) Irregularly sampled transit vehicles used as traffic sensors. *Transportation Research Record Issue 1719***,** 33-44.

GAULT, H. E. (1981) An on-line measure of delay in road traffic computer controlled systems. *Traffic Engineering and ControL,* 22 384-389.

GIPPS, P. G. (1997) The estimates of a measure of vehicle delay from detector output. *Transport Operations Research Group, Research Report No. 25.* University of Newcastle

HALL, D. L. & LLINAS, J. (1997) An introduction to multisensor data fusion. *Proceedings of the IEEE,* 85**,** 6-23.

HAMED, M. M., AL-MASAEID, H. R. & BANI SAID, Z. M. (1995) Short-term prediction of traffic volume in urban arterials. *Journal of Transportation Engineering,* 121**,** 249-254.

HEIDEMANN, D. (1994) Queue length and delay distributions at traffic signals. *Transportation Research Part B: Methodological,* 28 B**,** 377-389.

HELLINGA, B. & FU, L. (1999) Assessing expected accuracy of probe vehicle travel time reports. *Journal of Transportation Engineering,* 125**,** 524-530.

HOLM, C., ANZEK, M. & KASTELA, S. (2004) Travel time information service utilising mobile phone tracking. *Promet - Traffic - Traffico,* 16**,** 211-216.

HUNT, P. B., ROBERTSON, D. I., BRETHERTON, R. D. & WINTON, R. I. (1981) SCOOT - a traffic responsive method of co-ordinating signals. *TRL Laboratory Report 1014*.

IVAN, J. N. (1997) Neural network representations for arterial street incident detection data fusion. *Transportation Research Part C: Emerging Technologies,* 5**,** 245-254.

IVAN, J. N., SCHOFER, J. L., KOPPELMAN, F. S. & MASSONE, L. L. E. (1995) Real-time data fusion for arterial street incident detection using neural networks. *Transportation Research Record Issue 1497***,** 27-35.

KINNOCK, M. N. (1995) Towards fair and efficient pricing in transport: Policy options for internalising the external costs of transport in the European Union. European Commission Directorate-General For Transport-DG VII.

KLEIN, L. A. (2001) *Sensor Technologies and Data Requirements for ITS,* Boston, Artech House Books.

KLEIN, L. A., MILLS, M. K. & GIBSON, D. R. P. (2006a) Traffic Detector Handbook: Third Edition-Volume I. IN ADMINISTRATION, F. H. (Ed.).

KLEIN, L. A., MILLS, M. K. & GIBSON, D. R. P. (2006b) Traffic Detector Handbook: Third Edition—Volume II. IN ADMINISTRATION, F. H. (Ed.).

KLEIN, L. A., YI, P. & TENG, H. (2002) Decision support system for advanced traffic management through data fusion. *Transportation Research Record*.

KUWAHARA, M., CHUNG, E. & ISHIDA, T. (2004) Fundamental study on the issues of using probe data for OD estimation and route identification. *Proceedings of 11th World Congress on ITS (CD-ROM).*

KWON, T. M. (2006) Blind Deconvolution of Vehicle Inductance Signatures for Travel-Time Estimation *MN/RC-2006-06.* University of Minnesota Duluth, http://conservancy.umn.edu/bitstream/436/1/200606.pdf.

LAN, C. J. & DAVIS, G. A. (1999) Real-time estimation of turning movement proportions from partial counts on urban networks. *Transportation Research Part C: Emerging Technologies,* 7**,** 305-327.

LIGHTHILL, M. H. & WHITHAM, G. B. (1955) On kinematic waves. I. Flow movement in long rivers. II. A theory of traffic flow on long crowded roads. *Proceedings of the Royal Society, London,* A229**,** 281-345.

LIN, W. H., KULKARNI, A. & MIRCHANDANI, P. (2004) Short-term arterial travel time prediction for advanced traveler information systems. *Journal of Intelligent Transportation Systems: Technology, Planning, and Operations,* 8**,** 143-154.

LIN, W. H., KULKARNI, A. & MIRCHANDANI, P. (2006) Response to "comment on 'short-term arterial travel time prediction for advanced traveler information systems' by Wei-Hua Lin, Amit Kulkarni, and Pitu Mirchandani. *Journal of Intelligent Transportation Systems: Technology, Planning, and Operations,* 10**,** 45-47.

LIU, H., VAN ZUYLEN, H., VAN LINT, H. & SALOMONS, M. (2006) Predicting urban arterial travel time with state-space neural networks and Kalman filters. *Transportation Research Record.*

LOGENDRAN, R. & WANG, L. (2008) Dynamic travel time estimation using regression trees. *Project 304-351* Oregon Department of Transportation Research Unit and Federal Highway Administration http://www.oregon.gov/ODOT/TD/TP_RES/docs/Reports/2008/Dynamic_Travel_Time.pdf

LOWRIE, P. R. (1990) SCATS - Sydney Coordinated Adaptive Traffic System: A traffic responsive method of controlling urban traffic. *Sydney Co-ordinated Adaptive Traffic System*.

MARTIN, P. T. (1997) Turning movement estimation in real time. *Journal of Transportation Engineering,* 123**,** 252-260.

NAM, D. H. & DREW, D. R. (1999) Automatic measurement of traffic variables for intelligent transportation systems applications. *Transportation Research Part B: Methodological,* 33**,** 437-457.

NEWELL, G. F. (1982) *Applications of queueing theory* London New York - N.Y., Applications of queueing theory

NIST NIST/SEMATECH e-Handbook of Statistical Methods, http://www.itl.nist.gov/div898/handbook/, 13th February 2009.

OH, J. S., JAYAKRISHNAN, R. & RECKER, W. (2003) Section travel time estimation from point detection data. *In proceedings of the 82th Annual Meeting of Transportation Research Board.* Washington, D.C., U.S.A.

PARK, D. & RILETT, L. R. (1998) Forecasting multiple-period freeway link travel times using modular neural networks. *Transportation Research Record.*

PARK, D., RILETT, L. R. & HAN, G. (1999) Spectral basis neural networks for real-time travel time forecasting. *Journal of Transportation Engineering,* 125**,** 515-523.

PETTY, K. F., BICKEL, P., OSTLAND, M., RICE, J., SCHOENBERG, F., JIANG, J. & RITOV, Y. A. (1998) Accurate estimation of travel times from single-loop detectors. *Transportation Research Part A: Policy and Practice,* 32**,** 1-17.

RICE, J. & VAN ZWET, E. (2004) A simple and effective method for predicting travel times on freeways. *IEEE Transactions on Intelligent Transportation Systems,* 5**,** 200-207.

RICHARDS, P. I. (1956) Shockwaves on the highway. *Operations Research B,* 22**,** 81-101.

RITCHIE, S., PARK, S., OH, C., JENG, S.-T. & TOK, A. (2005) Field Investigation of Advanced Vehicle Reidentification Techniques and Detector Technologies - Phase 2. *California Partners for Advanced Transit and Highways (PATH). Research Reports: Paper prr-2005-8.*

http://repositories.cdlib.org/its/path/reports/prr-2005-8.

RITCHIE, S., PARK, S., OH, C. & SUN, C. (2002) Field Investigation of Advanced Vehicle Reidentification Techniques and Detector Technologies - Phase 1. *California Partners for Advanced Transit and Highways (PATH). Research Reports:UCB-ITS-PRR-2002-15.*

http://www.path.berkeley.edu/PATH/Publications/PDF/PRR/2002/PRR-2002-15.pdf.

ROBERTSON, D. I. & BRETHERTON, R. D. (1991) Optimizing networks of traffic signals in real time-the SCOOT method. *Vehicular Technology, IEEE Transactions on,* 40**,** 11-15.

ROBINSON, S. & POLAK, J. W. (2005) Modeling Urban Link Travel Time with Inductive Loop Detector Data by Using the k-NN Method. *Transportation Research Record,* 1935**,** 47-56.

ROSE, G. (2006) Mobile phones as traffic probes: Practices, prospects and issues. *Transport Reviews,* 26**,** 275-291.

SISIOPIKU, V. P. & ROUPHAIL, N. M. (1994a) Toward the use of detector output for arterial link travel time estimation: a literature review. *Transportation Research Record***,** 158-165.

SISIOPIKU, V. P. & ROUPHAIL, N. M. (1994b) Travel time estimation from loop detector data for Advanced Traveller Information Systems Application. *Technical Report, Illinois University Transportation Research Consortium.*

SISIOPIKU, V. P., ROUPHAIL, N. M. & SANTIAGO, A. (1994) Analysis of correlation between arterial travel time and detector data from simulation and field studies. *Transportation Research Record***,** 166-173.

SON, Y. T., CASSIDY, M. J. & MODANAT, S. M. (1995) Evaluating steady-state assumption for highway queueing system. *Journal of Transportation Engineering,* 121**,** 182-190.

SPIESS, H. (1990) Conical volume-delay functions. *Transportation Science,* 24**,** 153-158.

SRINIVASAN, K. K. & JOVANIS, P. P. (1996) Determination of number of probe vehicles required for reliable travel time measurement in urban network. *Transportation Research Record***,** 15-22.

STADTLUZERN (2008) http://www.stadtluzern.ch/.

STATHOPOULOS, A. & KARLAFTIS, M. G. (2003) A multivariate state space approach for urban traffic flow modeling and prediction. *Transportation Research Part C: Emerging Technologies,* 11**,** 121-135.

SUN, C. (2000) An investigation in the use of inductive loop signatures for vehicle classification *UCB-ITS-PRR-2000-4 PATH Research Report, March 2000* California.

SUN, C. & RITCHIE, S. G. (1999) Individual vehicle speed estimation using single loop inductive waveforms. *UCB-ITS-PWP-99-14 PATH Working Paper* California.

TAKABA, S., TAKABA, S., MORITA, T., HADA, T., USAMI, T. A. U. T. & YAMAGUCHI, M. A. Y. M. (1991) Estimation and measurement of travel time by vehicle detectors and license plate readers. IN MORITA, T. (Ed.) *Vehicle Navigation and Information Systems Conference, 1991*.

THOMAS, N. E. (1998) Multi-state and multi-sensor incident detection systems for arterial streets. *Transportation Research Part C: Emerging Technologies,* 6**,** 337-357.

TISATO, P. (1991) Suggestions for an improved Davidson travel time function. *Australian road research,* 21**,** 85-100.

TRB (1998) Highway Capacity Manual, Special Report 209. Washington D.C., National Research Council.

TRB (2000) Highway Capacity Manual. IN BOARD, T. R. (Ed.). Washington, D.C., National Research Council.

TSEKERIS, T. (2006) Comment on ‘‘Short-Term Arterial Travel Time Prediction for Advanced Traveler Information Systems’’ by Wei-Hua Lin, Amit Kulkarni, and Pitu Mirchandani. *Journal of Intelligent Transportation Systems: Technology, Planning, and Operations,* 10**,** 41-43.

TURNER, S. M. & HOLDENER, D. J. (1995) Probe vehicle sample sizes for real-time information: the Houston experience. IN DAILEY DANIEL, J. & HASELKORN MARK, P. (Eds.) *Vehicle Navigation and Information Systems Conference (VNIS).* Seattle, WA, USA, IEEE.

VAN AERDE, M., HELLINGA, B., YU, L. & RAKHA, H. (1993) Vehicle probes as real-time ATMS sources of dynamic O-D and travel time data. *Large Urban Systems - Proc., ATMS Conf.***,** 207-230.

VAN LINT, J. W. C., HOOGENDOORN, S. P. & VAN ZUYLEN, H. J. (2005) Accurate freeway travel time prediction with state-space neural networks under missing data. *Transportation Research Part C: Emerging Technologies,* 13**,** 347-369.

VICS (2008) http://www.vics.or.jp/english/.

VLAHOGIANNI, E. I., GOLIAS, J. C. & KARLAFTIS, M. G. (2004) Short-term traffic forecasting: Overview of objectives and methods. *Transport Reviews,* 24**,** 533-557.

VS-PLUS (2008) http://www.vs-plus.com/e/vsintro.htm.

WARDROP, J. G. (1968) Journey speed and flow in central urban areas. *Traffic Engineering and Control,* 9**,** 528-532.

WEBSTER, F. V. & COBBE, B. M. (1966) *Traffic Signals*, Road Research Technical Paper No. 56, Her Majesty's Stationery Office, London, England.

WESTERMAN, M., LITJENS, R. & LINNARTZ, J.-P. (1996) Integration Of Probe Vehicle And Induction Loop Data: Estimation Of Travel Times And Automatic Incident

Detection. *California Partners for Advanced Transit and Highways (PATH). Research Reports: Paper UCB-ITS-PRR-96-13.* .

XIE, C., CHEU, R. L. & LEE, D. H. (2001) Calibration-free arterial link speed estimation model using loop data. *Journal of Transportation Engineering,* 127**,** 507-514.

XIE, C., CHEU, R. L. & LEE, D. H. (2004) Improving arterial link travel time estimation by data fusion. *83rd Annual Meeting of the Transportation Research Board*.

YANG, J. S. (2007) Application of the Kalman filter to the arterial travel time prediction: A special event case study. *Control and Intelligent Systems,* 35**,** 79-85.

YIM, Y. (2003) The State of Cellular Probes. *California Partners for Advanced Transit and Highways (PATH). Research Reports: Paper UCB-ITS-PRR-2003-25.* http://repositories.cdlib.org/its/path/reports/UCB-ITS-PRR-2003-25

YOU, J. & KIM, T. J. (2000) Development and evaluation of a hybrid travel time forecasting model. *Transportation Research Part C: Emerging Technologies,* 8**,** 231-256.

YOUNG, C. P. (1988) A relationship between vehicle detector occupancy and delay at signal-controlled junctions. *Traffic Engineering and Control,* 29**,** 131-134.

ZHANG, H. M. (1999) Link-journey-speed model for arterial traffic. *Transportation Research Record***,** 109-115.

ZHANG, X. & RICE, J. A. (2003) Short-term travel time prediction. *Transportation Research Part C: Emerging Technologies,* 11**,** 187-210.

APPENDIX A TRAFFIC INDUCTIVE LOOP DETECTORS

This appendix provides brief overview of inductive loop detectors-widely available traffic data collection systems. Interested readers can refer to Klein (2001) and Klein et al., (2006a, 2006b) for detailed overview of different traffic data collection systems.

A.1 Inductive loop detector (ILD)

Inductive loop detectors (ILD) as the name implies are loop detectors that apply the simple principle of induction to detect vehicle over them. For this multiple turns of induction wires in loops are embedded in the pavement and connected to a control device. The wires are excited by a signal ranging in frequency from 10 kHz to 200 kHz. When a vehicle passes over or rests on the loop then the metal in the vehicle generates eddy currents which reduce the induction of the loop. The decreased inductance causes the resonance frequency to increase from its normal value. Traditionally, if the frequency change exceeds the threshold set by the sensitivity setting then the presence of a vehicle is defined.

Loop detector devices are presence type i.e., provide ‘1’ (on) and ‘0’ (off) information for the vehicle presence. In practice, both single and dual loop detectors are used. Single loop detectors can only provide the counts (flow) and occupancy. Most of the actuated signal controllers utilize single loop detectors. Dual loop detectors are mainly installed on freeways and consist of two single loop detectors on a short distance from each other on the same link. These detectors can also provide the speed considering the time difference between the signals produced between first and second loop.

A.1.1 DETECTOR ERROR

Data from detectors are generally accurate in free-flow conditions but less accurate when lane discipline is poor and when traffic is congested. Following are some of the reasons for overcounting and/or undercounting from the detector:

i. *Cross-talk*: primarily occur when one inductive loop (*A*) activates another loop detector (*B*) in adjacent lane or nearby. This leads to false detection of vehicle in loop *B*. For instance, say loop *A* and *B* are in adjacent lane, and when vehicle passes over loop *A*, then it changes the magnetic field of loop *A* which can interfere with the magnetic field of loop *B* and causing a false change in induction of loop *B*.

   The remedy for cross-talk includes: setting minimum spacing (at least 2 m) between the two adjacent detectors; different frequency settings for adjacent detectors; different number of turns in the loop for instance 3 turns in one and 4 turns in other etc.

ii. *Pulse break up*: involves gaps in detector actuation data, which may be incorrectly interpreted as different vehicles.

iii. *Closely spaced vehicle*: If the spacing between the vehicles is low for instance, during congested conditions then two consecutive vehicles may not be differentiated, resulting in detector undercounting.

iv. *Hanging (on or off)*: Detector may be malfunctioning and showing same value for a longer time period.

Most of the above issues can be addressed by data filter such as:

i. Pulses or gaps less than certain threshold can be ignored.

ii. Comparing detector *on* time with average *on* time of all the other detectors in the station.

iii. Comparing detector data against realistic threshold at regular time intervals.

A.2 Advanced loop detectors

The actual inductance curve produced by the vehicle passing by is not a simple peak. Due to complicated arrangement of metal part on the vehicle there are different sets of induction changes when the vehicle passes on the detector.

Advance detector data acquisition system for instance, digitizing the detector output and applying advance signal processing algorithms can provide key features of the vehicle's characteristics and behavior, rather than simply defining vehicle presence when the inductance change exceeds the threshold. These detectors can also be terms as *smart loop detectors* and are able to separate vehicles as well as measure their number of axles, vehicle type, speed and direction of movement. These detectors are often used in conjunction with automatic vehicle classification technology. These detectors can be used for vehicle reidentification and travel time measurements using pairs of loop detectors (*Refer to* Section 2.2.8).

A.3 Detector location on urban environment

In urban environment detectors are traditionally used for signal control, therefore their location on an urban link is primarily determined by the type of the signal controller. SCATS requires stop-line detectors where as SCOOTS requires detectors at the up-stream of the link. Certain Public Transport Priority Systems (PTPS) requires detectors at the mid-link. On an urban link there can be several combinations of different detector positions.

A combination of detectors at the survey site described in Section 6.2 (Lucerne City), in order of their position from the stop-line is as follows:

i. *Stop-line detectors*: are just before or after the stop-line marking at the intersection. They are 1.5 ~ 2 m in length.

ii. *Strategic detectors*: are slightly upstream of the stop-line and are 12 m in length. These detectors detect the queue and are not good for vehicle counts due to their longer lengths.

iii. *Call detectors*: They are approximately 60 m upstream of the stop-line and are 1.5 ~ 2 m in length. These detectors are used to define green-signal call for PTPS.

iv. *Traffic-jam detectors*: These detectors are near to up-stream entrance of the link and are of 5 m in length. Traffic-jam detectors as the name implies detect the queue extending to the up-stream entrance of the link.

APPENDIX B

DERIVATION OF AN EQUATION FOR ASSUMED DEMAND PATTERN

Following derivation is for the equation (3.4) (Chapter 3, section 3.2.3.1) for defining the proportions of counts during green phase in saturation flow pattern (n/N). Refer to Figure B-1, here:

N: is counts during green phase;

n: counts in saturation flow rate;

N_{max}: is the maximum counts during green phase, i.e., counts if flow is at saturation flow rate;

s: saturation flow rate;

g, *r* and *C*: are signal green time, red time and signal cycle length, respectively.

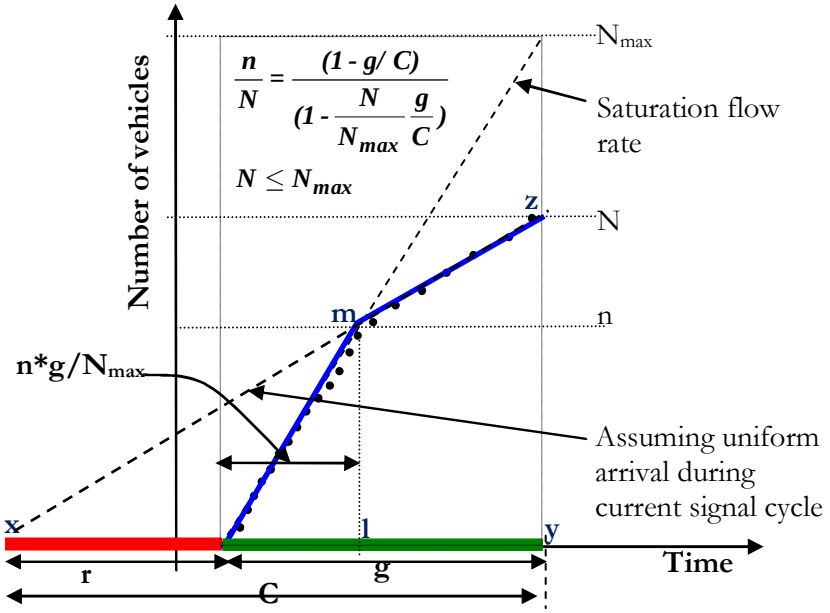

Figure B-1: Geometrical relationship between n and N, assuming uniform arrival during the current signal cycle.

$$N_{max} = (s * g);$$

If X < 1:

$$\Delta xyz \sim \Delta xlm \ (Similar\ Triangles);$$

$$\therefore \frac{yz}{xy} = \frac{lm}{xl}$$

$$\frac{N}{C} = \frac{n}{r + n * g / N_{max}}$$

$$\frac{n}{N}(1 - \frac{N}{N_{max}} * \frac{g}{C}) = (1 - g/C)$$

$$\frac{n}{N} = \frac{(1 - g/C)}{(1 - \frac{N}{N_{max}}\frac{g}{C})}$$

The developed relationship between n/N; N/N_{max} and g/C is presented in Figure B-2.

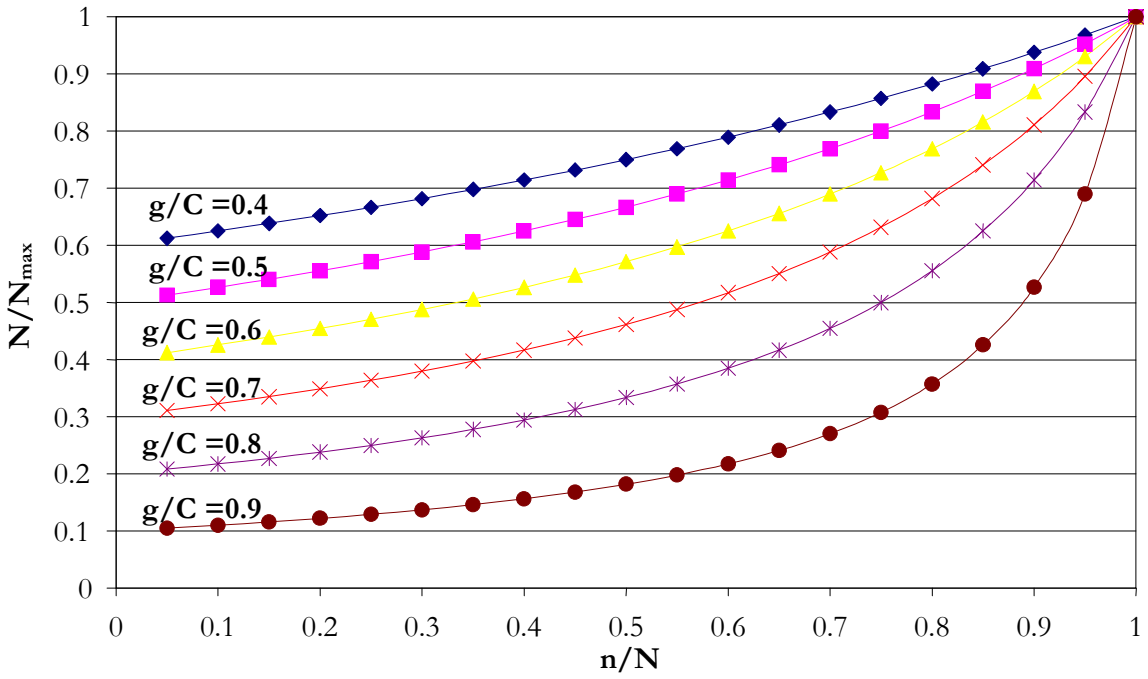

Figure B-2: Relationship between n/N; N/N_{max} and g/C for different counts and green split.

APPENDIX C AIMSUN

The appendix provides short introduction to AIMSUN. For detailed discussion refer to the user manual of AIMSUN.

AIMSUN is abbreviation for Advanced Interactive Microscopic Simulator for Urban and Non-Urban Networks. AIMSUN is a microscopic traffic simulator and the basic structure is as follows: Vehicles enter the network at network entry points and their movements through the network are determined by behavioral models such as, car following, lane changing, and gap acceptance. Each vehicle is assigned a set of vehicle and driver attributes which are used by the behavioral models to model the vehicle movement.

AIMSUN can function as either a stochastic model, where vehicles travel through the network based on turn probabilities, or a traffic assignment model using Origin Destination tables. It can also consider dynamic traffic assignment, where optimum vehicle paths between centroids are computed at the beginning of the simulation and then updated based on feedback from the network. Thus, route choice is based on actual traffic conditions and may vary at different points in the simulation.

The input to the AIMSUN simulator includes simulation scenario and set of simulation parameters that define the experiment. The scenario is composed of four types of data: network description, traffic control plan, traffic demand data and public transport plans. The simulation parameters are: fixed values that describe the experiment such as, simulation time, warm-up period, statistics interval, etc.; and variable parameters used to calibrate the models such as reaction times, lane changing zone, etc.

AIMSUN can provide continuous animated graphical representation of traffic network performance, statistical output data (flow, speed, journey times, delays, stops) and data gathered by the simulated detectors (counts, occupancy, speed). In addition, the software provided API access through which detailed traffic dynamics during simulation can be obtained and controlled as required by user.

Note: The results from a simulation model are reliable only when its parameters are properly calibrated for real world representation of traffic and its behavior. It is important that the

simulation model outputs are validated with field data. Properly calibrated simulation model has the potential to provide data for different traffic scenarios and hence can be used for number of traffic analysis and research purposes.

APPENDIX D RESULTS FROM CUPRITE TESTING

The results illustrated in this appendix are supplement to those presented in Chapter 4.

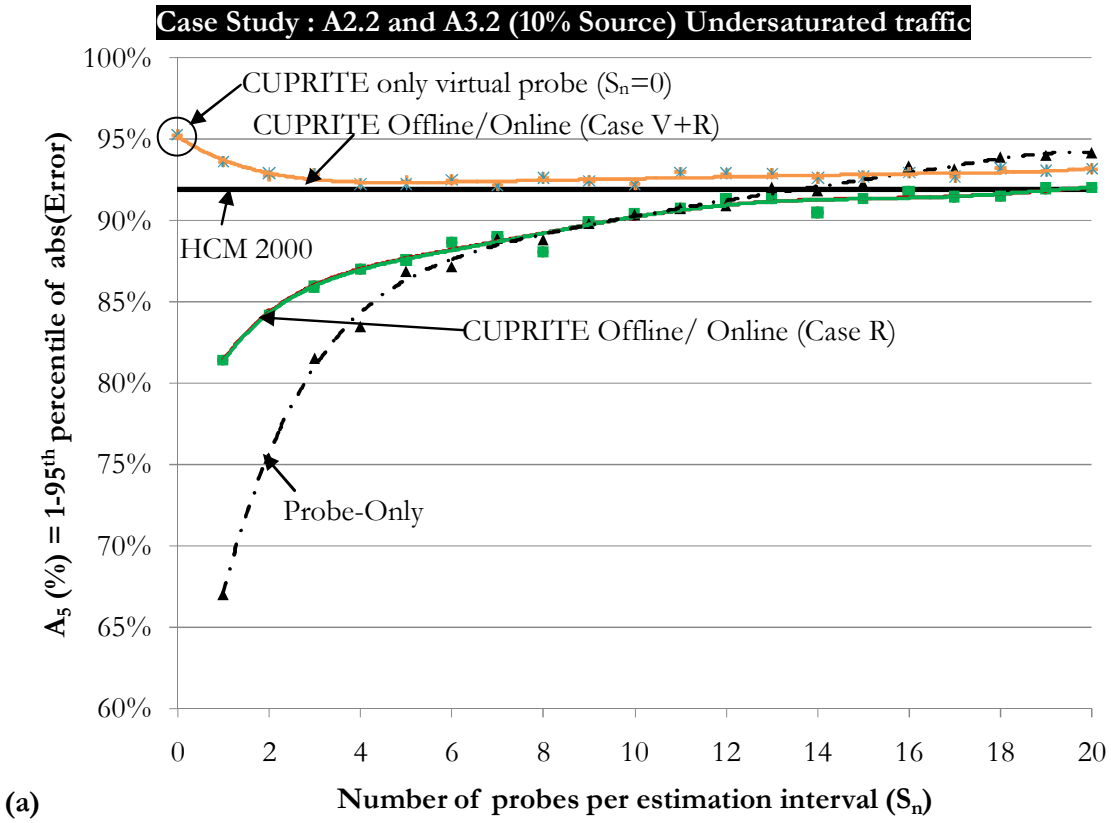

(a)

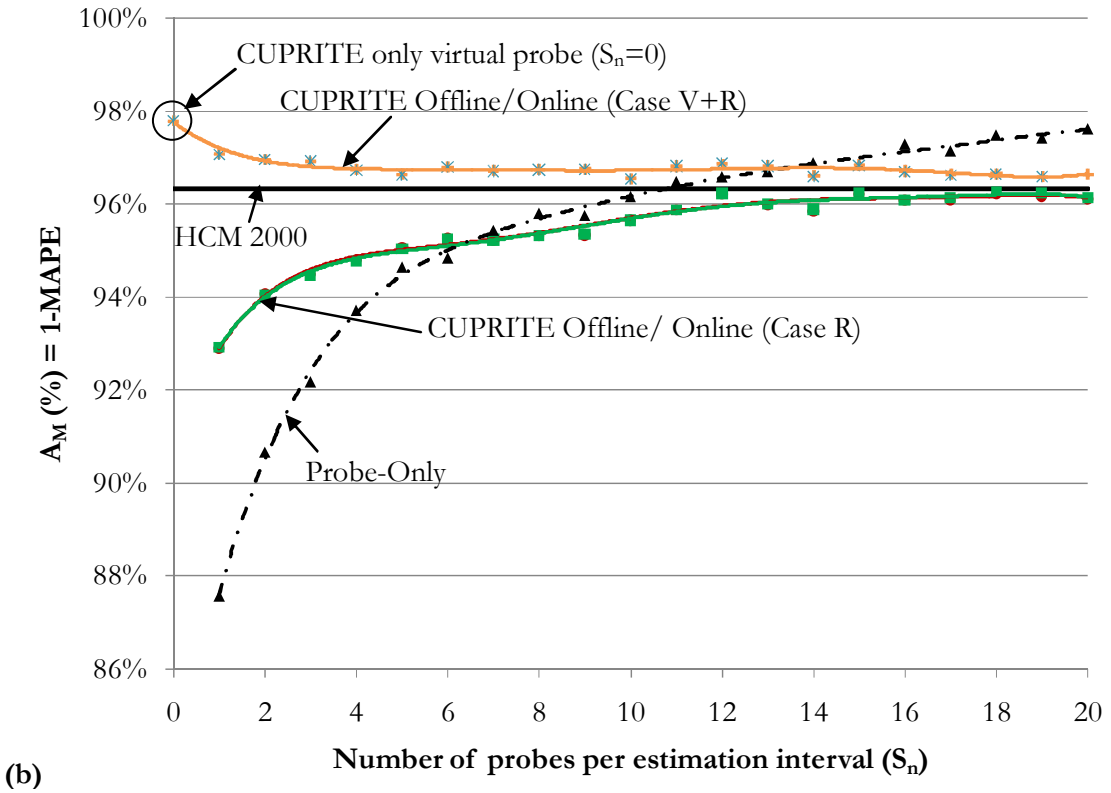

(b)

Figure D-1: Comparative results for 10% mid-link source during undersaturated traffic condition. Results for accuracy: (a) A_5 and (b) A_M versus S_n.

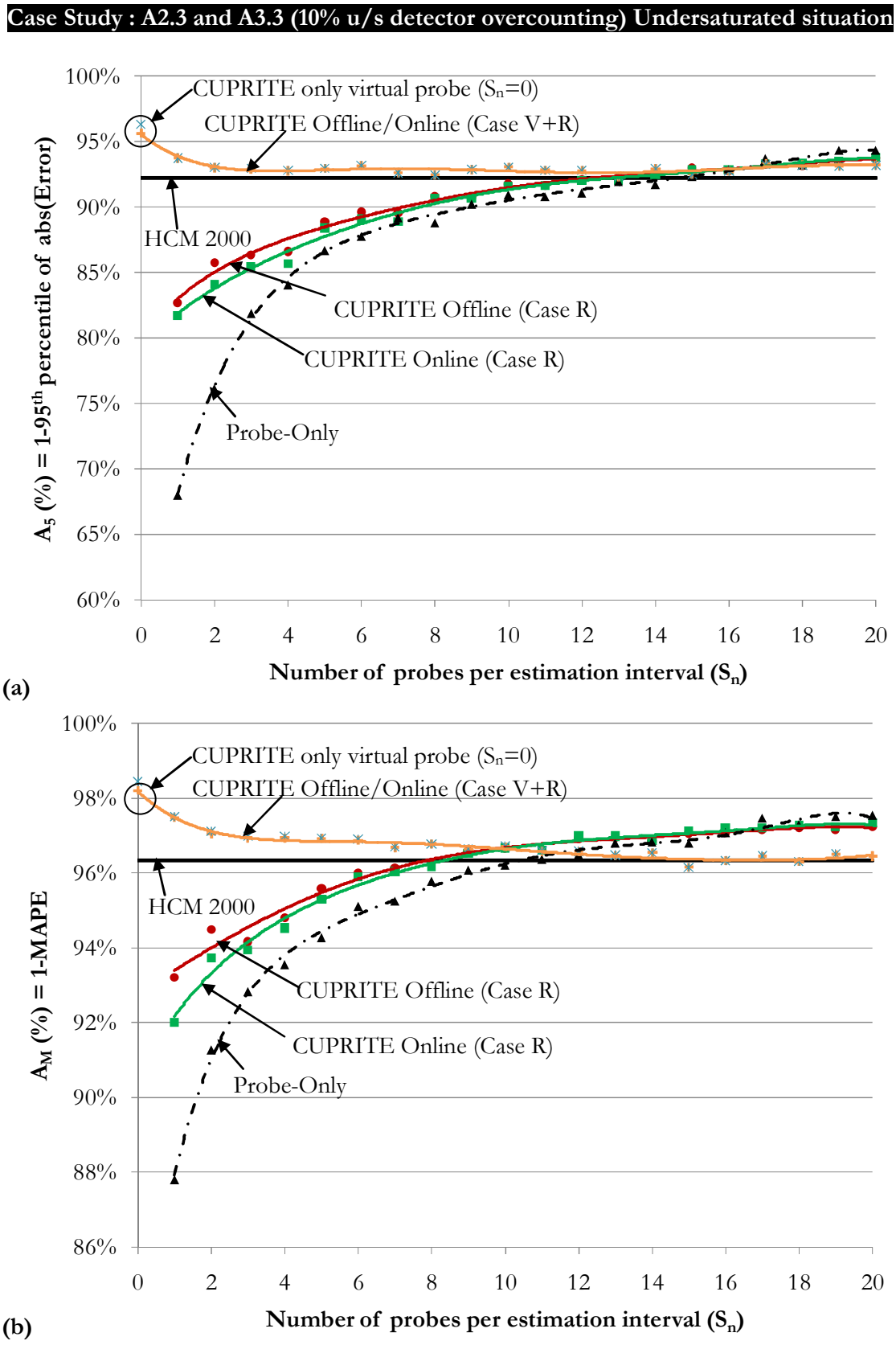

Figure D-2: Comparative results for 10% upstream detector overcounting during undersaturated traffic condition. Results for accuracy: (a) A_5 and (b) A_M versus S_n.

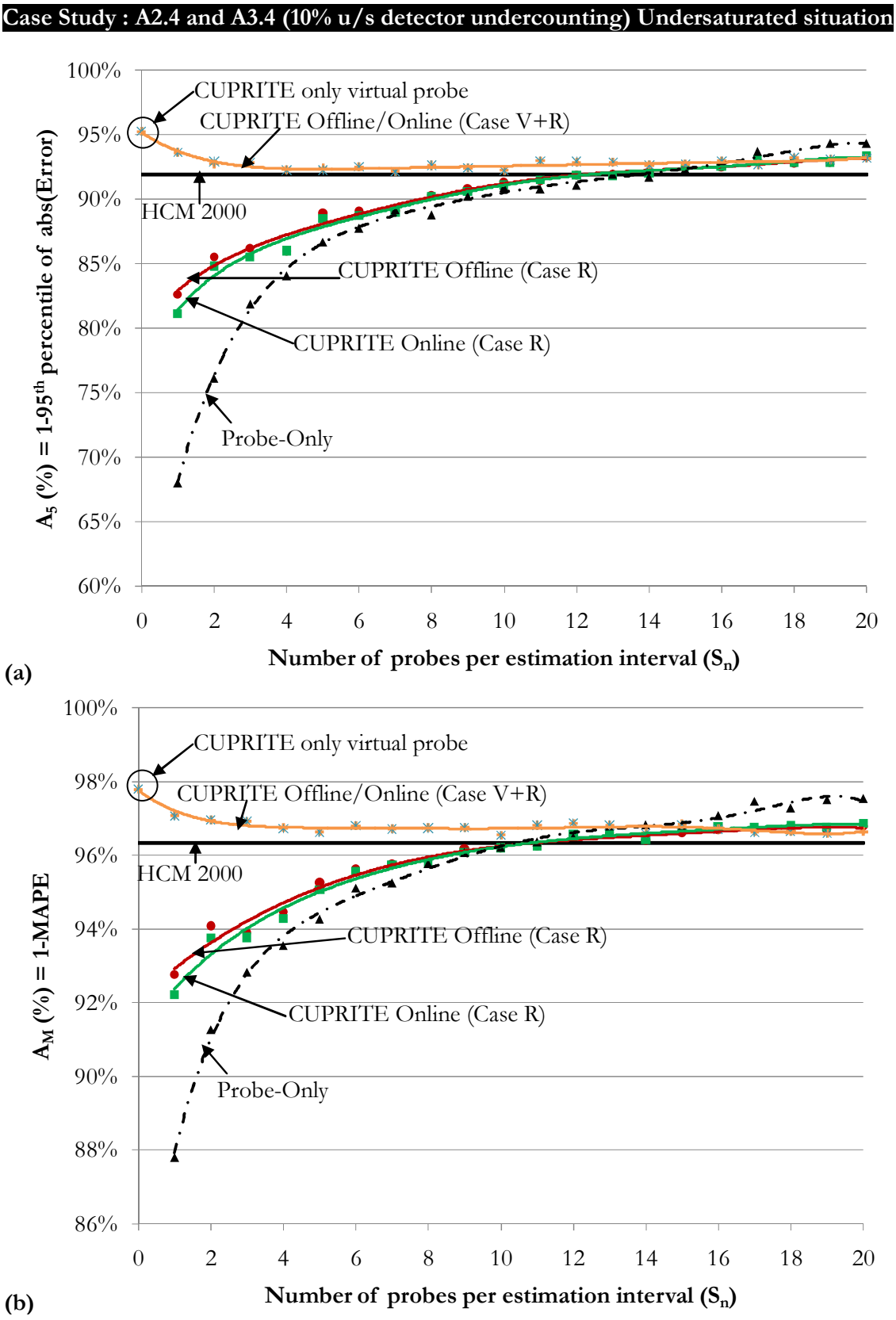

Figure D-3: Comparative results for 10% upstream detector undercounting case during undersaturated traffic condition. Results for accuracy: (a) A_5 and (b) A_M versus S_n.

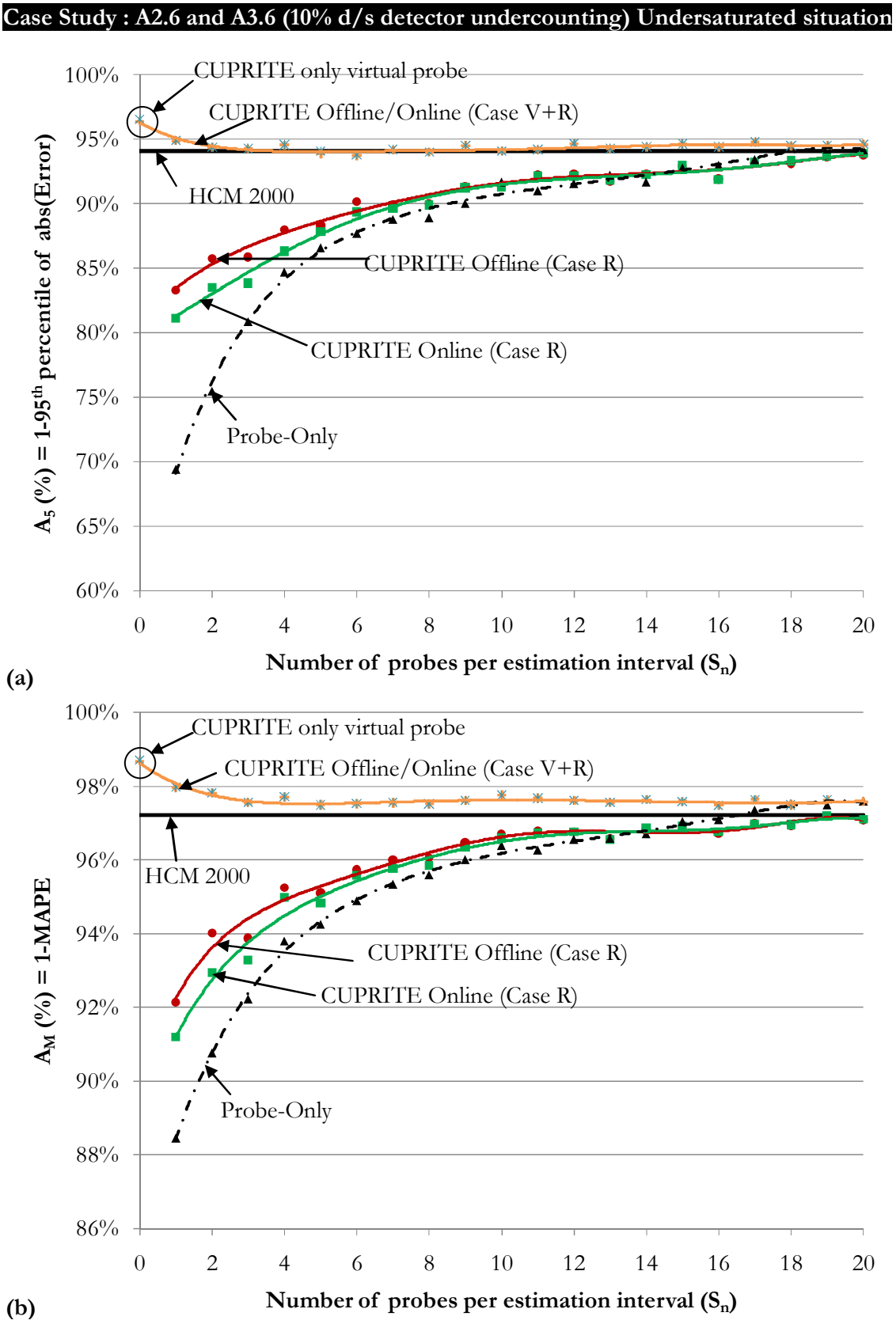

Figure D-4: Comparative results for 10% downstream detector undercounting case during undersaturated traffic condition. Results for accuracy: (a) A_5 and (b) A_M versus S_n.

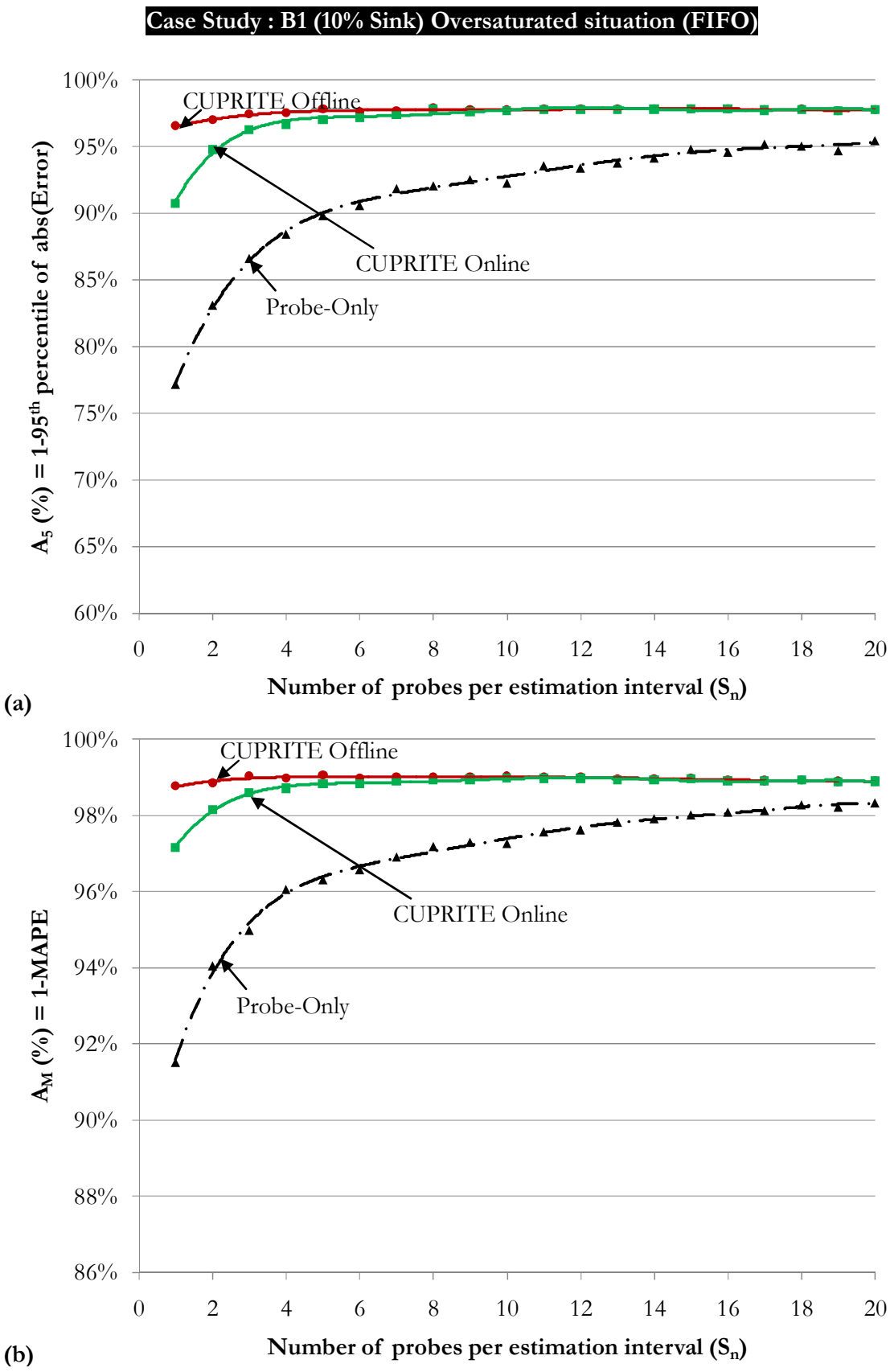

Figure D-5: Case B1 (10% sink) oversaturated traffic condition for FIFO discipline. Results for accuracy: (a) A_5 and (b) A_M versus S_n.

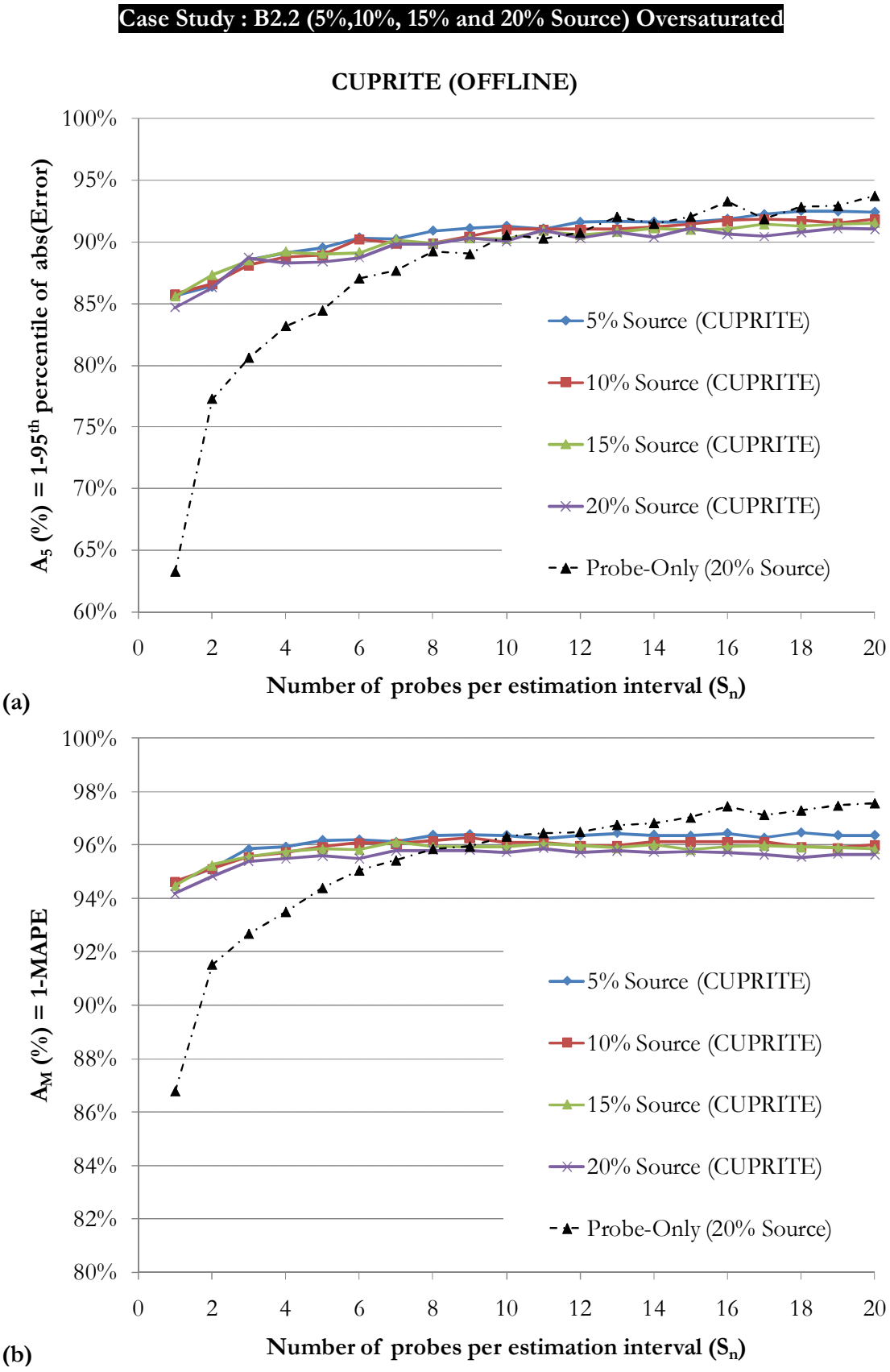

Figure D-6: CUPRITE Offline application for different source percentages (5%, 10%, 15% and 20%); oversaturated traffic condition; non-FIFO discipline. Results for accuracy: (a) A_5 and (b) A_M versus S_n.

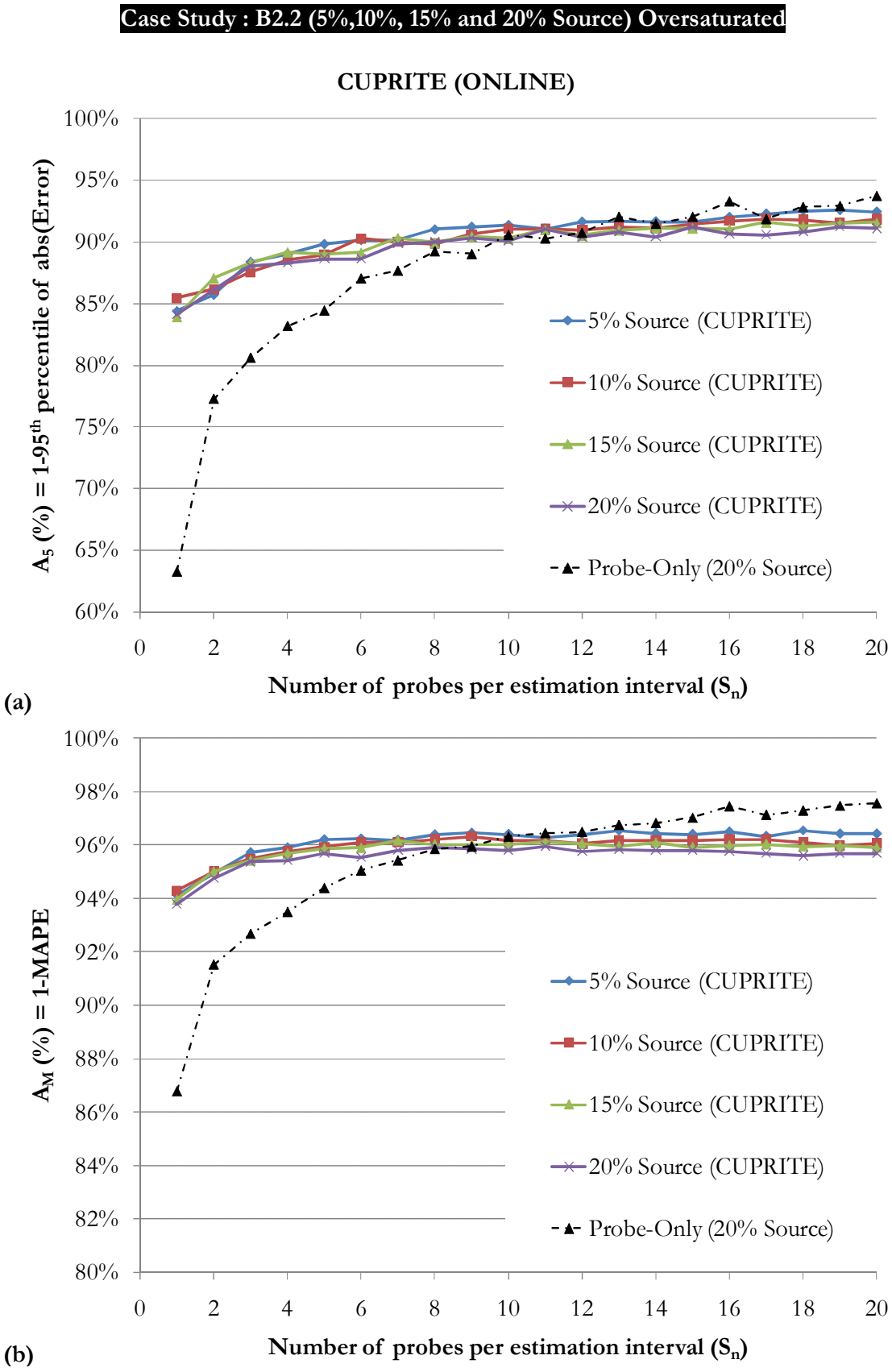

Figure D-7: CUPRITE Online application for different source percentages (5%, 10%, 15% and 20%); oversaturated traffic condition; non-FIFO discipline. Results for accuracy: (a) A_5 and (b) A_M versus S_n.

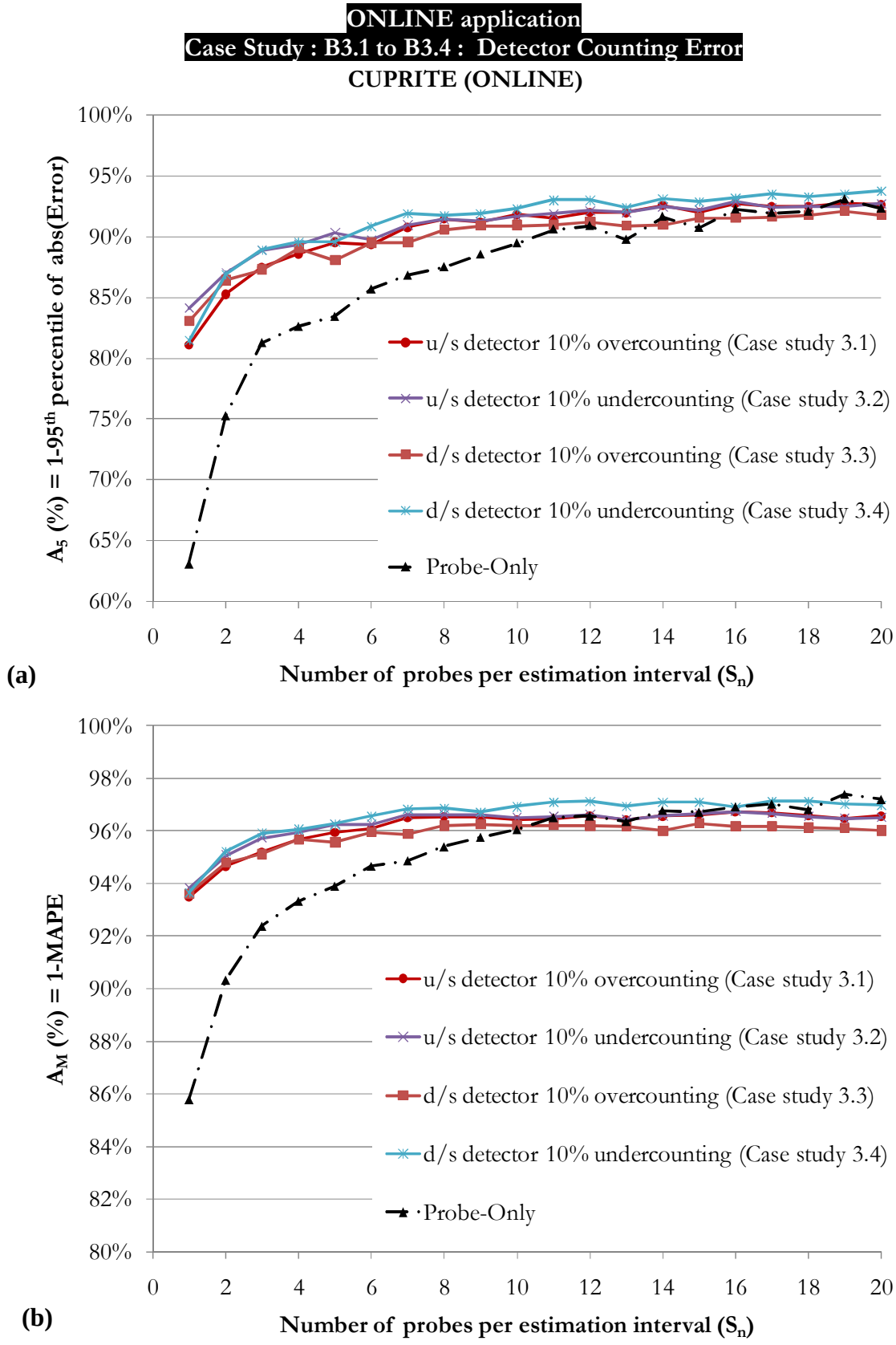

Figure D-8: Detector counting error with fixed number of probes per estimation interval (S_n) for Online application: Case B3. 1 to B3.4: (a) A_5 and (b) A_M versus S_n.

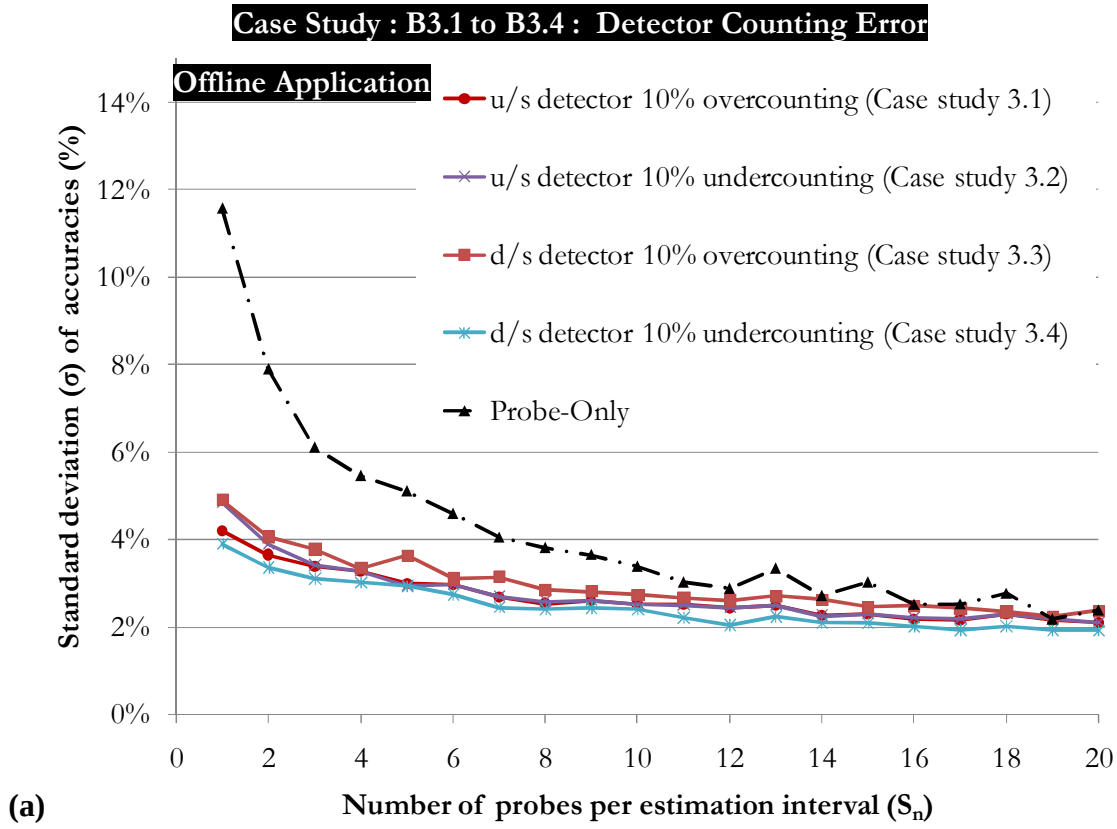

(a)

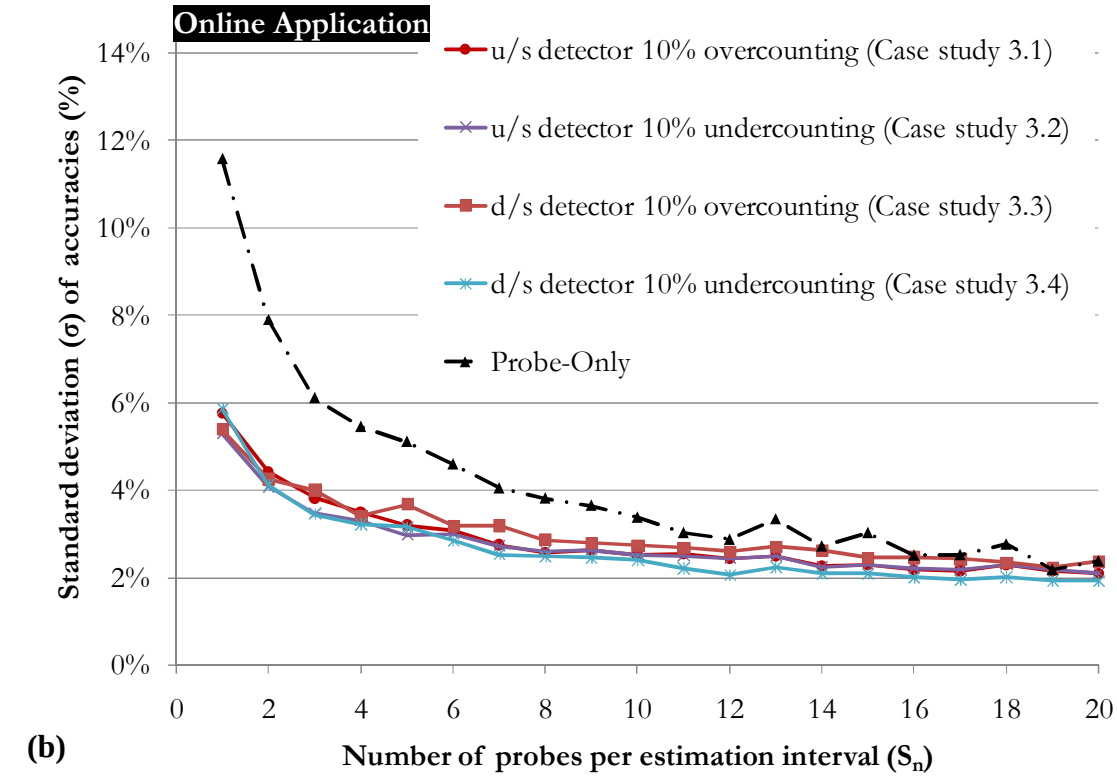

(b)

Figure D-9: Reliability of the estimate for case study (B3.1 to B3.4) on detector counting error with fixed number of probes per estimation interval (S_n) for a) Offline application and b) Online application.

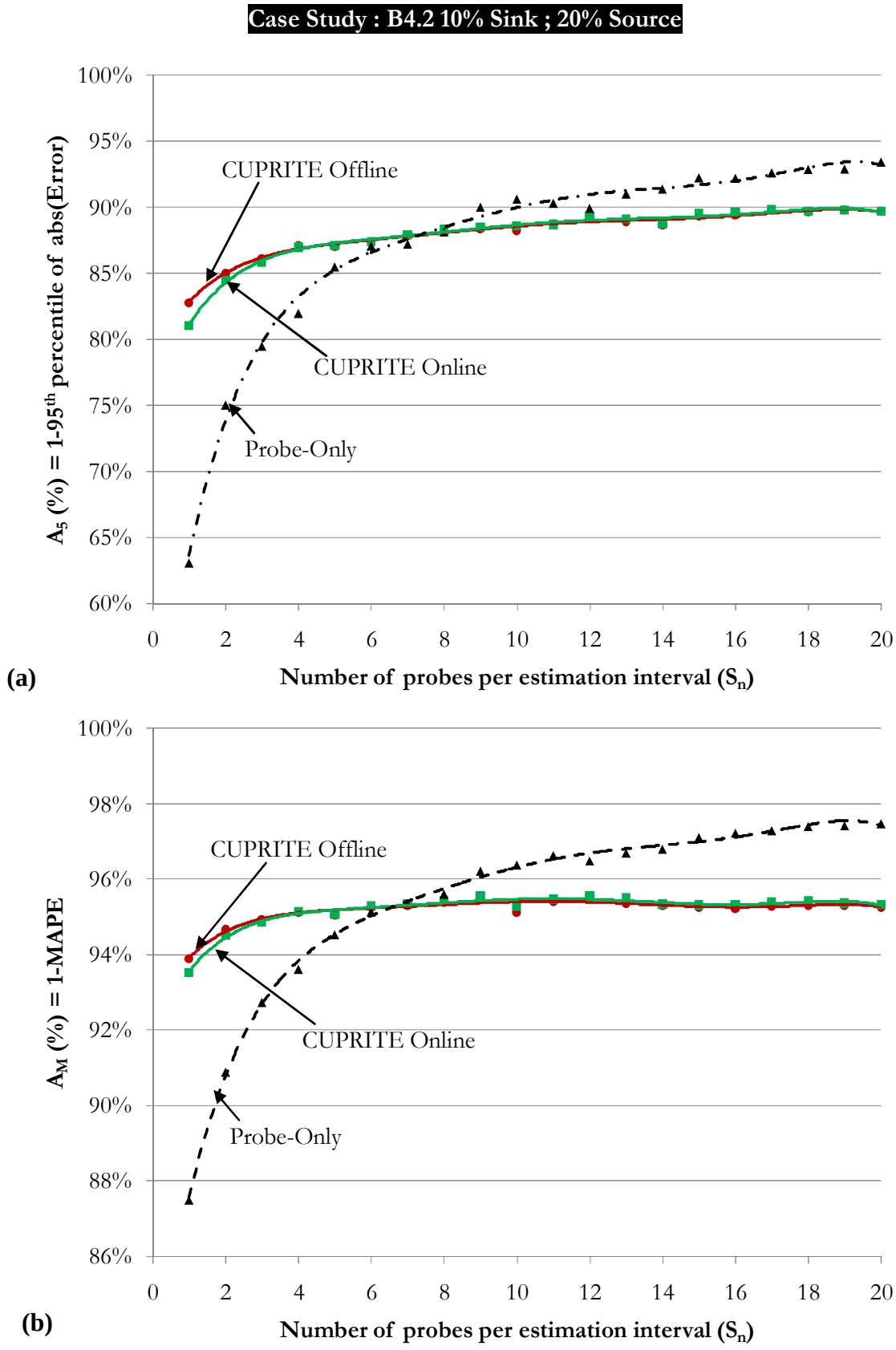

Figure D-10: Simultaneous presence of both sink and source. Case B4.2 (10% sink and 20% source): (a) A_5 and (b) A_M versus S_n.

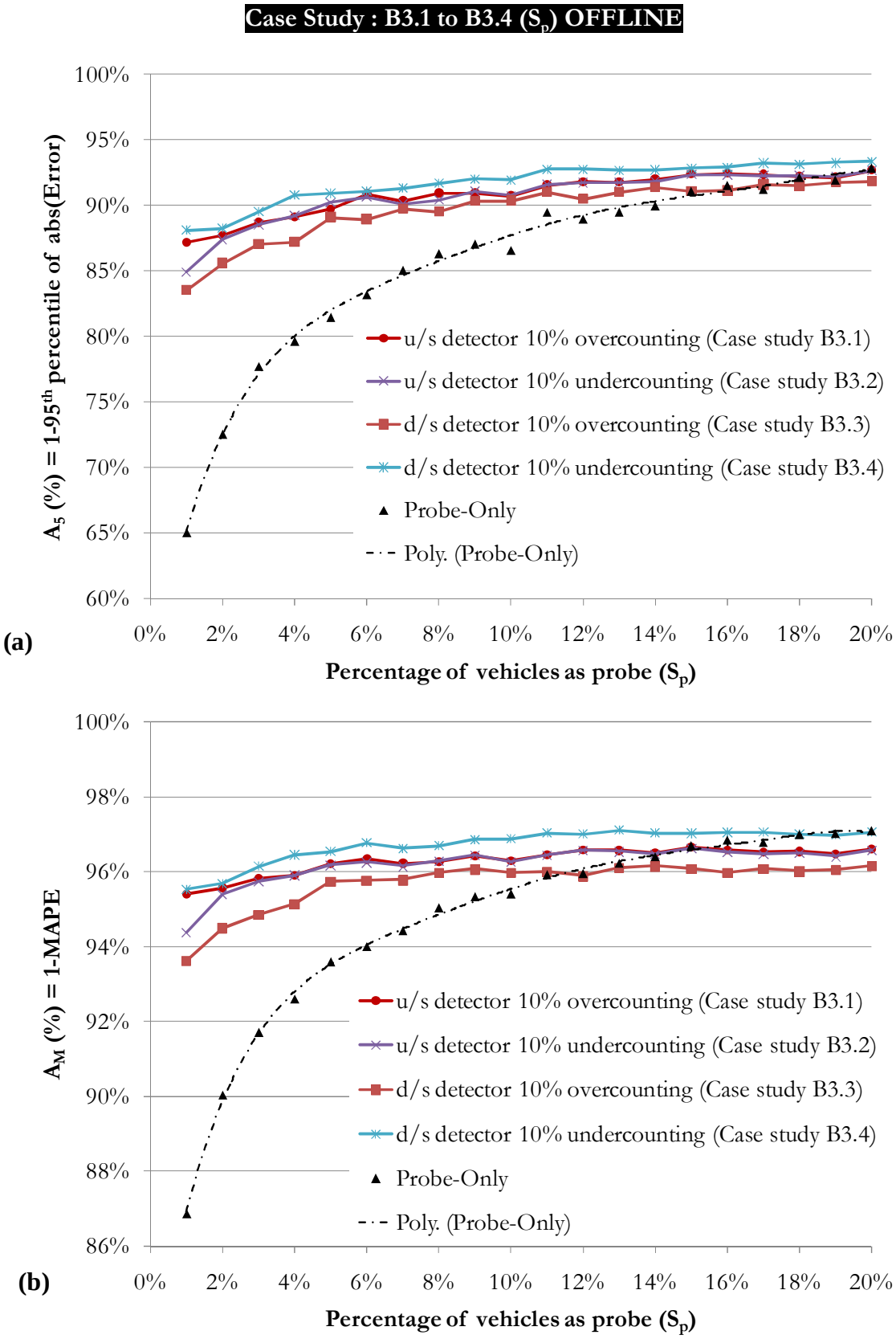

Figure D-11: Results for accuracy versus S_p case B3.1 to case B3.4 from CUPRITE offline application.

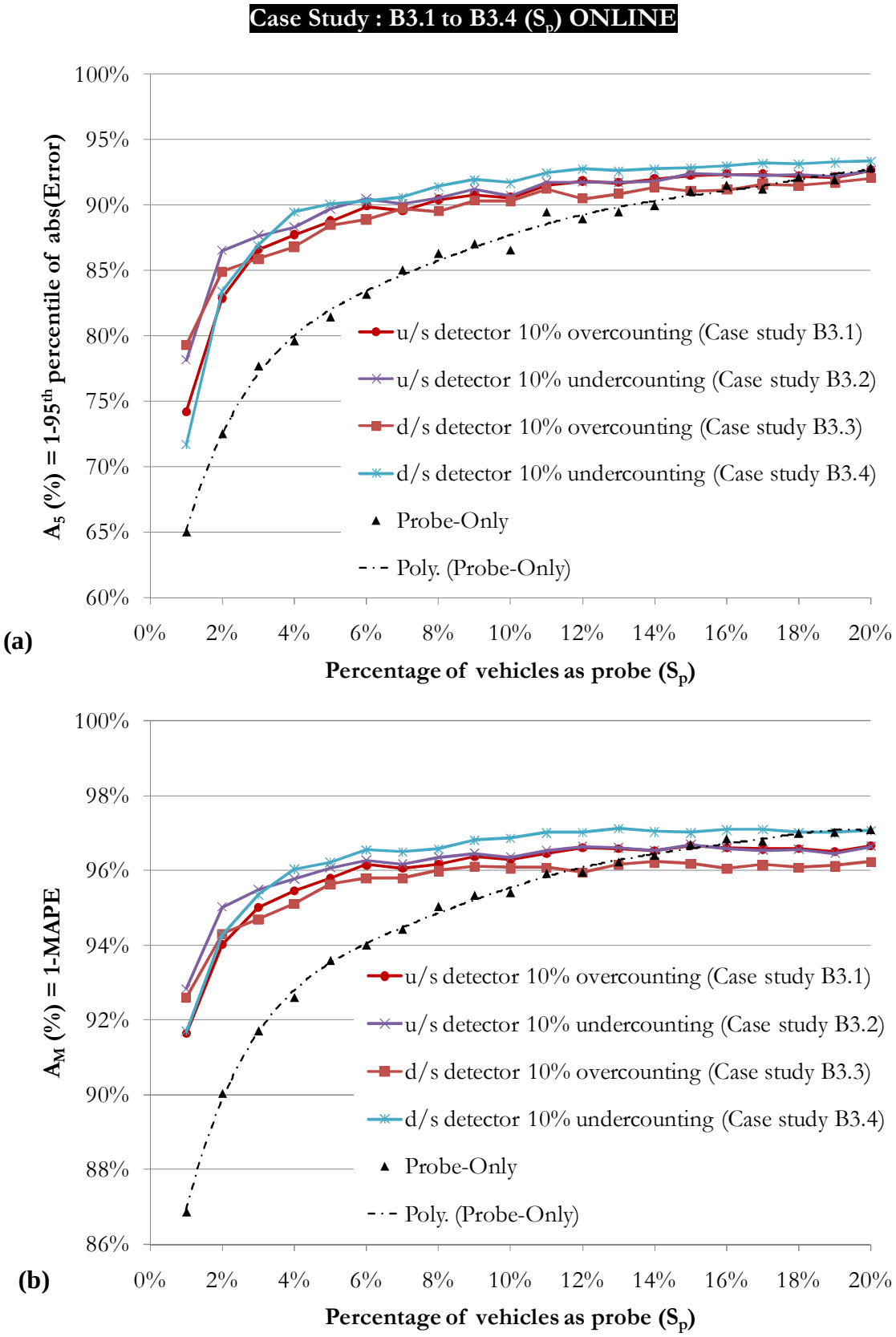

Figure D-12: Results for accuracy versus S_p case B3.1 to case B3.4 from CUPRITE online application.

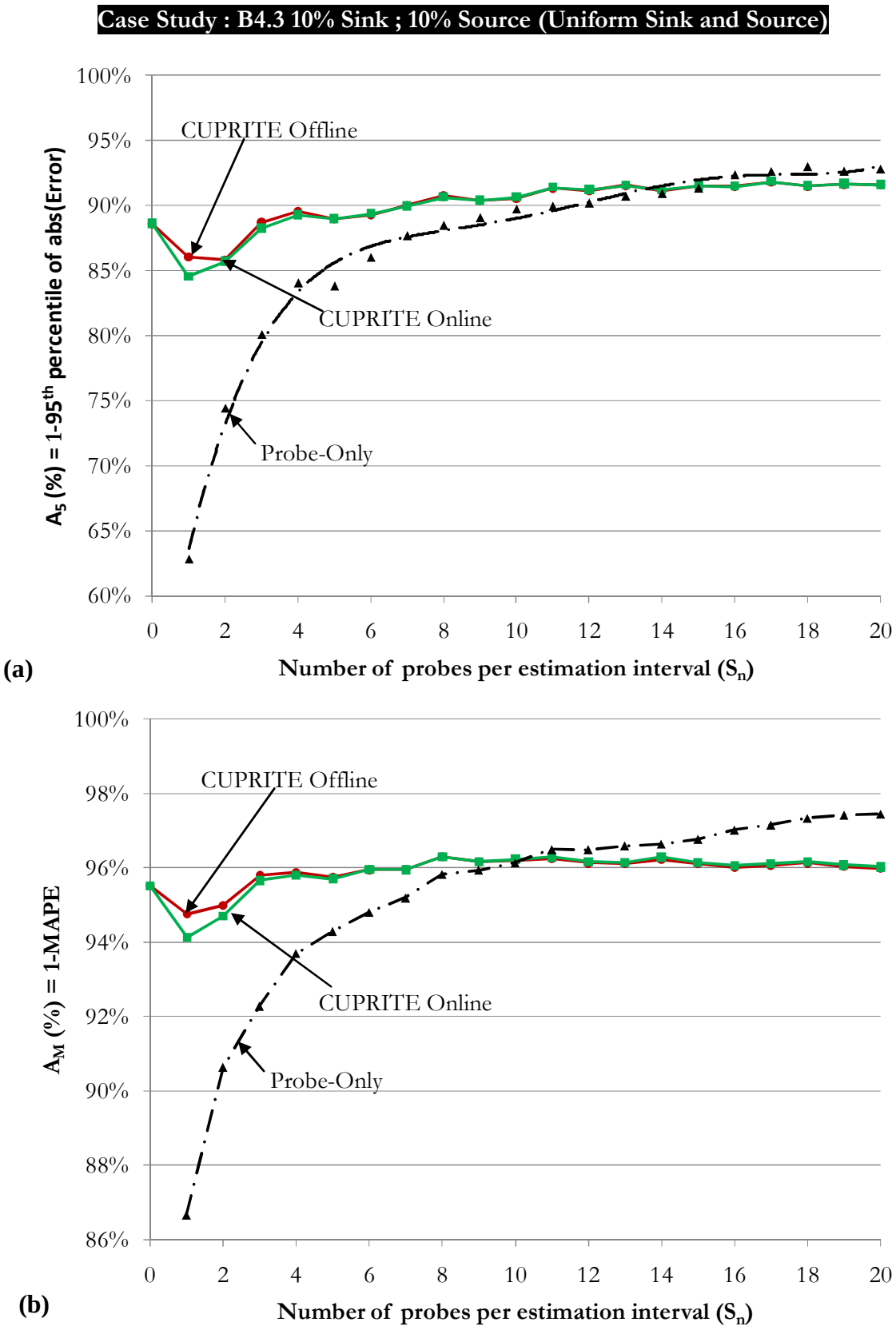

Figure D-13: Simultaneous presence of both sink and source. Case B4.3 (10% sink and 10% source): (a) A_5 and (b) A_M versus S_n.

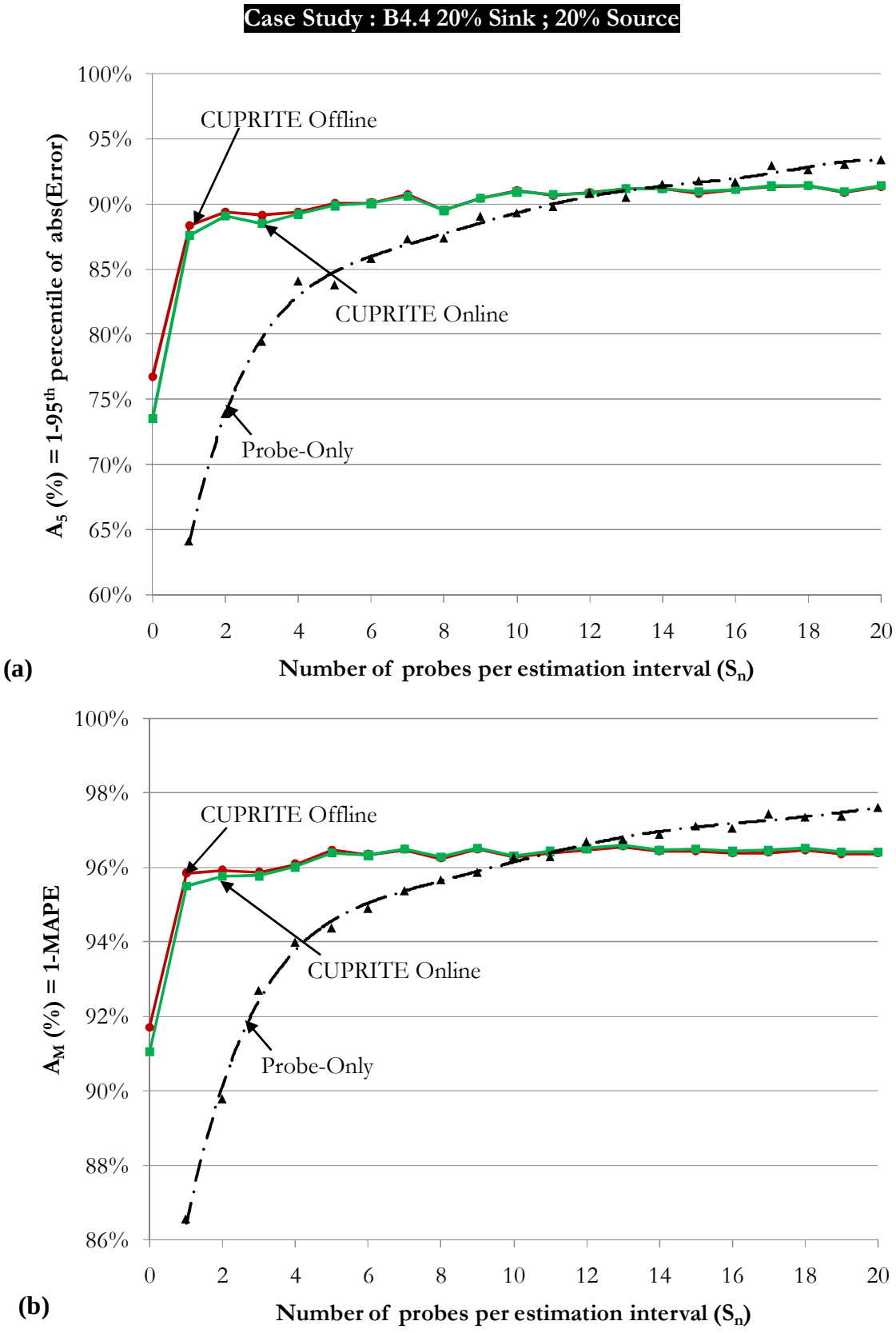

Figure D-14: Simultaneous presence of both sink and source. Case B4.4 (20% sink and 20% source): (a) A_5 and (b) A_M versus S_n.

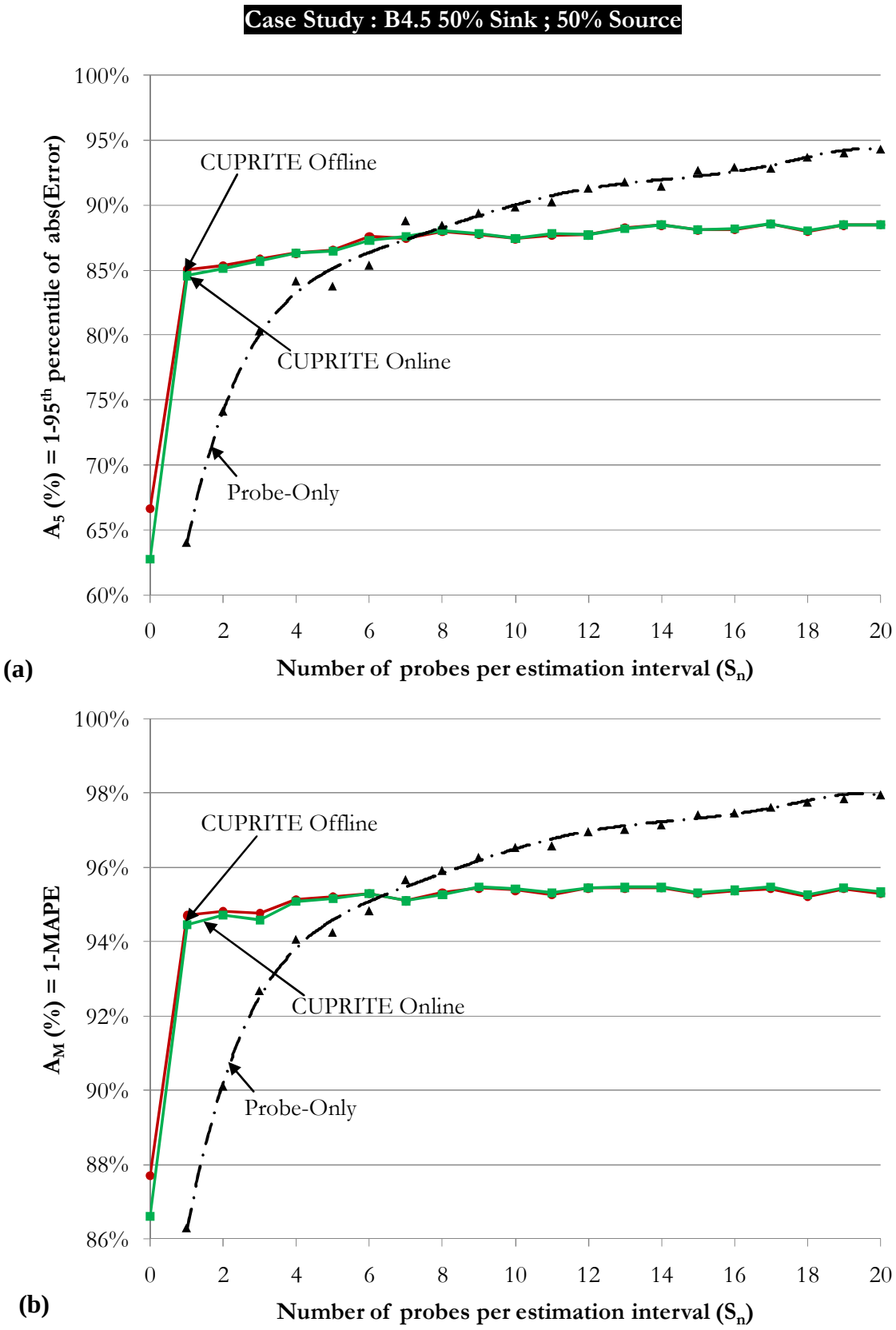

Figure D-15: Simultaneous presence of both sink and source. Case B4.5 (50% sink and 50% source): (a) A_5 and (b) A_M versus S_n.

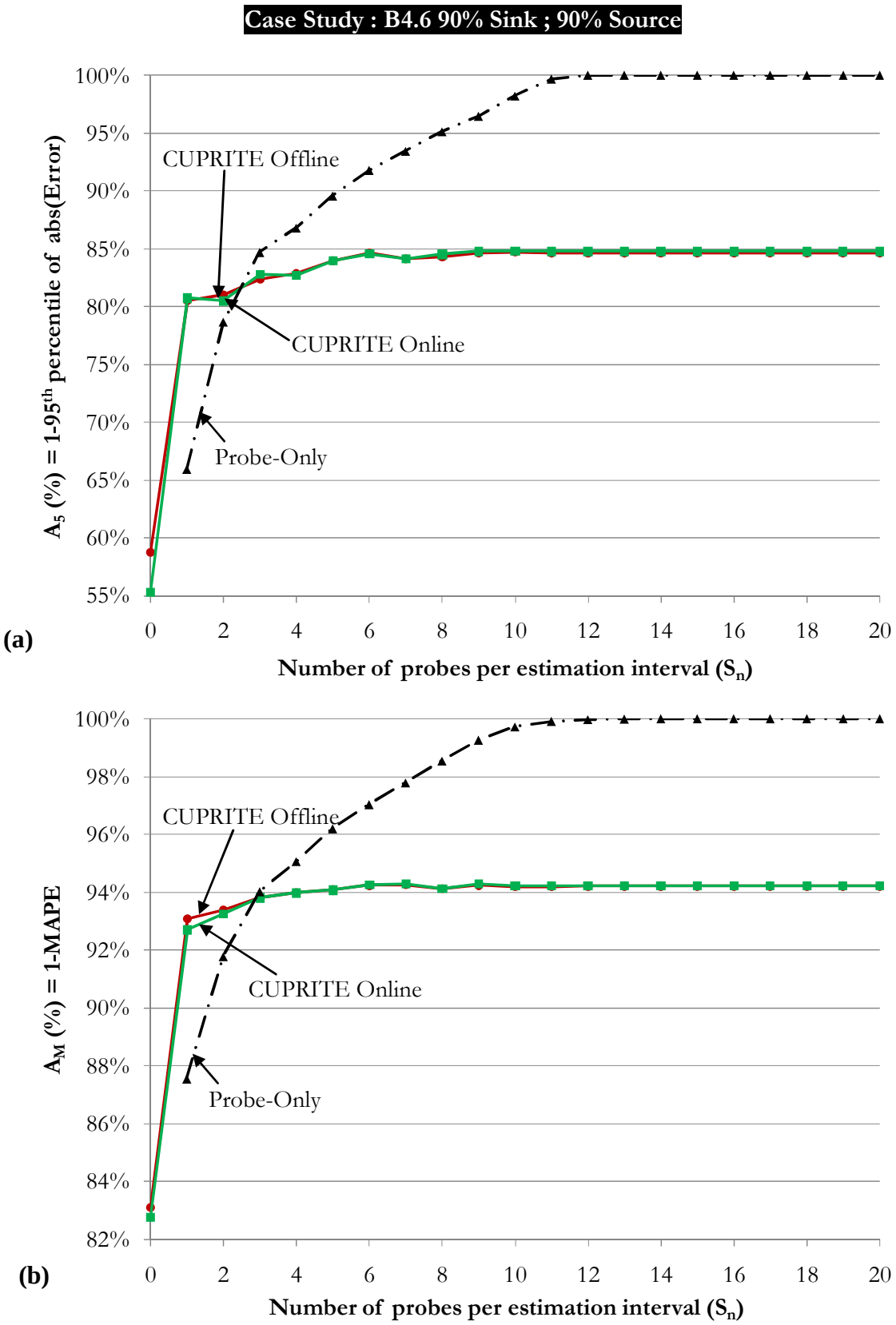

Figure D-16: Simultaneous presence of both sink and source. Case B4.6 (90% sink and 90% source): (a) A_5 and (b) A_M versus S_n.

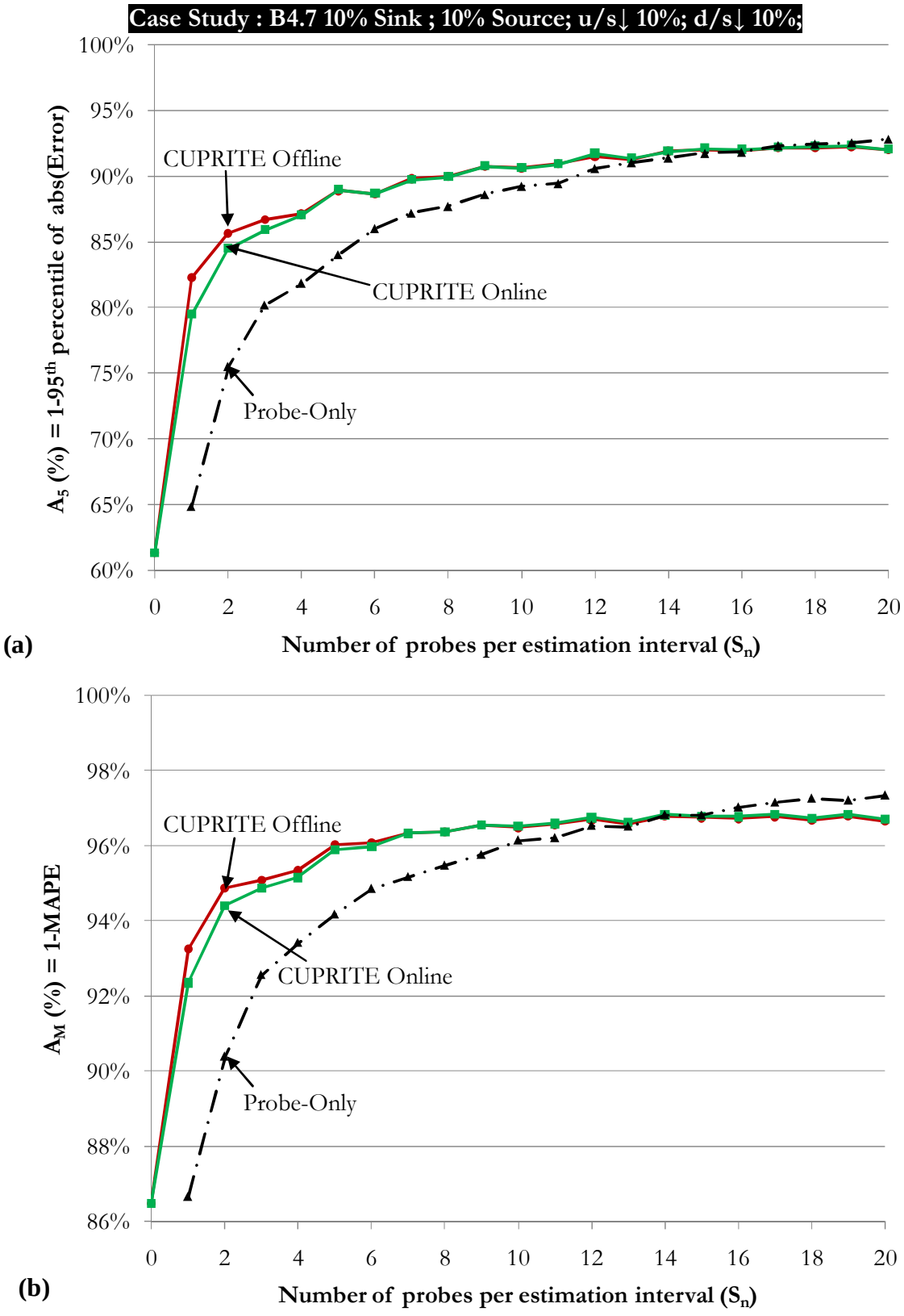

Figure D-17: Simultaneous presence of sink, source and detector counting error. Case B4.7 (10% sink; 10% source; both u/s and d/s detectors undercounting by 10%): (a) A_5 and (b) A_M versus S_n.

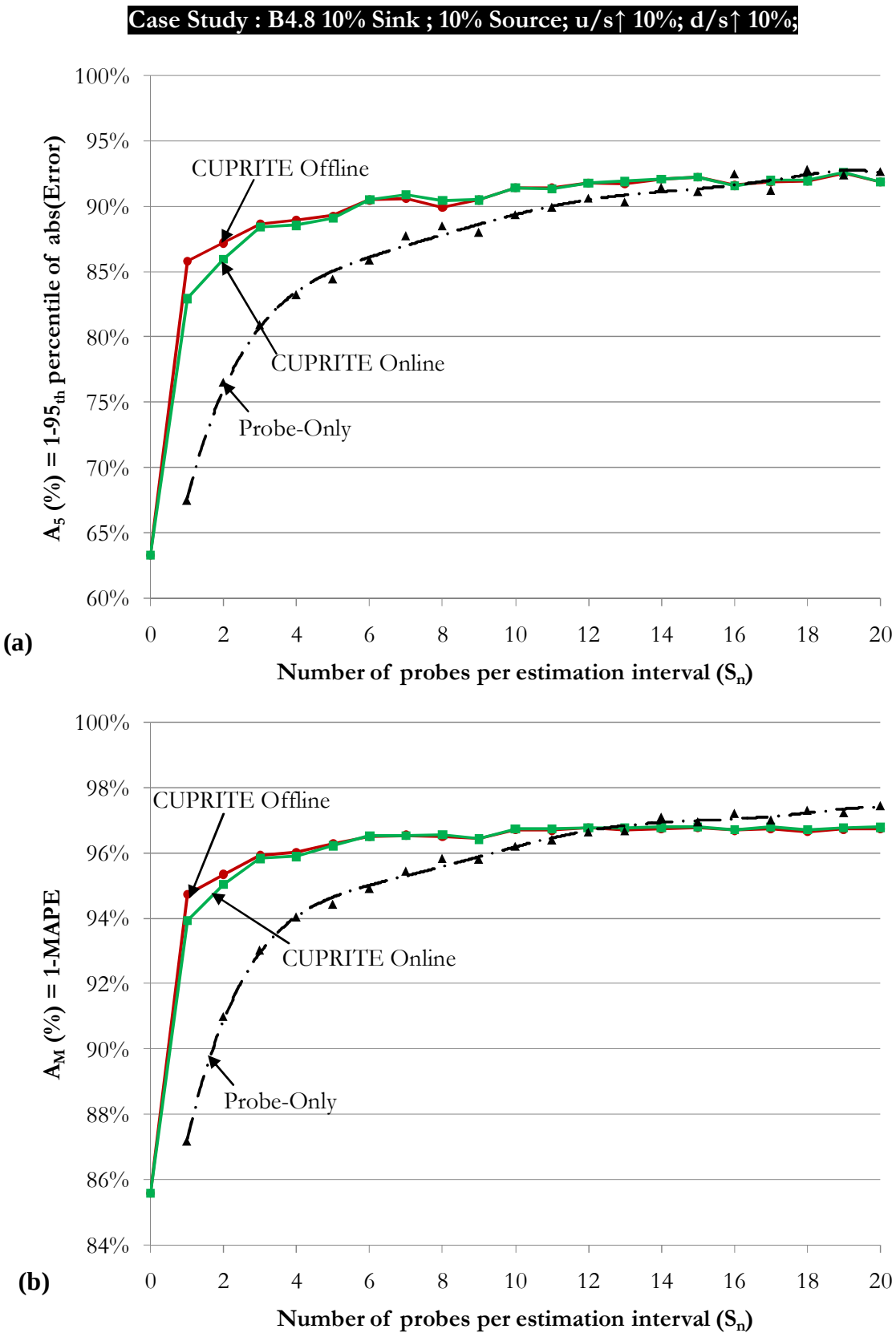

Figure D-18: Results for case B4.8 (10% sink; 10% source; both u/s and d/s detectors overcounting by 10%): (a) A_5 and (b) A_M versus S_n.

APPENDIX E NUMBER PLATE SURVEY

This appendix introduces the procedure employed for the survey.

A team of 28 observers were deployed to collect the time and vehicle ID (number plate) of vehicles observed at each survey station. Travel time from one station to another can be obtained by comparing the data from two survey stations. For this the vehicle ID at two stations is to be correctly noted. Number plate survey was continuous and to reduce human errors observers were grouped into different groups and instructed to work in shift, with regular rest periods.

Figure E-1: A survey station.

Figure E-1 illustrates a survey station (station K, *see* Figure 6-7) where an observer is performing a continuous voice recording. He is accompanied with second observer who logs few recorded values into a PDA which are later used to cross-check the number plate survey data at a station. The station is also equipped with a video camera, which records all the vehicles. The counts from the camera and recorded values can be used to know the capture percentage of survey. The video recording can also provide the actual turning ratio at the intersection. However, for the present study the data from video recorder is not required.

E.1 Raw data

We used handy digital voice recorders, each with capacity of more than three hours for continuous recording (*see* Figure E-2). A continuous voice recording was performed, where observer read out the first four digits of the number plate of a vehicle when it passes a predefined point (entrance of intersection). For instance, 86 86 was read out if the observed number plate is "LU 86869". At regular intervals time stamps were also recorded. The survey stations were entrance of intersections. Therefore, during signal red phase there was no vehicle entering the intersection. The observer read out the current time, as a time stamp, during each signal red phase. The number data includes car, bus and trucks. Motorcycles and bicycles are not reported.

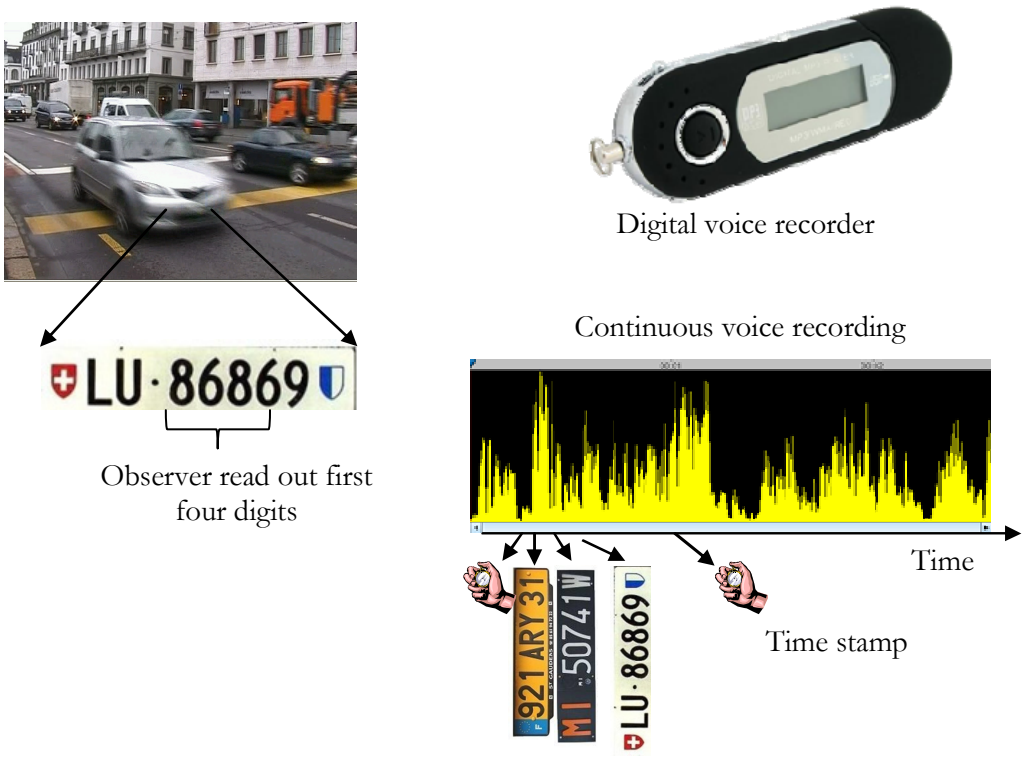

Figure E-2: Illustration of continuous voice recording of number plate survey.

E.2 Data entry

After the online collection of data, the data was processed offline to manually enter the recorded values into an electronic spreadsheet (*see* Figure E-3). For this the voice recording was played into a standard voice recorder (Windows Media Player) and the listened values were manually entered into a spreadsheet with two columns: Column 1 for the value recorded; and column 2 for the time on the media player corresponding to the frame when the recorded

value is listened. The latter column provides the relative difference in time between two recorded values. With time stamps recorded during the survey one can easily process the time corresponding to each number plate value. Following instructions were provided for entering data:

Step 1 Check the setting of the player. The play speed should be normal. For windows media player check: Play>PlaySpeed>Normal (or Ctrl+Shift+N).

Step 2 Listen to the recorded value. Listen only one value at a time e.g. if the recording is 3234 3452 6783 987… then pause after hearing 3234

Step 3 Enter in excel the value listened and the time displayed in the player.

Step 4 Repeat steps 2 and 3.

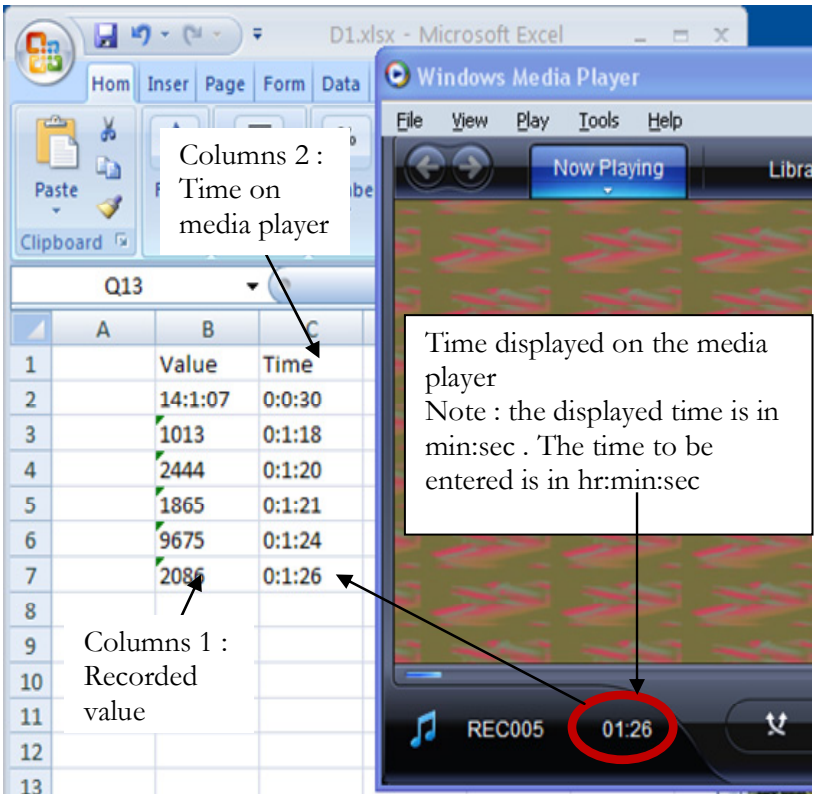

Figure E-3: Illustration of the procedure for data entry into spreadsheet.

APPENDIX F VALIDATION RESULTS FOR ROUTE A→F

This appendix provides results for travel time estimation for route A→I using *Extreme* based estimation; and *Component* based estimation. The components considered for latter case are: A→D_{Lft} and D_{Lft}→F. The results are supplement to the subsection 6.3.4

F.1 Extreme based estimation (A→F)

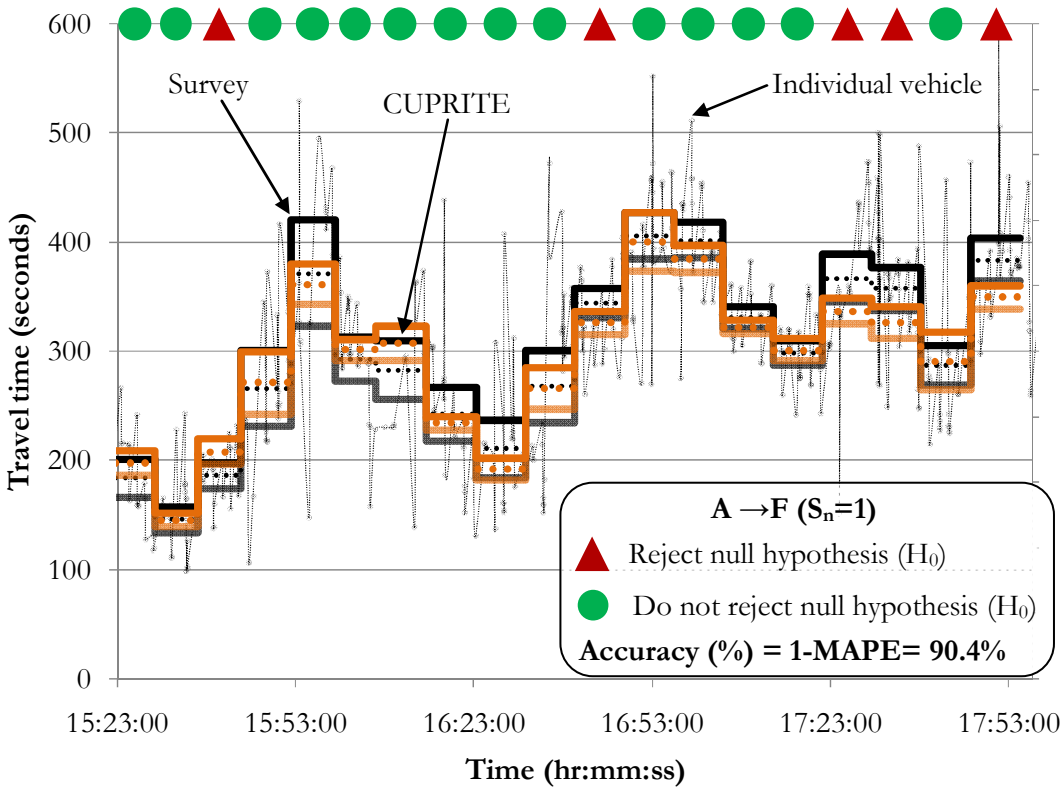

Figure F-1: *Extreme* based results for A→F (S_n=1).

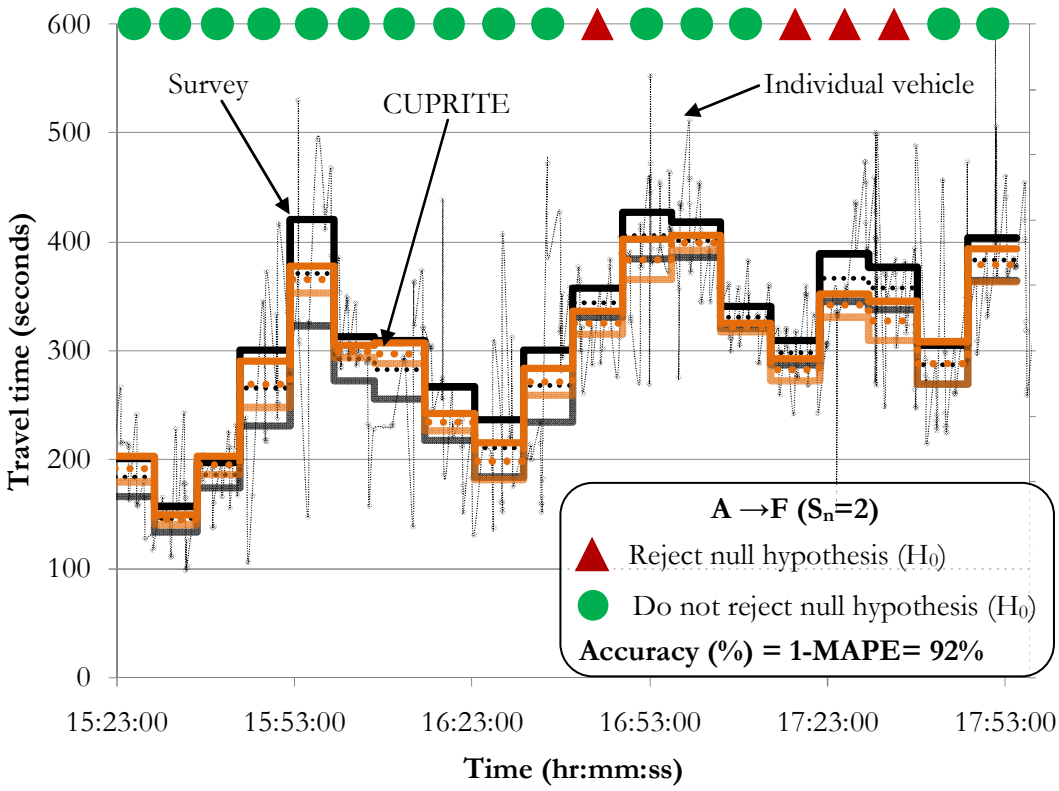

Figure F-2: *Extreme* based results for A→F (S_n=2).

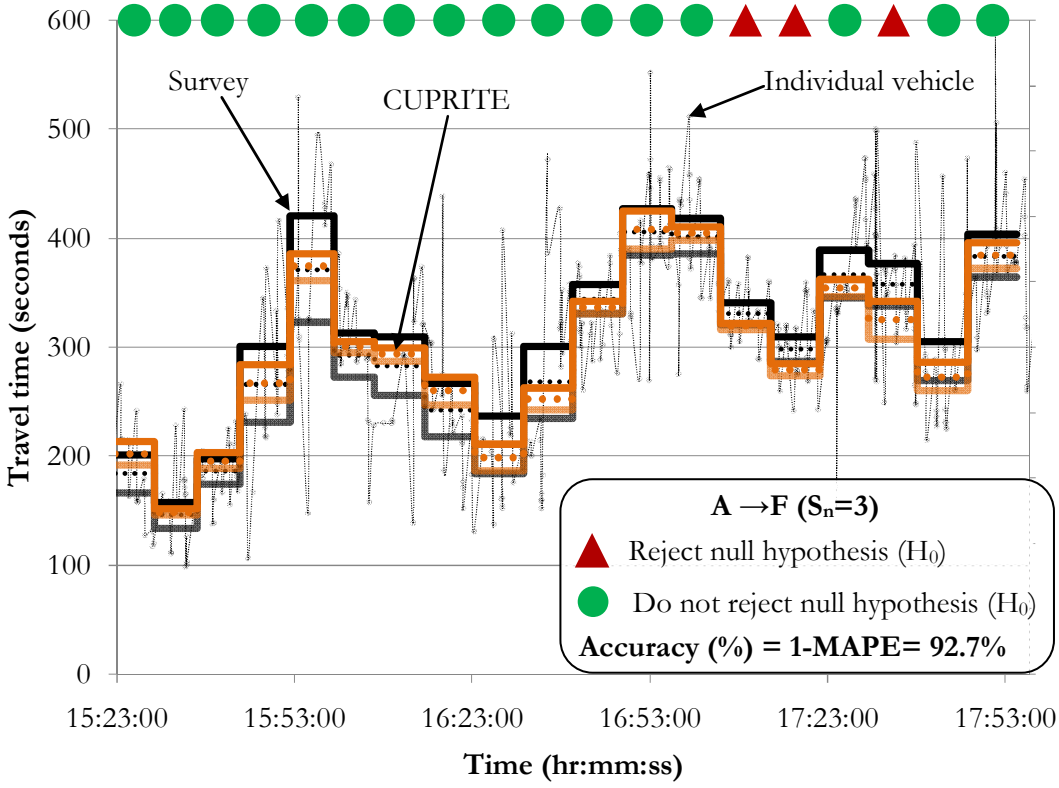

Figure F-3: *Extreme* based results for A→F (S_n=3).

F.2 Component based estimation (A→D_{Lft}→F)

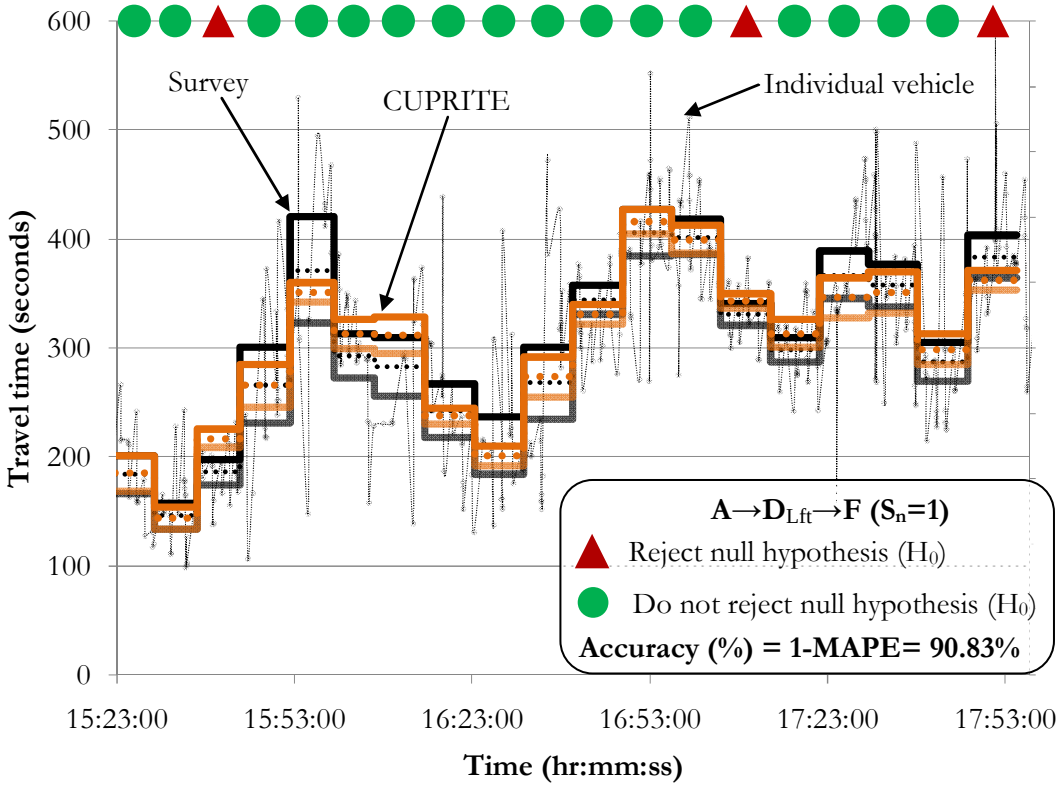

Figure F-4: *Component* based results for A→D_{Lft}→F (S_n=1).

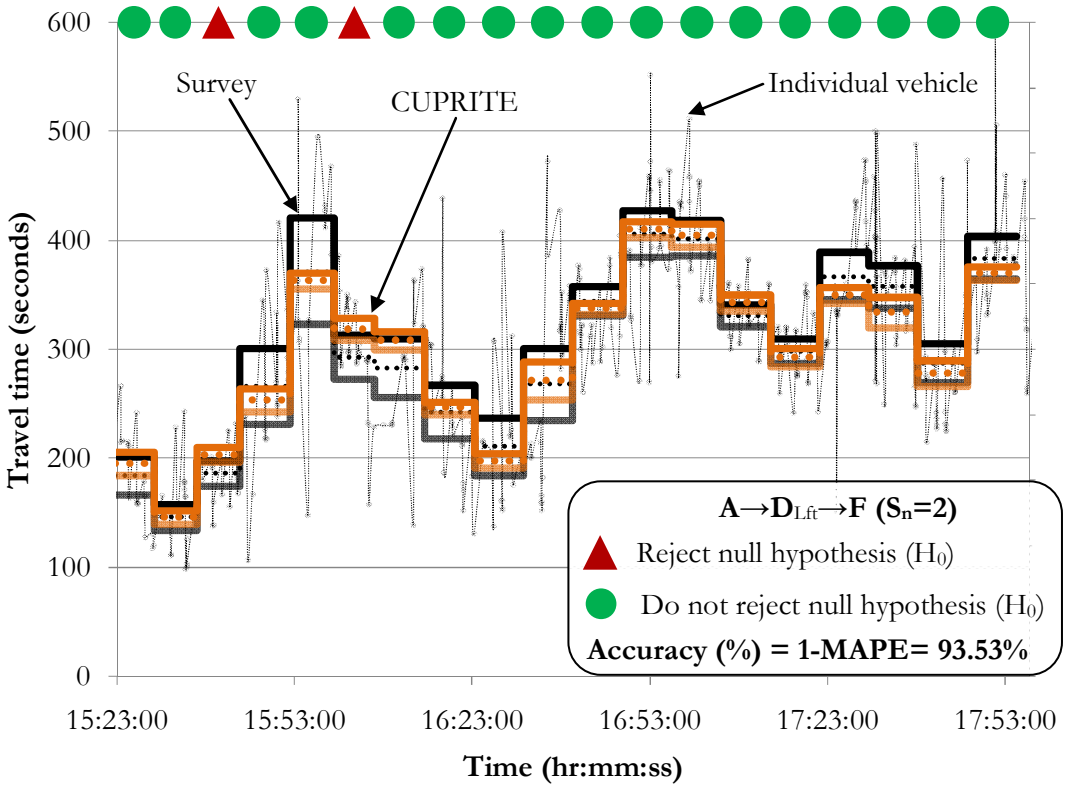

Figure F-5: *Component* based results for A→D_{Lft}→F (S_n=2).

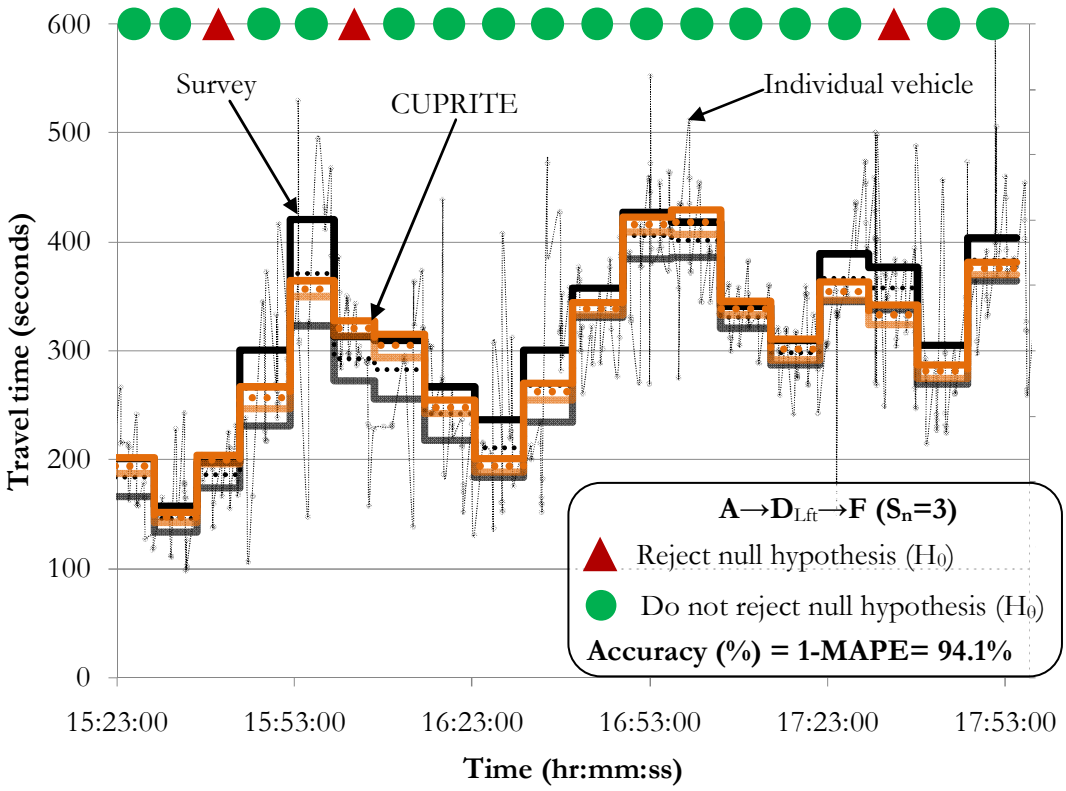

Figure F-6: *Component* based results for A→D_{Lft}→F (S_n=3).

APPENDIX G EXTENDED RESULTS FOR ROUTE D →I

In continuation to the validation results presented in section 6.3.2, this appendix contains results from intersection *D* to intersection *I* with travel time estimation interval of five signal cycles (at intersection *I*). The signal cycle time varies from 42 s to 55 s and on average the estimation interval is around 4 min.

G.1 Results for estimation interval of five signal cycle

Figure G-1 presents the number of survey vehicles per estimation intervals. It can be seen that few of the estimation intervals have less than three survey vehicles (i.e., period 22, 23 and 27). For estimation interval 23, there is only one survey vehicle. Statistically, if sample size is small then confidence bound is large and for sample size of one the confidence bound is infinite. Therefore, for period 23, the confidence bounds for survey travel time is not indicated in the results.

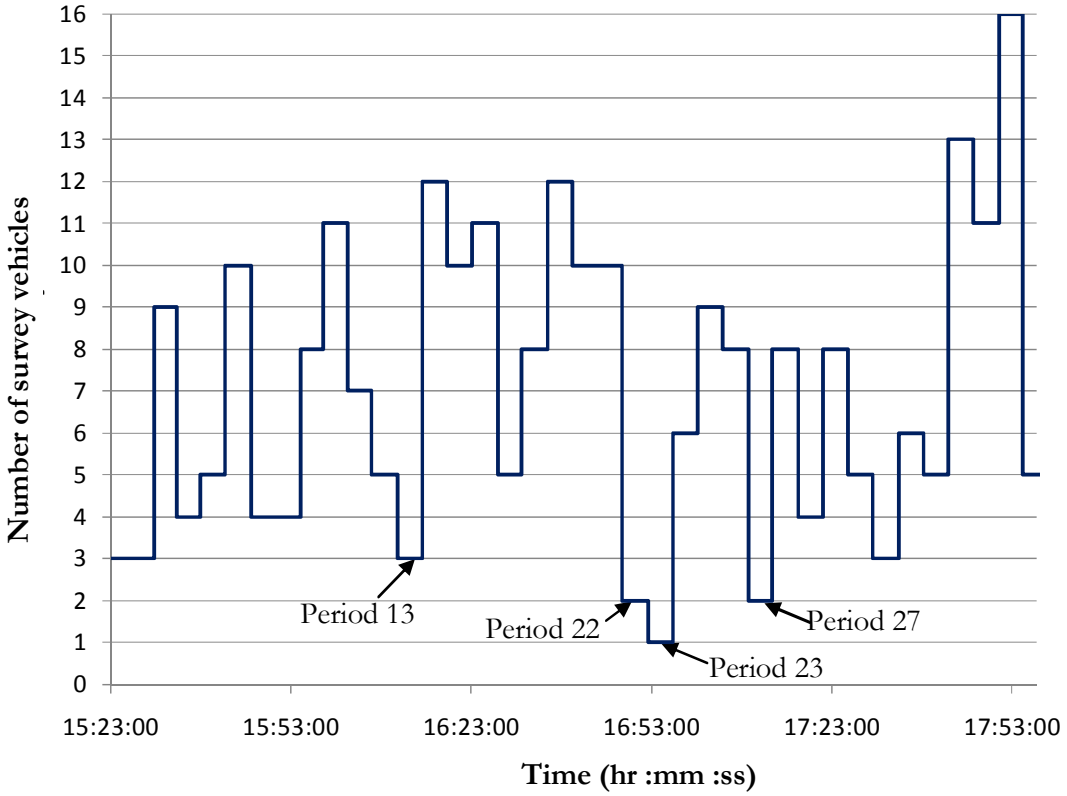

Figure G-1: Number of survey vehicles in estimation interval of 5 times the signal cycle.

Figure G-2, Figure G-3 and Figure G-4 presents the results with one, two and three probes per estimation interval, respectively. The accuracy increases from 88.7% to 93.5% with increase in number of probes from one to three. The estimation interval is around four minutes. From the results we can conclude that CUPRITE can capture the fluctuations in travel time on urban networks and can accurately estimate travel time for short estimation intervals.

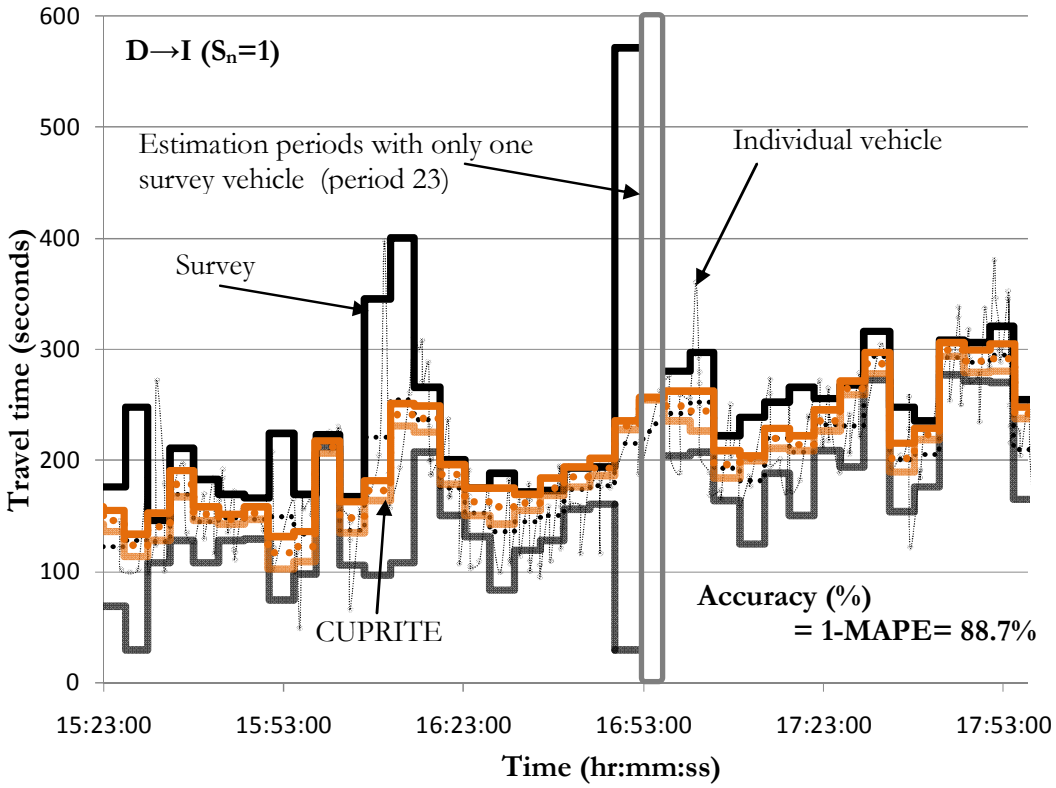

Figure G-2: *Extreme* based results for D→I (S_n=1).

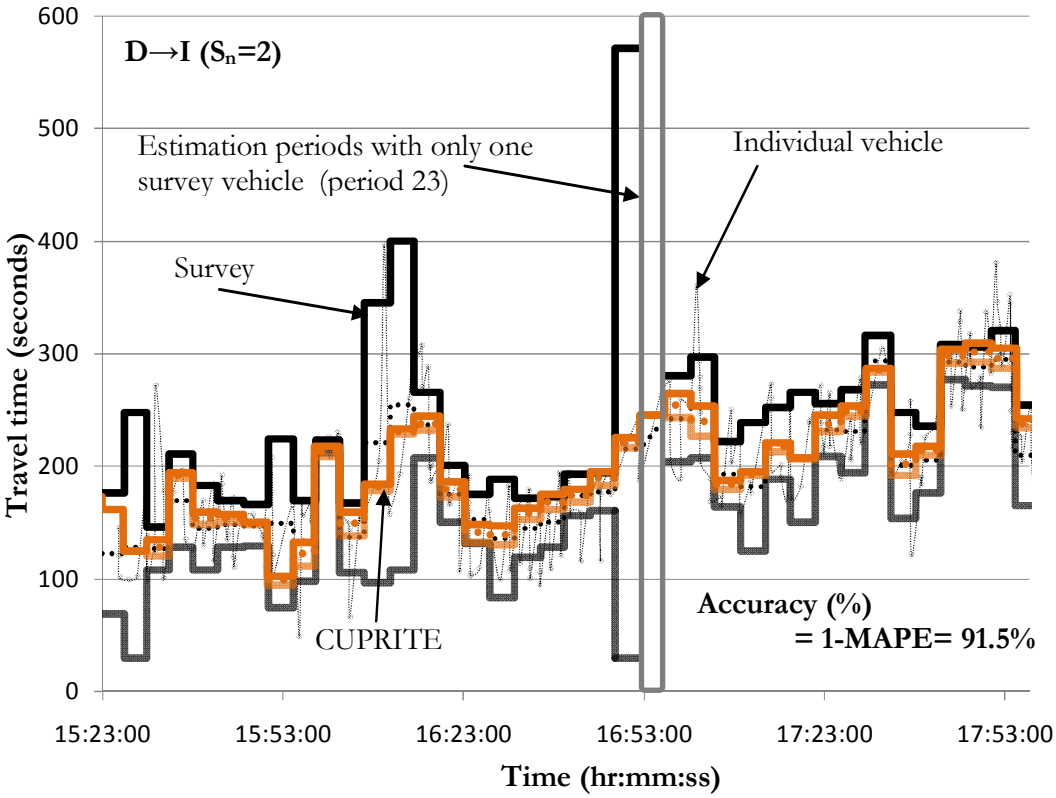

Figure G-3: *Extreme* based results for D→I (S_n=2).

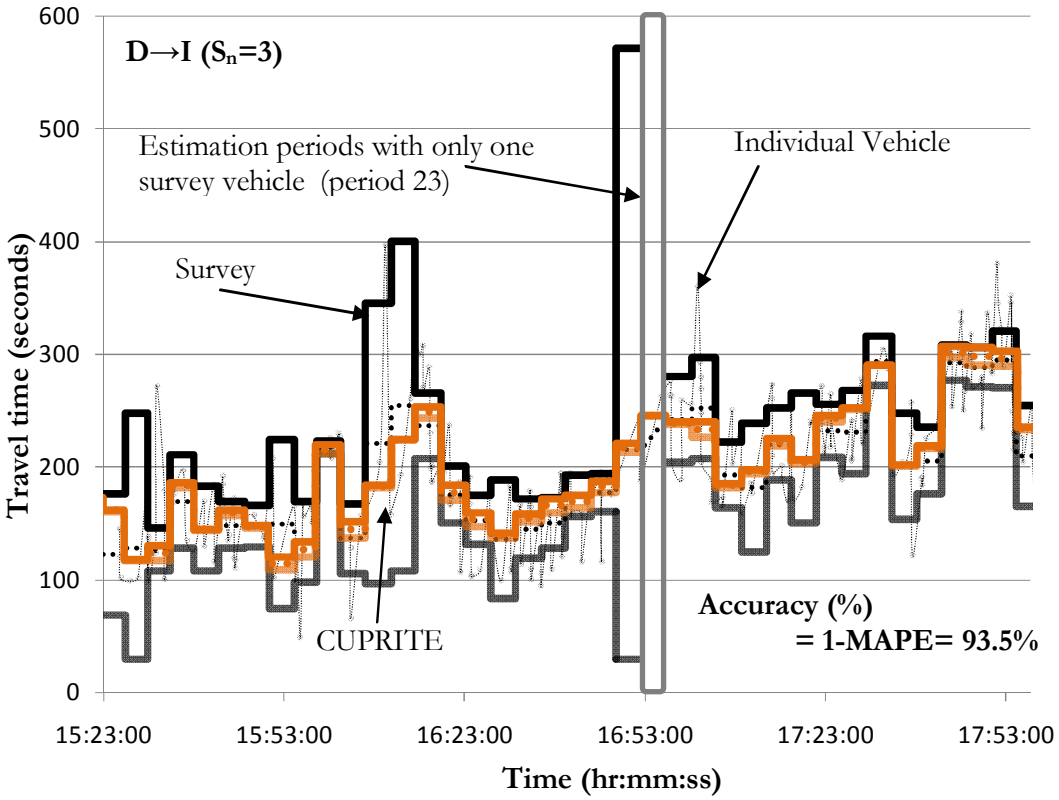

Figure G-4: *Extreme* based results for D→I (S_n=3).

G.2 Component based estimation (D→F→I)

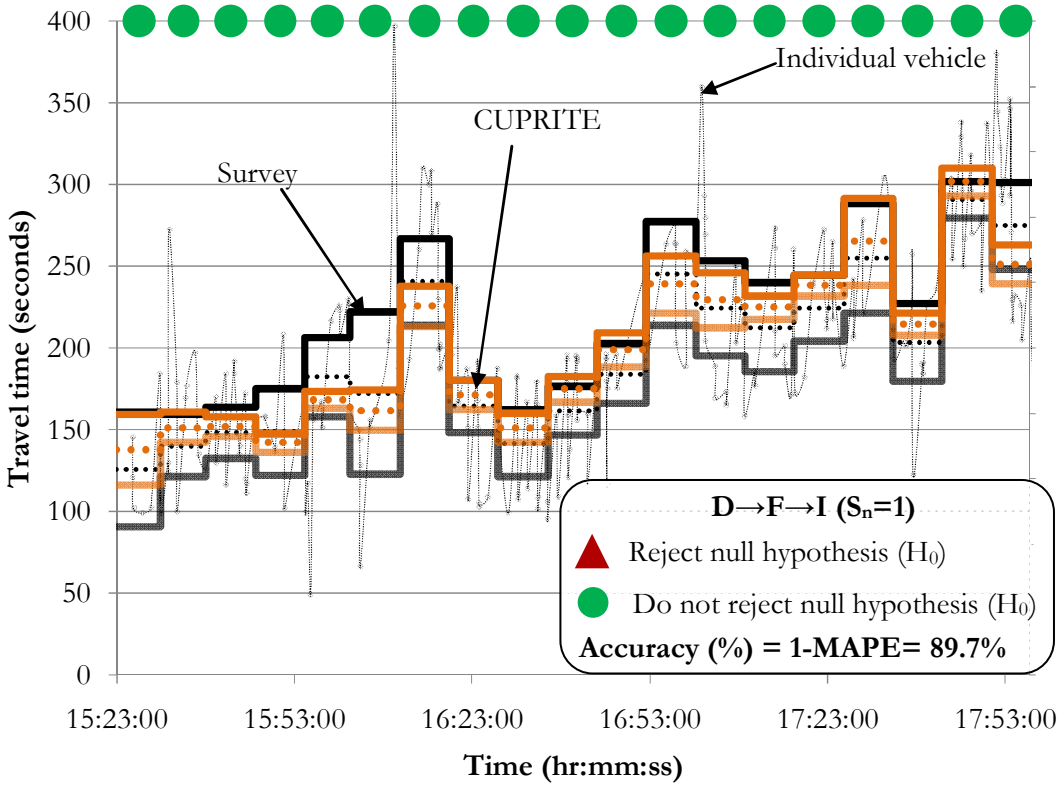

Figure G-5: *Component* based results for D→F→I (S_n=1).

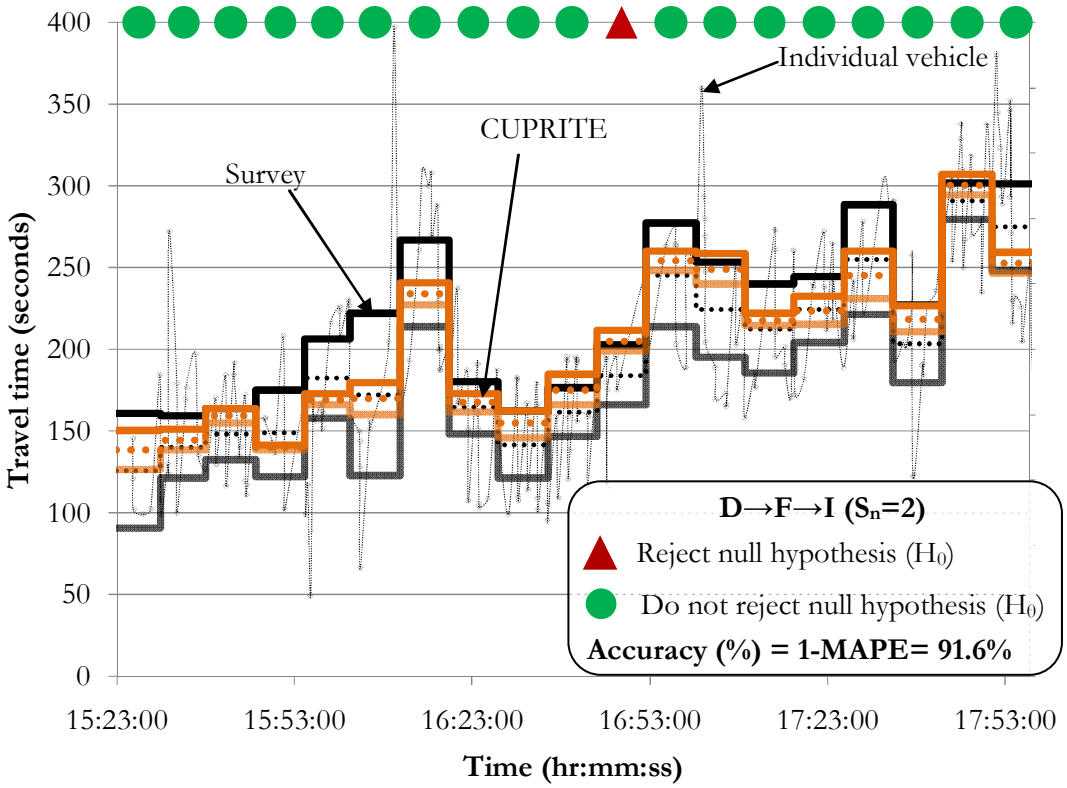

Figure G-6: *Component* based results for D→F→I (S_n=2).

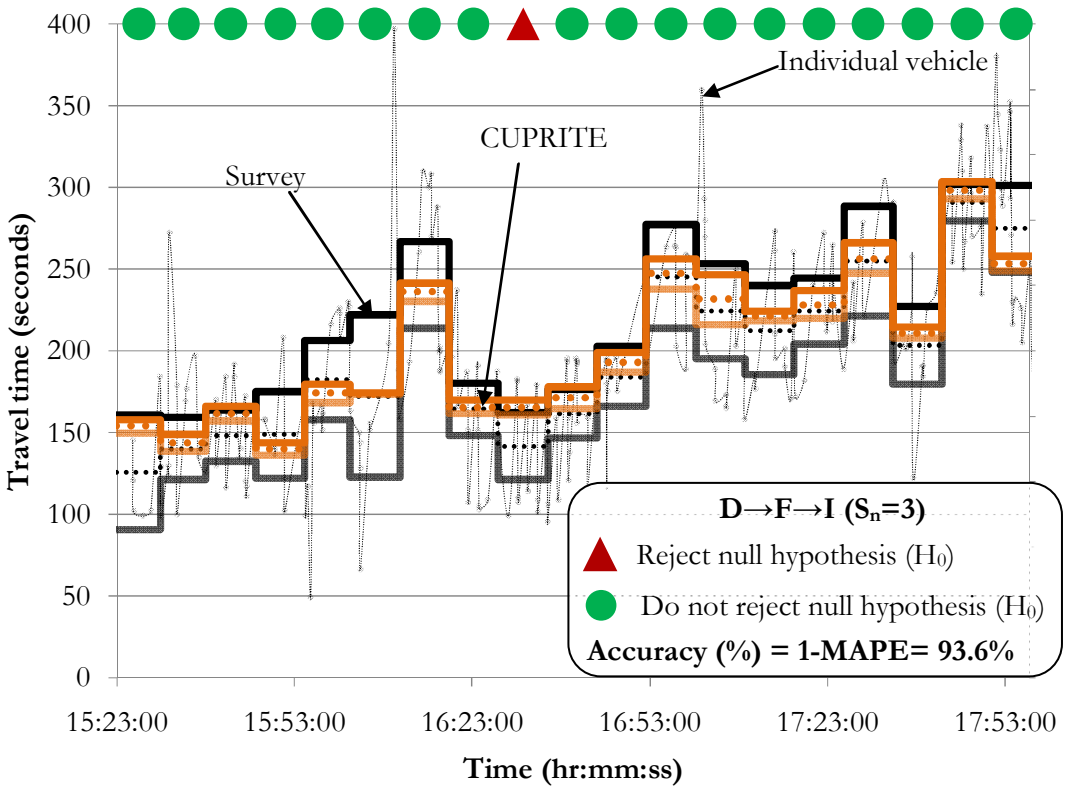

Figure G-7: *Component* based results for D→F→I (S_n=3).

APPENDIX H VALIDATION RESULTS FOR D→K

This appendix provides results for travel time estimation for route A→K using *Extreme* based estimation; and *Component* based estimation. The components considered for latter case are: D→F, F→I and I→K. The results are supplement to the subsection 6.3.4

H.1 Extreme based estimation (D→K)

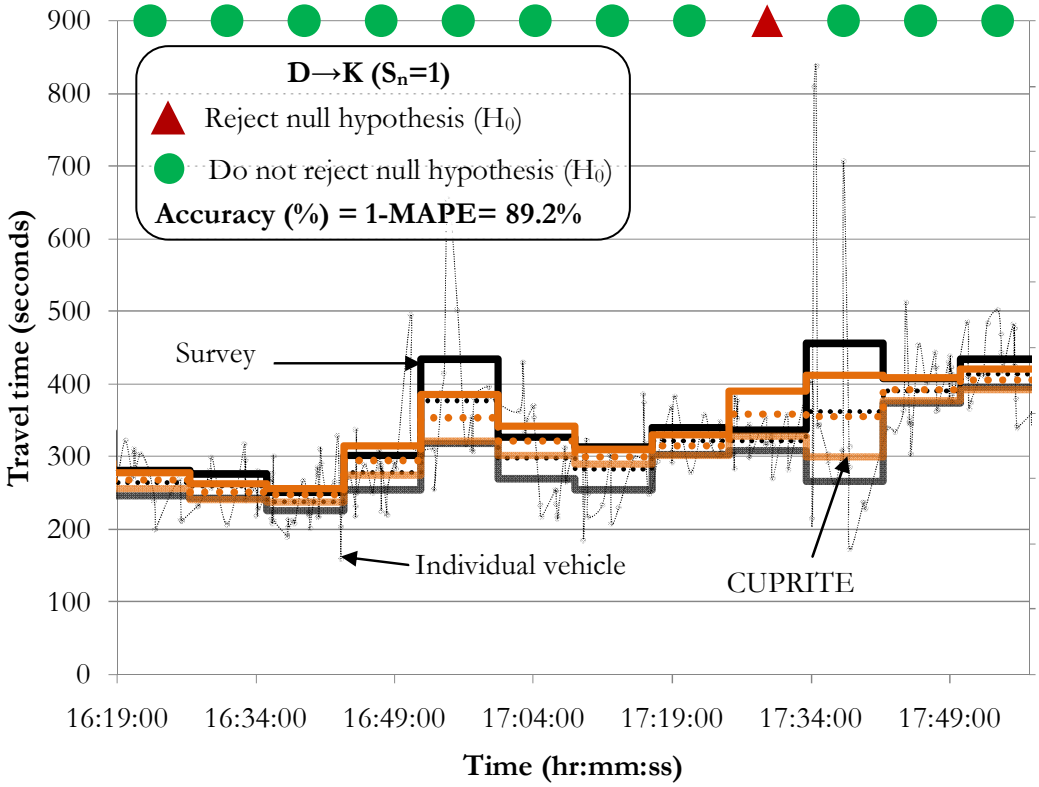

Figure H-1: *Extreme* based results for D→K (S_n=1).

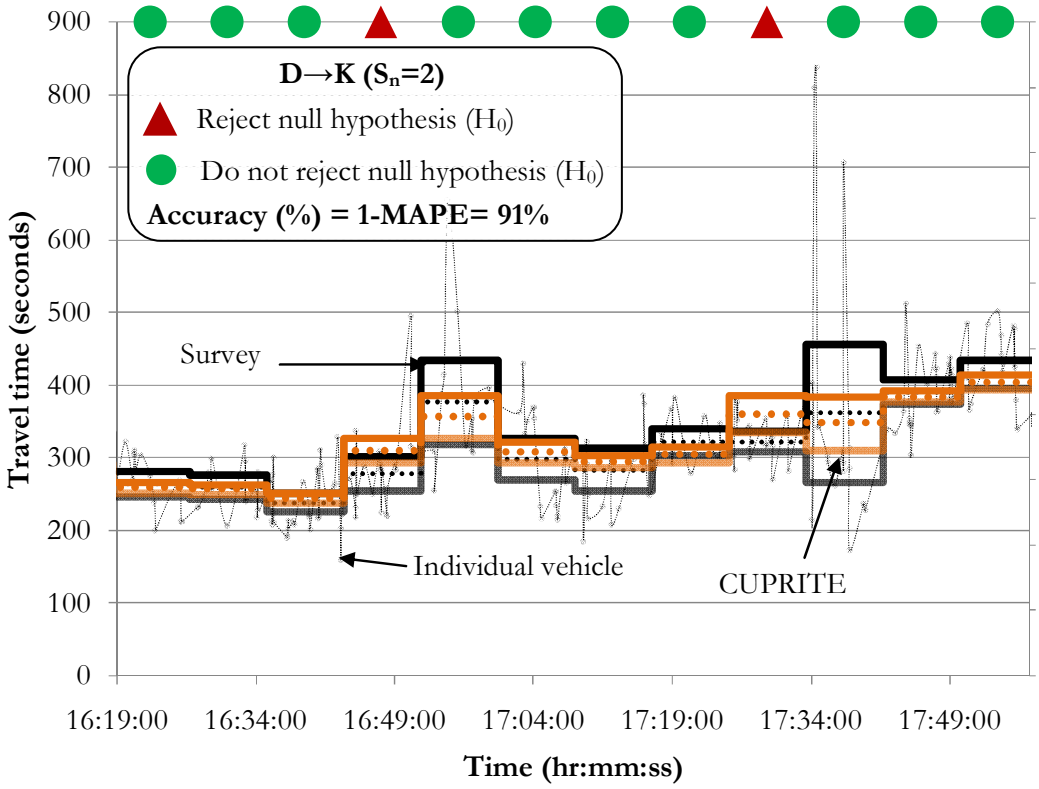

Figure H-2: *Extreme* based results for D→K (S_n=2).

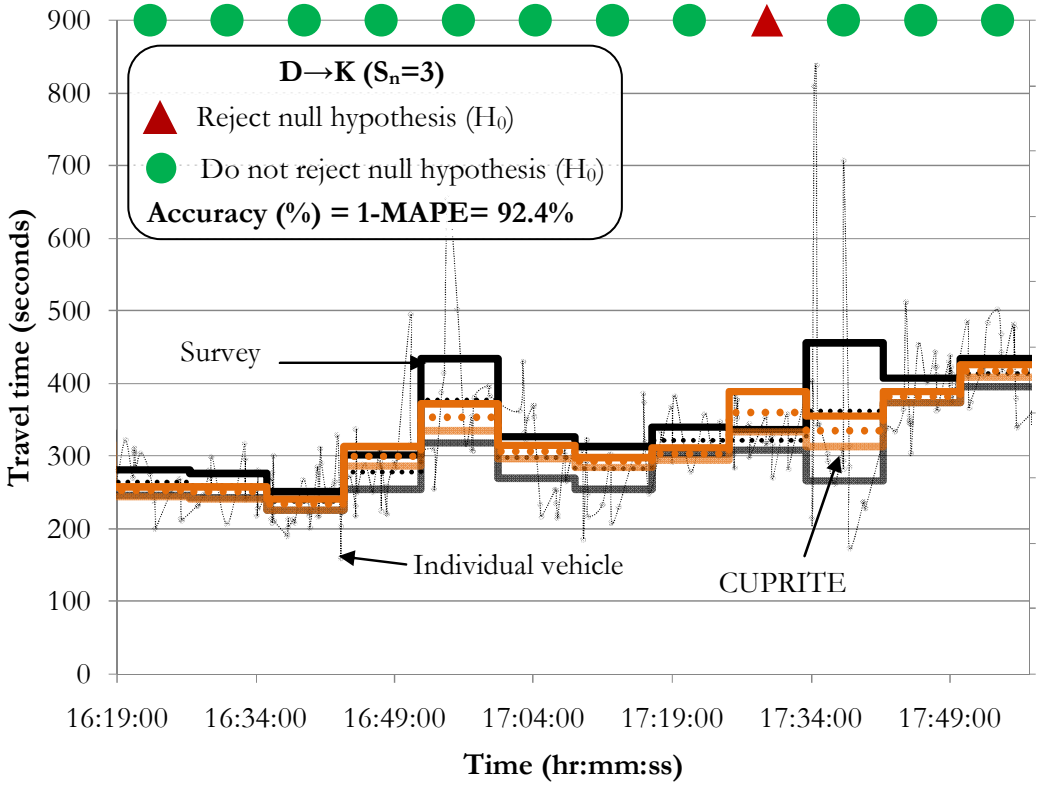

Figure H-3: *Extreme* based results for D→K (S_n=3).

H.2 Component based estimation (D→F→I→K)

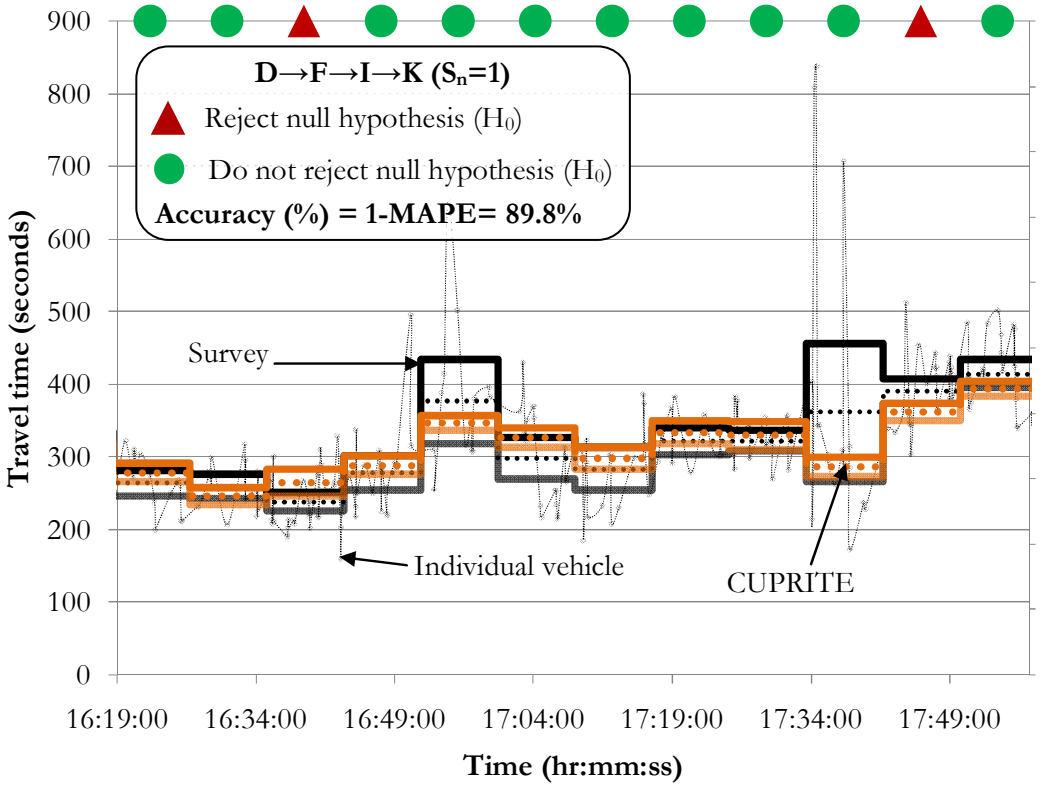

Figure H-4: *Component* based results for D→F→I→K (S_n=1).

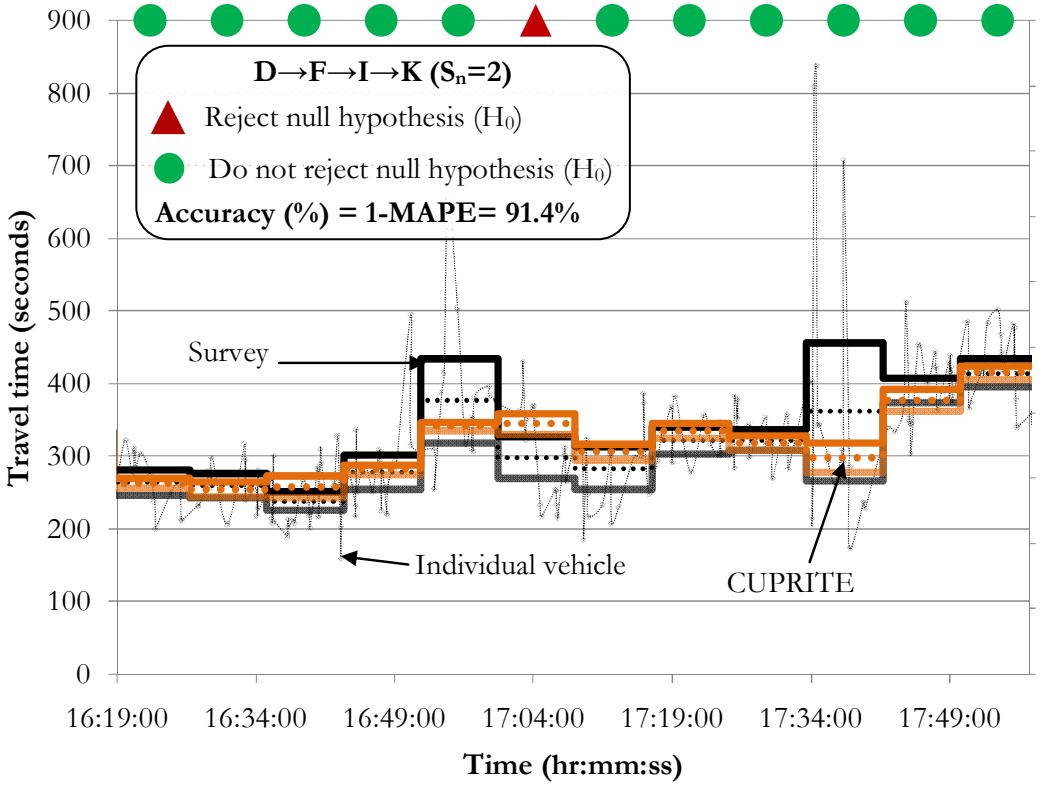

Figure H-5: *Component* based results for D→F→I→K (S_n=2).

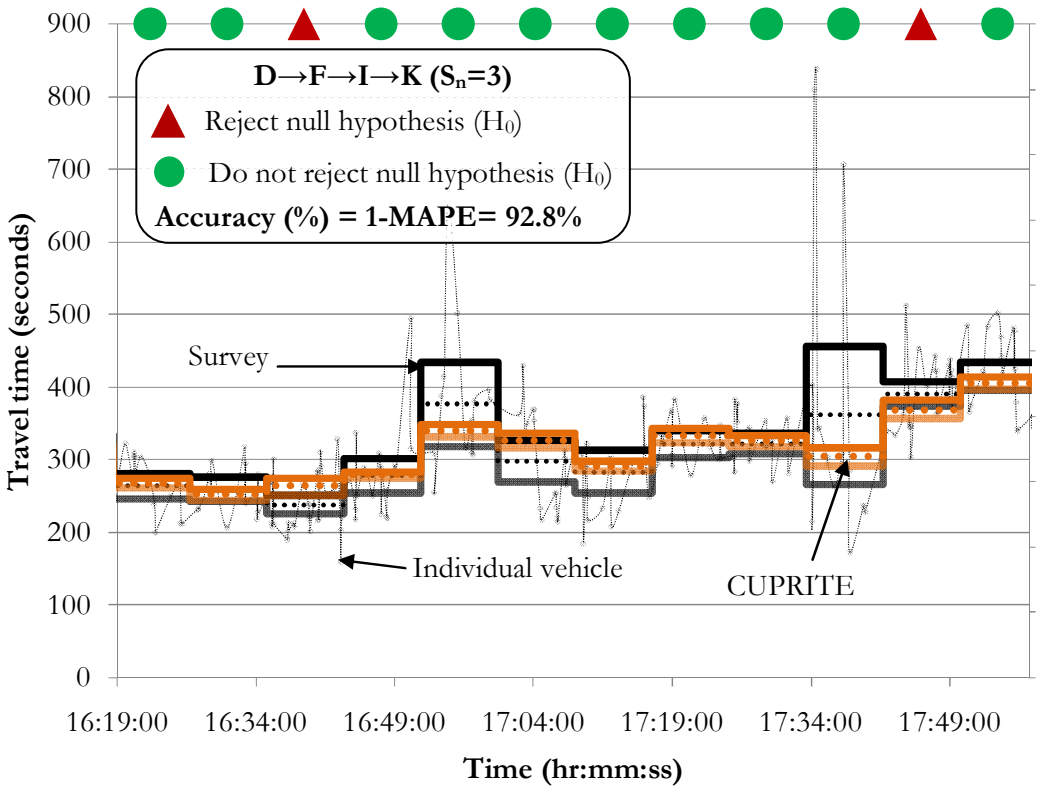

Figure H-6: Component based results for D→F→I→K (S_n=3).

APPENDIX I VALIDATION RESULTS FOR A→I

This appendix provides results for travel time estimation for route A→I using *Extreme* based estimation; and *Component* based estimation. The components considered for latter case are: A→D_{Lft}, D_{Lft}→F and F→I. The results are supplement to the subsection 6.3.4

I.1 Extreme based estimation (A→I)

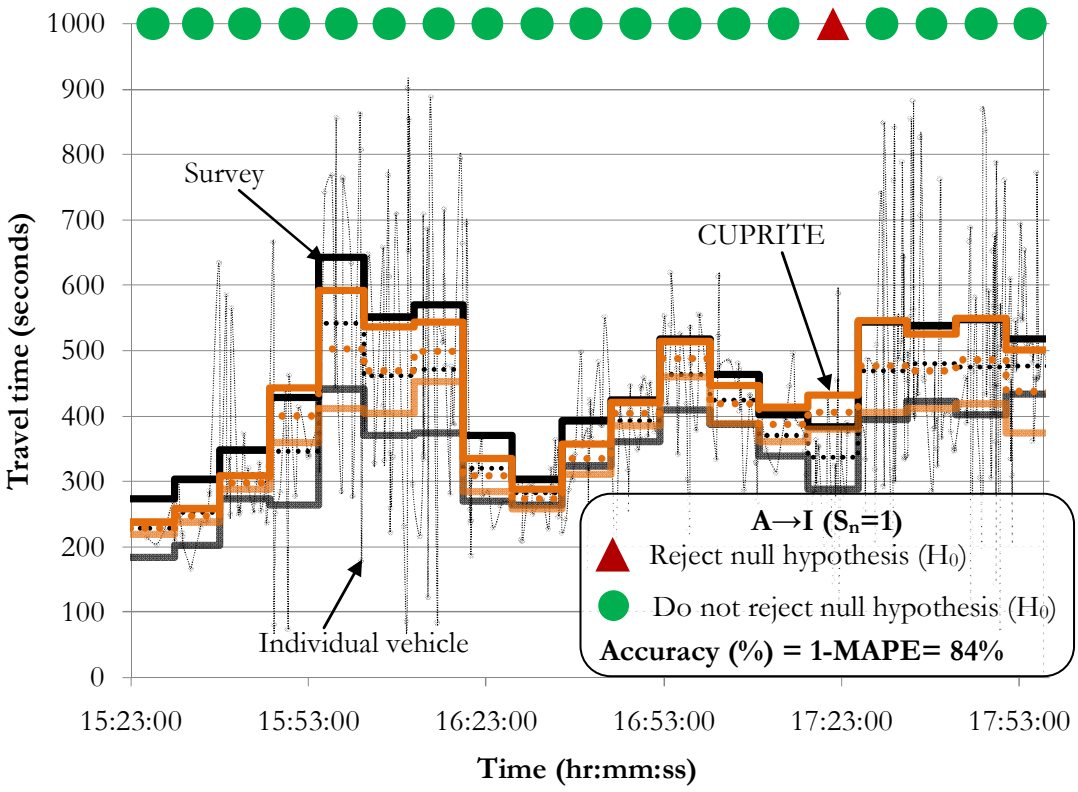

Figure I-1: *Extreme* based results for A→I (S_n=1).

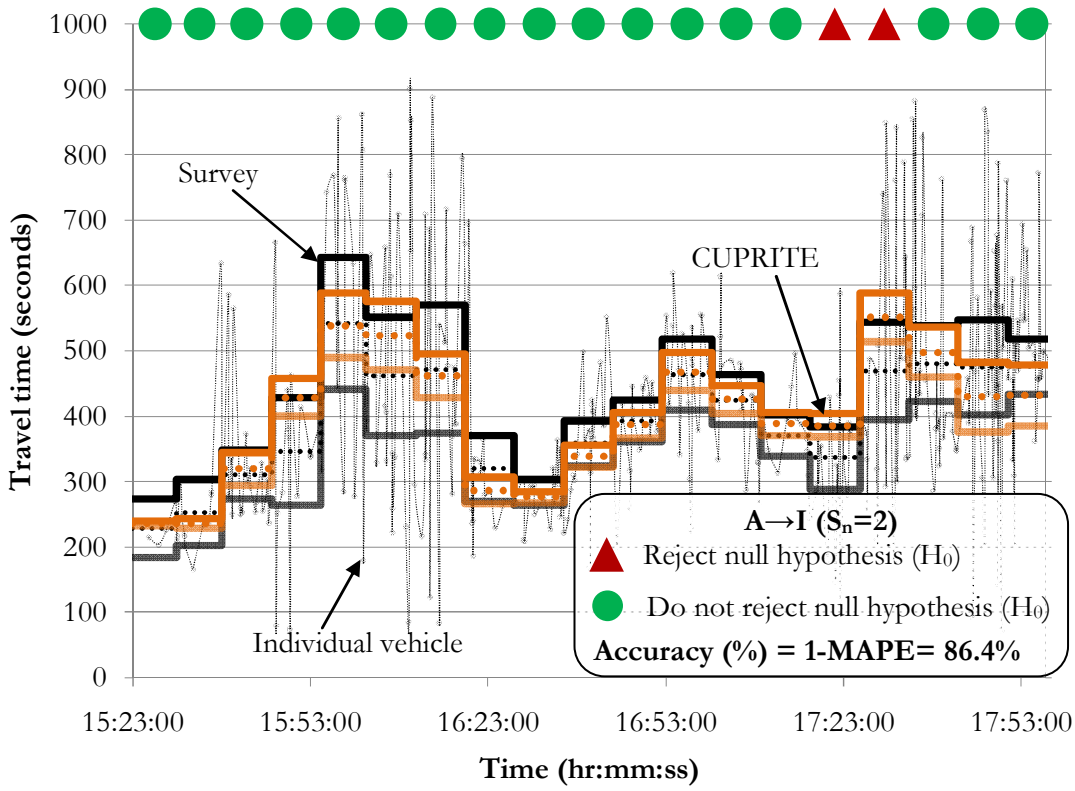

Figure I-2: *Extreme* based results for A→I (S_n=2).

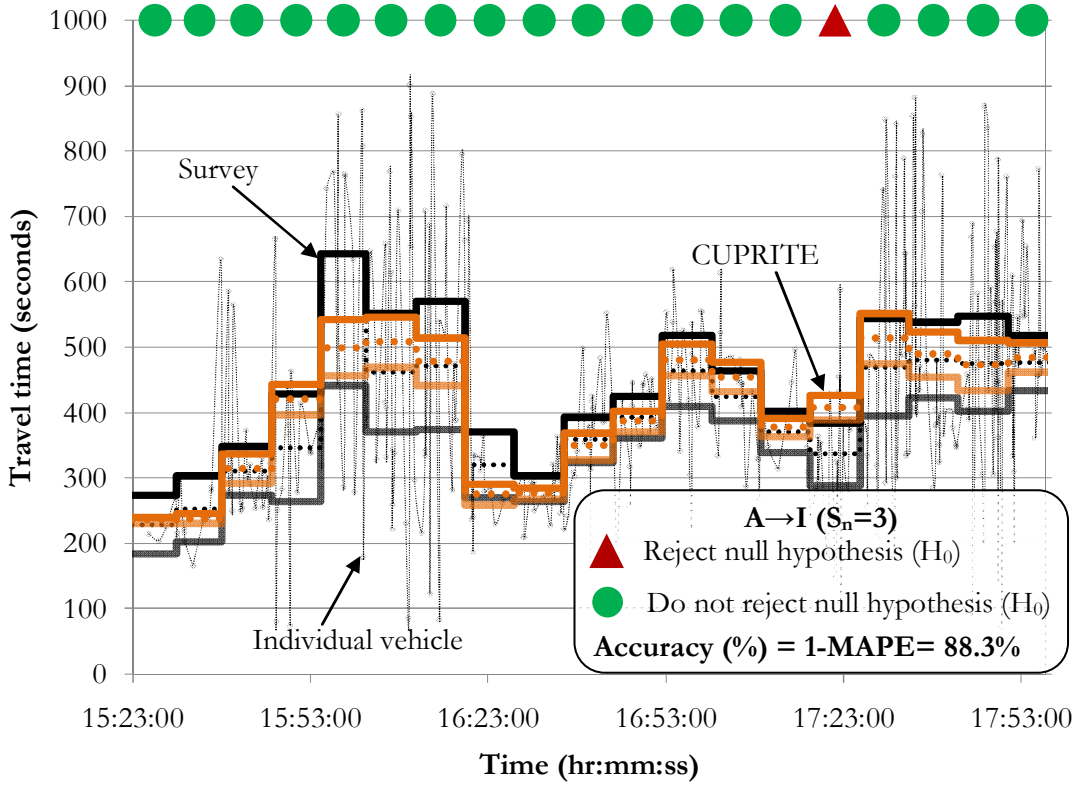

Figure I-3: *Extreme* based results for A→I (S_n=3).

I.2 Component based estimation (A→D_{Lft}→F→I)

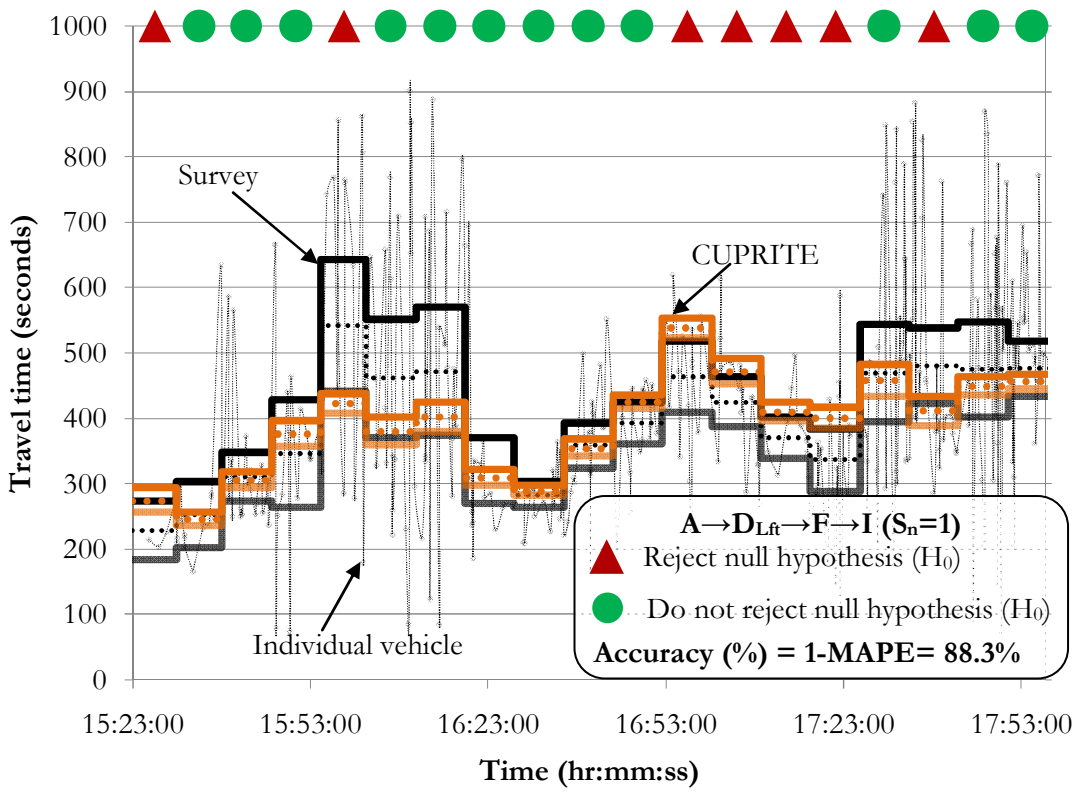

Figure I-4: *Component* based results for A→D_{Lft}→F→I (S_n=1).

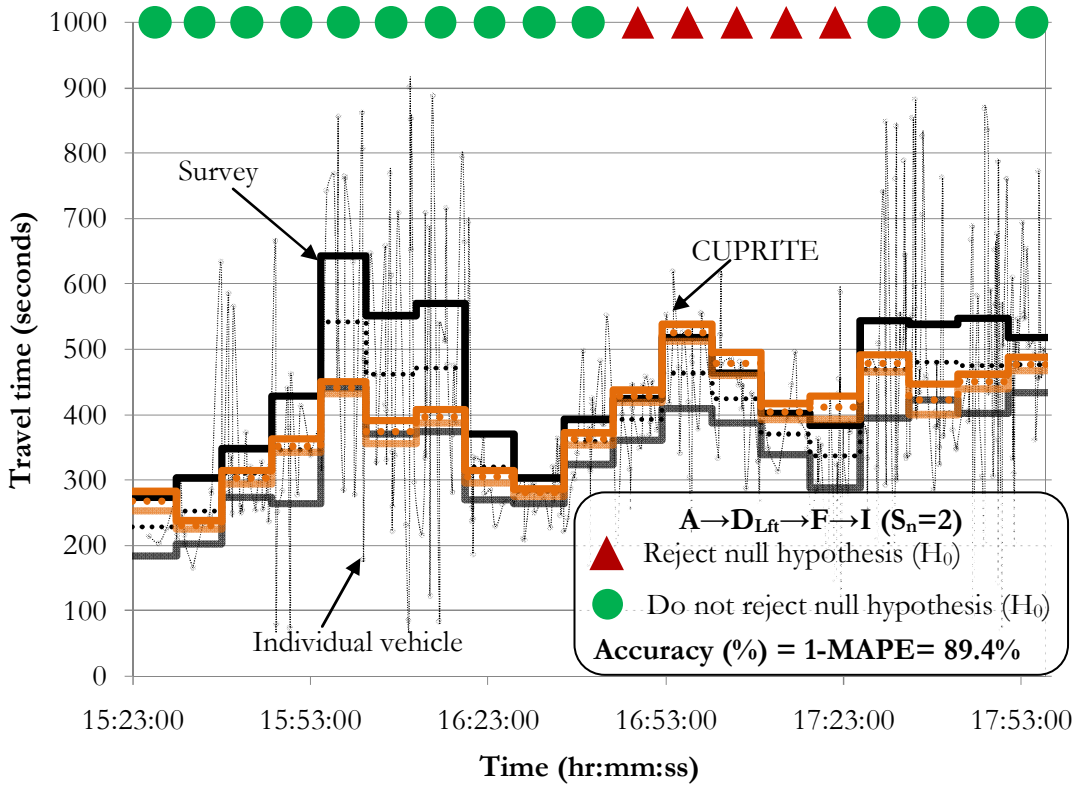

Figure I-5: *Component* based results for A→D_{Lft}→F→I (S_n=2).

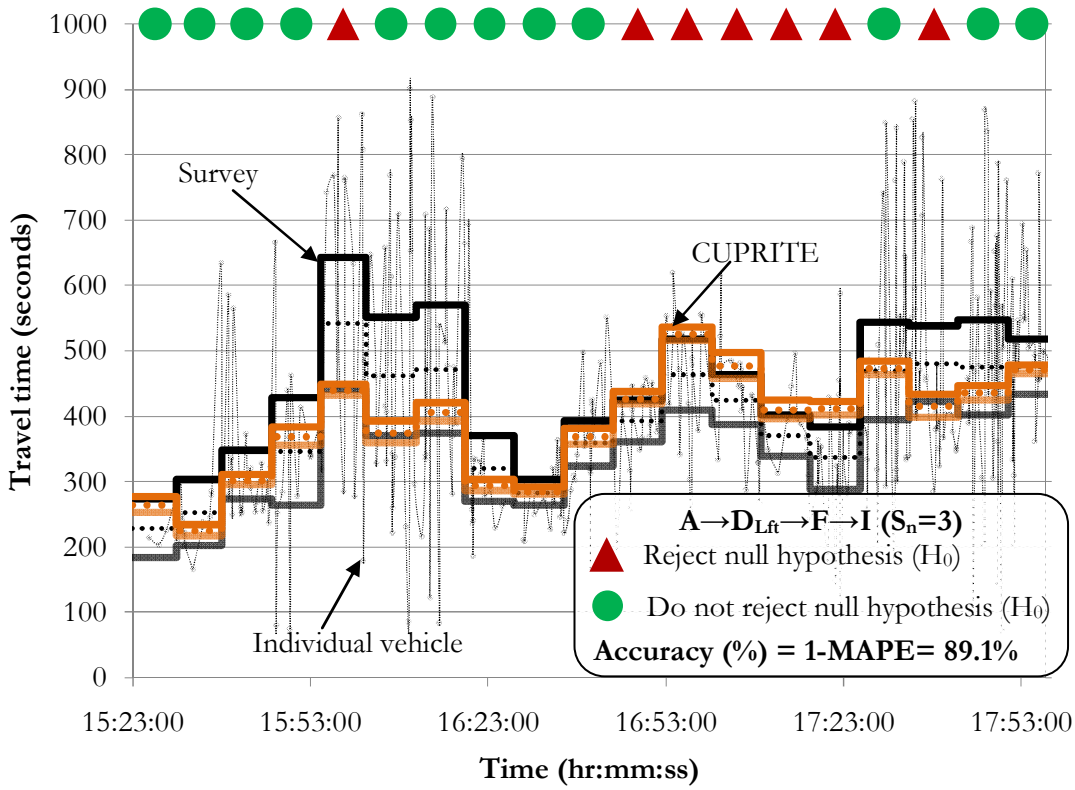

Figure I-6: *Component* based results for A→D_{Lft}→F→I (S_n=3).

APPENDIX J CUPRITE APPLICATION FOR ESTIMATION OF QUARTILE OF TRAVEL TIME

This appendix provides discussion on CUPRITE application for estimation of quartile of travel time.

By definition quartile is any value that divides the sorted data into equal parts:

i. Q_1: the first quartile is the 25^{th} percentile and 25% of the data is lower than Q_1.

ii. Q_2: the second quartile is the 50^{th} percentile (or median) and it divides the data into two equal parts.

iii. Q_3: the third quartile is the 75^{th} percentile and 75% of the data is lower than Q_3.

To obtain quartiles of travel time from CUPRITE we need to first estimate individual vehicle travel time. For this we apply the following slicing technique to define a pair of vehicles with similar travel time and thereafter estimate quartiles.

J.1 Slicing technique

We define cumulative plot as a polyline with *M* as the matrix of nodes for the polyline. For a travel time estimation interval, the total area A between the cumulative plots, is fragmented into different areas (A_i) (*see* Figure J-1), by horizontal cuts corresponding to the nodes at M_U (node matrix for U(t)) and M_D (node matrix for D(t)) and with the following constraint: For each fragmented area, A_i, if the counts, N_i, are above a certain threshold number, $N_{threshold}$, then the time interval for the arrival, t_{ui}, and departure, t_{di}, corresponding to the fragmented area should be below a certain threshold time interval ($t_{threshold}$). If not, then the area (A_i) is further fragmented by a horizontal cut to satisfy the constraints. The process is repeated until each fragmented area satisfies the constraints.

Finally, each fragmented area (A_i) represents the total travel time for the N_i number of vehicles. Assuming that these N_i number of vehicles experience similar travel time ($\overline{TT}_i$)

equals to the A_i/N_i. Finally, one can obtain the quartiles by sorting the travel time values obtained from all the sliced areas and corresponding number of vehicles.

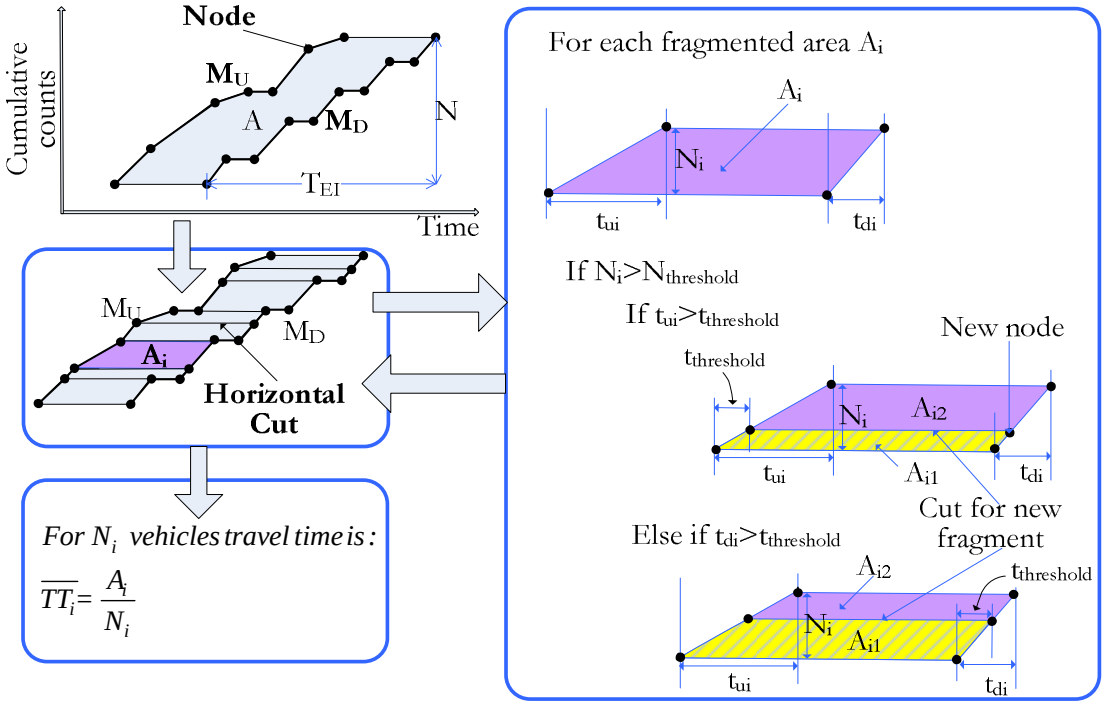

Figure J-1: Illustration for slicing the area between cumulative plots for defining travel time for different pair of vehicles within a estimation interval.

The algorithm for estimating quartiles using slicing method is as follows:

For an estimation interval say we have a two dimensional array with first column as list of A_i/N_i ($L_{A/N}$) and second column as list of N_i (L_N). Following steps are followed:

Step 1 Sort the array with respect to the values in the list $L_{A/N}$;

Step 2 Define a frequency list (L_f) by cumulating the values in the list L_N;

Step 3 Define N, as total number of vehicles in the estimation interval. This is the last element of the above frequency list;

Step 4 Define the index for the quartiles as follows:

Q_1_index = 0.25*N

Q_2_index = 0.5*N

Q_3_index = 0.75*N

Step 5 Quartiles are defined as the value corresponding to the j^{th} element of the sorted list $L_{A/N}$ where j is the rank of L_f such that:

if(j=0) and ($L_f[j] \geq Q_3$_index),

then $Q_3 = L_{A/N}[0]$

if(j>0) and ($L_f[j-1] < Q_3$_index) and ($L_f[j] \geq Q_3$_index),

then $Q_3 = L_{A/N}[j]$

Similarly, for Q_2 and Q_3;

Note: here the elements of the list start from rank 0.

For better understanding of the above algorithm a self explaining example is presented in the Figure J-2.

Original List			**Step 1** Sorted w.r.t Ai/Ni		**Step 2** [Cumulative Ni]	
$L_{A/N}$ [Ai/Ni]	L_N [Ni]		$L_{A/N}$ [Ai/Ni]	L_N [Ni]	L_f	
99.77	2.3		38.46	2.9	2.9	
68.49	2.3		43.82	2.5	5.4	
57.91	2.4		47.12	1.2	6.6	
43.82	2.5		48.35	2.9	9.5	< Q_1_index
76.20	3.2	**Q_1 →**	**56.29**	2.8	**12.3**	≥ Q_1_index
63.74	2.9		57.91	2.4	14.7	
56.29	2.8		60.77	3.2	17.9	
38.46	2.9		62.36	3.0	20.9	< Q_2_index
73.56	2.8	**Q_2 →**	**63.74**	2.9	**23.8**	≥ Q_2_index
62.36	3.0		64.86	3.5	27.3	
48.35	2.9		66.29	3.4	30.7	
77.70	3.1		68.49	2.3	33.0	< Q_3_index
83.96	3.1	**Q_3 →**	**73.56**	2.8	**35.8**	≥ Q_3_index
64.86	3.5		76.20	3.2	38.9	
60.77	3.2		77.70	3.1	42.1	
66.29	3.4		83.96	3.1	45.2	
47.12	1.2		99.77	2.3	47.5	

Step 3	N=	47.5
Step 4	Q_1_index =0.25*N =	11.87
	Q_2_index =0.5*N =	23.74
	Q_3_index =0.75*N =	35.61

Figure J-2: An example for quartile estimation using slicing method.

J.2 Application

The above defined slicing technique is applied on the Lucerne data described in Chapter 6 on a route from A→D_{Lft} and quartile Q_3 (75^{th} percentile) is estimated. The results are presented in Figure J-3, Figure J-4 and Figure J-5. Here the accuracy of the estimates from CUPRITE is defined as following:

$$Error_i = \left(\frac{\left|Q_{s_i} - Q_{C_i}\right|}{Q_{s_i}}\right)$$

$$MAPE = \sum_{i=1ton} \frac{Error_i}{n}$$

$$Accuracy(\%) = 1 - MAPE$$

Where: $Error_i$ is the absolute percentage error for i^{th} estimation interval; Q_{s_i} and Q_{C_i} are the Q_3 of survey travel time and travel time estimated from CUPRITE application during i^{th} estimation interval, respectively; n is the number of estimation intervals; and $MAPE$ is the Mean Absolute Percentage Error obtained from the CUPRITE application for different estimation intervals during survey period.

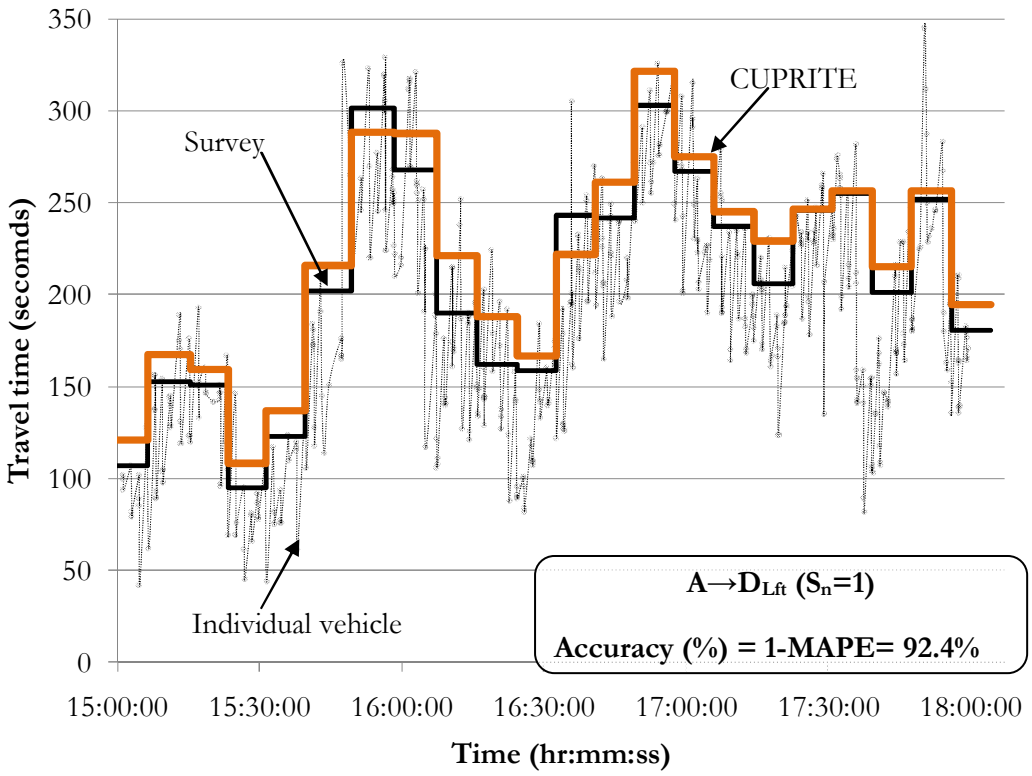

Figure J-3: Q_3 estimation using CUPRITE for route from A→D_{Lft} (S_n=1).

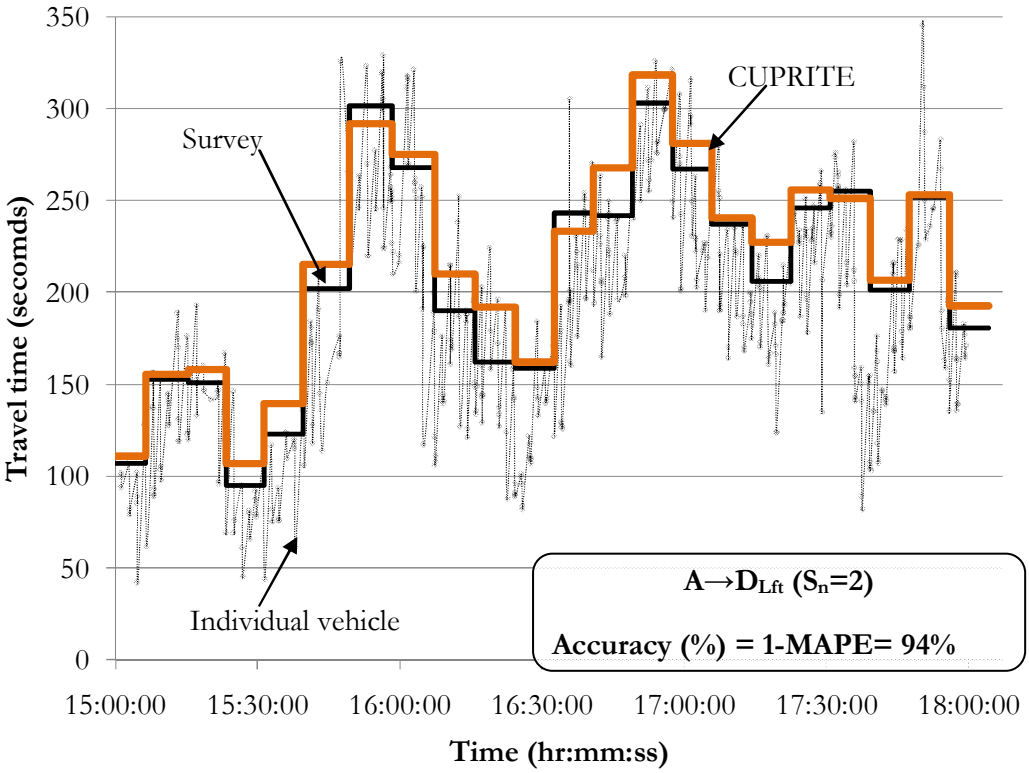

Figure J-4: Q_3 estimation using CUPRITE for route from A→D_{Lft} (S_n=2).

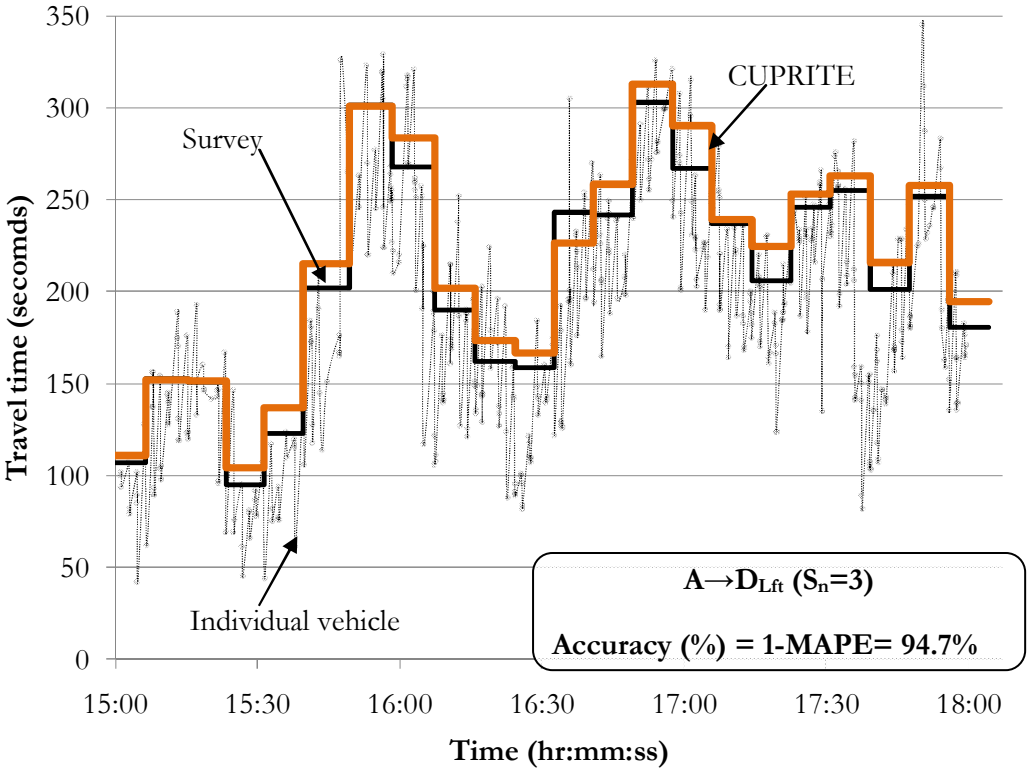

Figure J-5: Q_3 estimation using CUPRITE for route from A→D_{Lft} (S_n=3).

It is observed that the accuracy increases from 92.4% to 94.7% for increase in S_n from one probe per estimation interval to three probes per estimation interval. The results are similar to

what we have observed earlier for application of CUPRITE for mean travel time estimation (Refer to Figure 6-12 to Figure 6-14).

The above analysis indicates the potential of CUPRITE for quartile travel time estimation in addition to the average travel time estimation.

8 Curriculum vitae

Ashish BHASKAR

Phone: +41 (0) 21 693 23 41
Email: ashish.bhaskar@epfl.ch; abhaskar@gmail.com
Date of Birth: 21st January 1978
Nationality: Indian

Education

Master of Engineering in Civil Engineering, University of Tokyo, Tokyo, Japan *"A" grade in all academic courses at University of Tokyo- 20/20 credit*	*Oct 2002 - Sept 2004*
Bachelor of Technology in Civil Engineering, Indian Institute of Technology, Kanpur, India *Cumulative Grade point Average 8.4/10*	*July 1998 - May 2002*

Awards

[1] "Furuichi Award", for the outstanding research in the Department of Civil Engineering, University of Tokyo.

[2] "Morikawa Prize" for best presentation, Kyoto, Japan.

[3] Merit based scholarship awarded by Asian Development Bank.

Major research activity

CUPRITE: Doctoral dissertation *"A methodology (CUPRITE) for urban network travel time estimation by integrating multisource data".*	*March 2006-May 2009*
SIMNOISE: Study of vehicle noise under different operating conditions. Noise measurements were performed and the results of the study highlight the importance of considering different drivers behavior in noise modeling.	*Jan 2005-Feb 2006*
DRONE (area-wide Dynamic ROad traffic NoisE simulator): Integration of traffic noise model and traffic simulation model for areawide dynamic road traffic noise evaluation. Tested on Kawasaki city, Japan	*Oct 2002-Sept 2004*

Participation in the research team and research proposals

COST-TU0702 Network Vulnerability. This is EU COST action project	*Since 2008*
NEARCTIS Network of Excellence for Advanced Road Cooperative Traffic management in Information Society. This is an EU-FP 7 project	*Since 2007*

Teaching activities

Preparation of lectures and tutorials for following topics at graduate, master and doctoral level course: *Since 2005*

Traffic flow theory; Traffic signal control; Queueing theory; Statistical data analysis; Travel Demand Management.

Practical assignments: Tutor for master students to understand and use traffic simulation software AIMSUN and traffic noise assessment software CADNA.

Online **academic course management** using **MOODLE**. *Since 2008*

Other professional activities

Book: Transport Simulation-Beyond conventional approaches (EPFL Press) *2007-2008*

Assistant to the editor

Akcelik & Associates Pty Ltd, *Victoria, Australia* *2007 (part-time)*

Programmer for developing noise modules for SIDRA-TRIP

International Symposium on Traffic Simulation 2006 (ISTS06), *Lausanne, Switzerland* *September 2006*

Member of core group to organize the ISTS06 symposium.

Invited speaker

Journée Technique LAVOC, EPFL, Switzerland. Delivered talk on "Dynamic Road Traffic Noise Simulation". *September 2005*

Selected list of publications

Journal

[1] **Bhaskar, A.**, Chung, E., & Dumont, A-G., "Travel time estimation on urban networks with mid-link sources and sinks," Transportation Research Record 2009 (*in press*)

[2] **Bhaskar, A.,** Chung, E., & Kuwahara, M., "Development and implementation of the areawide Dynamic ROad traffic NoisE (DRONE) simulator," Transportation Research Part D: Transport and Environment, vol. 12, pp. 371-378, 2007

Book Chapters

[1] **Bhaskar, A.,** Chung, E., de Mouzon, O., & Dumont, A-G., "Urban network travel time estimation from stop-line loop detector data and signal controller data," WIT Transactions on the Built Environment, 96, 2007, pp 147-15

[2] Chung E., **Bhaskar, A.,** & Kuwahara, M., "Large area noise evaluation," in Highway and Urban Environment. vol. 12, Springer, Ed. Netherlands, 2007, pp. 579-589

[3] **Bhaskar, A.,** Chung, E., & Kuwahara, M., "Integration of Road Traffic Noise Simulator (ASJ) and Traffic Simulation (AVENUE) for Built-up Area," Advances in Transport Volume 16, 2004. pp 783-794

Refereed Conferences

[1] **Bhaskar, A.,** Chung, E., & Dumont, A-G., "Travel time estimation on urban networks with mid-link sources and sinks," Transportation Research Board 88th Annual Meeting, 11-15 January 2009, Washington D.C., USA

[2] **Bhaskar, A.,** Chung, E., Dumont, A-G., & de Mouzon, O., "Analytical Modelling and Sensitivity Analysis for Travel Time Estimation on Signalised Urban Network," in Transportation Research Board 87th Annual Meeting, 13-17 January 2008, Washington, D.C., USA

[3] **Bhaskar, A.,** Chung, E., & Dumont, A-G., "Benefits and Issues of Urban Network Travel Time Prediction," in 7th European Congress and Exhibition on Intelligent Transportation Systems and Services, 4-6 June 2008,Geneva, Switzerland

[4] **Bhaskar, A.,** Chung, E., Kuwahara, M., de Mouzon, O., & Dumont, A.-G., "Urban network travel time estimation from stop-line detector data and signal controller data," Thirteenth International Conference on Urban Transport and the Environment in the 21st Century 3 - 5 September 2007, Coimbra, Portugal

[5] Oshino, Y., Tsukui, K., Hanabusa, H., **Bhaskar, A.,** Chung, E., & Kuwahara, M. (2007) A Study of the Road Traffic Noise Prediction Model Taking into Account the Citywide Road Network. Inter-Noise 2007. Istanbul, Turkey.

[6] Chung, E., **Bhaskar, A.,** & Kuwahara, M., Large area noise evaluation. 8th Highway and Urban Environment Symposium, 12-14 June 2006, Nicosia, Cyprus.

[7] **Bhaskar, A.,** Chung, E., & Kuwahara, M., Integration of Road Traffic Noise Simulator (ASJ) and Traffic Simulation (AVENUE) for Built-up Area. 10th International Conference on Urban Transport and the Environment in the 21st century. Urban Transport X, 2004, Dresden, Germany

Date: 6th May, 2009